TOWARDS A HOLOGRAPHIC FRAMEWORK FOR COSMOLOGY

A DISSERTATION
SUBMITTED TO THE DEPARTMENT OF PHYSICS
AND THE COMMITTEE ON GRADUATE STUDIES
OF STANFORD UNIVERSITY
IN PARTIAL FULFILLMENT OF THE REQUIREMENTS
FOR THE DEGREE OF
DOCTOR OF PHILOSOPHY

Xi Dong

August 2012

This dissertation is online at: http://purl.stanford.edu/vd028jx9557

I certify that I have read this dissertation and that, in my opinion, it is fully adequate in scope and quality as a dissertation for the degree of Doctor of Philosophy.

Eva Silverstein, Primary Adviser

I certify that I have read this dissertation and that, in my opinion, it is fully adequate in scope and quality as a dissertation for the degree of Doctor of Philosophy.

Shamit Kachru

I certify that I have read this dissertation and that, in my opinion, it is fully adequate in scope and quality as a dissertation for the degree of Doctor of Philosophy.

Leonard Susskind

Approved for the Stanford University Committee on Graduate Studies.

Patricia J. Gumport, Vice Provost Graduate Education

This signature page was generated electronically upon submission of this dissertation in electronic format. An original signed hard copy of the signature page is on file in University Archives.

Abstract

Studies on black hole physics have lead to the holographic principle, which states that a quantum gravitational system can be captured by a theory living in fewer dimensions. Given the observed accelerating expansion of our universe, it has been a major challenge to understand the realization of the holographic principle in cosmology. In this dissertation we review our progress in building such a framework.

Starting from concrete AdS/CFT (anti de Sitter/conformal field theory) dual pairs, we obtain de Sitter (dS) and other general Friedman-Robertson-Walker (FRW) solutions by adding branes and other ingredients from string theory. In the de Sitter case, our brane construction gives a microscopic realization of the dS/dS correspondence. The degrees of freedom in the semi-holographic dual theory provide a parametric interpretation of the Gibbons-Harking entropy of the bulk de Sitter space.

In the FRW case, we focus on a family of simple FRW solutions sourced by magnetic flavor branes. These solutions have a holographic dual interpretation which decouples from gravity at late time, opening up the possibility of a precise duality. Time-dependent effects play a crucial role in these dual theories. In particular, we find that time-dependent couplings in a quantum field theory can strongly affect long-distance physics, effectively shifting the infrared operator dimensions and generalizing known unitarity bounds.

Acknowledgements

First and foremost I would like to thank my advisor, Eva Silverstein, for her constant support and guidance through the years. She has taught me how good theoretical physics is done, and her enthusiasm for physics always inspires me.

Throughout my graduate career at Stanford University, I have been very fortunate to have fruitful collaborations with Ning Bao, Daniel Harlow, Sarah Harrison, Bart Horn, Shamit Kachru, Shunji Matsuura, Eva Silverstein, Gonzalo Torroba, Huajia Wang, and Alexander Westphal. Daniel Harlow has been a fantastic friend with whom I worked through many problems together. I have learned a tremendous amount of quantum field theory and string theory from Gonzalo Torroba.

I have benefited greatly from interactions with other members of the Stanford Institute for Theoretical Physics and the SLAC Theory Group, especially Dionysis Anninos, Savas Dimopoulos, Daniel Green, Sean Hartnoll, Anson Hook, Jonathan Maltz, Michael Peskin, Michael Salem, Edgar Shaghoulian, Stephen Shenker, Douglas Stanford, Leonard Susskind, Vitaly Vanchurin, and Sho Yaida.

I have also been very fortunate to spend a year at the Kavli Institute for Theoretical Physics, UC Santa Barbara, as well as participating in many great programs there. I would like to thank especially Richard Eager, Thomas Faulkner, Zhengcheng Gu, Idse Heemskerk, Gary Horowitz, Nabil Iqbal, Vijay Kumar, Donald Marolf, David Morrison, Joseph Polchinski, and Matthew Roberts for many stimulating discussions.

For this dissertation I would like to thank my reading committee members: Eva Silverstein, Leonard Susskind, and Shamit Kachru for their time, interest and insightful comments. I would also like to thank Andras Vasy for being the chair of my dissertation defense committee.

Last and most, I would like to thank my family for all their love and support: for my parents who raised me with a love of science and supported me in all my endeavors, and for my wife Jing whose continuing encouragement and faithful support have made this dissertation possible. Thank you.

Xi Dong
Stanford University
August 2012

Contents

Abstract **v**

Acknowledgements **vi**

1 Introduction **1**

2 Micromanaging de Sitter holography **4**

2.1 Introduction 4

2.2 dS holography and microscopy 5

2.3 General techniques 11

2.3.1 The strategy for stabilization 12

2.3.2 Stabilization procedure 15

2.3.3 Effects from localized sources 18

2.4 dS_3 worked example 20

2.4.1 Brane construction 21

2.4.2 Stabilization mechanism 26

2.4.3 $D7$-$\overline{D7}$ stability analysis 34

2.4.4 Stabilizing other moduli 36

2.4.5 Localization of sources and the warp factor 39

2.4.6 Entropy and brane construction 42

2.4.7 Alternative examples 43

2.5 Discussion and Future Directions 45

3 FRW solutions and holography from uplifted AdS/CFT 48
3.1 Introduction: keeping it real . . . 48
3.2 FRW solution sourced by magnetic flavor branes . . . 52
3.2.1 Magnetic flavor branes . . . 52
3.2.2 Solution and warping . . . 55
3.2.3 $d-1$ Planck mass and its decoupling at late times . . . 61
3.2.4 Covariant entropy bound . . . 63
3.2.5 Basic relations among parameters . . . 65
3.3 Dynamics of particles and branes . . . 67
3.4 Degrees of freedom in FRW holography . . . 72
3.4.1 A microscopic count of degrees of freedom . . . 72
3.4.2 Deriving $\tilde{N}_{\rm dof}$ from the quasilocal stress tensor . . . 78
3.5 Correlation functions . . . 84
3.5.1 Massive Green's functions . . . 84
3.5.2 Massless Green's functions . . . 88
3.6 Future directions: Magnetic flavors and time-dependent QFT . . . 91
3.A Correlation functions in general CdL geometry . . . 93
3.A.1 Euclidean prescription . . . 93
3.A.2 Lorentzian prescription . . . 99
3.A.3 Our FRW spacetime . . . 103
3.A.4 Massive correlation functions . . . 106

4 Unitarity bounds and RG flows in time dependent QFT 108
4.1 Motivations . . . 108
4.2 Spacetime dependent double trace flows . . . 111
4.2.1 RG flow in the static limit . . . 112
4.2.2 Spacetime dependent case . . . 115
4.2.3 Long distance propagator . . . 118
4.2.4 Infrared physics and unitarity: two wrongs make a right . . . 121
4.3 Spacetime dependent RG flow for fermionic operators . . . 123
4.3.1 Results for the static theory . . . 124

4.3.2 Infrared dynamics of the spacetime dependent theory 127
4.4 Unitarity bounds in SUSY gauge theories and FRW holography . . . 128
4.4.1 $\mathcal{N} = 1$ Supersymmetric QCD plus singlets 129
4.4.2 Seiberg-Witten theory and flavor bounds 134
4.4.3 Static theory with $n > n_*$ massive flavors 138
4.5 Future directions 139
4.A Dynamical couplings and unitarity 140
4.B Gaussian theories with spacetime dependent masses 141
4.B.1 Bosonic model 142
4.B.2 Fermionic model 144
4.C Expansion of the two-point functions 145
4.C.1 Expansion around the nontrivial scale-invariant regime 145
4.C.2 Expansion around the free fixed point 147
4.D Higher-derivative toy model 149

5 Simple exercises to flatten your potential 152
5.1 Motivation: realizing your potential 152
5.1.1 Additional kinetic effects 155
5.2 Warmup: review of axion monodromy inflation 158
5.2.1 Flattening vs. moduli potential barriers 161
5.3 Workout: axions pushing on heavy fields 162
5.3.1 Bowflux: Sloshing of flux on fixed cycles 163
5.3.2 Puffing on the kinetic term 166
5.3.3 Weight lifting: pushing on moduli 168
5.3.4 Circuit training: toward more generic UV complete examples . 169
5.4 Cooldown 170

6 Analytic Coleman-De Luccia Geometries 172
6.1 Introduction 172
6.2 General Properties of the Coleman-De Luccia Geometry 173
6.2.1 Euclidean Preliminaries 173
6.2.2 Lorentzian Continuation 175

6.2.3 Constraints and a Definition 177
6.2.4 Compact Coleman-De Luccia Geometries 180
6.3 Examples 181
6.3.1 De Sitter Domain Walls 183
6.3.2 Decays from dS to dS 184
6.3.3 Decays from dS to Minkowski Space 187
6.3.4 Noncompact Examples 189
6.A Null Energy Condition 191
6.B A Bound on Parent dS Radius 192

Bibliography **195**

List of Tables

2.1 Ingredients for the brane construction of dS_3 21
2.2 Numerical example for a dS_3 solution 32

List of Figures

2.1 Compact brane constructions for de Sitter solutions 10

3.1 Contour C going above the double pole 98
3.2 (a) Contour C_a surrounding simple poles; (b) Coutour C_b surrounding a double pole and simple poles below 99

5.1 Combined data constraints on the tensor to scalar ratio r and the tilt n_s together with the predictions for power-law potentials 156
5.2 Effects of an inflationary flux on the three-term structure stabilized in a Minkowski minimum 163

6.1 Left: three regions of interest in the ξ plane for the Lorentzian continuation of a compact CDL geometry; Right: corresponding regions of the CDL Penrose diagram 177
6.2 A CDL geometry describing the decay from dS to dS 186
6.3 The geometry and potential describing a decay from dS to asymptotically Minkowski space 188
6.4 The potential leading to a CDL geometry describing the decay from Minkowski space to a crunching AdS 190
6.5 The geometry and potential for a decay from AdS to a crunch 190

Chapter 1

Introduction

At present we lack a fundamental theory of quantum gravity in cosmological backgrounds. String theory, widely considered the most promising candidate for such a theory, is still under active development. With the advent of the Matrix theory [1] and the AdS/CFT (anti de Sitter/conformal field theory) correspondence [2, 3, 4], string theory in certain Minkowski or AdS backgrounds became reasonably well-defined. Unfortunately, we have observed accelerated expansion and hence a positive cosmological constant in our universe. It therefore remains a major challenge to formulate string theory in cosmology.

Studies on black hole physics have lead to the holographic principle [5, 6], which is the statement that a gravitational system can be captured by a theory living in fewer dimensions. It has been viewed as a key property of the ultimate theory of quantum gravity. String theory appears to be holographic in a nontrivial way. In particular, both the Matrix theory and the AdS/CFT correspondence satisfy the holographic principle.

In this work, we review our progress in building a holographic framework for quantum gravity in cosmological backgrounds such as de Sitter or general Friedmann–Robertson–Walker (FRW) spacetime. Such a framework is essential not only conceptually, but also in making contacts with experiments that measure the cosmic microwave background radiation and allow us to "see" the very early universe. It could also lead to a better understanding of the ultimate fate of our universe.

Our general approach is to explore how our current understanding of string theory helps us resolve various puzzles, such as the nature of cosmological horizons, singularities, observables, and entropy. In Chapter 2 we develop tools to engineer de Sitter vacua with semi-holographic duals, using elliptic fibrations and orientifolds to uplift Freund-Rubin compactifications with CFT duals. The dual brane construction is compact and constitutes a microscopic realization of the dS/dS correspondence, realizing d-dimensional de Sitter space as a warped compactification down to $(d-1)$-dimensional de Sitter gravity coupled to a pair of large-N matter sectors. This provides a parametric microscopic interpretation of the Gibbons-Hawking entropy. We illustrate these ideas with an explicit class of examples in three dimensions, and describe ongoing work on four-dimensional constructions.

In Chapter 3, we present simple FRW solutions sourced by magnetic flavor branes and analyze correlation functions and particle and brane dynamics. To obtain a holographic description, we exhibit a time-dependent warped metric on the solution and interpret the resulting redshifted region as a Lorentzian low energy effective field theory in one fewer dimension. At finite times, this theory has a finite cutoff, a propagating lower dimensional graviton and a finite covariant entropy bound, but at late times the lower dimensional Planck mass and entropy go off to infinity in a way that is dominated by contributions from the low energy effective theory. This opens up the possibility of a precise dual at late times. We reproduce the time-dependent growth of the number of degrees of freedom in the system via a count of available microscopic states in the corresponding magnetic brane construction.

In Chapter 4 we generalize unitarity bounds on operator dimensions in conformal field theory to field theories with spacetime dependent couplings. Below the energy scale of spacetime variation of the couplings, their evolution can strongly affect the physics, effectively shifting the infrared operator scaling and unitarity bounds determined from correlation functions in the theory. We analyze this explicitly for large-N double-trace flows, and connect these to UV complete field theories. One motivating class of examples comes from our previous work on FRW holography, where this effect explains the range of flavors allowed in the dual, time dependent, field theory.

In Chapter 5 We show how backreaction of the inflaton potential energy on heavy

scalar fields can flatten the inflationary potential, as the heavy fields adjust to their most energetically favorable configuration. This mechanism operates in previous UV-complete examples of axion monodromy inflation – flattening a would-be quadratic potential to one linear in the inflaton field – but occurs more generally, and we illustrate the effect with several examples. Special choices of compactification minimizing backreaction may realize chaotic inflation with a quadratic potential, but we argue that a flatter potential such as power-law inflation $V(\phi) \propto \phi^p$ with $p < 2$ is a more generic option at sufficiently large values of ϕ.

In Chapter 6 we present the necessary and sufficient conditions for a Euclidean scale factor to be a solution of the Coleman-De Luccia equations for some analytic potential $V(\phi)$, with a Lorentzian continuation describing the growth of a bubble of lower-energy vacuum surrounded by higher-energy vacuum. We then give a set of explicit examples that satisfy the conditions and thus are closed-form analytic examples of Coleman-De Luccia geometries.

The work presented in Chapters 2 and 4 was done in collaboration with Bart Horn, Eva Silverstein, and Gonzalo Torroba, and was published in [7, 8]. The work presented in Chapter 3 was done in collaboration with Shunji Matsuura in addition to the aforementioned group, and was published in [9]. The work presented in Chapter 5 was done in collaboration with Bart Horn, Eva Silverstein, and Alexander Westphal, and was published in [10]. The work presented in Chapter 6 was done in collaboration with Daniel Harlow, and was published in [11].

Chapter 2

Micromanaging de Sitter holography

2.1 Introduction

We develop tools to engineer de Sitter vacua with semi-holographic duals, using elliptic fibrations and orientifolds to uplift Freund-Rubin compactifications with CFT duals. The dual brane construction is compact and constitutes a microscopic realization of the dS/dS correspondence, realizing d-dimensional de Sitter space as a warped compactification down to $(d-1)$-dimensional de Sitter gravity coupled to a pair of large-N matter sectors. This provides a parametric microscopic interpretation of the Gibbons-Hawking entropy. We illustrate these ideas with an explicit class of examples in three dimensions, and describe ongoing work on four-dimensional constructions.

The Gibbons-Hawking entropy of the de Sitter horizon [12] invites a microscopic interpretation and a holographic formulation of inflating spacetimes. Much progress was made in the analogous problem in black hole physics using special black holes in string theory whose microstates could be reliably counted, such as those analyzed in [13, 14, 15]; this led to the AdS/CFT correspondence [2, 3, 4]. In contrast, a microscopic understanding of the entropy of de Sitter space is more difficult for several reasons including its potential dynamical connections to other backgrounds (metastability), the absence of a non-fluctuating timelike boundary, and the absence

of supersymmetry.

In this chapter, we develop a class of de Sitter constructions in string theory, built up from AdS/CFT dual pairs along the lines of [16], which are simple enough to provide a microscopic accounting of the parametric scaling of the Gibbons-Hawking entropy. These models realize microscopically a semi-holographic description of metastable de Sitter space which had been derived macroscopically in [17, 18, 19]. It would also be interesting to connect this to other approaches to de Sitter holography such as [20, 21, 22] and to other manifestations of the de Sitter entropy such as [23, 24].[1] The construction is somewhat analogous to neutral black branes analyzed in [26].

We will begin in §2.2 by explaining the salient features of the holographic duality and of the de Sitter construction which realizes it microscopically. In §2.3 we will lay out our methods in more detail, applying them to worked examples of dS_3 in §2.4. Finally, §2.5 discusses further directions and ongoing work, including dS_4 constructions in progress.

2.2 dS holography and microscopy

A semi-holographic duality follows simply by recognizing the de Sitter static patch as a warped compxactification

$$ds^2_{dS_d} = dw^2 + \sin^2\left(\frac{w}{R_{dS}}\right) ds^2_{dS_{d-1}}. \tag{2.1}$$

The warp factor $\sin^2(w/R_{dS})$ goes to zero at $w = 0, \pi R_{dS}$ and rises to a finite maximum in between, implying two warped throats and a propagating graviton in $d-1$ dimensions. Such a semi-holographic duality is familiar in the study of warped compactifications (such as [27]) and Randall-Sundrum models [28]. In these systems, the bulk of the throats admits a dual description in terms of a field theory (as in [29]), but the finite maximum of the warp factor implies that this field theory is cut off at a finite scale and coupled to gravity [28, 30, 31]. The main observation in [17, 18, 19] was that the same statements apply to de Sitter (2.1).

[1] See [25] for a different proposal.

This macroscopic derivation of a holographic description leaves open the question of what degrees of freedom build up the two throats microscopically. In this work, we find that 'uplifting' AdS/CFT brane constructions to de Sitter space automatically produces the two-throat structure, while revealing (example by example) the microscopic degrees of freedom that build up the throats.

Before turning to the detailed examples, let us explain the main features of the construction and its realization of de Sitter holography. Freund-Rubin solutions of the form $AdS_d \times B^n \times T^{10-d-n}$, with B^n positively curved and with fluxes threading through the compactification, provided the first examples of the holographic AdS/CFT duality [2, 3, 4]. These can be described in terms of a d-dimensional effective potential (as in [32, 33, 34, 35, 36, 37, 38, 39]), with a negative curvature-induced term arising from the dimensional reduction of the Einstein term $\sqrt{g}\mathcal{R}$, played off against a positive term from the flux energy.

In the dual brane construction, these fluxes and the corresponding geometry arise from the presence of color branes (e.g. D3-branes in the canonical $AdS_5 \times S^5$ example and D1-D5 for $AdS_3 \times S^3 \times T^4$) probing the space transverse to their worldvolume directions. The space probed by these branes takes the form of a cone with base B^n,

$$ds^2 = dw^2 + R(w)^2 ds_B^2 \tag{2.2}$$

with $R(w) = w$. For our purposes it will be useful to review how this comes about in the following way. The equations of general relativity applied to the radius $R(w)$ of the base require

$$\frac{(dR/dw)^2}{R^2} \sim +\frac{1}{R^2} \tag{2.3}$$

with the + sign corresponding to the positive curvature of B^n. This is a radial analogue of the Friedmann equation of cosmology, with R'/R (prime denoting differentiation with respect to the radial coordinate w) playing the role of Hubble, and we have included only the curvature term on the right hand side because this is all that contributes in the absence of the color branes. This has the solution $R = w$, giving the metric $ds^2 = dw^2 + w^2 ds_B^2$ of a noncompact cone.

In the presence of the color branes, the near horizon AdS_d solution arises from

a competition of the positive curvature of B_n against flux terms which must be included on the right hand side of (2.3) along with the curvature of the d noncompact dimensions.

Starting from these Freund-Rubin solutions, we will next add ingredients to "uplift" the AdS solution to dS, deriving an effective potential which has minima with positive cosmological constant. Then, we will ask what becomes of the original AdS/CFT brane construction in the process of uplifting.

The method we will use to achieve the uplifting is to introduce, among other things,
(i) Contributions which overcompensate the positive curvature in the original Freund-Rubin compactification. One such ingredient is an elliptic fibration of the T^{10-n-d} over B^n,

$$\begin{array}{rl} T^{10-n-d} \rightarrow & \mathcal{Y}_{10-d} \\ & \downarrow \\ & B^n \end{array} \tag{2.4}$$

which introduces negative contributions to the scalar curvature that compete with the negative potential term in the original Freund-Rubin compactification [16]. NS5-branes at real codimension two on the base B also compete with its curvature. D-branes wrapping all of B^n (along with suitably stabilized anti-branes or other sources canceling their charge) dominate in the expansion in inverse radii and can play an important role in the uplifting, though they are subdominant in the string coupling and hence must be combined with other sources.
(ii) Orientifolds, at higher codimension than the leading uplifting term, to generate the intermediate negative term in the potential required to obtain a metastable minimum.

We will explain this and related methods in a detailed class of $(A)dS_3$ examples in the remainder of the chapter; further examples in four dimensions are in progress [40]. For now, let us assume such a construction exists and analyze its effect on the brane construction and the structure of the resulting holographic dual.

Elliptic fibrations (i) can be thought of as a configuration of 5-branes as in [41, 42,

43]; we will call these "stringy cosmic 5-branes (SC5s)". Since they are extended in the radial direction, they are flavor branes and in general introduce both electric and magnetic matter. Neveu-Schwarz branes and spacefilling D-branes also contribute flavors. Orientifolds (ii) project the D-brane theory onto a different gauge group, flavor group, and matter content, with unitary groups replaced by orthogonal or symplectic groups.

More significantly, we would like to understand what happens to the space – the analog of the cone described above – on which the color branes live. We will in particular consider what uplifting does to the equation (2.3) satisfied by R (the radial modulus of the base) in the absence of the flux contributed by the color branes. In general, this problem is more complicated than in the simplest AdS/CFT models: removing the flux will destabilize many moduli in general, leading to radial and/or time evolution of more than just R. In a given construction, one may study this in detail. However, there is a general qualitative feature of the de Sitter brane construction which follows more simply.

Let us start with a configuration, at some initial time, in which the non-radial moduli are independent of w, and carry zero kinetic energy. We can then focus on the radial modulus R, solving its equation of motion by letting it vary radially with w. Given the uplifting, the radial Friedmann equation is now of the form

$$\frac{R'(w)^2}{R^2} \sim -\frac{1}{R^{n_1}} + \frac{const}{R^{n_2}} \tag{2.5}$$

We have taken into account that the positive-curvature term in (2.3) has been overcompensated. We have also included the orientifold stress-energy of the uplifted model, and in order for this to provide an intermediate negative term in the potential we must have $n_1 < n_2$.[2]

Since $n_2 > n_1$, there will be points at which $R'(w) = 0$, so the radius R grows to a maximum size and then proceeds to decrease again. In the analogue Friedmann equation, this is like a closed universe in the radial direction. (Note that since we

[2]For the purposes of the present heuristic discussion, we have not included kinetic mixing of moduli; we will address this below in (2.25) and find that it does not change the qualitative result.

are discussing spatial rather than temporal evolution, the case of a closed universe follows from negative rather than positive curvature.) The cone of the AdS/CFT brane construction has become a compact space in the de Sitter case.

Now let us add back in the color branes. In the AdS case, we place color branes at the tip of a cone, and they warp the geometry to produce a Freund-Rubin flux compactification. In the dS case, since the radial direction is compact, there is a second tip where R shrinks to zero size. If we put color branes at one tip and anti-branes at the other, this again generates the flux which plays off against the other ingredients to stabilize the compactification. The two tips in the brane construction correspond to the two warped throats comprising the de Sitter static patch. That is, the brane construction corresponding to the uplifted model has automatically produced a microscopic realization of these throats!

As in the cosmological analogue, this geometry can develop curvature singularities at the tips where $R(w)$ shrinks to zero size; these are radial analogues of a big bang and big crunch. These generalize the conical singularity in familiar AdS/CFT examples. The nature of the singularities depends on the powers n_1 and n_2 arising in (2.5). The second (orientifold) term dominates the right hand side of (2.5) near $R = 0$. In the case of negative curvature, $n_1 = 2$ and $n_2 > 2$; in this case the orientifold term induces a timelike singularity which is worse than conical. This has to do with the singularity at the cores of the orientifolds, which would be interesting to resolve. However, in our construction below this question is evaded, as the leading R-dependences in (2.5) will yield $n_1 = 0, n_2 = 2$ at fixed string coupling.

In the presence of the flux corresponding to N_c color branes, the right hand side of the radial Friedmann equation (2.5) acquires one or more additional terms of the form $\sim -N_c^2/R^{2n}$ (with $2n > n_2$). This dominates at small R and prevents the crunch or bang singularity from happening. Once all the ingredients are included in a way which yields a complete stabilization mechanism, R' goes to zero for all w (as the moduli are stabilized) and the right hand side of (2.5) acquires new terms including the d-dimensional de Sitter curvature.

In the regime of couplings applicable to the de Sitter solution, the color branes are best described in terms of their dual gravity solution. The first, simplest examples of

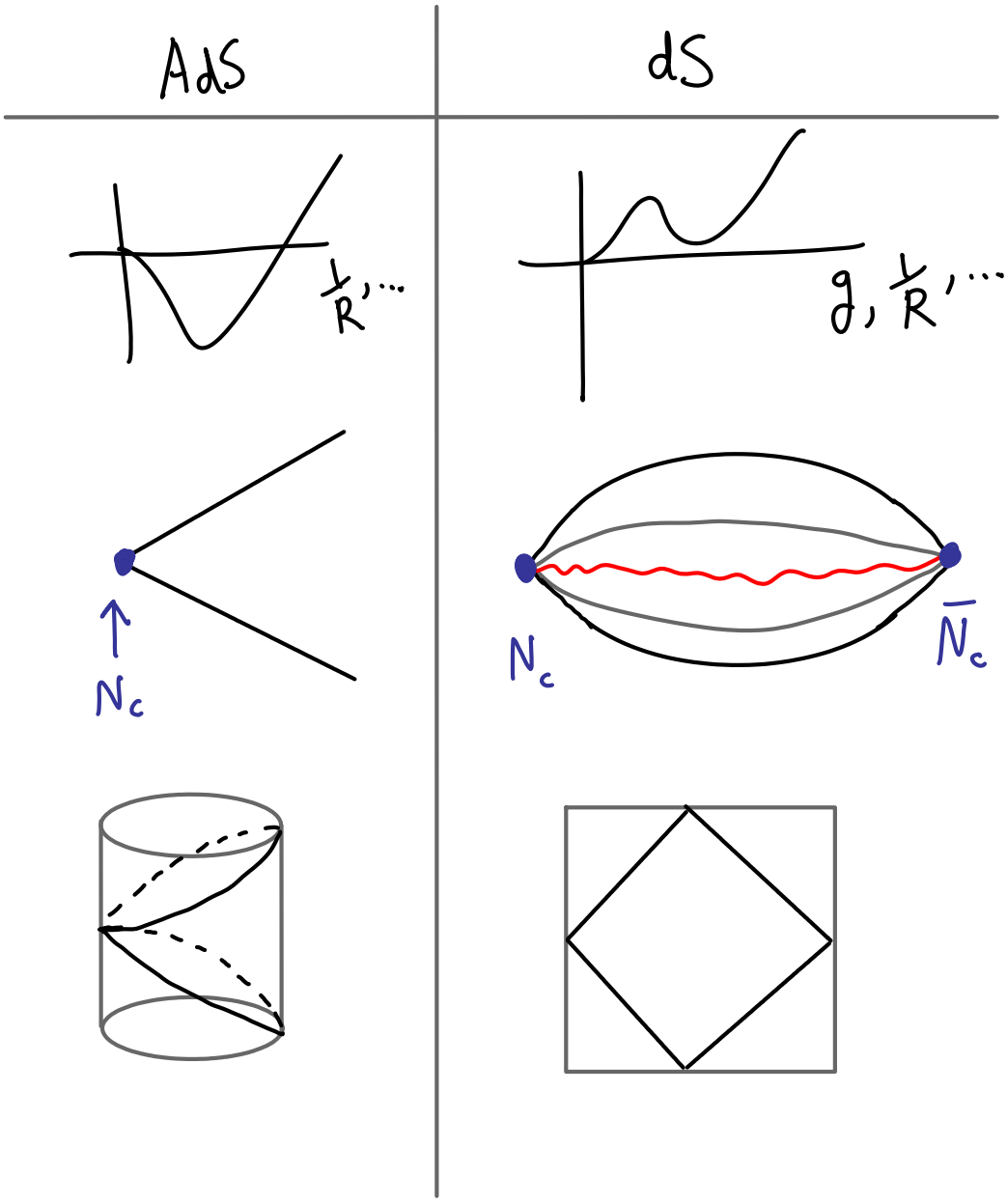

Figure 2.1: de Sitter brane constructions are compact as a result of the net positive potential energy carried by the flavor branes, curvature, and orientifolds. The two tips with color branes or antibranes correspond to the two warped throats of dS_d in the dS_{d-1} slicing.

AdS/CFT dual pairs had a line of fixed points connecting the regimes of weak and strong coupling in the low energy limit of the brane construction. In cosmological solutions such as this (and also for generic gauge/gravity duals, even some such as [44] closely related to the original examples of AdS/CFT), there is not a line of maximally symmetric solutions allowing one to continue between weak and strong couplings regimes of the brane construction. One may, however, consider weakly coupled, but less symmetric, time dependent backgrounds by analyzing the runaway region near weak coupling and/or large radius.

As we discussed above, the dS/dS correspondence is 'semiholographic' in the sense that the Planck mass is finite and $(d-1)$-dimensional gravity does not decouple. Nevertheless, as we will show below, the dS entropy can be understood parametrically in terms of the degrees of freedom of the brane system. The reason for this is fairly simple – the ingredients we add to uplift add a small number of flavors and projections to the original AdS brane system, which does not change its entropy as a function of large quantum numbers such as the dimensions of the color groups.

2.3 General techniques

Our technique for stabilizing moduli while uplifting AdS/CFT dual pairs can be thought of as a combination of two familiar methods: Freund-Rubin stabilization, and the identification of elliptically fibered manifolds with branes on their base. In this section, we discuss the general methods involved in this construction before coming to an explicit class of examples in §2.4.

de Sitter model-building in string theory (without a connection to a known holographic dual) has proceeded actively since the discovery of the late-time acceleration of the universe (see e.g. [32, 33, 34, 35, 36, 37, 38, 39] for some reviews with various perspectives on the problem). Following work anticipating the landscape and its role in interpreting the cosmological constant [45, 46], early constructions make use of the positive leading potential from supercriticality [47, 48] or from anti-D3-branes [49] in warped flux compactifications [27] with non-perturbative contributions to the superpotential. The latter scenario has provided rich ground for low-energy

supersymmetric model building in cosmology and particle physics, but particularly for the goal of understanding de Sitter holography microscopically it may be advantageous to seek simple and explicit de Sitter solutions using perturbative ingredients [50, 51, 52, 53, 54, 55, 56, 57, 58, 59, 60, 61].

In this line of development, one lesson thus far has been that brane sources with tension $\sim 1/g_s^2$ play a very useful role in de Sitter stabilization; certain no go results follow in their absence. These are a priori more difficult to control at weak string coupling than D-branes. One way in which the present work builds further in this direction is to realize such objects via elliptic fibration [42, 43, 16], which incorporates their backreaction. (In some cases we will find that the core sizes of required solitonic branes are controllably small in any case.)

2.3.1 The strategy for stabilization

With their backreaction taken into account, the sets of N_{Dp} color branes described above are replaced by corresponding RR fluxes,

$$\int_{\Sigma^{8-p}} F_{8-p} = N_{Dp} \;\Rightarrow\; F_{8-p} \sim \frac{N_{Dp}}{\mathrm{vol}(\Sigma^{8-p})} \tag{2.6}$$

where $\mathrm{vol}(\Sigma^{8-p})$ denotes the volume of the surface threaded by the flux. Here we set $\alpha' = 1$ and simplify the formulas by omitting numerical factors such as 2π; these will be taken into account in the explicit analysis in §2.4. Also, the metric signature is taken to be $(-+\ldots+)$.

We look for solutions which are locally of the form

$$dS_d \times B_n \times T^{10-n-d} \tag{2.7}$$

in the presence of background fluxes (2.6), plus the flavor branes and orientifolds. The radius of dS_d is denoted by R_{dS}. Notice that in general these localized sources will break the isometries of $B_n \times T^{10-n-d}$.

There are two different approaches to this problem. First, one can work directly in ten dimensions, looking for solutions to the equations of motion derived from the

(string frame) action

$$S = \frac{1}{2\kappa_{10}^2}\int \sqrt{-g^{(10)}}\left[e^{-2\phi}(\mathcal{R}^{(10)} + 4(\nabla\phi)^2 - \frac{1}{2}|H_3|^2) - \frac{1}{2}|\tilde{F}_n|^2\right] + S_{CS} + S_{loc}\,. \quad (2.8)$$

Here S_{CS} denotes the type II Chern-Simons terms, and S_{loc} stands for contributions from localized sources,

$$S_{loc} = -T_p\int \sqrt{-g^{p+1}}\,. \quad (2.9)$$

This method is preferable when practical. However, explicit solutions to the equations of motion can be easily obtained only when enough isometries are present, which is not the case here.

Instead, we will analyze the d-dimensional effective field theory derived by compactifying (2.8) on $B_n \times T^{10-n-d}$, anticipating a solution with internal dimensions small with respect to the de Sitter radius R_{dS}. This requires identifying the light scalar fields which must be stabilized,[3] computing their effective potential, and finding a minimum with positive cosmological constant. In fact a minimum is not strictly necessary: in order to study accelerated expansion, one requires that any tachyonic masses be small compared to the Hubble scale of the de Sitter solution. A holographic or semi-holographic description of this situation would be interesting in itself.

To begin with, we will derive an approximate d-dimensional moduli potential by averaging the localized sources over the internal space, ignoring the warp factor. Then it must be checked that such a solution can be lifted to a full 10d configuration. The 10d consistency conditions will be discussed in §2.3.3 and addressed in our specific model in §2.4.

Three of the moduli consist of the dilaton and internal volumes[4]

$$\tilde{R}_0^n \equiv \langle \mathrm{vol}(B_n)\rangle \quad , \quad L_0^{10-n-d} \equiv \langle \mathrm{vol}(T^{10-n-d})\rangle. \quad (2.10)$$

[3] which we will loosely refer to as "moduli"

[4] We use a tilde on the base size $\tilde{R}_0$ because in explicit models such as orbifolds, the base may be anisotropic and we will find it useful to reserve the notation R for the curvature radius of the base.

In terms of these, the d-dimensional Planck scale from dimensional reduction is

$$(M_d)^{d-2} = \frac{\tilde{R}_0^n L_0^{10-n-d}}{g_{s,0}^2} \,. \tag{2.11}$$

It is useful to introduce fluctuating fields with vanishing VEV,

$$g_s = g_{s,0} e^{\phi} \;,\; \tilde{R} = \tilde{R}_0 e^{\sigma_R} \;,\; L = L_0 e^{\sigma_L} \,. \tag{2.12}$$

At fixed Planck scale, ϕ, σ_R and σ_L have kinetic terms independent of the overall volume.

The effective action becomes

$$S_{eff} = M_d^{d-2} \int \sqrt{-g^{(d)}} e^{-2\phi + n\sigma_R + k\sigma_L} \, \mathcal{R}^{(d)} + \dots \,, \tag{2.13}$$

where here $k = 10 - n - d$. The dependence of the Einstein term on the fluctuating scalars is removed by a Weyl rescaling,

$$g^{(d)}_{E\mu\nu} \equiv \left(e^{-2\phi + n\sigma_R + k\sigma_L}\right)^{2/(d-2)} \, g^{(d)}_{\mu\nu} \,. \tag{2.14}$$

From now on we work in Einstein frame and drop the 'E' subindex. Then, the action takes the form

$$S_{eff} = \int \sqrt{-g^{(d)}} \, \left[M_d^{d-2} \left(\mathcal{R}^{(d)} - G_{ij} \, g^{\mu\nu} \partial_\mu \sigma^i \partial_\nu \sigma^j \right) - \mathcal{U} \right] \,. \tag{2.15}$$

The (positive definite) kinetic term metric G_{ij} for the moduli σ^i follows by dimensionally reducing $\int \sqrt{-g^{(10)}} \mathcal{R}^{(10)}$ on $B_n \times T^{10-n-d}$ in Einstein frame.[5] In our normalization for the moduli, G_{ij} has order one eigenvalues that depend on d and n. There is kinetic mixing between R and L ($G_{RL} \neq 0$), reflecting the fact that the overall volume modulus arises from the combination $\tilde{R}^n L^k$.

[5] When backreaction from localized sources is important, a slightly more complicated metric ansatz is required and kinetic terms receive warping corrections. We refer the reader to [62, 63, 64] for details. Here we will consistently work in the limit of small warping, where such effects can be ignored.

The d-dimensional Einstein frame potential energy reads

$$\begin{aligned}\mathcal{U} &\equiv M_d^d \left(\frac{g_s^2}{\tilde{R}^n L^{10-d-n}}\right)^{d/(d-2)} \left[-\frac{1}{g_s^2}\int \sqrt{g^{(10-d)}}\left(\mathcal{R}^{(10-d)} - 4(\nabla\phi)^2 - \frac{1}{2}|H_3|^2\right) + \right. \\ &+ \left. \sum_{loc,\, q} T_q \,\mathrm{vol}(\Sigma_{q+1-d}) + \tilde{R}^n L^{10-n-d} \sum_p \frac{N_{Dp}^2}{\mathrm{vol}(\Sigma^{8-p})^2}\right] . \end{aligned} \tag{2.16}$$

The first two factors come from the Weyl rescaling and the fact that we work at fixed d-dimensional Planck mass M_d. The second term inside the square brackets is the contribution from the localized sources (2.9), and Σ_{q+1-d} is the cycle wrapped by the q-brane along the internal directions. For D-branes/O-planes, $T_q \sim 1/g_s$; NS5, KK5 and SC5-branes have tension $T \propto 1/g_s^2$ that can compete against curvature if they sit at real codimension two on the base B_n.[6] The last term is produced by the flux backreaction eq. (2.6) from the color branes.

So far, we are ignoring contributions from the warp factor derived carefully in [65, 66, 67] which we will address below. Note that as is standard, with the Weyl rescaling factor in place each term in the effective potential goes to zero at weak coupling or large radius.

2.3.2 Stabilization procedure

Minima of Eq. (2.16) are conveniently analyzed with the "abc" method of [50], as follows. Before adding the torus fibration, we have curvature

$$\mathcal{R}^{(10-d)} \sim \frac{1}{R^2}\,, \tag{2.17}$$

where as mentioned above, the curvature radius R may differ from the n^{th} root of the volume $\tilde{R}$ in anisotropic models such as orbifolds. The potential energy from positive

[6] The 10d dilaton can vanish or blow up at the cores of localized sources. In our discussion, g_s denotes the d-dimensional field, which corresponds to an average value of the 10d mode away from the sources. A similar comment applies to the complex and Kähler moduli of T^{10-n-d}, which can degenerate at the positions of SC5 branes.

curvature is

$$\mathcal{U}_R \sim -M_d^d \left(\frac{g_s^2}{\tilde{R}^n L^{10-n-d}}\right)^{2/(d-2)} \frac{1}{R^2}\,. \tag{2.18}$$

The calculations simplify in terms of the variable

$$\eta \equiv \frac{1}{R}\left(\frac{g_s^2}{\tilde{R}^n L^{10-n-d}}\right)^{1/(d-2)} \tag{2.19}$$

which gives $\mathcal{U}_R \sim -M_d^d \eta^2$. We note the useful relation between the Planck scale (2.11) and the stabilized value of the moduli,

$$M_d = (\eta_0 R_0)^{-1}\,. \tag{2.20}$$

Stringy cosmic branes and NS5 branes give positive contributions to η^2, competing with and potentially over-cancelling the curvature potential energy if they arise at real codimension two on the base B_n. Orientifold planes and D-branes contribute terms of order $\eta^{(d+2)/2}$ with opposite signs; the net effect should give a negative coefficient in front of $\eta^{(d+2)/2}$ (denoted below by $-b(\sigma)$, with $b(\sigma) > 0$). Flux energy scales like η^d and always gives a positive coefficient $c(\sigma) > 0$. Putting everything together, we find an effective potential with the structure

$$\mathcal{U} = M_d^d\, \eta^2 \left(a(\sigma) - b(\sigma)\eta^{(d-2)/2} + c(\sigma)\eta^{d-2}\right)\,, \tag{2.21}$$

where here σ^I are the moduli different from the combination in Eq. (2.19). The functions $a(\sigma)$, $b(\sigma)$ and $c(\sigma)$ are computed from (2.16).

Let us first consider the AdS case, where only the fluxes (related to color branes) and positive internal curvature are kept:

$$a(\sigma) = -1\,,\ b(\sigma) = 0\,,\ c(\sigma) = R^d \tilde{R}^n L^{10-n-d} \sum_p \frac{N_{Dp}^2}{\mathrm{vol}(\Sigma^{8-p})^2}\,. \tag{2.22}$$

The σ fields are stabilized at the critical points of $c(\sigma)$ (denoted by σ_0). Plugging

this back into eq. (2.21) gives a minimum

$$\eta_0^{d-2} = \frac{2}{d\, c_0}\ ,\ \mathcal{U}_0 = -M_d^d\, \frac{d-2}{d}\eta_0^2 \tag{2.23}$$

and a cosmological constant (see eqs. (2.15) and (2.20))

$$\Lambda_{min} = \frac{\mathcal{U}_0}{M_d^{d-2}} = -\frac{d-2}{d}\frac{1}{R_0^2}\,. \tag{2.24}$$

Of course, this is the well-known result that Freund-Rubin solutions supported only by flux and positive curvature have an AdS radius of the same order of magnitude as the internal curvature radius, $R_{AdS}^2 \approx R_0^2$.

Moving on to the dS case, the ingredients described above give uplifting terms that set $a(\sigma) > 0$, orientifolds plus D-branes to set $b(\sigma) > 0$, and flux contributions as in the AdS case. It is instructive to first analyze the background solution in the absence of color branes (a and b nonzero, but $c = 0$). This will make contact with the discussion of the radial Friedmann equation (2.5).

We focus on the radial evolution (coordinate w in the slicing of Eq. (2.1)) of the volume moduli R and L. As discussed above, generically some of the moduli will become time dependent; here we restrict to an initial time where the kinetic energy is small compared to the gradient energy from radial variation. Neglecting this time dependence we can extremize the effective action (2.15) with respect to $g_{00}^{(d)}$, obtaining

$$G_{ij}\nabla^w\sigma^i\nabla_w\sigma^j = \frac{d-2}{d}\mathcal{R}^{(d)} - \frac{\mathcal{U}}{M_d^{d-2}}\,. \tag{2.25}$$

The left hand side is a positive definite quadratic combination of $R'(w)/R$ and $L'(w)/L$. In general, $R'(w) \neq 0$ sources radial dependence in L through the kinetic mixing. We can solve for $L'(w)/L$ in terms of $R'(w)/R$. Then using the expression (2.16) for the potential energy, the right hand side of Eq. (2.25) has the structure discussed in (2.5) (after a conformal rescaling that relates 10- and d-dimensional Einstein frames). Namely, $\mathcal{U}$ has both positive and negative contributions so that the right hand side in (2.25) admits nontrivial roots for R. $R(w)$ grows until it reaches

this value, and then decreases again. As discussed in §2.2, the effective description reveals that the background space is compact.

Next, placing the color branes and antibranes at the tips $R = 0$ gives a nonzero $c(\sigma)$. There exists a solution with positive energy for

$$1 < \frac{4ac}{b^2} < \frac{(d+2)^2}{8d}\,, \tag{2.26}$$

evaluated at the minimum of the other moduli σ^I. The strategy is to first minimize

$$\delta(\sigma) \equiv \frac{4ac}{b^2} - 1 \tag{2.27}$$

at a small value, with the potential and minimum then becoming

$$\mathcal{U} = M_d^d\,\eta^2\left(a\left(1 - \frac{b}{2a}\eta^{(d-2)/2}\right)^2 + \frac{b^2}{4a}\delta\,\eta^{d-2}\right) \Rightarrow \eta_0^{(d-2)/2} = \frac{2a_0}{b_0}\,. \tag{2.28}$$

The positive cosmological constant gives a dS radius

$$R_{dS}^2 \approx \frac{R_0^2}{\delta_0 a_0}\,. \tag{2.29}$$

Small values of δ and/or a then lead to solutions with small internal dimensions relative to the de Sitter radius. This was studied for AdS compactifications in [16], and will arise in a different way in the examples in the present work.

2.3.3 Effects from localized sources

Let us now discuss the ten dimensional consistency of the solutions. Using the dimensionally reduced theory, approximating the sources as smeared, we have explained how the ingredients described above can combine to give a solution of the form $dS_d \times B_n \times T^{10-n-d}$. Now we shall analyze the model from a 10d perspective. We would like to understand under what circumstances there exists a 10d solution to Eq. (2.8) that, after averaging over the internal space, gives results approximately consistent with the ones derived from (2.16).

The equations of motion must be solved pointwise in ten dimensions. Some of the ingredients such as O-planes are localized in the internal dimensions; i.e. their charge and stress-energy are delta-function supported in some directions. According to the effective theory (2.16), these O-planes play off against fluxes and net negative internal curvature to stabilize the moduli. However, the fluxes and internal negative curvature are not delta-function localized at the positions of the O-planes, and so these effects alone cannot play off of each other pointwise to give 10d solutions.

The missing contributions come from p-forms and warping [65, 66, 67], which must be consistently included in the effective potential. As we will shortly review, these effects are small when the sources are dilute enough or have little enough tension that the gravitational and RR potentials they source are small in the bulk of the internal geometry. In our construction in the next section, this will hold for D-branes and orientifold planes; the elliptic fibration itself does not correspond to well-localized sources, but contributes to the curvature-induced potential energy in a manner we can compute using a sigma model.

Let us discuss explicitly the gravitational backreaction. Gravitational and p-form effects are of the same order of magnitude for BPS objects, so the two analyses are parallel. As argued in e.g. [65, 66, 67], the contribution that accounts for the localized stress-energy of the sources is a warp factor e^A multiplying the $(A)dS_d$ metric which varies over the internal dimensions (as well as conformal factors in the internal metric, depending on one's conventions for the fiducial internal metric). We will look for solutions with $A \ll 1$ away from the cores of the localized sources.

The equation of motion for the warp factor is of the form

$$\nabla^2 A - (\nabla A)^2 = -\mathcal{R}^{(10-d)} + g_s^2 \, |F|^2 + g_s^2 \, T^{loc} - g_s^2 \, \mathcal{U} \tag{2.30}$$

where we have replaced various powers of e^A by 1, anticipating a solution with $A \ll 1$. Here $\mathcal{R}^{(10-d)}$ is curvature, F is flux and $\mathcal{U}$ is the d-dimensional effective potential, a constant independent of the internal coordinates. This equation has the property that for delocalized sources the right hand side would vanish and no nontrivial warp factor would be generated.

The corrections to the effective potential $\mathcal{U}$ are of order $(\nabla A)^2/g_s^2$. If $A \ll 1$, and hence $\nabla^2 A \gg (\nabla A)^2$, this means that the corrections are negligible. That is, the $\nabla^2 A$ term dominates over the $(\nabla A)^2$ term in the equation of motion, providing a mechanism to solve the 10d equations in the presence of the unsmeared, localized sources; while at the same time the correction to the effective potential is of order $(\nabla A)^2$, a subdominant effect. Here we are assuming that no special tuning or cancellations occur among the terms in the effective potential.

As mentioned above, a similar criterion applies to the p-form potential fields. The corrections to the effective potential are of order $|\nabla C_p|^2$ (as can be read directly from the ten-dimensional action (2.8)), while the equations of motion require nonzero $\nabla^2 C_p$.

2.4 dS_3 worked example

Our dS_3 construction builds up from the venerable D1-D5 system [14, 15] corresponding to an $AdS_3 \times S^3/\mathbb{Z}_k \times T^4$ near-horizon geometry (with the $\mathbb{Z}_k$ acting freely on the S^3). The freedom to take the orbifold order k large will be used to stabilize the internal curvature at a small value. Before analyzing the dS_3 construction in detail, we should point out that in our model the internal curvature and string coupling, though consistently small, cannot be taken to be parametrically small. Indeed, specific details of the internal geometry will be found to limit the order of k and the amount of flux that can be turned on in order to get a dS solution. Ongoing constructions in higher dimensions [40] suggest that this is not a general property of our approach.

To summarize the construction: we will first consider a nontrivial fibration – allowing the T^4 to vary its shape or size over the $S^3/\mathbb{Z}_k$ – as in [16, 41, 42, 43].

$$\begin{array}{rl} T^2 \times T^2 \to & \mathcal{Y}_7 \\ & \downarrow \\ & S^3/\mathbb{Z}_k \end{array} \tag{2.31}$$

This, together with a set of NS5-branes, will contribute positive curvature energy

and help to 'uplift' the negative potential energy of the $S^3/\mathbb{Z}_k$. We will then include orientifolds which produce an intermediate negative term in the potential. Fluxes corresponding to the color D1- and D5-branes contribute a third set of positive terms.

We begin by discussing these ingredients in detail in §2.4.1. In §2.4.2 we obtain the 3d effective potential and find a dS_3 solution with the radii and string coupling self-consistently stabilized. Other modes are included in §2.4.3 and §2.4.4, and the construction is analyzed from the 10d viewpoint in §2.4.5. In §2.4.6 we estimate the de Sitter entropy, and we end in §2.4.7 by commenting on other three-dimensional alternative examples.

2.4.1 Brane construction

Our construction requires ingredients which are collected in Table 2.1. We will shortly

	0	1	2	3	4	5	6	7	8	9
$D1$	x	x								
$D5$	x	x					x	x	x	x
$O5$	x	x		x	x				x	x
$O5'$	x	x	x			x	x	x		
$\rho 5$	x	x	x	x					x	x
$\rho 5'$	x	x			x	x	x	x		
NS5	x	x		x	x		x		x	
NS5$'$	x	x	x			x		x		x
$D7$, $\overline{D7}$	x	x	x	x	x	x		x	x	
$D7'$, $\overline{D7'}$	x	x	x	x	x	x	x			x

Table 2.1: Ingredients for the brane construction of dS_3

explain each of these ingredients. First let us describe the underlying geometry. The T^4 lies along the 6789 directions. The 2345 directions correspond to the radial and $S^3/\mathbb{Z}_k$ directions. As discussed above, the radial direction is compact due to the effects of flavor branes and curvature. The color D1 and D5 branes (and the corresponding antibranes) are then placed at the tips where $S^3/\mathbb{Z}_k$ vanishes. From the expression for the potential energy below, in the present construction these are conical singularities.

Let us denote $\phi_1 = x_2 + ix_3$, $\phi_2 = x_4 + ix_5$. We can realize the S^3 as a Hopf

fibration: $|\phi_1|^2 + |\phi_2|^2 = R^2$, with the fiber circle along the $\gamma \equiv \arg(\phi_1) + \arg(\phi_2)$ direction. The base $\mathbb{CP}^1$ of the Hopf fibration is given by gauging this direction. The $\mathbb{Z}_k$ orbifold acts as $(\phi_1, \phi_2) \to e^{2\pi i/k}(\phi_1, \phi_2)$, i.e. by a shift on γ. The scalar fields we must stabilize include the string coupling g_s, the sizes $R\sqrt{\alpha'}$, $R_f\sqrt{\alpha'}$ of the base and fiber of the $S^3/\mathbb{Z}_k$, and the size $L\sqrt{\alpha'}$ of the T^2 factors in the geometry. We will address these first. In general, we must consider all deformations of the 10d fields which are sourced by our ingredients to check if any are unstable. We will find that axions and anisotropic metric modes are either projected out or are stabilized by the dynamics of our model.

The ingredients are as follows:

• (1) a variation of the Kähler moduli $\rho = b_T + iL^2$ of each T^2 over the base $\mathbb{CP}^1$. Here $b_T \sim B_{67}L^2 = B_{89}L^2$ comes from the 67 and 89 components of the NS-NS two-form potential.

This introduces complex codimension-two branes, i.e. "stringy cosmic fivebranes" (SC5-branes), as was described in [42, 43]; ρ degenerates at points on the $\mathbb{CP}^1$ corresponding to the positions of these branes. In general, both the complex structure moduli τ and the complexified Kähler moduli ρ of the T^2 fibers could become singular, corresponding to two types of stringy cosmic fivebranes, which we shall call τ5- and ρ5-branes respectively. In the present construction, for simplicity we will use only ρ5-branes.

The set of ρ5-branes makes two important contributions to the potential energy. First, recall that a varying complex structure τ over the base $\mathbb{CP}^1$ subtracts from the scalar curvature. Since T-duality interchanges τ-fibrations with ρ-fibrations, the same holds for the ρ5-branes. A slightly more subtle effect is the following. Appropriate sets of (p,q) ρ5-branes set boundary conditions for $\rho = b_T + iL^2$ at their cores, fixing the size L of (and the axion b_T on) the corresponding T^2 fiber to be some value L_* (and b_*), usually of string scale. As we introduce other ingredients into our construction, they can cause the (averaged) size L of the T^2 fibers to increase, and the variation of

L (and b_T) results in extra gradient energy of order

$$\int_{\mathcal{Y}_7} d^7y\sqrt{g}\frac{|\nabla\rho|^2}{g_s^2\rho_2^2} \sim \frac{\hat{n}_\rho}{g_s^2R^2(\alpha')^{3/2}}\frac{L^4R^3}{k}\left(\left(\log\frac{L^2}{L_*^2}\right)^2+\frac{(b_T-b_*)^2}{L^4}\right) \tag{2.32}$$

deriving from the curvature of the fibration. We write $\hat{n}_\rho$ here to denote the number of stacks of coincident ρ5-branes which introduce a boundary condition. This is distinct from the total number of ρ5-branes. We will use the contribution from the gradient energy sourced by the ρ5-branes to help stabilize L.

To be specific, we will use the following ρ5-brane configuration. Let us describe it in terms of its T-dual, in order to provide a geometrical description in terms of a gauged linear sigma model (GLSM) [68]. For reasons which will become clear shortly, we will find it useful to consider branes which locally pin the elliptic fibers at an order one value in string units, using as few branes as possible to accomplish this. We take a (2,2)-supersymmetric GLSM with charges

Φ_1	Φ_2	X_1	Y_1	Z_1	P_1	X_2	Y_2	Z_2	P_2
0	0	2	3	1	-6	0	0	0	0
0	0	0	0	0	0	2	3	1	-6
6	6	0	0	-1	0	0	0	-1	0

(2.33)

under a $U(1)^3$ gauge symmetry. The D-terms take the form

$$\begin{gathered}\textstyle\sum_{j=1}^2(2|x_j|^2+3|y_j|^2+|z_j|^2-6|p_j|^2-\ell)^2 \\ +\left(6|\phi_1|^2+6|\phi_2|^2-|z_1|^2-|z_2|^2-\xi\right)^2\end{gathered} \tag{2.34}$$

Here the Fayet-Iliopoulos parameters correspond to size moduli $\xi\sim R^2$ and $\ell\sim L^2$.

We take a gauge-invariant superpotential of the form

$$\int d^2\theta\sum_{j=1}^2 P_j\left\{Y_j^2-X_j^3-Z_j^6g_j(\phi_1,\phi_2)-X_jZ_j^4f_j(\phi_1,\phi_2)\right\} \tag{2.35}$$

with $g_1=\phi_1$, $g_2=\phi_2$ of degree 1 and $f_j=0$ in order to respect the gauge invariances

(2.33). This gives the T^2 fibrations as the vanishing loci of Weierstrass polynomials of the form

$$y_j^2 - x_j^3 - z_j^6 g_j(\phi) - x_j z_j^4 f_j(\phi) = 0 \ , \text{ for } j = 1, 2 \, .$$

Each T^2 degenerates over a codimension 2 surface, $\phi_1 = 0$ or $\phi_2 = 0$ respectively. These each correspond to singularities with fixed $\rho \to e^{i\pi/3}$. Since $f = 0$ everywhere, the fibration has constant

$$\rho = \rho_* = j^{-1}(0) = e^{i\pi/3}$$

everywhere, not just at these special points where the ρ5-branes sit. In our complete construction, other ingredients will source ρ, and deviations from the constant value ρ_* will cost gradient energy (2.32).

So far, the two T^2s vary over a base $\mathbb{CP}^1$ with homogeneous coordinates ϕ_1 and ϕ_2. In this model as it stands, there is a (spacetime supersymmetric) $\mathbb{Z}_6$ orbifold singularity at $z_1 = z_2 = 0$ descending from the third $U(1)$ gauge symmetry in the table (2.33).

In our model of interest (2.31), the base is not in fact $\mathbb{CP}^1$; it is instead a $\mathbb{Z}_k$ orbifold of a Hopf fibration over this $\mathbb{CP}^1$, a Lens space. In the GLSM, the third $U(1)$ gauge transformation parameterizes the Hopf fiber. For our purposes, we need the model obtained by reducing this continuous gauge identification to a $\mathbb{Z}_k$ identification.

As in [16] we can obtain the elliptic fibration over S^3 (including the Hopf fiber) as the base of a cone. We introduce the radial direction of this cone along with the Hopf fiber by adding another chiral field Φ_0 to the GLSM, assigning Φ_0 charge -10 under the third $U(1)$. (We insist here that the sum of charges cancel, producing a non-compact Calabi-Yau fourfold, in order to preserve SUSY among the ρ5-branes.) In order to incorporate the $\mathbb{Z}_k$ orbifold we also mod out by

$$(\phi_1, \phi_2, z_1, z_2) \to (\alpha^6 \phi_1, \alpha^6 \phi_2, \alpha^{-1} z_1, \alpha^{-1} z_2)$$

where $\alpha = e^{2\pi i/k}$ (with the other fields invariant).

From the vanishing of the discriminant $\Delta = 27g^2 + 4f^3$, this model introduces $n_\rho = 4$ ρ5-branes, significantly fewer than the 24 which would fully cancel the curvature of

the $\mathbb{CP}^1$. This agrees with the fact that beta function for the Fayet-Iliopoulos (FI) parameter $R^2 \sim \xi$ describing the size of the base is $(12-2)/12 = 20/24$ times what it would be in the absence of the nontrivial fibration. (This beta function is proportional to the curvature; in the GLSM it is proportional to the sum of the charges of the fields under the $U(1)$ gauge symmetry corresponding to this FI parameter.) In this model, the number of defects itself is 2; i.e. $\hat{n}_\rho = 2$ in (2.32). We will use these numbers for definiteness in our analysis.

Since we do not require the fibration to nearly cancel the curvature, the singularities analyzed in [16] do not arise. A priori we do not require a hierarchy between the dS and internal curvatures in order to study conceptual questions about de Sitter holography; however, we will obtain such a hierarchy in our explicit construction below for somewhat different reasons from those in [16].

The additional ingredients are as follows:

• (2) N_{D5} units of RR F_3 flux on the $S^3/\mathbb{Z}_k$, and N_{D1} units of RR F_7 flux on $\mathcal{Y}_7$ (2.31).

• (3) An orientifold five-plane wrapped on an unorbifolded S^1 in $S^3/\mathbb{Z}_k$ times one T^2. The O5-plane acts as an orientation reversal combined with a reflection on the other T^2 and on two of the directions of the $S^3/\mathbb{Z}_k$. We include a second O5-plane on an orthogonal S^1 and the other T^2. Note that the orbifold enhances the effect of the orientifold planes relative to the ρ5-branes and other sources which wrap the fiber circle. In general in de Sitter model building, one needs a negative intermediate term in the potential which competes with the leading term. This requires the ratio of their coefficients to be large; in our case this ratio is given effectively by k.

In terms of the elliptic fibration given above, the orientifold projection acts as $\phi_1 \to \mp\overline{\phi}_1$, $\phi_2 \to \pm\overline{\phi}_2$, and x_j, y_j, z_j, and P_j are also projected to their conjugates.

It is interesting to study this effect – that orientifolds counteract positive energy sources – in a ten dimensional description. The O5 metric, at distances large compared to the string scale, looks like

$$ds^2 = (1-(\alpha' g_s/r^2))^{-1/2}(-dt^2+dx_\parallel^2) + (1-(\alpha' g_s/r^2))^{1/2} dx_\perp^2 \tag{2.36}$$

The O-planes contract the space around them, more strongly so near the object. Now consider starting from a metric with a deficit angle induced by a stringy cosmic brane, and orientifold it. The contraction induced by the O5 will have a more pronounced effect near its core than farther away, since the effect dies off at large r away from the O5. This reduces the deficit angle.

• (4) An NS5-brane wrapped on an unorbifolded S^1 in $S^3/\mathbb{Z}_k$ and stretched along a one-cycle of each T^2. Include another one wrapped on orthogonal directions. For future convenience, we will take these branes to wrap along the orientifold loci in the base $\mathbb{CP}^1$, which has the effect of reducing the NS5-brane tensions and of projecting out their slippage modes. An important issue which we will address below is the backreaction of these NS5-branes. In our ultimate construction below we will ensure that their core sizes are significantly smaller than the base radius.

• (5) Dp-branes and anti-Dp-branes: to begin with, we will consider a D7-brane wrapped on $S^3/\mathbb{Z}_k$ and stretched along a one-cycle of each T^2, and an anti D7-brane wrapped on the same cycle but in a different discrete Wilson line vacuum. Include also another such pair wrapping the other cycle of each T^2. We put each anti-brane in a nontrivial discrete Wilson line vacuum in order to prevent perturbative brane-antibrane annihilation, as we will explain in §2.4.3. In order to decrease the curvature of the base B_n, we will find that a simple variant with D5-branes replacing the D7-branes is advantageous. We will discuss this below in section §2.4.7 after working through the D7-brane version of the model.

These ingredients all together break supersymmetry. However, pairwise many preserve supersymmetry and hence do not attract or repel to leading order. As in the standard AdS_3 model, the D1-D5 color branes are replaced by fluxes in the solution. In particular, all the other ingredients are pairwise mutually supersymmetric except the $D7$-$\overline{D7}$ pair, whose stability we will explain in detail below.

2.4.2 Stabilization mechanism

To begin with, we will write down a naïve 3d effective potential obtained by averaging each source over the compact directions. This procedure ignores warping which

develops as a result of the varying degree of localization of the sources in the internal dimensions [65, 66, 67]. We will show this to be a self-consistent approximation by analyzing the form of the equations determining the warp factor, finding that the warping necessary to solve the 10d equations of motion contributes a subdominant term to the 3d potential energy (as discussed in general terms in §2.3.3). In essence, we find that the stabilized values of the coupling and inverse radii are small enough to justify our expressions for the stress energy contributed by the various ingredients we have listed.

We denote the radii of the base and fiber of the $S^3/\mathbb{Z}_k$ in string units by R and R_f, so that the volume of $S^3/\mathbb{Z}_k$ is $2\pi^2 R^2 R_f$. Below we find $R_f \sim R/k$. Note that the curvature radius of $S^3/\mathbb{Z}_k$ is R. The radii of the T^4 are denoted by L_6, L_7, L_8, and L_9 with $L_6 L_7 L_8 L_9 \equiv L^4$. We also need to consider the field $b_T \sim L^2 B_{67} = L^2 B_{89}$ sourced by the ρ5-branes. Define

$$\tilde{\eta} \equiv \frac{g_s}{R^2 L^2}\,, \quad \beta \equiv \frac{k R_f}{R}\,. \tag{2.37}$$

We find it more convenient to work with the combination $\tilde{\eta}$ instead of the variable $\eta = k\tilde{\eta}^2/\beta$ defined in (2.19). Transforming to $3d$ Einstein frame as in (2.16), we obtain

$$\begin{aligned}\mathcal{U} \approx & 16 M_3^3 k^3 \left\{ \left(4\pi^2 - \frac{2\pi^2}{3\beta^2} \left[24 - n_\rho - \hat{n}_\rho \left(\left(\log \frac{L^2}{L_*^2} \right)^2 + \frac{(b_T - b_*)^2}{L^4} \right) \right] + \frac{\pi k n_{NS5}}{L^2 \beta^3} \right) \frac{\tilde{\eta}^4}{k} \right. \\ & \left. - \left(2\pi R^2 - \frac{n_{D7} R^4 \beta}{2k} \right) \frac{\tilde{\eta}^5}{\beta^3} + 4\pi^2 \left(N_{D5}^2 L^4 + \frac{(N_{D1} + b_T^2 N_{D5})^2}{L^4} + 2 b_T^2 N_{D5}^2 \right) \frac{k\tilde{\eta}^6}{\beta^4} \right\}\end{aligned} \tag{2.38}$$

Here M_3 is the reduced Planck mass. The first term is the metric flux contribution from the Hopf fibration over $\mathbb{CP}^1$, and the second term (i.e. the square bracket) represents the net curvature introduced by the elliptic fibration (2.4), with the presence of ρ5-branes. The boundary values L_* and b_* are determined from the GLSM as

$$\rho_* = b_* + i L_*^2 = e^{i\pi/3}\,.$$

The third contribution to $\tilde{\eta}^4$ comes from the tension of NS5-branes.

The $\tilde{\eta}^5$ term receives a negative contribution from the O5-planes, plus a positive term from the D7- and anti D7-branes. For the RR flux contributions we have three terms, the first coming from $|F_3|^2$, the second from $|F_7+\frac{1}{2}B_2\wedge B_2\wedge F_3|^2$ (which can be understood by T-dualizing the type IIA coupling $|F_4+\frac{1}{2}B_2\wedge B_2\wedge F_0|^2$ three times), and the final term from $|B_2\wedge F_3|^2$ (since we do not have F_5 in our construction).[7]

We have included numerical factors such as 2π, according to

$$T_p = \frac{1}{(2\pi)^p g_s \alpha'^{(p+1)/2}}\ ,\ 2\kappa_{10}^2 = (2\pi)^7\alpha'^4\,,$$

and the quantization of the p-form fluxes

$$\frac{1}{(2\pi\sqrt{\alpha'})^{p-1}}\int_{\Sigma_p} F_p \in \mathbb{Z}\,.$$

In this expression for the potential, and elsewhere, we have set $\alpha'=1$ for simplicity. The various sets of flavor branes including the elliptic fibration, and the orientifolds, are supersymmetric in themselves and also pairwise supersymmetric with each other. As a result, their contributions to the potential are well approximated by their underlying BPS tension formulae. Not all factors are known precisely, however; for example the term proportional to $\log(L^2)$ is an approximation of the gradient term (2.32) by $\nabla^2 \to \frac{2}{3R^2}$ which we believe to be a reasonable estimate up to factors close to one (based on computations with trial sinusoidal wavefunctions).

We have included the effect of the orientifolds as well as the $\mathbb{Z}_k$ projection in reducing the volume, but we do not know the precise internal geometry taking into account the effects of all the ingredients. In our best controlled examples below, we will find that starting from the above expression for the potential energy, the curvature

[7] We should point out that although naïvely the zero modes from B_{67} and B_{89} would be projected out by the orientifolds, a nonzero expectation value $b_*\neq 0$ is allowed because $\rho_* = e^{i\pi/3}$, $e^{2\pi i/3}$ are related by a modular transformation. As explained around (2.32), the fluctuation $b_T \sim L^2 B_{67} = L^2 B_{89}$ away from b_* has nontrivial dependence along the internal directions, so it does not correspond to a zero mode. Physically, this variation is sourced by a competition between $\rho 5$ branes and RR fluxes. With these caveats, we will sometimes refer to b_T as an "axion"; however, it should not be confused with the B_2 zero modes analyzed below in §2.4.4.

in string units, $\mathcal{R}\alpha'$, comes out to be of order 10^{-3} (with other examples giving $\mathcal{R}\alpha' \sim 10^{-2}$ or 10^{-1} depending on the details of the Dp-branes used in the construction). For this reason, although we will not obtain parametrically large radii, we expect corrections to be reasonably small. Because we will tune the de Sitter cosmological constant to be somewhat smaller than the internal curvature scale, $\mathcal{O}(\alpha')$ corrections can affect the depth of the de Sitter minimum. However, since the individual terms in the potential are much larger than this, these effects should only shift the stabilized values of the moduli by a small amount.

At this point it may be useful to emphasize an important distinction between curvature radii and size moduli. The curvature of our internal dimensions goes like $1/R^2$, but does not get large when the radii R_f and L of the Hopf and elliptic fibrations become small. These can (and will) be closer to the string scale than R without driving up the curvature and resulting α' corrections.

The potential (2.38) has the form

$$\mathcal{U} \sim M_3^3(a\tilde{\eta}^4 - b\tilde{\eta}^5 + c\tilde{\eta}^6) \tag{2.39}$$

which allows us to use the 'abc' technique in [50] to stabilize the moduli. We first minimize $4ac/b^2$ as a function of all other moduli besides $\tilde{\eta}$ –see discussion around (2.26). If we can use discrete quantum numbers to tune the minimal value of $4ac/b^2$ to be close to but slightly greater than 1, the potential (2.39) will have a de Sitter minimum with $\tilde{\eta}$ stabilized near

$$\tilde{\eta} \approx \frac{2a}{b} \approx \frac{b}{2c}\,. \tag{2.40}$$

The only R dependence of the potential comes from the coefficient b, so we can easily minimize it with respect to R at

$$R^2 = \frac{2\pi k}{n_{D7}\beta}\,. \tag{2.41}$$

After that the middle term is reduced to $-2\pi^2 k\tilde{\eta}^5/(n_{D7}\beta^4)$ and $4ac/b^2$ becomes

$$\frac{4ac}{b^2} = \frac{16n_{D7}^2}{k^2}\left\{\beta^4 - \frac{1}{6}\left[24 - n_\rho - \hat{n}_\rho\left(\left(\log\frac{L^2}{L_*^2}\right)^2 + \frac{(b_T - b_*)^2}{L^4}\right)\right]\beta^2 + \frac{kn_{NS5}}{4\pi L^2}\beta\right\} \times\left(N_{D5}^2 L^4 + \frac{(N_{D1} + b_T^2 N_{D5})^2}{L^4} + 2b_T^2 N_{D5}^2\right) \tag{2.42}$$

Let us focus next on the stabilization of β. This follows from the factor in curly brackets, which has a three-term structure analogous to (2.39):

$$\{\dots\} \equiv \tilde{a}\beta - \tilde{b}\beta^2 + \beta^4 \tag{2.43}$$

where

$$\tilde{a} = \frac{kn_{NS5}}{4\pi L^2}\ ,\ \tilde{b} = \frac{1}{6}\left[24 - n_\rho - \hat{n}_\rho\left(\left(\log\frac{L^2}{L_*^2}\right)^2 + \frac{(b_T - b_*)^2}{L^4}\right)\right] \tag{2.44}$$

In this case, if we can minimize $\tilde{a}^2/\tilde{b}^3$ with respect to L and b_T at

$$\frac{\tilde{a}^2}{\tilde{b}^3} = \frac{4}{27} + \epsilon, \tag{2.45}$$

with a small positive ϵ (analogously to $1 \lesssim 4ac/b^2$), then we can minimize $\{\dots\}$ with respect to β at a positive small value of $\{\dots\}$,

$$\{\dots\} = \frac{3}{4}\tilde{b}^2\epsilon\ \ ,\ \ \beta = \sqrt{\frac{\tilde{b}}{3}}\left(1 - \frac{9}{8}\epsilon\right)\ . \tag{2.46}$$

This will in turn help us to tune $4ac/b^2$ to be slightly larger than 1 and will give a parametrically small string coupling.

Minimizing $\tilde{a}^2/\tilde{b}^3$ with respect to the axion b_T gives $b_T = b_*$. The RR flux contributions to the potential want to push b_T to 0 but as long as ϵ is small they are subdominant and only cause a small deviation away from $b_T \approx b_*$. Therefore $\tilde{b}$ is

reduced to $\frac{1}{6}[24 - n_\rho - \hat{n}_\rho(\log(L^2/L_*^2))^2]$. Minimizing $\tilde{a}^2/\tilde{b}^3$ respect to L^2 requires

$$24 - n_\rho - \hat{n}_\rho \left(\log \frac{L^2}{L_*^2}\right)^2 = 3\hat{n}_\rho \log \frac{L^2}{L_*^2} \tag{2.47}$$

which we would like to satisfy with a large (though limited) L. This relation determines L, and then Eq. (2.45) fixes kn_{NS5},

$$kn_{NS5} = \frac{4\pi}{3}\beta\hat{n}_\rho \left(\log \frac{L^2}{L_*^2}\right) L^2 + \mathcal{O}(\epsilon)\,. \tag{2.48}$$

Therefore, the order of the orbifold is limited by L.

An explicit example of an appropriate ρ fibration was given above, with $n_\rho = 4$ and $\hat{n}_\rho = 2$. With these numbers, we find $L = 2.5$ and $kn_{NS5} = 88$; this gives $\epsilon = 0.0016$.

Before going on, let us note that in order to minimize $4ac/b^2$ with respect to L (and requiring (2.48)), it is enough to take

$$L^2 = \sqrt{\frac{N_{D1}}{N_{D5}} + b_*^2}. \tag{2.49}$$

This is also the scaling of the D1-D5 AdS solution. However, this is not strictly necessary, because deviations from this equality produce a tadpole from the flux factor that is suppressed by ϵ as compared to the mass squared responsible for the first equality. Such a contribution then causes only a small deviation from the solution (2.47). For simplicity, though, in the formulas below we specialize to the scaling $L^4 \sim N_{D1}/N_{D5}$.

Altogether we obtain (dropping numerical factors)

$$\frac{4ac}{b^2} \sim \frac{n_{D7}^2}{k^2}\left[24 - n_\rho - \hat{n}_{\rho 5}(\log(L^2/L_*^2))^2\right]^2 \epsilon N_{D1}N_{D5} \sim 1. \tag{2.50}$$

Setting $n_{NS5} \sim n_{D7} \sim 1$, Eq. (2.45) implies that parametrically $k \sim L^2 \approx \sqrt{N_{D1}/N_{D5}}$, and (2.50) reduces to $N_{D5} \sim 1/\sqrt{\epsilon}$, which gives large N_{D5} and even larger N_{D1}. With them it should be possible to tune $4ac/b^2$ to be close to but slightly greater than

1. After minimizing $4ac/b^2$ we find a de Sitter minimum at $\tilde{\eta} \approx 2a/b \sim \epsilon/k^2$. The moduli and dS radius scale as follows with the parameters:

$$R_f \sim \frac{R}{k}, \quad R^2 \sim L^2 \sim k \sim \sqrt{\frac{N_{D1}}{N_{D5}}}, \quad N_{D5} \sim \sqrt{\frac{1}{\epsilon}}, \quad g_s \sim \epsilon, \quad R_{dS}^2 \sim \frac{R^2}{\epsilon} \tag{2.51}$$

Note that we have obtained large radius and weak string coupling, thanks to the small ϵ. From eq. (2.29), tuning $a \propto \epsilon$ to be small also produces a hierarchy $R_{dS} \gg R$. So our model features parametrically small internal dimensions (compared to the dS scale), giving a gap between 3d moduli and internal KK excitations.

Importantly, the size of L is limited by (2.47). The fact that this relation is logarithmic helps drive up the value of L, but it is limited by the size of the other terms; as mentioned above we take the minimal values we can obtain for n_ρ and $\hat{n}_\rho$.

Numerical example

We can check this numerically for the potential estimated above, and the results are summarized in Table 2.2. Here $n_{NS5} = 2$ and $n_{D7} = 4$ are the fewest number of

Input data	
n_ρ	4
$\hat{n}_\rho$	2
ρ_*	$\exp(i\pi/3)$
n_{NS5}	2
n_{D7}	4
k	44
N_{D1}	156
N_{D5}	5

Stabilized moduli	
R	9.2
kR_f	7.5
L	2.5
b_T	0.48
g_s	0.02
ϵ	0.002
$4ac/b^2$	1.003

Table 2.2: Numerical example for a dS_3 solution

branes required for the setup to have the necessary symmetries in the T^4 directions. As can be seen from the above tables, our initial data fix the moduli in a de Sitter minimum. The axion is stabilized at $b_T = 0.48$ very close to $b_* = 0.5$.

Comparing these numbers to the parametrics above, we see that numerical prefactors break the parametric degeneracy between L and R; also, N_{D5} is somewhat

smaller than expected, but nevertheless $g_s \ll 1$. The relation $L^2 = \sqrt{N_{D1}/N_{D5}}$ has not been enforced exactly, but this is a small effect since the contribution of the corresponding tadpole will be suppressed by $\mathcal{O}(\epsilon)$. The primary use of the flux quantum numbers N_{D1} and N_{D5} was not to fix L, as might be supposed from the form of the effective potential, but to keep $4ac/b^2$ within the allowed range. Interestingly, it is even possible to stabilize all moduli without color fivebranes as long as $\epsilon \ll 1$. In particular we find a dS minimum with $N_{D1} = 262$, $N_{D5} = 0$, and all other parameters approximately as above. We will comment further on this possibility when we discuss the scaling of the entropy.

It is worth commenting on the size of ϵ, since taking $\epsilon \ll 1$ is responsible for achieving a weak string coupling and also boosts the number of degrees of freedom. In particular, in three-term stabilization mechanisms (as opposed to the two-term Freund-Rubin mechanism), there is a priori extra freedom to tune the (A)dS radius large. Our ability to tune ϵ small is limited by the size of the large quantum numbers in the problem. We can express this in terms of $k \sim L^2$ (which is limited by (2.47)). For example, if we shift $k \to k+1$, we shift (2.45) and hence ϵ by $\sim kN_{D5}/N_{D1} \sim 1/k$. Shifting N_{D1} by one would seem to shift ϵ by an amount of order $1/N_{D1}$, however, this effect is suppressed by ϵ and the effect of changing N_{D1} is negligible when ϵ is small.

The mass matrix is positive definite for the input data and the stabilized values found above, and yields masses of order $1/R$ and $\sqrt{\epsilon}/R$. This follows from the fact that the canonically normalized fields are $\sigma_R \equiv M_3^{1/2} \log R, \sigma_L \equiv M_3^{1/2} \log L, \Phi \equiv M_3^{1/2} \log g_s$ and $\sigma_f \equiv M_3^{1/2} \log R_f$. Differentiating $\mathcal{U}$ twice with respect to each σ yields contributions of the order of a typical term in $\mathcal{U}/M_3$ which sources it; this is of order $1/R^2$ for the moduli σ_f and σ_L, and of order ϵ/R for σ_R and Φ. To the extent that we tune the de Sitter minima to be smaller than the height of the moduli barriers, these masses are larger than the de Sitter Hubble scale, and for $\epsilon \ll 1$, the masses of σ_L, σ_f are parametrically larger. For the numbers given above, the smallest of the masses is about one order of magnitude above the Hubble scale.

Higher order corrections

Finally, let us consider α' and quantum corrections. Quantum effects are controlled by $g_s^2 \sim \epsilon$, and are further suppressed by the KK scale $1/R^2$ (they have to vanish in the limit in which supersymmetry is restored). These can therefore be safely ignored.

On the other hand, a slightly conservative estimate for the size of the $\mathcal{O}(\alpha')$ corrections to the GLSM is given by the curvature

$$\alpha' \mathcal{R} \sim \frac{8}{R^2} \sim 0.1 \tag{2.52}$$

in the example above. The factor of 8 comes from relating the $\mathbb{CP}^1$ and S^3 radii. This is on the edge of control, since we do not understand all $\mathcal{O}(1)$ factors arising from the backreacted geometry and from the gradient energy terms. Such corrections will not affect the moduli stabilization barriers, which are not suppressed by ϵ, but can alter the stabilized value of the Hubble scale.

Strictly speaking, when studying the numerics for the case of small ϵ we must start with the corrected effective potential to leading order in $\mathcal{O}(\alpha')$ and then tune k to find ϵ small and positive, of order $\gtrsim 1/k$. We stress once again that the numerics quoted in our example are meant to illustrate the stabilization procedure but are not to be taken as exact. However, metastable de Sitter solutions from our effective potential are quite generic, and we expect the exact solution to be not qualitatively different. Moreover, at the end of the section we present a simple way of pushing the curvature to significantly smaller values, by replacing the flavor D7-branes by flavor D5-branes.

2.4.3 $D7$-$\overline{D7}$ stability analysis

Let us now elaborate on the stability of the D7- and anti D7-brane pairs, ingredient (5) above. These wrap a T^2 fiber and the full $S^3/\mathbb{Z}_k$. The latter introduces fractional Wilson line vacua. There are k distinct Wilson line vacua (i.e. non-gauge-equivalent

flat connections)

$$\left(e^{i\int_{fiber}A}\right)^k = 1 \quad \Rightarrow \quad \int_{fiber} A = \frac{2\pi n}{k}\ , \quad n = 0, \ldots, k-1. \tag{2.53}$$

Explicit expressions for these vacua on a Lens space $S^3/\mathbb{Z}_k$ were given in e.g. [69]. Let us put the D7-branes in their $n = 0$ vacuum and the anti D7-branes in a vacuum with $n \sim k/2$. We must assess potential instabilities of this configuration from brane-antibrane strings (assessing whether there is a tachyon), and from gauge field modes. Because the fiber circle is small, for some purposes it is useful to analyze this in a T-dual description.

One can see by periodicity of the gauge field or by T-duality that the size of the circle seen by the Wilson lines is of order

$$\tilde{R}_f \sim \frac{1}{R_f} \sim \frac{k}{R} \sim \sqrt{k} \tag{2.54}$$

where in the last two relations we used our stabilization mechanism (2.51). This circle being much larger than string scale, the brane and antibrane are separated by a parametrically large distance even if they sit at the same position on the transverse T^2.

Next let us analyze the Wilson lines for potential instabilities. Because the Wilson line vacua are discrete, there is a positive contribution to the mass squared in varying away from the corresponding flat connection. This scales like the square of the field strength. Since $F \sim \delta A/R$ (R being the size of the space transverse to the fiber circle), this mass squared goes like $1/R^2$.

There is also a negative contribution to the mass squared from the attraction of the brane and antibrane. This can perhaps be seen and estimated most easily in a T-dual description, with an inverted circle radius (2.54) and a T-dual string coupling $\tilde{g}_s \sim g_s/R_f \sim g_s k/R$. The (anti) D7-branes are turned into (anti) D6-branes, wrapping the base $\mathbb{CP}^1$ times the T^2 and sitting in diametrically opposite positions on the dual circle. The attractive potential between each brane/antibrane

pair is (using the scaling $\tilde{R}_f \sim \sqrt{k} \sim R$)

$$\mathcal{U}_{7\bar{7}} \sim -M_3^3 \left(\frac{g_s^2}{R^2 R_f L^4}\right)^3 \left(\tilde{g}_s^2 \times \frac{1}{\tilde{g}_s^2} \times R^2 L^2\right) \sum_{n_1,n_2,n_3=-\infty}^{\infty} \frac{1}{|\vec{x} - \vec{n}R|}. \tag{2.55}$$

The first factor here is the usual Einstein frame conversion factor, the $\tilde{g}_s^2$ is the 10d Newton's constant in the T-dual frame, the $1/\tilde{g}_s^2$ is the product of tensions, the $R^2 L^2$ is the volume over which the D6-branes are wrapped, and the last factor is the codimension 3 potential. The sum over $\vec{n} = (n_1, n_2, n_3)$ represents the compactification; we can work on the covering space with a periodic array of localized sources, and then later project by translations in order to compactify.

This potential gives a negative mass squared to the attraction mode between the brane and antibrane pair. Expanding around $x \sim R/2$, we get

$$\mathcal{U}_{7\bar{7}} \sim -M_3^3 \left(\frac{g_s^2}{R^2 R_f L^4}\right)^3 \frac{L^2}{R} \left(x - \frac{R}{2}\right)^2. \tag{2.56}$$

Switching to a canonically normalized kinetic term $\mathcal{L}_{kin} \sim R^2 L^2 \dot{x}^2/\tilde{g}_s \sim \dot{\phi}^2$, we get the negative contribution to the mass squared from the attraction of the brane and antibrane pair:

$$\delta m^2 \sim -M_3^3 \left(\frac{g_s^2}{R^2 R_f L^4}\right)^3 \frac{L^2}{R} \frac{\tilde{g}_s}{L^2 R^2} \sim -\frac{g_s}{R^2}. \tag{2.57}$$

Although this is parametrically of the same order of magnitude as the Hubble scale (remember that the Hubble scale is tuned), it is parametrically smaller than the positive mass squared arising in deformation away from a flat connection. This mode is therefore perturbatively stable.

2.4.4 Stabilizing other moduli

So far we have addressed R, R_f, L, b_T, g_s and the $D7$-$\overline{D7}$ stability. In this section we will address the other possibly light directions in scalar field space. In order to holographically formulate inflationary spacetimes, we must require that all modes be lifted, or if tachyonic that the tachyonic mass be much smaller than the de Sitter

Hubble scale.

Axions

First, there are potentially light scalars arising as axions from the RR forms and from the B-field. The zero modes surviving the orientifold projection are

$$\begin{aligned} C_2 &= c_1\, dx^6 \wedge dx^7 + c_2\, dx^8 \wedge dx^9 \\ B_2 &= b_1\, dx^7 \wedge dx^8 + b_2\, dx^6 \wedge dx^9 + b_3\, dx^6 \wedge dx^8 + b_4\, dx^7 \wedge dx^9\,. \end{aligned} \tag{2.58}$$

The zero modes from C_0, B_{67} and B_{89} are projected out by the orientifold action. (Recall that the field $b_T \sim L^2 B_{67} = L^2 B_{89}$ analyzed before varies along the internal dimensions, so it does not correspond to a zero mode; see discussion around Eq. (2.32)). Finally, the scalars from C_4 threading nontrivial cycles are projected out by the orientifold action.

We have analyzed the dependence of the potential energy of these modes coming from fluxes and from the wrapped D-branes, finding a positive mass matrix for our parameters. This follows more simply by noting first that the underlying D1-D5 AdS/CFT system has no tachyons (even allowed tachyons) from axions. The additional ingredients which uplift the system to de Sitter do not render their mass matrix tachyonic. The orientifolds as just noted project out some modes. The Dp-branes contribute positive masses to Neveu-Schwarz axions along their worldvolumes; similarly, NS5-branes would contribute positively to the mass squareds for RR axions, though in any case those along the NS5-brane worldvolumes are projected out by the O-planes. The stabilization of L works slightly differently in the de Sitter case as compared to AdS. This affects the mass matrix for the b axions, but in a way that yields a positive mass squared solution for appropriate values of N_{D1}/N_{D5}, including those of our numerical examples.

The ρ fibration contributes a subtle effect lifting C_2, as follows. S-dualizing the $|\tilde{F}_7|^2$ term described above and integrating by parts gives a term proportional to $|B_2 \wedge C_2 \wedge F_3|^2$.[8] The combined effect of F_3 flux through the base $S^3/\mathbb{Z}_k$ and $B_2 =$

[8] See e.g. [70]. The expressions for $\tilde{F}_7$ and $\tilde{H}_7$ can be understood by using S- and T-duality and

$b_*(dx^6 \wedge dx^7 + dx^8 \wedge dx^9)$ produced by the $\rho 5$ branes gives positive mass terms to both c_1 and c_2 in (2.58).

Moduli of the elliptic fibration and NS5-branes

The moduli of the elliptic fibration are flat to leading order since they come from superpotential terms in a (2,2) sigma model. In the explicit model given above with linear polynomials $g^{(j)}(\phi)$, there is only one such deformation.

The NS5-branes wrap contractible cycles in the base $\mathbb{CP}^1$ and could possess slippage modes if they were not wrapped on the orientifold loci in these directions. In this case the NS5-branes are frozen in place by the orientifold action. It can be checked that the full solitonic field configuration corresponding to the NS5-brane is compatible with the orientifold action; the compatibility condition is equivalent to the condition that these ingredients be mutually supersymmetric.

Anisotropic deformations

The setup in Table 2.1 is rather symmetric, and the potential is automatically extremized with respect to directions that break the symmetry. However, we must ensure that such directions are not too tachyonic. It is energetically favorable for orientifolds to wrap larger cycles. Because of this, the O5 and O5$'$ contribute negatively to the mass squared for anisotropies of the tori. However, the $\rho 5$-branes and NS5-branes contribute positively to the mass squared of these modes. The quantity $4ac/b^2$ (2.42) is deformed in the following way by these contributions

$$\frac{4ac}{b^2} \propto \frac{\epsilon \tilde{b}^2 + \gamma_1 \phi^2}{b_0^2 + \gamma_2 \phi^2} \tag{2.59}$$

where γ_1 and γ_2 are positive quantities which do not scale down with ϵ. The γ_2 term comes from the orientifold. The tachyonic mass squared that it imparts is suppressed by the power of ϵ in the numerator. There is no such suppression of the positive mass squared from the $\rho 5$s or NS5s. So the net effect is a positive mass squared for these

from the anomalous D-brane couplings $S_{WZ} = \int e^B \wedge \sum_p C_p$.

anisotropic modes.[9]

However, anisotropies of the base are more subtle. The O-planes that we have prescribed can elongate without breaking any of the symmetry. To see this, we can coordinatize the S^3 as follows. Set $\tilde{\phi}_1 \equiv x_3 + ix_4 \equiv \rho_1 e^{i\gamma_1}, \tilde{\phi}_2 \equiv x_2 + ix_5 \equiv \rho_2 e^{i\gamma_2}$. The round S^3 metric is

$$ds^2 = |d\tilde{\phi}_1|^2 + |d\tilde{\phi}_2|^2 = d\rho_1^2 + \rho_1^2 d\gamma_1^2 + d\rho_2^2 + \rho_2^2 d\gamma_2^2 \tag{2.60}$$

with $\rho_1^2 + \rho_2^2 = R^2$. Using this latter relation, we can set $\rho_1 = R\sin\kappa, \rho_2 = R\cos\kappa$ with $0 \leq \kappa \leq \pi/2$. This gives metric

$$ds^2 = d\kappa^2 + \sin^2\kappa d\gamma_1^2 + \cos^2\kappa d\gamma_2^2 \tag{2.61}$$

The O5 lies along γ_1 at $\kappa = 0$, while the O5′ lies along γ_2 at $\kappa = \pi/2$. It is possible to shrink the κ direction without breaking any of the symmetry, elongating the γ directions to maintain constant volume. Therefore, the O-planes alone produce a tadpole in this direction.

However, because of the tuning down of ϵ above, the NS5-branes and ρ5-branes each contribute more to the forces in the problem. Indeed, while the O-planes compete against the net term $\{\dots\} \propto \epsilon \ll 1$ above (2.43), NS5-branes and ρ5-branes contribute larger, individual contributions to $\{\dots\}$. The NS5-branes push oppositely to the orientifold planes. The ρ5-branes stretch in the κ direction, so the combined effects of the ρ5-branes and NS5-branes together stabilize this direction.

2.4.5 Localization of sources and the warp factor

After having found a consistent solution in the 3d effective theory, we should analyze the ten dimensional consistency of the construction. Following the discussion in §2.3.3, let us argue that the localization of the sources will not appreciably change

[9]The mode $L_{78}^2 \neq L_{69}^2$ is a special case: the only contribution is a positive mass term from D7-branes. The energy of the other ingredients (NS5s, ρ5s and orientifolds) is independent of this field. In the case where the D7-branes are replaced by flavor D5s wrapping $S^3/\mathbb{Z}_k$, this direction becomes flat at the classical level.

the potential (2.38), though it requires taking into account a slowly varying warp factor.

In the effective 3d theory (2.38) the localized sources (for instance O5 planes) play off against fluxes and net negative internal curvature to stabilize the moduli. Since these are not delta-function localized at the positions of the O5-planes, solving the 10d EOMs pointwise requires a warp factor e^A multiplying the $(A)dS_3$ metric which varies over the internal dimensions [65, 66, 67]:

$$ds^2 = e^{2A(y)} ds^2_{AdS_3} + e^{-2A(y)} \tilde{g}_{ij} dy^i dy^j \tag{2.62}$$

Recall from the discussion around (2.30) that if the equation for the warp factor can be solved (by having nonzero $\nabla^2 A$) with $A \ll 1$, then the corrections to the effective potential are negligible since they are of order $(\nabla A)^2/\kappa^2$. This provides a mechanism for solving the 10d equations in the presence of localized sources while keeping corrections to the potential subdominant. Therefore, let us check that in the present construction the condition $A \ll 1$ holds away from the cores of the localized sources (whose tensions already take the cores into account).

First consider the O5-planes as a source for A. Note that the fiber circle being small, these effectively wrap a T-dual circle of size $\tilde{R}_f \sim 1/R_f$; there are three directions $\vec{y}_\perp$ transverse to the O5s. Schematically we have

$$\nabla^2 A(\vec{y}_\perp) \sim \frac{1}{g_s} \frac{1}{R_f} g_s^2 \sum_{n_R, n_1, n_2} \delta^{(3)}(\vec{y}_\perp - \vec{y}_0 - \vec{n} R) + \text{other sources}, \tag{2.63}$$

the first factor here being the $1/g_s$ tension, the second the wrapped T-dual circle, and the g_s^2 factor arising from Newton's constant κ^2. Once again, we can work on the covering space with a periodic array of localized sources, and then later project by translations in order to compactify. Let us look at A at a point $\vec{y}_\perp$ halfway in the

middle of the localized O5 sources. This gives us

$$A\left(\frac{R}{2},\frac{L}{2},\frac{L}{2}\right) \sim g_s \frac{1}{R_f} \sum_{n_R,n_1,n_2} \frac{1}{\sqrt{R^2\left(n_R-\frac{1}{2}\right)^2 + L^2\left(n_1-\frac{1}{2}\right)^2 + L^2\left(n_2-\frac{1}{2}\right)^2}} + \text{contributions from other sources.} \tag{2.64}$$

In the covering space, the sum on $\vec{n}$ represents the contributions from localized sources farther and farther away from the point $\vec{y}_\perp$. As discussed above, if all sources were smeared, the gradient of A would cancel. So the full expression for A, including all localized and homogeneous sources, is essentially the difference between the sum on $\vec{n}$ and the integral over $\vec{n}$. Since L and R are of the same order of magnitude, the overall contribution to the warp factor is $A \sim \mathcal{O}(g_s)$, and the localization of the source can be ignored. Similarly, the gravitational potential sourced by the D7-branes is suppressed by g_s, leading to $A \ll 1$ when combined with the full complement of sources.

The ρ5-branes would produce $A \sim 1$ in a similar way if we treated them as putatively localized sources of stress-energy. Indeed, they do have long-range effects on the geometry; they correspond to a nontrivial fibration (2.4) described by a Weierstrass model. The corrected target space is described by the infrared regime of the gauged linear sigma model (GLSM) presented above. Their contribution to the curvature and hence to the moduli potential is of the same form as it would be in the naïve estimate based on the tension of an isolated brane. The most familiar example of this is the case of elliptically fibered Calabi-Yau manifolds, where the fibration exactly cancels the curvature of the base. This occurs for example in the case of 24 stringy cosmic fivebranes on a base $\mathbb{CP}^1$. More generally, the GLSM beta function ~ 24 for the running of the FI parameter ξ corresponding to the size R^2 of the base is shifted by the elliptic fibration to $\sim (24 - n_\rho)$.

We expect similar statements to hold for the NS5-branes (ingredient (4) above). By themselves, these NS5-branes could be described including backreaction in a half-flat approximation by recognizing them à la [42, 43] as a different set of ρ5-branes with monodromy $\rho \to \rho + 1$. These are holomorphic with respect to a different choice of complex coordinates on the $\mathbb{R}^4 \times T^4$ of our brane construction, so it is

not trivial to describe both sets of ρ5-branes using the same GLSM. However, the two sets are mutually supersymmetric and their BPS tensions combine additively. (They are U-duals of D-brane combinations with 4 Neumann-Dirichlet directions; such combinations have no binding energy.) For this reason we expect their contributions to be well described by the tensions we included in the moduli potential (2.38), at least in cases where their core size is sufficiently small. In the D7-brane model so far considered, this is marginal; the core size of the NS5 is not smaller than R, as we will discuss below in §2.4.7. However, the variants in §2.4.7 involving D5-branes will push the parameters to where the NS5-brane has a string-scale core, much smaller than R. It would be useful to develop techniques to simultaneously control multiple types of $1/g_s^2$-tension branes more explicitly.

2.4.6 Entropy and brane construction

Given the above scalings (2.51), the entropy scales parametrically like

$$\mathcal{S} \sim M_3 R_{dS} \sim \frac{L^4 R^4}{k g_s^2 \epsilon^{1/2}} \sim \frac{k N_{D1} N_{D5}}{\epsilon^{3/2}} \tag{2.65}$$

This scaling of the entropy is the same as in the corresponding AdS model when $\epsilon < 0$. This makes sense, since the ρ5-brane flavors and the orientifold projections are only of order 1 in number, so that the scaling is as in the corresponding D1-D5 AdS orbifold quiver theory up to an enhancement by $\epsilon^{-3/2}$. This factor can be understood as in section 3.5 of [16]: pull out a color brane from a tip of the cone, and count the number of ways of winding strings around the base of the cone up to an energy cutoff comparable to the energy of a string stretching radially to the tip. This gives an enhancement factor $\sim (R_{dS}/R)^3 \sim \epsilon^{-3/2}$. As a result, we can read off the parametric scaling of the Gibbons-Hawking entropy from the D1-D5 system.

Many details come into the precise coefficient over which we have no control at present. As in [16], our main handle on the holographic dual is through its brane construction. It would be interesting to develop tools to study this theory in more

detail.[10] With the brane construction in hand, however, one can immediately study further questions of interest such as the microscopic description of decays out of the metastable dS vacuum and their holographic description.[11]

As mentioned in §2, this model has a brane construction for which the radially evolving R, at fixed initial values of the other moduli, solves the equation (2.5)

$$\frac{R'(w)^2}{R^2} \sim -1 + \frac{const}{R^2} \tag{2.66}$$

for which the singularities at the tips $R \to 0$ are conical. The first term here comes from the D7-branes and anti D7-branes, and the second includes the O5-planes which are at codimension two on the base.

It is also possible to stabilize the construction with $N_{D5} = 0$, as mentioned ealier. In this case the parametric scaling is

$$\mathcal{S} \sim M_3 R_{dS} \sim \frac{L^4 R^4}{k g_s^2 \epsilon^{1/2}} \sim \frac{N_{D1}^2}{k \epsilon^{3/2}} \tag{2.67}$$

In this case the tuning of ϵ plays the dominant role. It would be interesting to understand this case better as it does not appear to arise directly from a known AdS/CFT dual pair, as is the case for most models in the landscape.

2.4.7 Alternative examples

In this subsection we provide two alternative examples in which the radius of curvature R is pushed to larger values and we therefore have better control of α' corrections.

First, we can replace the D7- and anti D7-branes with a single pair of D5- and anti D5-branes wrapping the $S^3/\mathbb{Z}_k$, and put them in different Wilson line vacua to

[10] An intriguing possibility is that as in [71], the holographic duals may only exist as cutoff theories.

[11] Other macroscopic proposals for de Sitter holography which are based on different ways of slicing the spacetime include [20, 21, 22]. It would be interesting to study whether our dS construction building from AdS/CFT might also provide a microscopic realization of these ideas.

prevent perturbative brane-antibrane annihilation:

	0	1	2	3	4	5	6	7	8	9
$D5$, $\overline{D5}$	x	x	x	x	x	x				

(2.68)

The stabilization proceeds as before with the middle term $-b\tilde{\eta}^5$ in the effective potential replaced by

$$\frac{\mathcal{U}}{M_3^3} \supset -16k^3 \left(2\pi R^2 - \frac{n_{D5} R^4 \beta}{2kL^2}\right) \frac{\tilde{\eta}^5}{\beta^3} \,. \tag{2.69}$$

This gives

$$R^2 = \frac{2\pi k L^2}{n_{D5}\beta} \,, \tag{2.70}$$

and the rest of the stabilization proceeds as before. Note that n_{D5} is the number of flavor D5- and anti D5-branes as specified above, which should be distinguished from N_{D5}, the number of color D5-branes wrapping different directions in our brane construction. With $n_{D5} = 2$, we find $R \approx 33$ (as compared to $R \approx 9$ in the model with flavor D7 branes); now α' corrections are of order $8/R^2 = 7 \times 10^{-3}$.

We can push R to even larger values by wrapping the flavor D5-branes on an unorbifolded S^1 in the $S^3/\mathbb{Z}_k$, the fiber $S^1/\mathbb{Z}_k$, and one of the T^4 directions:

	0	1	2	3	4	5	6	7	8	9
$D5$	x	x	(x)	x	x	(x)	x			
$D5'$	x	x	x	(x)	(x)	x		x		

(2.71)

Here the parentheses indicate that the true D5-brane locus is a combination of these dimensions. Note that we do not need to include anti D5-branes here because the D5-branes are wrapping a contractible cycle in the $S^3/\mathbb{Z}_k$, but in order to stabilize the anisotropic mode $L_{78}^2 \neq L_{69}^2$ we need two D5-branes wrapping the 6 and 7 directions respectively. Again, the middle term of the effective potential is replaced by

$$\frac{\mathcal{U}}{M_3^3} \supset -16k^3 \left(2\pi R^2 - \frac{\pi n_{D5} R^3 \beta}{kL}\right) \frac{\tilde{\eta}^5}{\beta^3} \tag{2.72}$$

which stabilizes $R = 4kL/(3n_{D5}\beta)$. With $n_{D5} = 2$, the value of R is further increased

from 33 to 91, with the α' corrections of order $8/R^2 = 1 \times 10^{-3}$.

Another advantage of these two alternative constructions is that the size of the NS5-brane core is much smaller than the radius R. A simple way of looking at this is to take the T-dual along the fiber direction R_f: the NS5-branes are turned into KK5-branes with a fiber size $\tilde{R}_f = 1/R_f = k/(\beta R)$. In our previous construction with D7-branes, this size is of the same order of magnitude as R, as we can see from the parametric scaling $R^2 \sim k$. However, if we replace the D7-branes with D5-branes as in the first example above, we have $R^2 \sim kL^2 \sim k^2$ and the fiber size $\tilde{R}_f \sim k/R \sim 1$ is much smaller than R. In the second example above, we have $R^2 \sim k^2L^2 \sim k^3$ and the fiber size $\tilde{R}_f \sim k/R \sim 1/\sqrt{k}$ is again much smaller than R. This is also confirmed by the numerics: with the previous D7 construction we have $\tilde{R}_f = k/(\beta R) = 5.9$ not much smaller than $R = 9.2$, with the first D5 construction we have $\tilde{R}_f = 1.64$ much smaller than $R = 33$, and with the second D5 construction we have $\tilde{R}_f = 0.59$ much smaller than $R = 91$.

The $D7$-$\overline{D7}$ stability analysis can be repeated in the first D5 example, with analogous results: there is a negative mass squared of Hubble scale, but the deformations away from the flat connection give large positive contributions to the mass squared and keep the mode perturbatively stable. In the second example, the D5-branes are mutually supersymmetric but may possess slippage modes because they wrap contractible cycles on the base $\mathbb{CP}^1$; placing the branes at the orientifold loci (the effect on their tension is already included in (2.72)) projects these modes out and freezes the branes in place.

2.5 Discussion and Future Directions

Similar methods apply to the construction of semi-holographic de Sitter models in other dimensions. Work on four dimensional examples of this kind is in progress [40]. A promising class of candidate models arises from type IIA string theory on an orientifold of an elliptic fibration over B_4 (e.g. $\mathbb{CP}^2$ or $\mathbb{CP}^1 \times \mathbb{CP}^1$) which overcompensates the curvature energy of B_4, along with RR 2-form and 6-form flux as well as additional flavor branes.

This work raises many interesting questions about the nature of the dual implied by the brane constructions. Let us make a few comments here. The compactness of the brane construction implies propagating $d-1$-dimensional gravity. As we have discussed, the fact that this is coupled to a matter sector with large entropy makes for a useful albeit semi-holographic duality; $d-1$-dimensional gravity is weakly interacting over a large range of scales because of the enhancement of the $d-1$-dimensional Planck mass induced by the large number of species. (In the $d=3$ case studied explicitly in this chapter, the $d-1$ dual is Liouville gravity coupled to a large-c matter sector, as anticipated macroscopically in [17, 18, 19] and proposed for somewhat different reasons in [21, 22].) By the same token many other modes are dynamical. In particular flavor groups are dynamical in $d-1$ dimensions, i.e. the flavor symmetry is weakly gauged; the flavor groups have a large number $\sim N_c$ of matter fields charged under them which screen their interactions. This is analogous to the weak dynamical gravity in the $d-1$ dimensional description, with large-c matter sector.

One basic question is whether the $d-1$-dimensional matter theory here is UV complete by itself (and just happens to be coupled to gravity in the case that it arises as part of a dual for de Sitter). Another possibility, analogous to the situation obtained for non-supersymmetric warped throats in [71], is that the matter theory only exists as a low energy effective theory. In general, we would like to understand the couplings of the matter degrees of freedom to Liouville gravity in our setup.

A related question concerns the microscopic interpretation of the entropy. So far we obtained a parametric result, but not the precise coefficient. Even in AdS/CFT, obtaining the precise coefficient is difficult; for example in the $\mathcal{N}=4$ supersymmetric Yang Mills theory there is a famous ratio of $3/4$ between the strong and weak coupling results. In the present case, the coupling to $d-1$-dimensional gravity is a further complication. In particular, altogether the central charge vanishes in a theory of gravity, something borne out by the macroscopic calculations in [17, 18, 19]. Perhaps in the case $d-1=2$, the *effective* central charge is the appropriate notion of a count of degrees of freedom; this is sensitive to the matter contribution.

Our construction is reminiscent of the attempt [26] to count Schwarzschild entropy

with a brane-antibrane system. In the present case, there is a variety of brane constructions which reflects the landscape of possible solutions: each de Sitter solution corresponds to a definite brane construction.

Our solutions eventually decay. Decay modes include the strongly coupled, exponentially suppressed version of brane-antibrane annihilation: Schwinger decay of the flux dual to the color branes. The decay of de Sitter solutions into each other or to regions of zero or negative cosmological constant is central in many attempts to formulate the landscape *en masse*, and concrete input from microscopic brane constructions may be useful.

Chapter 3

FRW solutions and holography from uplifted AdS/CFT

3.1 Introduction: keeping it real

At present we lack a complete theoretical framework for cosmology. One approach to this problem is to try to organize cosmology holographically, building on the success of the AdS/CFT correspondence. Doing so is not trivial for a number of reasons related to the tendency of cosmological solutions to mix with each other and the absence of a simple timelike boundary. Dynamical gravity, or an integration over metrics, is part of the putative lower-dimensional dual in various attempts so far to generalize the AdS/CFT correspondence to cosmology and describe a complete set of observables; this includes dS/CFT [20, 72] at least as it is interpreted in [73],[1] dS/dS [18, 19] and FRW/CFT [21, 22]. Despite the lower dimensional gravity, the formulation of a significant part of the system in terms of a large matter sector is a nontrivial step, one which has recently been put on more solid footing microscopically [7]. Nonetheless it is important to understand whether a more precise formulation might exist.

[1] For this example, there may at least be a subset of observables which correspond to a precise non-gravitational CFT as described in [73], where the CFT computes the wavefunction of the universe. However, this wavefunction is a functional of the metric which one must ultimately integrate over. See the recent work [74] for more discussion of this question.

The structure of UV complete cosmological solutions will likely be useful in answering this question.[2] In this chapter, we present and analyze concrete cosmological solutions which are sourced by a generic ingredient – magnetic flavor branes – used to uplift AdS/CFT systems [16] to cosmology. With sufficiently many magnetic flavor branes, no nonsingular static solutions exist, but time-dependent solutions do exist which are nonsingular at late times; these solutions are nonsingular at all times if obtained from a bubble nucleation process. (Another interesting class of dynamical F-theory solutions was studied in the earlier work [75], which emphasized the point that no physical restriction on the number of 7-branes exists once the generic possibility of time dependence is included.) We will introduce a holographic interpretation of this class of solutions, employing the following basic strategy.

First, we find a warped metric on our spacetime and interpret the two highly redshifted regions in terms of a pair of low energy effective theories. This is a generalization of the observation in [18, 19] that metastable d-dimensional de Sitter spacetime is a warped compactification with two throats and propagating $(d-1)$-dimensional gravity.[3] This line of reasoning of course goes back to the original arguments [2, 4, 3, 77] that the highly redshifted core region of a stack of branes should be equivalent to a field theory, since it represents low energy degrees of freedom decoupled from the ambient Planck scale. We verify that particles are stable in the infrared region, though color branes out on their approximate Coulomb branch propagate up the throat. We call this phenomenon "motion sickness"; as we will discuss later on it is not fatal.

The next step is to compute the $(d-1)$-dimensional Newton constant: this reveals that the $(d-1)$-dimensional graviton decouples at late times, in a way analogous to a Randall-Sundrum theory with the "Planck brane" taken off to infinity. This, and the growth of the entropy at late times [78], is consistent with the possibility of an ultimately precise holographic dual decoupled from gravity. Although gravity decouples in this promising manner, we will see that the way the field theory induces a growing Planck mass is through a rapidly growing number of degrees of freedom, rather than

[2] In the somewhat analogous context of black hole physics, study of concrete string theoretic examples led to microstate counts and ultimately the AdS/CFT correspondence.

[3] More recently, a description in terms of two CFTs coupled to gravity was motivated in another way by [76].

via a growing cutoff on the effective field theory. That is, the system at late times behaves like a theory which is holographic and non-gravitational, but with a finite cutoff for the dual theory. Cutoff quantum field theory is in principle well defined, but many questions remain about its detailed implementation in gauge/gravity duality.[4]

In fact, we find a nontrivial match between the time-dependent number of degrees of freedom in the $(d-1)$-dimensional dual theory, computed using the gravity side in three different ways, with an estimate of the number of available microscopic degrees of freedom on the magnetic flavor branes responsible for the uplift to cosmology. The states we count are drawn from the infinite algebras discussed in [80, 81], cut off at finite time by backreaction and topological consistency criteria. As we will describe below, as currently formulated this count is consistent with basic group-theoretic requirements, but is not fully derived. It is subject to two assumptions about unknown quantities – the first is a plausible conjecture made but not proved in [80, 81], and the second regards the number of charged matter representations which arise. With these assumptions, our count consistently reproduces the gravity-side result in a general class of solutions in different dimensions in a way that appears nontrivial, and generalizes the parametric microscopic estimate of the dS entropy of [7] to FRW cosmologies. These results seem rather encouraging, and motivate further study of time-dependent field theories with sufficiently many magnetic flavors to provide candidate duals for cosmological solutions.

Our formulation of the holographic dual as a Lorentzian-signature field theory (or effective field theory) maintains standard reality and unitarity properties; in particular the number of degrees of freedom in the matter sector is a positive real number. There are other interesting approaches to de Sitter or FRW holography which define the dual on a spacelike (Euclidean) surface, and it would be interesting to study the relation between these different formulations.[5] It may be useful to note, however, that because of the ultimate requirement of integrating over metrics, the argument for defining the

[4]There has been interesting recent progress in relating radial slices to RG scale in AdS/CFT [79], but the detailed dictionary remains to be understood, and is subject to various important subtleties such as the fact that different types of gravity-side particles have different relationships between their energy and their radial position.

[5]In particular, an interesting approach to a concrete example of dS/CFT can be found in [82]. See also [83, 84, 85] for a formal analytic continuation of certain cosmological computations.

theory on the boundary of the spacetime does not trivially generalize from AdS to dS or FRW solutions. Microscopically, large-radius de Sitter solutions in string theory do not arise as a simple continuation of AdS solutions, which turns the flux imaginary in the Freund-Rubin solution. The physically consistent metastable dS solutions that are known arise instead by uplifting AdS solutions with a more complicated collection of stress-energy sources. As we will see, defining a Lorentzian-signature dual via our warped metric does not a priori force us to forego a complete dual description: our warped solution decompactifies at late times, somewhat analogously to Randall-Sundrum with the Planck brane removed to infinity.

Another basic motivation for this work is to further develop our understanding of the structure of time-dependent and cosmological solutions in string theory. We compute correlation functions of massive and massless particles in our geometry; the latter requires a careful treatment of pseudotachyon modes [86]. The structure of these correlation functions should tell us much more about holography on our solutions, the detailed analysis of which we leave for future work. One intriguing feature is that the two-point function of Kaluza-Klein modes is a power law, rather than exponential.

This chapter is organized as follows: In the next section we present FRW solutions sourced by magnetic flavor branes uplifting Freund-Rubin compactifications. We exhibit a warped metric on the solution, indicating a low energy sector corresponding to an effective field theory. In Section 3.3, we show that particles remain stably in the throat at late times, and color branes move up the throat. This theory is cut off and coupled to gravity at finite times, but the Planck mass and the number of degrees of freedom go off to infinity at late times in a manner that is dominated by contributions of the warped region, raising the possibility that the dual completes to a precise non-gravitational theory in this limit. We compute the number of field theoretic degrees of freedom in several macroscopic ways in Sections 3.2 and 3.4.2, and also present, in Section 3.4.1, a count of brane degrees of freedom which agrees with the macroscopic predictions given certain assumptions. In Section 3.5, we study the two-point correlation functions of scalar fields in our solutions, in the massive and massless cases; a full derivation is relegated to Appendix 3.A. Finally, we conclude in Section 3.6, and outline directions for future study.

3.2 FRW solution sourced by magnetic flavor branes

We would like to understand whether FRW cosmology in d dimensions, which occurs for example after decays of metastable de Sitter, admits a $(d-1)$-dimensional holographic dual description. Our strategy is to look for a warped metric on the FRW solutions derived from uplifted AdS/CFT solutions in string theory. We then interpret the infrared region of the warped metric – the region of strong gravitational redshift – in terms of a dual effective field theory (EFT). Finally, we analyze whether the EFT might become a self-contained quantum field theory (QFT) in the far future, since the entropy bound and the $(d-1)$-dimensional Planck mass go to infinity in that limit.

3.2.1 Magnetic flavor branes

The simplest AdS_d/CFT_{d-1} dual pairs arise from Freund-Rubin compactifications on a positively curved Einstein manifold Y stabilized by flux. These can be understood as the near-horizon backreacted solution obtained from color branes placed at the tip of a cone $\mathcal{C}$ with base Y.

We will uplift to cosmological solutions by adding heavy branes which reverse the sign of the curvature of Y. Consider first the $AdS_5 \times S^5$ solution of type IIB string theory, with the S^5 viewed as a Hopf fibration over a base $\mathbb{CP}^2$ (there are many similar examples with S^5 replaced by a more general Einstein space Y). As discussed in [16], there is a natural ingredient which competes with the internal curvature: (p,q) 7-branes at real codimension two on the $\mathbb{CP}^2$, wrapping the Hopf fiber circle and extended along AdS_5. Such branes can be described using F-theory [87, 88, 89], which geometrizes the varying axio-dilaton, and one finds that 36 7-branes are required to exactly cancel the curvature of the $\mathbb{CP}^2$. Similarly, 24 7-branes are required to exactly cancel the curvature of a $\mathbb{CP}^1$, which arises as the base of the Hopf fibration in examples with a compactification on S^3, such as $AdS_3 \times S^3 \times T^4$. In the latter case, alternatively one can use "stringy cosmic 5-branes"[41, 42, 43], elliptic fibrations with the torus fiber coming from the T^4. See for instance [7], where SC5-branes together with other ingredients are used to cancel the curvature of $\mathbb{CP}^1$.

Let us denote the elliptic fibration over the base $B = \mathbb{CP}^m$ – the $\mathbb{CP}^m$ with 7-branes at real codimension two – by $\hat{B}$, and the entire uplifted compactification by $\hat{Y}$. Parameterize the number n of 7-branes or stringy cosmic branes in all cases by defining a quantity

$$\Delta n \equiv n - n_{\text{flat}} \tag{3.1}$$

such that $\Delta n = 0$ corresponds to a flat uplifted base $\hat{B}$.

In the AdS case $\Delta n < 0$, such configurations including their backreaction on the geometry can be described relatively simply using F-theory. On the field theory side, these systems have magnetic flavors, arising in the brane construction from (p, q) strings stretching between D3-branes and the (p, q) 7-branes [90, 91].

Bringing 7-branes together in a time-independent manner generically introduces singularities. For sufficiently few 7-branes, it is understood how these singularities are resolved physically, giving enhanced symmetries and/or light matter fields. In a gauged linear sigma model (i.e. toric) description of the geometry of the elliptic fibration, singularities appear as additional branches in the target space [68]. A criterion for physically resolved singularities of these static solutions [16] is that the central charge of the additional branch be less than that of the main target space of the sigma model. In this case, one may formulate a brane construction with 7-branes intersecting at the tip of a cone, at which the color branes are placed.

This geometry and the backreacted solutions were described in [44, 16]. Its salient features are captured by the five dimensional theory obtained by compactifying on S^5 and adding the potential energy of the 7-branes. The effective potential in 5D Einstein frame is

$$\mathcal{U} \sim M_5^5 (R_f R^4)^{-2/3} \left(\frac{R_f^2}{R^4} + \frac{\Delta n}{R^2} + \frac{N_c^2}{R^8 R_f^2} \right) \tag{3.2}$$

where $R_f\sqrt{\alpha'}$ is the size of the fiber circle S_f^1, and $R\sqrt{\alpha'}$ is the size of the uplifted base $\hat{B}$. The first term is from the metric flux of the S^1 fiber, and the second is the net contribution of the internal curvature and seven-branes. In this F-theory setting

there is generically no global mode of g_s. There are additional scalar fields from 7-brane moduli, which are relatively flat as discussed in [16]. A simple case to consider is one in which the dilaton is fixed at an $SL(2,\mathbb{Z})$ invariant point, via the mechanisms discussed in [44]. The third term comes from N_c units of 5-form flux corresponding to the color branes. The middle term will concern us most in this work; it comes from the 7-brane sources.

The 7-branes wrap $AdS_5 \times S^1_f$ times a two-cycle in the base, and in the dimensionally reduced theory we do not keep track of their positions in the compact directions. As reviewed in [16], the geometrical understanding [87, 88, 89] of 7-branes as an elliptic fibration makes it possible to calculate their leading contribution to the curvature, and hence to the potential energy (3.2). One can study the geometry by realizing it as the target space of a gauged linear sigma model [68]. In this description, the beta function for the size of the negatively curved internal space has the same scaling but opposite sign as in the case of a $\mathbb{CP}^m$, by an amount Δn that depends on the number of 7-branes. The deformations of the 7-brane configuration are superpotential terms in the sigma model and are intrinsically lighter. We can for convenience focus on configurations where the string coupling has been fixed at $g_s \sim 1$, enforced by appropriate combinations of 7-branes; it is also interesting to consider the orientifold limit [92]. The static solutions with $\Delta n < 0$ are then described by minima of (3.2) [16].

Bringing $\Delta n \geq 0$ branes together in a *static* configuration leads to singularities which violate the above condition for allowed singularities, with the central charge of the singular branch being larger than that of the main target space. From the point of view of the description (3.2), $\Delta n \geq 0$ leads to a decompactification limit. Moreover, in such a configuration the states that transform under the infinite algebras realized on (p,q) 7-branes [80, 81], which are broken for separated 7-branes, appear to come down to zero mass. These effects hint that an infinite set of degrees of freedom may ultimately be involved in formulating physics in the generic case of $\Delta n > 0$, and we will return to this point after developing a controlled gravitational description of uplifted solutions.

In general, we should allow for time-dependent backreacted solutions [75]. As we will explain shortly, the 7-branes need not come together anywhere at late times,

and in appropriate examples (such as [7]). An initial singularity may be avoided by matching to a Coleman-de Luccia tunneling process in the past (as described in Appendix 3.A), though we will in any case focus on the late time physics in the present work.

3.2.2 Solution and warping

Let us now introduce our solutions for $\Delta n > 0$. It is interesting to analyze this class of solutions both from a ten-dimensional perspective and using the d-dimensional description obtained by compactification on the uplifted space $\hat{Y}$. Below, we will exhibit a precise 10d solution, but let us begin with the d-dimensional description.

In the case $d = 5$, we have an effective potential (3.2) for the scalar fields R and R_f. With $\Delta n > 0$, the 7-branes overcompensate the contribution of the curvature to the effective potential, so they turn the base $\mathbb{CP}^2$ into a net negatively curved space $\hat{B}$, whose curvature scales with R as if it were a hyperbolic space. All terms in the potential (3.2) are positive in this case, and we look for time-dependent solutions where the radii evolve with time (along with the FRW scale factor $a(t)$ in the d-dimensional theory).

As we will see momentarily, the d-dimensional FRW equations along with the equations of motion for the scalar fields R and R_f admit a time-dependent solution where at late times R and the scale factor expand with time, and the fiber circle R_f remains constant. The dominant term in the potential energy (3.2) in this solution is the term proportional to $\Delta n/R^2$, since the others decay more quickly at large R and fixed R_f. In particular, the 5-form flux corresponding to the color branes is very subdominant at late times. We will make contact with this in Section 3.3, when analyzing the dynamics of color branes in our solutions.

Specifically, we find the scale factor $a(t) \propto t$, while $R \propto t^{3/7}$ and R_f approaches a constant. The mass of a KK mode on the uplifted base is

$$m_{KK} \sim \frac{n_{KK}}{R} \times \frac{M_5}{(R^4 R_f)^{1/3}} \propto \frac{n_{KK}}{t} \tag{3.3}$$

where the second factor here is the conversion to Einstein frame. This means that, as

in the original examples of AdS/CFT [2], there is no hierarchy between the internal dimensions and the curvature scale in d dimensions. It is likely possible to use the method developed in [16] to obtain a hierarchy of scales, but as we will see shortly our solution is very simple in 10 dimensions.

These scalings can be obtained self-consistently by noting that in this limit the dominant contribution to the energy is given by the 7-branes and curvature, while the fluxes dilute faster. The FRW equations become

$$\begin{aligned} 4\,\frac{\ddot{a}}{a} &= -\frac{28}{3}\frac{\dot{R}^2}{R^2} + \frac{2}{9}M_5^2(R^4R_f)^{-2/3}\frac{\Delta n}{R^2} \\ 12\,\frac{\dot{a}^2}{a^2} + 12\,\frac{K}{a^2} &= \frac{28}{3}\frac{\dot{R}^2}{R^2} + \frac{2}{3}M_5^2(R^4R_f)^{-2/3}\frac{\Delta n}{R^2}\,. \end{aligned} \tag{3.4}$$

Here K is the spatial curvature of the FRW metric. Looking for a solution of the form $a(t) = ct$, the first equation gives

$$R(t) = \left(\frac{7M_5}{3\sqrt{42}}\frac{\Delta n^{1/2}}{R_f^{1/3}}\right)^{3/7} t^{3/7}\,. \tag{3.5}$$

Plugging in the second equation yields $K = -1$ (i.e. an open FRW solution) and $c^2 = 7/3$ with $a(t) = ct$. Note that there will also be a dynamical equation for $R_f(t)$; however, analyzing this equation of motion shows that it is self-consistently frozen in place in the regime above. This and other features of the solution will be very clear in the 10d solution we will present shortly. Numerical studies of the equations of motion for $a(t)$, $R(t)$, and $R_f(t)$ show that the solution above is an attractor for a range of initial conditions.

Let us now analyze the 10d solution. So far we have focused on (p, q) 7-branes, but similar considerations apply more generally to FRW cosmologies sourced by other branes realized as elliptic fibrations, such as stringy cosmic 5-branes. More generally, other types of sources may be involved. For example, in decay from the metastable dS_3 solution in [7], the uplifting contribution arises in part from stringy cosmic 5-branes but also from other sources such as NS5-branes. In general, it is interesting to consider the FRW phase corresponding to the leading source at late times. The elliptic

fibrations we consider here are natural sources which contribute to the curvature at leading order, and we will continue to focus on this case here.

We then consider a d-dimensional FRW spacetime and an internal space that can be described as a Hopf fibration over a base $\mathbb{CP}^m$. As we argued before, as far as the evolution of the size R of the base goes, the uplifted base $\hat{B}$ (the elliptic fibration over $\mathbb{CP}^m$) behaves like a hyperbolic space $\mathbb{H}_{2m}$ of real dimension $2m$. Compactifying on this, we find the following Ricci-flat string-frame metric, which is hence a vacuum solution of Einstein's equation:

$$ds_s^2 = -dt_s^2 + \frac{t_s^2}{c^2} dH_{d-1}^2 + \frac{t_s^2}{\hat{c}^2} d\hat{B}_{2m}^2 + dx_f^2, \tag{3.6}$$

where $c^2 = (d+2m-2)/(d-2)$, $\hat{c}^2 = (d+2m-2)/(2m-1)$, and

$$dH_{d-1}^2 = d\chi^2 + \cosh^2\chi \, dH_{d-2}^2 \tag{3.7}$$

is the metric on a noncompact, unit hyperboloid of dimension $d-1$. $d\hat{B}_{2m}^2$ is the metric on our uplifted, negatively curved compact base space of dimension $2m$. Although in this work we are concerned with generic configurations with $\Delta n > 0$ branes uplifting AdS/CFT solutions, the solution above also describes the dynamics of a compactification on $S^1 \times \mathbb{H}_{2m}/\Gamma$, a circle times a compact hyperbolic space. In that case, the dilaton is meaningful (as oppposed to in F-theory); nevertheless, since our solution is Ricci-flat in 10d string frame, the dilaton is not sourced in this solution.

In this solution we only included the effects of the flavor branes. In the $\Delta n < 0$ case of AdS/CFT, the flux corresponding to color branes plays a leading role in the backreacted solution. However, in the present case at late times the flux dilutes away and is subdominant, as we emphasized above. Furthermore, since the contribution from the metric flux (first term in (3.2)) can also be neglected and the fiber size becomes constant at late times, we have approximated the fiber direction by an S^1 factor in the geometry.[6] In some cases, there may be additional transverse dimensions

[6] Although the metric flux is subdominant in the solution, it does affect the topology; in particular the fiber circle remains contractible. This feature will play a role in our count of brane degrees of freedom in Section 3.4.1. The nontrivial fibration of the circle is a feature of the AdS/CFT dual pair

(such as the T^4 in models based on $AdS_3 \times S^3 \times T^4$), which we suppressed in the metric (3.6).

Let us now compactify down to d dimensions. The volume of the compactification manifold $\hat{Y}$ is

$$\mathrm{Vol}(\hat{Y}) \propto R_f R^{2m} \propto t_s^{2m}, \tag{3.8}$$

where we have not kept track of time-independent coefficients and have used $R \sim t_s$ from (3.6). Going to the d-dimensional Einstein frame

$$g^{(d)}_{\mu\nu,E} = \left(\frac{\mathrm{Vol}(\hat{Y}) M_{10}^8}{M_d^{d-2}} \right)^{2/(d-2)} g^{(d)}_{\mu\nu,s}, \tag{3.9}$$

we get an FRW metric of the form

$$ds_E^2 = -dt^2 + c^2 t^2 dH^2_{d-1} \ , \tag{3.10}$$

where

$$c^2 = \frac{d+2m-2}{d-2} \ , \qquad t \propto t_s^{c^2} \ . \tag{3.11}$$

Cases of particular interest are uplifts of $AdS_5 \times S^5$, with $c^2 = 7/3$ ($d = 5$, $m = 2$) and uplifts of $AdS_3 \times S^3 \times T^4$, with $c^2 = 3$ ($d = 3$, $m = 1$). This reproduces the results obtained using the d-dimensional theory: $R(t) \propto t^{1/c^2}$, in agreement with (3.5).

Since $c > 1$, the scale factor is expanding faster than in curvature dominated FRW (a.k.a. flat spacetime in Milne coordinates). In general, $\Delta n > 0$ corresponds to $c > 1$, and we will find it very useful to contrast our results for $c > 1$ with the case of flat space ($c = 1$). Our holographic interpretation will apply consistently for $c > 1$, and will not apply to flat spacetime.

We may change variables by setting

$$t = (\eta^2 - w^2)^{c/2} \ , \ \chi = \frac{1}{2} \log \frac{\eta + w}{\eta - w}, \tag{3.12}$$

which we are uplifting to FRW cosmology, so the metric flux may be an important element even though its energetic contribution is subdominant. More generally, it would be interesting to develop a holographic duality for the solution without any metric flux.

and the metric (3.10) becomes

$$ds^2 = c^2(\eta^2 - w^2)^{c-1}\left(dw^2 - d\eta^2 + \eta^2 dH^2_{d-2}\right). \tag{3.13}$$

This metric exhibits warping for $c > 1$, which corresponds to $\Delta n > 0$. We want to understand the spectrum and dynamics of degrees of freedom that are redshifted to low energies.

It is useful to consider a closely related time coordinate $t_{UV} = \eta^c$, giving metric

$$ds^2 = c^2\left(t_{UV}^{2/c} - w^2\right)^{c-1} dw^2 + \left(1 - \frac{w^2}{t_{UV}^{2/c}}\right)^{c-1}\left(-dt_{UV}^2 + c^2 t_{UV}^2 dH^2_{d-2}\right). \tag{3.14}$$

On the UV slice $w = 0$, we have $t_{UV} = t$. In this metric the warp factor

$$f(w, t_{UV}) \equiv \left(1 - \frac{w^2}{t_{UV}^{2/c}}\right)^{(c-1)/2} \tag{3.15}$$

and the metric component g_{ww} depend only weakly on the coordinate time at late times:

$$\left|\frac{\partial_{t_{UV}} f}{\partial_w f}\right| \sim \left|\frac{\partial_{t_{UV}} g_{ww}}{\partial_w g_{ww}}\right| \sim t_{UV}^{-(1-1/c)} \to 0 \qquad \text{as} \qquad t_{UV} \to \infty \tag{3.16}$$

where in the last equivalence we have evaluated a point at constant warp factor, i.e. constant $w/t_{UV}^{1/c}$. This is not a covariant quantity, but neither is the redshifted energy and the small value of the ratio (3.16) may simplify some calculations at late times.

There are other ways of writing the FRW spacetime as a warped product metric: as a simple example, we may pass to the conformal time $T = \frac{1}{c}\log(t_{UV}/\ell)$ in the $(d-1)$-dimensional theory, where ℓ is an arbitrary length scale. We can absorb the scale factor ct_{UV} (in $d-1$ dimensions) into the warp factor and write the warped metric as

$$ds^2 = c^2(\ell^{2/c}e^{2T} - w^2)^{c-1}dw^2 + c^2\ell^2 e^{2cT}\left(1 - \frac{w^2}{\ell^{2/c}e^{2T}}\right)^{c-1}(-dT^2 + dH^2_{d-2}). \tag{3.17}$$

The dual theory now lives on a static (non-expanding) space $\mathbb{R} \times \mathbb{H}_{d-2}$. This is similar

to the AdS/CFT correspondence written on global vs. Poincaré slicing, or other slicings with an expanding or static hyperboloid [93]. These various slicings describe a dual theory living on different spacetimes. In our case, a complication is the presence of time-dependent couplings and (in general) a time-dependent metric for the field theory. Furthermore, since the dual theory is not conformal, the conformal transformation that removes the factor e^{2cT} also modifies the running couplings, as we discuss in Section 3.2.5. Other, more general slicings may lead to even more complicated dual descriptions: for instance, using Gaussian normal coordinates starting from a central spatial slice (hyperbolic or otherwise) gives different w-dependences in the temporal and spatial warp factors. Although we will stick to the simpler example given above in this work, it would be interesting to consider the existence of dual theories for more general slicings.

Again, using the warped metric given above, we wish to determine what light (meaning energy $\ll$ bulk Planck mass M_d) degrees of freedom there are. Given a region of strong gravitational redshift, i.e. a region of light states in our gravity solutions, the system may have a right to a field theory description as in the low energy regime of the usual AdS/CFT.

The proper time interval between two events of coordinate interval Δt_{UV} is

$$\Delta T(w, t_{UV}) = \Delta t_{UV} \left(1 - \frac{w^2}{t_{UV}^{2/c}}\right)^{(c-1)/2} . \tag{3.18}$$

This redshift factor is, of course, 1 for $c = 1$ (flat spacetime), and for $c > 1$ it is smaller than 1. This indicates gravitational redshift for probes of proper energy $\sim 1/\Delta T$ (fixed in units of the d-dimensional Planck mass M_d). Energies of such probes are redshifted down by a factor of $f(w, t_{UV})$ defined in (3.15). As we mentioned above, this is time-dependent as well as dependent on the "radial" scale w, but its w dependence is stronger (3.16). Slices of constant $w/{t_{UV}}^{1/c}$ are then slices of constant scale. In terms of the coordinates given in (3.12), this corresponds simply to slices of constant χ.

This effect arises in the absence of any flux, suggesting that the flavor branes (or

more generally the geometry they source) support dynamical degrees of freedom in the EFT region.[7]

It is important to note that basic degrees of freedom such as KK modes, oscillating closed strings, 7-7 strings and junctions, D-branes, and so on do not have fixed masses in units of M_d. Their masses depend on $t = (t_{UV}^{2/c} - w^2)^{c/2}$, leading to $t_{UV}^{2/c} - w^2$ dependence in ΔT in (3.18). This is analogous to radially-dependent masses in AdS/CFT.[8] For KK modes on the uplifted base, KK and winding modes on the fiber, strings, and 7-7 strings/junctions we obtain respectively

$$m_{KK} \propto \frac{1}{t}\,, \quad m_f \propto m_{\rm str} \propto \frac{1}{t^{1-1/c^2}}\,, \quad m_{77} \propto \frac{1}{t^{1-2/c^2}}\,. \tag{3.19}$$

We will analyze their dynamics in Section 3.3. For our examples, the specific values for the exponents are, respectively, -1, $-4/7$, $-1/7$ for $m = 2$, $d = 5$, and -1, $-2/3$, $-1/3$ for $m = 1$, $d = 3$.

3.2.3 $d-1$ Planck mass and its decoupling at late times

As in Randall-Sundrum theory (RS) [28], we can compute the $(d-1)$-dimensional Newton constant $G_{N,d-1}$ by dimensionally reducing on the w direction. This yields

$$\frac{1}{G_{N,d-1}} \equiv M_{d-1}^{d-3} \sim M_d^{d-2} \int_0^{t_{UV}^{1/c}} dw \sqrt{-\tilde{g}} \tilde{g}^{t_{UV} t_{UV}} \tag{3.20}$$

$$\sim M_d^{d-2} \int_0^{t_{UV}^{1/c}} dw \left(1 - \frac{w^2}{t_{UV}^{2/c}}\right)^{\frac{(d-2)(c-1)}{2}} t_{UV}^{1-1/c} \sim M_d^{d-2} t_{UV}. \tag{3.21}$$

[7] In some examples of AdS/CFT obtained by color branes probing the tip of a cone, there are closed string moduli at the tip, for example ones corresponding to Fayet-Iliopoulos terms. The question was raised in those examples of whether these modes are dynamical. There, the fact that the cone itself was unwarped supports the conclusion that the FI term is a parameter, not a field. In more general cases such as ours, however, the answer may be different.

[8] For example, in AdS/CFT compactified on a circle, momentum modes on the circle become radially-dependent masses for which the redshift factor precisely cancels out, and there are many other examples one could consider.

where by $\tilde{g}_{\mu\nu}$ we mean the factors that appear in the d-dimensional metric but not in the $(d-1)$-dimensional metric. Thus at finite times, we have a warped compactification with propagating $(d-1)$-dimensional gravity as in the dS/dS correspondence [18, 19], but as $t_{UV} \to \infty$ gravity decouples.

This raises the possibility of a more precise field theory dual in the far future. A simple but nontrivial test of this possibility is the following. In a general warped compactification [94, 27, 49], a diverging $(d-1)$-dimensional Planck mass can arise in (at least) two ways:

(1) A leading contribution may come from the warped throat (the effective field theory), as in RS with a Planck brane moving off to infinity. In this case, as the Planck brane goes off to infinity the holographic dual becomes a pure QFT decoupled from gravity, i.e. the effective field theory completes to a full QFT.

(2) Instead, in a more general warped compactification the leading contribution may come from the volume of the compactification manifold, with the warped throat subdominant. In this case, the effective field theory does not complete to a full QFT which captures the full system.

Let us check which of these possibilities is realized in our system. First, let us elaborate on the behavior (1) above in the case of RS. This consists of an AdS_5 spacetime

$$ds^2 = \frac{r^2}{R_{AdS}^2}\left(-dt^2 + d\vec{x}^2\right) + \frac{R_{AdS}^2}{r^2}dr^2 \tag{3.22}$$

up to a finite radial scale r_{UV}. The 4-dimensional Planck mass M_4 is given by dimensionally reducing on the radial direction:

$$M_4^2 \sim M_5^3 \int_0^{r_{UV}} dr\sqrt{-\tilde{g}}\tilde{g}^{tt} \sim M_5^3 \frac{r_{UV}^2}{R_{AdS}} \sim \tilde{N}_{dof,AdS}\Lambda_{c,RS}^2 \tag{3.23}$$

In the last relation here, which indicates that the Planck mass is induced by the field theory degrees of freedom, we used that the central charge of the field theory scales like $\tilde{N}_{dof,AdS} \sim M_5^3 R_{AdS}^3$ [95] and that the energy scale of the cutoff is $\Lambda_{c,RS} = r_{UV}/R_{AdS}^2$.

For our purposes, it will be useful to belabor this result in the following way. First, let us break up the calculation (3.23) into two pieces: the integral over r from

0 to $\epsilon\, r_{UV}$, and the rest of the integral from $\epsilon\, r_{UV}$ to r_{UV}, where ϵ is a fixed constant between 0 and 1. This separates an IR contribution $r < \epsilon\, r_{UV}$ (corresponding to energies below $\epsilon\, r_{UV}/R^2_{AdS}$) from a UV contribution for $r > \epsilon\, r_{UV}$, using an arbitrary reference scale $\epsilon\, r_{UV}/R^2_{AdS}$ that is fixed in terms of the UV cutoff as we increase r_{UV}. The ratio of the two contributions is a constant as the Planck brane moves off to infinity. In particular, the infrared region continues to contribute a leading piece to the 4-dimensional Planck mass.

Let us analyze the same question in our FRW case. First, define a scale M_* dividing the UV and IR regions of our throat via

$$\frac{M_*}{M_{UV}} \equiv \epsilon \;\Rightarrow\; w_* = t_{UV}^{1/c}\sqrt{1-\epsilon^{2/(c-1)}}\,. \tag{3.24}$$

In terms of this, we can work out the ratio of UV to IR contributions to the Planck mass (3.21), obtaining

$$\frac{UV}{IR} = \frac{\int_0^{\sqrt{1-\epsilon^{2/(c-1)}}} dy(1-y^2)^{(d-2)(c-1)/2}}{\int_{\sqrt{1-\epsilon^{2/(c-1)}}}^1 dy(1-y^2)^{(d-2)(c-1)/2}} = \text{constant}\,. \tag{3.25}$$

Thus our setup behaves similarly to case (1), raising the possibility of a pure field theory dual capturing the FRW physics at late times.

3.2.4 Covariant entropy bound

An important quantity that characterizes a field theory is its number of degrees of freedom. For example, if we cut off a theory with a lattice, we require some number $\tilde{N}_{\rm dof}$ of degrees of freedom per lattice point to define it. That is, we denote the number of field theoretic degrees of freedom by $\tilde{N}_{\rm dof}$. We would like to understand this quantity in our putative holographic theory, generalizing the analysis given in [95]. There, an infrared cutoff on the radial coordinate in AdS was related to a UV cutoff in the corresponding QFT. Even in ordinary AdS/CFT this UV cutoff is not understood very precisely, however: it is not literally a lattice cutoff since it does not break the isometries of the space on which the field theory lives, and the UV/IR

relation works differently for different types of probes on the gravity side. However, gravitational calculations of the entropy of thermal states and of the central charges in the field theory reproduce the behavior expected from an identification of $\tilde{N}_{\rm dof}$ with the number of degrees of freedom per lattice point, and we may revert to that language.

We will compute the time dependence of this quantity in several distinct ways in the present work, including a count of available states on the magnetic flavor branes, obtaining the same answer. On the gravity side, a measure of the number of degrees of freedom is given by the covariant entropy bound [96, 97] on the entropy passing through an observer's past light sheet. As emphasized in [78], for FRW solutions (unlike the metastable de Sitter phase) the entropy bound grows to infinity at late times.

Let us work this out explicitly in our solution. We start by choosing a spherically symmetric set of coordinates on (3.10)

$$ds_E^2 = -dt^2 + c^2 t^2 \left(\frac{dr^2}{1+r^2} + r^2 d\Omega_{d-2}^2 \right) . \tag{3.26}$$

Consider an observer at the origin ($r = 0$) in our space at time t_0. The past light cone of this observer is foliated by spheres of size $\rho = r(t)ct$, where $r(t)$ is determined by

$$\int_0^r \frac{dr}{\sqrt{1+r^2}} = -\int_{t_0}^t \frac{dt}{ct} \qquad \Rightarrow \quad r(t) = \frac{1}{2}\left[\left(\frac{t_0}{t}\right)^{1/c} - \left(\frac{t}{t_0}\right)^{1/c} \right]. \tag{3.27}$$

For $c > 1$, the sphere grows to a maximal size $\rho_{max} \propto t_0$ and then begins to shrink (because of the contraction of the FRW universe) as we go back in time.

The conjectured entropy bound [96, 97] is given by the area of this maximal sphere in Planck units. From this we obtain, substituting the time t_0 of the observer by t,

$$\mathcal{S} \sim M_d^{d-2} t^{d-2}. \tag{3.28}$$

(For $c = 1$, the sphere never reaches a maximal size, but instead keeps growing,

indicating a diverging entropy bound even at finite time.) In our case, the entropy going to infinity at late times also suggests the possibility of a precise dual of our FRW phase when $t \to \infty$; this jibes with the infinite warped throat we develop at late times in our solution.

3.2.5 Basic relations among parameters

We are now in a position to list some basic relations between several quantities in our system: the $(d-1)$-dimensional Planck mass, the number of field theoretic degrees of freedom $\tilde{N}_{\rm dof}$ in the effective field theory (EFT), and the cutoff Λ_c of the EFT. These relations will enable us to solve for their dependence on time t_{UV}. We will derive $\tilde{N}_{dof}$ independently using the quasilocal stress tensor below in §3.4.2, obtaining the same result for its dynamics as is predicted by the simple considerations of this section.

First, since the $(d-1)$-dimensional Planck mass is largely induced by the field theory (as we just found in the previous subsection), we have the relation

$$\tilde{N}_{\rm dof}\,\Lambda_c^{d-3} \sim \frac{1}{G_{N,d-1}} \equiv M_{d-1}^{d-3} \sim M_d^{d-2} t_{UV} \tag{3.29}$$

where Λ_c is the cutoff of our effective field theory.

In our $(d-1)$-dimensional theory, we expect a nontrivial quantum energy density. If we assume that this is an order one fraction of the source of Hubble expansion in the dual, we obtain a second relation comes from the Friedmann equation in the $(d-1)$-dimensional theory:

$$H_{d-1}^2 = \frac{1}{t_{UV}^2} \sim \tilde{N}_{\rm dof}\Lambda_c^{d-1} G_{N,d-1}. \tag{3.30}$$

Here $H_{d-1} = 1/t_{UV}$ is Hubble in the $(d-1)$-dimensional theory obtained by dimensional reduction on w in (3.14).

Putting these together, we find

$$\tilde{N}_{\rm dof} \sim M_d^{d-2} t_{UV}^{d-2}\,, \qquad \Lambda_c \sim \frac{1}{t_{UV}}\,. \tag{3.31}$$

This result is consistent with the entropy discussed in the last subsection if we assume the basic relation

$$\mathcal{S} \sim \tilde{N}_{\rm dof} \Lambda_c^{d-2} \, {\rm Vol}_{d-2} \tag{3.32}$$

where ${\rm Vol}_{d-2} \sim t_{UV}^{d-2}$ is the volume of space in the dual theory. The result (3.31) is also consistent with the result for $\tilde{N}_{\rm dof}$ below in (3.4.2).

It is also possible to define the theory on a non-expanding lattice using the coordinatization (3.17), where the $(d-1)$-dimensional theory lives on $\mathbb{R} \times \mathbb{H}_{d-2}$. In this case a calculation analogous to (3.21) gives

$$\tilde{N}_{\rm dof} \Lambda_c^{d-3} \sim \frac{1}{G_{N,d-1}} \sim M_d^{d-2} \ell e^{(d-2)cT} \sim \frac{M_d^{d-2} t_{UV}^{d-2}}{\ell^{d-3}}. \tag{3.33}$$

In this case, the Friedmann equation requires that

$$0 = H_{d-1}^2 = G_{N,d-1} \rho + \frac{1}{\ell^2} \tag{3.34}$$

where ℓ is the curvature scale of the hyperbolic spatial slices. One implication of this is that the energy density must compensate the time dependence in the Newton constant. If we assume again that the energy density is of order $\tilde{N}_{\rm dof} \Lambda_c^{d-1}$, we obtain the relation

$$G_{N,d-1} \tilde{N}_{\rm dof} \Lambda_c^{d-1} \sim \frac{1}{\ell^2} \tag{3.35}$$

In this case, we then get

$$\tilde{N}_{\rm dof} \sim M_d^{d-2} t_{UV}^{d-2} \, , \qquad \Lambda_c \sim \text{constant}. \tag{3.36}$$

Again, this agrees with the covariant entropy bound and with the independent derivation of $\tilde{N}_{\rm dof}$ we find below in (3.4.2). Note that the cutoffs in (3.31) and (3.36) are related by a conformal rescaling: to obtain the effective field theory on $\mathbb{R} \times \mathbb{H}_{d-2}$, we have to remove the overall factor e^{2cT} in (3.17) by a conformal transformation. This should be compared with the corresponding term in (3.14) where there is no such factor. Since our theory does not have a conformal symmetry, this conformal transformation changes the running coupling constants and other scale dependent

quantities. We can see this explicitly in that the gravitational coupling $G_{N,d-1}$ is different in the two cases.

For both slicings, the final result agrees with the scaling (3.28) from the covariant entropy bound, since at late times $t \sim t_{UV}$. Thus if we think of the cutoff as a lattice cutoff, the system builds up entropy by accumulating degrees of freedom per lattice point, rather than by increasing the number of lattice points. In Section 3.4.1 we will provide an independent count of $\tilde{N}_{\rm dof}$ using the magnetic brane construction, finding that the infinite store of degrees of freedom on our $\Delta n > 0$ set of 7-branes, cut off by backreaction criteria, precisely reproduces this behavior. As described above, these results are consistent with the possibility of a complete non-gravitational field theory dual at late times, albeit one with a finite cutoff for the field theory. The growth of $\tilde{N}_{\rm dof}$ is consistent with this interpretation: in a field theory with time-dependent masses and couplings, the number of degrees of freedom below a fixed cutoff scale will generically change with time. In our case, it increases rapidly.

3.3 Dynamics of particles and branes

So far, we have presented our d-dimensional cosmological solution, exhibited a warped metric on it, and derived basic properties of its $(d-1)$-dimensional description, a candidate holographic dual. In this section we study the motion of particles and branes in our geometry. Their motion in the highly redshifted (infrared) region is related to the long distance dynamics of the putative holographic dual. For simplicity we will consider the $d = 5$ case; general dimensionalities d can be studied in a similar fashion.

Our goals are twofold. First, we would like to better understand the role of the color sector in our theory, given that the 5-form flux is subdominant in the solution and warping arises without it. Secondly, we want to check whether the infrared degrees of freedom in the highly redshifted (warped) throat are stable. In general, it would be interesting to understand what additional criteria – beyond the presence of strong warping – might need to be satisfied in order to obtain a holographic dual capturing the low energy degrees of freedom (see [98, 99] for some earlier discussion

of this question). One natural physical criterion is that the strength and variation of the warp factor be such that light particles remain in the warped region.[9]

The results are as follows: color branes (D3-brane domain walls) are not stable in the IR region of our warped geometry, but particles (massive (3.19) and massless) do remain in the infrared region. These facts can be seen in a simple way from the original metric (3.6) (they follow equivalently from a similar analysis using the warped metric).

In the case $d = 5$, $m = 2$, the 10-dimensional string frame metric is (3.6)

$$ds^2 = -dt_s^2 + \frac{t_s^2}{c^2}(d\chi^2 + \cosh^2\chi\, dH_3^2) + \frac{t_s^2}{c^2}d\hat{B}_4^2 + dx_f^2\,, \tag{3.37}$$

where dH_3^2 is the metric on a unit 3-dimensional hyperbolic space $\mathbb{H}_3$ and $c^2 = 7/3$. As mentioned above, slices of constant scale in our warped metric (3.14) translate into slices of constant χ, and the two infrared regions correspond to large $|\chi|$.

The isometries of the 4-dimensional hyperboloid, and the corresponding conserved momenta, imply that particles that start moving out in the χ direction continue propagating to larger $|\chi|$ as time goes on. Massless particles head toward null infinity, traveling on null geodesics $d\chi = c\, dt_s/t_s$, so that

$$\chi_{\text{massless}}(t_s) = c\log(t_s/t_0). \tag{3.38}$$

Massive particles at a fixed point on $\mathbb{H}_3$ are governed by the Born-Infeld action

$$S_{\text{massive}} = -\int dt_s m(t_s)\sqrt{1 - \dot{\chi}^2 t_s^2/c^2} \tag{3.39}$$

where the particle mass $m(t_s)$ can depend on time in our system. In particular, the string-frame counterparts of (3.19) are:

$$m_{KK,s} \propto \frac{1}{t_s}\,, \quad m_{str,s} \propto m_{f,s} \propto 1\,, \quad m_{77,s} \propto t_s\,. \tag{3.40}$$

[9]We thank D. Marolf and J. Polchinski for this suggestion.

The conserved momentum is

$$p = \frac{\delta \mathcal{L}}{\delta \dot{\chi}} = \frac{m(t_s)\dot{\chi} t_s^2/c^2}{\sqrt{1 - \dot{\chi}^2 t_s^2/c^2}}. \tag{3.41}$$

A particle at fixed $\chi = \chi_0$ (with $\dot{\chi} = 0$ initially) stays at χ_0; a particle moving toward the bottom of either throat continues to do so as $t_s \to \infty$. We can solve for $\dot{\chi}$ using (3.41), giving

$$\dot{\chi} = \frac{cp}{t_s \sqrt{p^2 + m(t_s)^2 t_s^2/c^2}}. \tag{3.42}$$

From this we see that in all cases (3.40), $\dot{\chi} \to 0$ at late times.

At this point we should note that the two-dimensional slice of the spacetime traced out by t and χ (at a fixed point on the $\mathbb{H}_3$) is simply flat space, with metric $-dt^2 + c^2 t^2 d\chi^2$. In that subspace alone, the low energy region we are defining is a version of a Rindler horizon. Since $c > 1$ the spacetime is not flat overall, and the curvature affects generic particle trajectories and quantum mechanical wave packets, but a classical calculation of test particle trajectories does not sense this effect.

We get the same result, of course, by working directly in the d-dimensional warped metric given above. There, to analyze particle dynamics we solve the equations of motion for a particle with a mass of the form $m(\eta, w) \sim (\eta^2 - w^2)^\kappa$ (with κ given by (3.19) for some of the basic particles in our system). In our solution, this is obtained by varying the action

$$S_{\text{massive}} = -\int d\eta \; m(\eta, w) \; c(\eta^2 - w^2)^{(c-1)/2} \sqrt{1 - (dw/d\eta)^2}. \tag{3.43}$$

At late η, this yields a solution of the form

$$w = c_1 \eta + \frac{c_2}{\eta^b} \tag{3.44}$$

with $b = 2\kappa + (c-1)$. In the examples discussed above (KK modes, closed strings, and 7-7 strings) $b \geq -1$, with equality occurring for the case of KK modes. Again, this means that such particles stay in the infrared region we just defined if they start out there. Note that when transformed back into regular coordinates t, χ, the subleading

piece is important to allow the particles to propagate in time.

A D3-brane, on the other hand, experiences a force pushing it up the warped throat. Its Born-Infeld action in 10d string frame is of the form

$$S_{D3} \sim -T_3 \int dt_s \left(\frac{t_s}{c}\right)^3 \cosh^3\chi \sqrt{1-\dot{\chi}^2 t_s^2/c^2}, \tag{3.45}$$

where T_3 is the D3-brane tension. The $\cosh^3\chi$ factor introduces a force pushing the brane to smaller values of $|\chi|$. It is straightforward to verify, as we will do momentarily, that as a result of this force the D3-branes come up the throat. We will call this phenomenon "motion sickness."[10]

Let us start from (3.37) in the dimensionless conformal time $\tilde{t} = c\log(t_s/\ell)$, where ℓ is an arbitrary length scale. The equation of motion that follows from the DBI action is

$$\frac{d}{d\tilde{t}}\left(e^{4\tilde{t}/c}\cosh^3\chi\,\frac{\chi'}{\sqrt{1-\chi'^2}}\right) + 3e^{4\tilde{t}/c}\cosh^2\chi\,\sinh\chi\,\sqrt{1-\chi'^2} = 0\,, \tag{3.46}$$

where we took the D3-brane position to depend on time only, and here $\chi' \equiv d\chi/d\tilde{t}$ represents the derivative with respect to the conformal time.

Deep in the IR of either of our warped throats (e.g. the one with $\chi \gg 1$), (3.46) can be reduced to a first order differential equation for χ'. Integrating this equation reveals that after some time ($\tilde{t} > 1$) the probe D3-brane propagates up the throat and escapes from the IR region, reaching the UV slice $\chi = 0$ within a finite time.[11] It is interesting to note that it takes longer and longer for the branes to escape to this slice at later and later times t_s: from (3.45), we have $|\dot{\chi}| < c/t_s$.

Let us remark briefly on the significance of the motion sickness and its time dependence, which should provide useful clues as to the nature of the dual theory. Firstly, it is worth recalling that motion of color sector eigenvalues up the throat

[10] This is a relative of Fermi seasickness, though the term "Technicolor Yawn" [100] most colorfully illustrates the connection between this class of phenomena and warped throats.

[11] If we set up the system with some 5-form flux (rather than starting with explicit D3-branes), it would be interesting to determine whether, and at what rate, D3-branes are nucleated. The analysis in this section shows that once present, color branes do not remain in the warped region for all time.

occurs in some familiar examples of AdS/CFT. One example is the case of $\mathcal{N} = 4$ supersymmetric Yang-Mills theory on a compact negatively curved space [93, 101], where the eigenvalues are subject to a negative quadratic potential. This theory is unitary, because the eigenvalues take forever to get to infinity. The system is properly treated by putting the eigenvalues in a scattering state. Another example is Fermi seasickness [102], where finite density effects draw color branes up the warped throat. If one cuts off these theories by embedding them in a warped compactification then the effect would take a finite time as long as the Planck mass is finite.

A new element in the present case is that the magnetic branes support some warping by themselves, and the color sector is subdominant in the solution. As we have just seen, particles stay down the warped throat created by the magnetic branes, suggesting that the holographic dual may be built from degrees of freedom living on them.

Altogether, there are two reasons motion sickness does not appear to be fatal in our system: (i) the fact that there is an infrared region in the absence of the color D3-branes, and (ii) the fact that even in familiar examples of gauge/gravity duality where the color branes are responsible for all the warping, unitarity is not necessarily sacrificed in the presence of a potential which pushes color branes toward the UV. There are two approaches one can take: (1) eject the offending color branes (treating the color sector as negligible, since the flavor branes provide warping anyway), or (2) wait it out (keeping the color branes in the game, since the instability takes longer at larger t_s).

In particular, in trying to better understand the field theory dual it may remain useful to think about starting with a color sector in place, since the ejection of the branes takes longer and longer as $t_s \to \infty$. As we will see in the next section, however, the number of degrees of freedom is well accounted for by junction states living on the 7-branes themselves.

3.4 Degrees of freedom in FRW holography

In Section 3.2 we found that the covariant entropy bound and the number of degrees of freedom per lattice point in the holographic dual grow as t^{d-2}. Now we will suggest a microscopic explanation for this time-dependent growth in terms of states associated to 7-7 strings and string junctions. These are natural candidates to account for the growing $\tilde{N}_{\rm dof}$, because bringing together $\Delta n > 0$ (p,q) 7-branes in a static way leads to infinite dimensional algebras [80, 81] that are realized on light states. We make this counting and the assumptions which go into it precise in Section 3.4.1.

In the gravity side, the magnetic flavor branes lead to warping and to an IR region, as we discussed in the previous sections. In the AdS/CFT correspondence, a warped geometry produces a nontrivial quasilocal stress tensor that can be used to compute the CFT energy momentum tensor and the central charge. In Section 3.4.2 we generalize this method to cosmological solutions. This provides an independent calculation of $\tilde{N}_{\rm dof}$ that agrees with the microscopic count and with the results in §3.2.5).

3.4.1 A microscopic count of degrees of freedom

In this chapter we are focusing on quantities we can calculate under control in our gravity solutions, determining from them various basic features of the putative cutoff field theory dual. This includes several independent computations showing that the number of field theoretic degrees of freedom grows with time as $\tilde{N}_{\rm dof} \propto t_{UV}^{d-2}$. In this section, we will seek a microscopic accounting of these states. In general, such a count is not guaranteed to work in any simple way; even in systems with a weak coupling limit and a large number of unbroken supercharges, $\tilde{N}_{\rm dof}$ generally suffers corrections in going from weak to strong coupling. For example, the two are related by a factor of 3/4 in the $\mathcal{N} = 4$ super Yang-Mills theory, and by a more nontrivial interpolation in other examples. Nonetheless, it is interesting to ask whether any natural count of states reproduces the parametric behavior of $\tilde{N}_{\rm dof}$ in a given example.

Rather than going to weak coupling, one may trade fluxes for branes, turning on the corresponding scalar fields, and study the microstates which are evident in that

phase [103]. For example, in the $\mathcal{N} = 4$ super Yang-Mills theory if we go out on the Coulomb branch by introducing N_c explicit D3-brane domain walls, the N_c^2 degrees of freedom of the dual gauge theory become more manifest. In that example, of course, the D3-branes source the warping, accounting for the low energy sector that indicates the existence of the field theory dual [2].

In our solutions, the 7-branes source warping in themselves. As with flavor branes in AdS/CFT, they do not come together in the backreacted solution (our time dependent solution), but in the corresponding (singular) static solution they intersect at a point (where the color branes are placed in the brane construction). Since they source some warping (like color branes normally do), there is a possibility that there are fundamental degrees of freedom of the dual theory that live on their intersection. Since they dominate at late times (and since the color branes suffer from motion sickness), they may account for the lion's share of $\tilde{N}_{\rm dof}$. We will explore this possibility in this section, finding rather encouraging results.

Consider string and string junction states stretching between 7-branes. For the generic case of $\Delta n > 0$, there is an infinite dimensional algebra generated by these junctions [80, 81].[12] If the fiber circle were not contractible, they could also a priori carry arbitrarily large momentum and winding quantum numbers around that direction. However, they ultimately back react on the geometry, the fiber circle is ultimately contractible, and Kaluza-Klein momenta are cut off by the giant graviton effect [107], so at any finite time only finitely many states are available. In this section, we will estimate the total number of degrees of freedom $\tilde{N}_{\rm dof}$ at late times by counting junctions up to a cutoff determined by backreaction and topology. We will be concerned with the t-dependence of $\tilde{N}_{\rm dof}$, and will not keep track of time-independent factors.[13] The resulting count of brane degrees of freedom will precisely match the behavior

$$\tilde{N}_{\rm dof} \sim t_{UV}^{d-2} \tag{3.47}$$

[12] There have been similar intriguing appearances of large algebras organizing states and/or dynamics in works such as [104, 105, 106].

[13] In the future it might be very interesting to analyze the factors arising from group theory to characterize the dual theory in more detail. The present calculation suggests that this is on the right track.

found above from macroscopic considerations (3.31). As we will describe below, this statement is based on two assumptions we will specify.

Let us parameterize a state by the number $n_{\rm str}$ of strings it contains stretching among the 7-branes, the winding number n_f on the fiber circle, and the momentum number k_f on the fiber circle. We will ultimately analyze all cases, with various dimensionalities for the compact and noncompact directions. Let us start with the specific case of $d = 5$, $m = 2$ (i.e. uplifted $AdS_5 \times S^5$).

We can bound $n_{\rm str}$ by the requirement that the core size of the set of $n_{\rm str}$ strings not exceed R, to avoid strong backreaction. The core size is determined from the gravitational potential, which goes like $1/r^{d_\perp - 2}$, where $d_\perp$ is the codimension (e.g. $1/r$ for particles in 3+1 dimensions, $1/r^4$ for D3-branes in ten dimensions, and so on). In our case, we need to take into account that the fiber circle is much smaller than R, so the effective codimension of the strings is 7 rather than 8. With $n_{\rm str}$ strings, the core size is given by

$$\frac{n_{\rm str}}{r_{\rm core}^5} \sim 1. \tag{3.48}$$

From this, the condition that this size not exceed the size R of the base $\mathbb{CP}^2$ is

$$r_{\rm core} \sim n_{\rm str}^{1/5} \leq R \sim t_s \sim t^{3/7} \qquad \Rightarrow \quad n_{\rm str} \leq t^{15/7}. \tag{3.49}$$

The strings can wind around the fiber circle also. If they wind $R/R_f \sim t_s \sim t^{3/7}$ times, they can detect that the fiber is contractible. So let us cut off the windings at

$$n_f \leq t^{3/7}. \tag{3.50}$$

The string may also have momentum $k_f/(R_f\sqrt{\alpha'})$ along the fiber circle. There is not a topological cutoff on k_f as for windings; the momentum is a conserved charge. However, the tower of momentum modes does not go up forever. Ultimately, it was shown in [107] that Kaluza-Klein momenta are naturally cut off in UV-complete string theoretic examples of AdS/CFT in exactly the right way to mirror the operator content of the dual field theory. In the present case, there is an important crossover at a lower scale. We may view our states as bound states of Kaluza-Klein gravitons and

(p,q) string junctions. For sufficiently small k_f, i.e. $k_f/R_f \ll R$, the energy of each stretched string is of order $R/\sqrt{\alpha'}$; the gravitons are well bound to the strings. But when k_f crosses over to become much larger than RR_f, they are not strongly bound and the system as a whole behaves like a set of relativistic Kaluza-Klein gravitons of total momentum $k_f/(R_f\sqrt{\alpha'})$. (Ultimately, as in [107], these gravitons grow into giants.) Since the gravitons are not strongly bound to the stretched strings (if bound at all), the state may no longer be fundamental. Because of this crossover, we will count k_f only up to $RR_f \sim t^{3/7}$:

$$k_f \leq t^{3/7}. \tag{3.51}$$

Finally, we need to determine whether there are additional combinatorial factors which depend on $n_{\rm str}$ arising from the algebra generated by the junctions. To start, let us consider the configurations classified in [80, 81]. There, one starts from a subset $\mathcal{S}_0$ of the (p,q) 7-branes which generates a finite Lie algebra $\mathcal{G}_0$. One then considers junctions with some prongs ending on the $\mathcal{S}_0$ branes, transforming under $\mathcal{G}_0$ according to their weight vector λ under $\mathcal{G}_0$. The rest of the prongs of these junctions form a set of n_Z strings with charge (p,q); these end on the remaining 7-branes (or some subset of them) denoted collectively by Z. The works [80, 81] show that a junction with weight λ and asymptotic charge $n_Z(p,q)$ satisfies a relation

$$\lambda\cdot\lambda = -\mathbf{J}^2 + n_Z^2(f(p,q)-1). \tag{3.52}$$

Here $\mathbf{J}^2 \geq -2$ is the self-intersection of the junction, and $f(p,q)$ is a specific function of the asymptotic charges (see for example eqn. (2.9) of the second reference in [80, 81]). Since $\lambda\cdot\lambda \geq 0$, $f(p,q) \geq 1$ in the generic cases where the full system builds up an infinite algebra $\mathcal{G}_{inf}$. In particular, for $f(p,q) > 1$ the right hand side of (3.52) can become large and positive by increasing n_Z, and the equation may be satisfied with longer and longer weight vectors λ in $\mathcal{G}_0$. (This is in contrast to the cases with $f(p,q) < 1$, where at most a finite number of weights can satisfy (3.52).) It is conjectured in [80, 81] that states with $\mathbf{J}^2 = -2$ have the special feature that they can be realized by "Jordan Open Strings", strings that end on two of the 7-branes (crossing cuts emanating from the 7-branes in the process). We will count these

strings.

Given that, next we need to know if there are any multiplicities in the tower of available states which grow with $n_{\rm str}$ at large $n_{\rm str}$. As mentioned below (5.52) of the first reference in [80, 81], given a weight vector of length squared $\lambda \cdot \lambda$, there is a degeneracy given by the dimension of its Weyl orbit. However, this number cannot grow arbitrarily large; it is bounded by the dimension of the Weyl group of $\mathcal{G}_0$. In particular, if we consider any individual representation of $\mathcal{G}_0$, the number of weight vectors degenerate with the longest weight vector is given by the Weyl group, and does not grow with n.

There are additional degeneracies in the weight lattice beyond those required by Weyl reflections, but these involve multiple representations. As long as the number of these representations which arise in our physical system do not grow too fast with $n_{\rm str}$, the count we propose here holds up. It would be interesting to analyze this explicitly for specific Lie groups. This question of which charged matter representations appear in F theory compactifications has been studied previously in string theory for phenomenological model building, and similar techniques may be useful in the present case.

Next, let us consider more general configurations which build up $\Delta n > 0$. One way to think about these is by iterating the procedure just described, considering junctions stretching between the entire set of 7-branes corresponding to the infinite group $\mathcal{G}_{inf}$, and an additional (p, q) 7-brane. This works similarly to the above case, except now the Cartan matrix of the $\mathcal{G}_{inf}$ set of sevenbranes is of indefinite signature. This by itself would allow for an infinite number of weight vectors of a fixed length squared (schematically of the form $\lambda_+^2 - \lambda_-^2$ given the indefinite metric). So in the equation (3.52) there would be an infinite number of solutions even for *finite* n_Z. However, this infinite number is itself cut off by insisting that the corresponding junctions be made up of at most of order $n_{\rm str}$ strings. This limits λ_+ and λ_- above to be at most of order $n_{\rm str}$ in length, and counting their degeneracy is similar to the above count for finite groups.

Putting this all together, the number of available degrees of freedom is obtained

from the product of the maximum values of $n_{\rm str}$, n_f, and k_f:

$$\tilde{N}_{\rm dof} \sim (n_{\rm str} n_f k_f)_{\rm max} \sim t^{15/7+2\times 3/7} = t^3 = t^{d-2} \tag{3.53}$$

for $d = 5$.

Next, let us work out $\tilde{N}_{\rm dof}$ for $d = 3$, $m = 1$ (i.e. an FRW uplift of $AdS_3 \times S^3 \times T^4$). In this case, the T^4 is of fixed size, independent of t, so (3.48) becomes

$$\frac{n_{\rm str}}{r_{\rm core}} \sim 1. \tag{3.54}$$

As a result, (3.49) becomes

$$r \sim n_{\rm str} \leq R \sim t_s \sim t^{1/3} \qquad \Rightarrow \quad n_{\rm str} \leq t^{1/3} \tag{3.55}$$

Again, the strings can wind around the fiber circle as well. If they wind $R/R_f \sim t_s \sim t^{1/3}$ times, they see that the fiber is contractible. So we cut off the windings at

$$n_f \leq t^{1/3} \tag{3.56}$$

and also the momentum

$$k_f \leq t^{1/3}. \tag{3.57}$$

Altogether we get

$$\tilde{N}_{\rm dof} \sim (n_{\rm str} n_f k_f)_{\rm max} \sim t = t^{d-2} \tag{3.58}$$

for $d = 3$.

Having checked it now for two examples, let us finally consider all cases, varying the dimensionalities of the FRW spacetime and the uplifted internal base space. For d noncompact FRW dimensions and a $2m$ dimensional uplifted base space, together with one fiber circle and $9 - d - 2m$ toroidal directions, we have

$$n_{\rm str} \leq t_s^{d+2m-4}, \qquad n_f \leq t_s, \qquad k_f \leq t_s \tag{3.59}$$

where t_s is the 10-dimensional string frame time coordinate (3.6). So $\tilde{N}_{\rm dof}$ goes like

t_s^{d+2m-2}. Recall that t_s goes like t^{1/c^2} in terms of the Einstein frame time coordinate (3.10), and $c^2 = (d+2m-2)/(d-2)$ (3.11). Therefore for the general case, we have

$$\tilde{N}_{\rm dof} \sim t^{d-2}\,, \tag{3.60}$$

whose time dependence agrees precisely with the macroscopic calculations of $\tilde{N}_{\rm dof}$.

3.4.2 Deriving $\tilde{N}_{\rm dof}$ from the quasilocal stress tensor

In the AdS/CFT correspondence, there are several ways to compute the number of degrees of freedom per lattice point of the CFT. For instance, Brown and Henneaux [108] used the conformal structure of asymptotically AdS_3 to identify the central charge, which was rederived from different points of view in [109, 110]. The conformal anomaly can also be computed from the variation of the renormalized effective action under a conformal transformation [3, 111]. Those analyses, however, depend highly on the conformal symmetry, or on the asymptotic structure of AdS spacetime. Since our spacetime does not have such a structure, we need to apply other methods.

One possible method is to excite our FRW spacetime and produce a black hole with a hyperbolic horizon in the IR region. The horizon entropy will be identified with that of the effective field theory, from which we could extract $\tilde{N}_{\rm dof}$. This is analogous to the entropy computation of an AdS black hole in [112].

Another method, which will be applied here, is to compute Brown and York's quasilocal stress tensor [113] and identify it with the expectation value of the stress tensor in the boundary theory. In the context of AdS/CFT, this was used to compute the Casimir energy and $\tilde{N}_{\rm dof}$ of the boundary theory in [114, 115, 116, 110]. This method can be generalized to the dS/dS correspondence [18, 19] and to our FRW model. In order to see how it works, let us first review the definition of the quasilocal stress tensor and then use it to calculate $\tilde{N}_{\rm dof}$ of the dual theories in both dS/dS and FRW.

Quasilocal stress tensor

Let us consider a spacetime manifold $\mathcal{M}$ with a timelike boundary $\partial\mathcal{M}$ and space-time metric $g_{\mu\nu}$. This boundary could be a regularized one at some coordinate cutoff r_c. Let n_μ be the outward pointing normal vector to $\partial\mathcal{M}$, normalized so that $n_\mu n^\mu = 1$. The induced metric on the boundary is given by

$$\gamma_{\mu\nu} = g_{\mu\nu} - n_\mu n_\nu, \tag{3.61}$$

where a pullback onto $\partial\mathcal{M}$ is understood. The Einstein action including a boundary term is

$$S = \frac{M_d^{d-2}}{2}\int_{\mathcal{M}} d^dx\sqrt{-g}(\mathcal{R} - 2\Lambda) - M_d^{d-2}\int_{\partial\mathcal{M}} d^{d-1}x\sqrt{-\gamma}\Theta + M_d^{d-2}S_{\rm ct}[\gamma_{ab}], \tag{3.62}$$

where Θ is the trace of the extrinsic curvature of the boundary

$$\Theta_{\mu\nu} = -\gamma_\mu{}^\rho\nabla_\rho n_\nu, \tag{3.63}$$

$S_{\rm ct}$ is a suitably chosen local functional of the intrinsic geometry γ_{ab} of the boundary, and a, b are coordinate indices on the boundary. The quasilocal stress tensor [113] is given by

$$\tau^{ab} \equiv \frac{2}{\sqrt{-\gamma}}\frac{\delta S}{\delta\gamma_{ab}} = M_d^{d-2}\left(\Theta^{ab} - \Theta\gamma^{ab} + \frac{2}{\sqrt{-\gamma}}\frac{\delta S_{\rm ct}}{\delta\gamma_{ab}}\right). \tag{3.64}$$

The AdS/CFT correspondence relates the expectation value of the stress tensor $\langle T_{ab}\rangle$ in the dual field theory to the limit of the quasilocal stress tensor τ_{ab} as the regularized boundary at r_c is taken to infinity:

$$\sqrt{-h}h^{ab}\langle T_{bc}\rangle = \lim_{r_c\to\infty}\sqrt{-\gamma}\gamma^{ab}\tau_{bc}, \tag{3.65}$$

where h_{ab}, the background metric on which the dual field theory is defined, is related to the boundary metric γ_{ab} by a conformal transformation. The counterterms in $S_{\rm ct}[\gamma_{ab}]$ are chosen appropriately so as to cancel all divergences when the limit is taken. This has a natural interpretation on the dual field theory side: we use local

counterterms to obtain a finite, renormalized expectation value of the stress tensor in the field theory.

$\tilde{N}_{\mathbf{dof}}$ in AdS/CFT and dS/dS

Let us calculate the quasilocal stress tensor in AdS_d and dS_d, both sliced by dS_{d-1}. The metric is given by

$$ds^2_{(A)dS_d} = R^2 dw^2 + f(w)^2 ds^2_{dS_{d-1}}, \qquad ds^2_{dS_{d-1}} = h_{ab} dx^a dx^b, \tag{3.66}$$

where $f(w) = \sinh w$ for AdS_d and $\sin w$ for dS_d. Here R is the curvature radius of both $ds^2_{(A)dS_d}$ and $ds^2_{dS_{d-1}}$.

In the AdS_d case, the AdS/CFT correspondence says that the bulk is dual to a boundary conformal field theory living on dS_{d-1}. In the dS_d case, the dS/dS correspondence [18, 19] conjectures that the bulk is dual to two effective field theories living on dS_{d-1}, both of which are cut off at an energy scale $1/R$ and coupled to $(d-1)$-dimensional gravity and to each other.

Coming back to our calculation, let us choose a regularized boundary at $w = w_c$. It has an induced metric $\gamma_{ab} = f(w)^2 h_{ab}$, where h_{ab} is the dS_{d-1} metric on which the field theory is defined. The extrinsic curvature tensor is

$$\Theta_{ab} = -\frac{1}{R} f(w_c) f'(w_c) h_{ab}, \tag{3.67}$$

and before adding the counterterms the quasilocal stress tensor is given by

$$\tau_{ab} = \frac{(d-2)M_d^{d-2}}{R} f(w_c) f'(w_c) h_{ab} = \begin{cases} \dfrac{(d-2)M_d^{d-2}}{R} (\sinh w_c \cosh w_c) h_{ab}, & \text{for } \mathrm{AdS}_d, \\ \dfrac{(d-2)M_d^{d-2}}{R} (\sin w_c \cos w_c) h_{ab}, & \text{for } \mathrm{dS}_d. \end{cases} \tag{3.68}$$

In the AdS_d case, the stress tensor is divergent as w_c goes to infinity, and the counterterms in S_{ct} renormalize it to

$$\tau_{ab} \sim \frac{M_d^{d-2}}{R} e^{-(d-3)w_c} h_{ab} \tag{3.69}$$

for large w_c, so the limit in (3.65) becomes finite and gives $\langle T_{ab}\rangle \sim (M_d^{d-2}/R)h_{ab}$.[14] Matching this to the expectation value of the CFT stress tensor on dS_{d-1} with $\tilde{N}_{\rm dof}$ degrees of freedom per lattice point

$$\langle T_{ab}\rangle \sim \frac{\tilde{N}_{\rm dof}}{R^{d-1}} h_{ab}, \tag{3.70}$$

we arrive at the correct number of degrees of freedom per lattice point

$$\tilde{N}_{\rm dof} \sim M_d^{d-2} R^{d-2} \tag{3.71}$$

in the context of AdS/CFT. In fact we do not have to take w_c to infinity to get this parametric result. We could set w_c to be of order 1 and forget about the counterterms (because there are no divergences to cancel if w_c is fixed at order 1, and including the counterterms would only change the numerical coefficients which we are not keeping track of). This gives the same parametric result for $\tilde{N}_{\rm dof}$.

This perspective is important for the dS/dS correspondence, because in this case the w coordinate is bounded and we cannot take w_c to infinity. What we can do is fix w_c at order 1, and by the same argument we get $\tilde{N}_{\rm dof} \sim M_d^{d-2} R^{d-2}$. This means that the number of degrees of freedom per lattice point for the dual theory on dS_{d-1} is parametrically the same as the Gibbons-Hawking entropy of dS_d. This was confirmed by the concrete brane construction for the dS/dS correspondence in [7].

It is interesting to note that the quasilocal stress tensor (3.68) vanishes at $w_c = \pi/2$ in the dS_d case. This does not contradict our previous result $\tilde{N}_{\rm dof} \sim M_d^{d-2} R^{d-2}$, because one can reliably deduce $\tilde{N}_{\rm dof}$ of the dual field theory only well below its cutoff. The "UV slice" $w_c = \pi/2$ corresponds exactly to the energy scale where the effective field theory is cut off and coupled to gravity. The vanishing of the quasilocal stress tensor is reminiscent of the gravitational dressing effect discussed in [18, 19]. As we shall see in the next subsection, this also happens in our FRW spacetime.

Before going on, we should note that the advantage of being able to take w_c

[14] Strictly speaking, the limit is nonzero only for odd d. In even (bulk) dimensions, the limit vanishes and so does the trace anomaly of a CFT in odd (boundary) dimensions. We can still get $\tilde{N}_{\rm dof}$ by other means.

to infinity in the AdS_d case is that we can calculate the exact $\tilde{N}_{\rm dof}$ including the numerical coefficients. To demonstrate this, let us work for simplicity in $d = 3$. Only one counterterm is needed in this case, which is simply a cosmological constant on the boundary: $S_{\rm ct} = -(1/R)\int_{\partial\mathcal{M}}\sqrt{-\gamma}$. The quasilocal stress tensor becomes

$$\tau_{ab} = \frac{M_3}{R}(\sinh w_c \cosh w_c - \sinh^2 w_c)h_{ab}, \tag{3.72}$$

which gives $\langle T_{ab}\rangle = (M_3/2R)h_{ab}$ upon taking w_c to infinity. The stress tensor from $\tilde{N}_{\rm dof}$ free massless scalar fields in dS_2 may be calculated in a standard way,[15] giving $\langle T_{ab}\rangle = (\tilde{N}_{\rm dof}/24\pi R^2)h_{ab}$. This can also be obtained from the trace anomaly $\langle T^a_a\rangle = (c/24\pi)\mathcal{R}$ of a two-dimensional CFT. Matching this result to the quasilocal stress tensor, we arrive at

$$c \equiv \tilde{N}_{\rm dof} = 12\pi M_3 R, \tag{3.73}$$

which agrees exactly with [111, 110].

$\tilde{N}_{\rm dof}$ in the FRW dual

Let us now calculate the quasilocal stress tensor in our FRW spacetime. We start with the warped metric

$$ds_d^2 = c^2(\eta^2 - w^2)^{c-1}(dw^2 - d\eta^2 + \eta^2 dH_{d-2}^2), \tag{3.74}$$

and choose the regularized boundary to be a surface of constant α where α is defined by $w = \alpha\eta$ with $0 < \alpha < 1$. This is a hypersurface of constant energy scale relative to the UV cutoff: $\alpha \approx 1$ corresponds to the IR, while $\alpha \ll 1$ corresponds to the UV. The exact value of α is not essential in our analysis, as long as it is of order 1. This is because our main interest is the parametric dependence of the quasilocal stress tensor on η (or t_{UV}), and this is not affected by the exact location of the hypersurface. One may also consider RG flows in our FRW geometry, as in AdS or dS [118, 119, 120, 121, 122], and relate $\tilde{N}_{\rm dof}$ in the IR to its value in the UV. The

[15] For two-dimensional (and therefore conformally flat) spacetimes one can use Eq. (6.136) of [117]. Note that their metric convention is the opposite of ours.

η-dependence of $\tilde{N}_{\rm dof}$ is not affected by the energy scale.[16]

From the coordinate transformation $\chi = \frac{1}{2}\log\frac{\eta+w}{\eta-w}$, a hypersurface of constant α is also a hypersurface of constant $\chi = \operatorname{arctanh}\alpha$, so it is much easier to calculate the quasilocal stress tensor in the usual FRW coordinates

$$ds_d^2 = -dt^2 + c^2t^2(d\chi^2 + \cosh^2\chi\, dH_{d-2}^2). \tag{3.75}$$

The induced metric on the regularized boundary at $\chi = \chi_c$ is given by

$$\gamma_{ab}dx^a dx^b = -dt^2 + c^2t^2\cosh^2\chi\, dH_{d-2}^2, \tag{3.76}$$

and the extrinsic curvature can be calculated as

$$\Theta_{tt} = 0, \qquad \Theta_{ij} = -\frac{\tanh\chi_c}{ct}\gamma_{ij}, \tag{3.77}$$

where i, j are the coordinate indices on $\mathbb{H}_{d-2}$. The quasilocal stress tensor is given by

$$\tau_{tt} = (d-2)\frac{M_d^{d-2}}{ct}(\tanh\chi_c)\gamma_{tt}, \qquad \tau_{ij} = (d-3)\frac{M_d^{d-2}}{ct}(\tanh\chi_c)\gamma_{ij}, \tag{3.78}$$

It is interesting to note that this corresponds to a perfect fluid with equation of state $w = (d-3)/(d-2)$. It has vanishing pressure in $d = 3$.

The next step is to calculate the expectation value of the stress tensor in the dual field theory, which lives on the background metric $h_{ab} = \gamma_{ab}$ and has $\tilde{N}_{\rm dof}$ degrees of freedom per lattice point:

$$\langle T_{ab}\rangle \sim \frac{\tilde{N}_{\rm dof}}{t^{d-1}}h_{ab}. \tag{3.79}$$

This can be obtained either on dimensional grounds or by using Eq. (6.134) of [117], noting that γ_{ab} is conformally flat. Let us set χ_c to be of order 1 as this is equivalent to setting α to be of order 1. We match $\langle T_{ab}\rangle$ to the quasilocal stress tensor (3.78)

[16] $\alpha = 1$ is a singular surface and we do not set the hypersurface there. In a broader picture, this singular surface is replaced by the Coleman–de Luccia instanton and connected to the parent de Sitter space.

and obtain

$$\tilde{N}_{\rm dof} \sim M_d^{d-2} t_{UV}^{d-2}, \tag{3.80}$$

where we have replaced t with t_{UV} because on a hypersurface of constant α we have $t = (1-\alpha^2)^{c/2} t_{UV} \sim t_{UV}$ from (3.13). This is in agreement with the microscopic count of the number of degrees of freedom.

Just as in the dS/dS correspondence, the quasilocal stress tensor (3.78) vanishes at $\chi_c = 0$, corresponding to the UV slice $w = 0$. Again this suggests renormalization from the $(d-1)$-dimensional gravitational effects.

3.5 Correlation functions

In this section we compute two-point functions for massive and massless scalar fields in our solution. These should provide detailed information about the nature of the $(d-1)$-dimensional theory. That theory lives on an FRW geometry, has time-dependent and scale-dependent couplings, and is necessarily strongly coupled in order to reproduce a large-radius gravity solution. We will leave a complete interpretation of our Green's functions to future work, but will note some of their interesting features below.

3.5.1 Massive Green's functions

In AdS/CFT it is well understood how gravitational scattering amplitudes behave like field theory correlators. For example, massive propagators in the bulk (which are exponentially suppressed in flat space) turn into power-law CFT two-point functions in the dual theory through the effects of the warp factor, which is a strong function of the radial distance r. Because of the warp factor, geodesics do not go along fixed-r trajectories; they can take advantage of the warp factor and go along a shorter path by moving in the radial direction. This leads to the power law rather than exponential correlators. (A simple discussion of this can be found in [95].)

Let us ask the analogous question in our case. Our dual theory is formulated on an FRW spacetime and has a time and scale-dependent coupling corresponding to

the radius R of $\hat{B}$, which depends on $t = (t_{UV}^{2/c} - w^2)^{c/2}$. (As noted above (3.16), this quantity depends more strongly on the radial scale coordinate w than on time t_{UV}.) As we saw in Section 3.2.5 and Section 3.4, our theory is cut off at a finite scale, but accumulates additional field theoretic degrees of freedom as time evolves forward. As a result, the theory is not conformally invariant. Nonetheless we will see that there is one sector of massive bulk fields – KK modes on the base $\hat{B}$ – which have power law correlators.

We will now compute the leading behavior of the 2-point Green's functions for particles of mass $m(t) \propto t^{-\alpha}$ in our geometry. To find the dominant trajectory, we must solve the equations obtained by varying the action

$$S = -\int d\lambda\, m(t)\sqrt{\dot{t}^2 - c^2 t^2\left(\dot{\chi}^2 + \cosh^2\chi\,\dot{\tilde{\chi}}^2 + \dots\right)}, \tag{3.81}$$

where "dot" represents a derivative with respect to the worldline coordinate λ and $dH_{d-1}^2 = d\chi^2 + \cosh^2\chi(d\tilde{\chi}^2 + \sinh^2\tilde{\chi}\, d\Omega_{d-3}^2)$. We are interested in computing the propagator between the points $(t, \chi, \tilde{\chi})$ and $(t, \chi, \tilde{\chi} + \Delta\tilde{\chi})$. Note that because of the time-dependent mass, the calculation of the dominant trajectory is not equivalent to a calculation of the geodesic distance between the two points in our spacetime.

Our result can only depend on time t and on the geodesic distance L between two points in $\mathbb{H}_{d-1}$ because of the isometries of $\mathbb{H}_{d-1}$. For two points on the same χ-surface, the geodesic distance L in $\mathbb{H}_{d-1}$ is given by[17]

$$\cosh L = \cosh^2\chi\,\cosh\Delta\tilde{\chi} - \sinh^2\chi\,. \tag{3.82}$$

The central (UV) slice of our warped geometry is at $\chi = 0$. We will be interested both in Green's functions formulated deep in the IR at $\chi \gg 1$, and also in Green's functions formulated at the UV slice $\chi = 0$.

Since the propagator can only depend on t and on the geodesic distance L, it is actually easier to do the calculation at constant $\tilde{\chi}$ and varying χ, and at the end

[17]This is the hyperbolic law of cosines, and it can be obtained by analytic continuation from a similar formula on a sphere, or simply from the dot product in the embedding space.

replace this by L. Consider a particle with mass

$$m(t) = \frac{n_\alpha}{t^\alpha}\,, \tag{3.83}$$

where n_α is a constant of dimension $1-\alpha$. In the $d=5$ case, $\alpha = 1$, $4/7$, and $1/7$ for KK modes, closed strings, and 7-7 strings, respectively. Define the new coordinates

$$\tau = \frac{t^{1-\alpha}}{1-\alpha}, \qquad y = (1-\alpha)c\chi, \qquad (\alpha \neq 1) \tag{3.84}$$

and

$$\tau = \log(t/\ell), \qquad y = c\chi, \qquad (\alpha = 1). \tag{3.85}$$

Let us first address the KK modes. Setting $n_1 \equiv n_{KK}$ we see that the action (3.81) at constant $\tilde{\chi}$ reduces to

$$S = -n_{KK}\int d\lambda\sqrt{\dot{\tau}^2 - \dot{y}^2} \qquad (\alpha = 1). \tag{3.86}$$

This is equivalent to the action for a particle with a constant mass in flat spacetime. The resulting two-point function is $e^{-n_{KK}\Delta y}$, exponentially suppressed in $\Delta y = c\Delta\chi = cL$.

However, this is a *power law* suppression in the geodesic distance ΔX in the $(d-1)$-dimensional spacetime $-dt_{UV}^2 + c^2 t_{UV}^2 dH_{d-2}^2$ on which the $d-1$ theory lives. Working at $\chi = 0$, we have the geodesic distance $L = \Delta\tilde{\chi}$ according to (3.82). We can see the power law behavior by making a coordinate transformation

$$X = t_{UV}\sinh(c\tilde{\chi})\ ,\ T = t_{UV}\cosh(c\tilde{\chi})\,, \tag{3.87}$$

where the metric is Minkowskian on the plane spanned by X and T. Taking our two points at the same T, i.e. taking $\tilde{\chi}_1 = -\tilde{\chi}_2 = \Delta\tilde{\chi}/2$, we obtain the geodesic distance (for $\Delta\tilde{\chi} \gg 1$)

$$\Delta X = 2t_{UV}\sinh(c\Delta\tilde{\chi}/2) \approx t_{UV}e^{c\Delta\tilde{\chi}/2}, \tag{3.88}$$

and hence our exponential result in $\Delta\tilde{\chi}$ becomes a power law in ΔX. The Green's

function is of the form

$$G(\Delta x) \sim e^{-n_{KK}cL} \sim e^{-n_{KK}c\Delta\tilde{\chi}} \sim \frac{1}{(\Delta x)^{2n_{KK}}}, \tag{3.89}$$

where $\Delta x \equiv \Delta X/ct_{UV}$ is the comoving geodesic distance.

This result is quite intriguing, as we obtain power law correlators from a massive KK mode propagator, which is reminiscent of what happens in ordinary AdS/CFT. However, here the mechanism for this involves the time dependence of the mass. The propagator deep in the IR (large χ) and for large $\Delta\tilde{\chi}$, has an additional exponential suppression as a function of χ,

$$G(\chi; \Delta x) \sim e^{-n_{KK}cL} \sim e^{-n_{KK}c(2\chi+\Delta\tilde{\chi})} \sim e^{-2cn_{KK}\chi}\frac{1}{(\Delta x)^{2n_{KK}}}\,, \tag{3.90}$$

where we used $L \approx 2\chi + \Delta\tilde{\chi}$ from the large χ, $\Delta\tilde{\chi}$ limit of (3.82). Recalling that $\chi = \frac{1}{2}\log\frac{\eta+w}{\eta-w}$ (3.12), we find that the propagator has a power law scaling with w/η. This energy scaling of the correlator is again characteristic of a CFT, where power-law wavefunction renormalization is produced by nontrivial anomalous dimensions. Note that these formulas only apply in the $c > 1$ case, since for $c = 1$ the KK masses are constant, and we do not get warping or this power law behavior.

Next, let us analyze the correlation functions for other massive scalar fields, those for which $\alpha \neq 1$.

$$S = -n_\alpha \int d\lambda \sqrt{\dot{\tau}^2 - \tau^2\dot{y}^2} \qquad (\alpha \neq 1). \tag{3.91}$$

This action is equivalent to the action for a particle with constant mass n_α in the Milne universe, and the dominant trajectory is obtained by analytic continuation from flat space:

$$S_{cl} = 2in_\alpha\tau \sinh\frac{\Delta y}{2}\,, \tag{3.92}$$

where the sign can be determined by the $-i\epsilon$ prescription implicit in the square root. Approximating the propagator by $e^{iS_{cl}}$ and rewriting the action in terms of the

geodesic distance L obtains

$$G(t;L) \sim \exp\left[-2n_\alpha \frac{t^{1-\alpha}}{1-\alpha} \sinh\frac{(1-\alpha)cL}{2}\right] . \tag{3.93}$$

Let us consider the massive fields with $\alpha < 1$ (closed strings and 7-7 strings) at large $\Delta\tilde{\chi} \gg 1$, in which case we have $L \approx \Delta\tilde{\chi} + 2\log\cosh\chi$ from (3.82). Note that this expression is valid for both small and large χ. In terms of the geodesic distance ΔX (3.88) in the $(d-1)$-dimensional FRW spacetime, the massive Green's function (3.93) has (for large $\Delta\tilde{\chi} \gg 1$) an exponential suppression

$$G(t;\Delta X) \sim \exp\left[-n_\alpha \frac{t^{1-\alpha}}{1-\alpha}\left(\frac{\Delta X}{t_{UV}}\right)^{1-\alpha} (\cosh\chi)^{c(1-\alpha)}\right] \sim \exp\left[-n_\alpha \frac{(\Delta X)^{1-\alpha}}{1-\alpha}\right], \tag{3.94}$$

where we have used $t_{UV} = t(\cosh\chi)^c$ from the coordinate transformation (3.12). It is interesting to note that the $\alpha < 1$ Green's function in this form is independent of χ (although there could be χ-dependent prefactors that we have not kept track of).

These $\alpha < 1$ fields become parametrically heavy at late times, dying away at long distances as compared to the KK modes with their power law correlators. But they remain part of the theory: as we have seen in Section 3.4.1, the set of 7-7 strings and junctions which do not strongly backreact on the geometry make a leading contribution to the count of degrees of freedom. This is somewhat reminiscent of off-diagonal matrix elements in the $\mathcal{N} = 4$ SYM theory out on its Coulomb branch: these are parametrically heavy at large AdS radius as compared to KK modes, but they cannot be decoupled from the system.

3.5.2 Massless Green's functions

One can potentially learn about the field theory dual of a warped gravity solution such as ours by studying the massless correlation functions. In this section, we give the correlation function of a massless scalar field in our open FRW spacetime, considering the case where it comes from a Coleman–de Luccia (CdL) decay [123]. Details on deriving correlation functions in a general d-dimensional CdL geometry, including

an explicitly Lorentzian prescription without the need to analytically continue the eigenmode expansion, are presented in Appendix 3.A.

The calculation is of interest more generally, as it requires developing tools to treat pseudotachyon modes [86] which arise from Hubble expansion. These are infrared modes which do not oscillate with time, but also do not grow large enough to significantly affect the background solution. Such modes arise for $c > 1$, as explained in Section 3.A.3. In general, these may be treated by putting them in a scattering state and computing correlation functions as expectation values in this state. The method we use here involves choosing a particular state, the Hartle-Hawking vacuum that one obtains from the analytic continuation of the Euclidean CdL geometry.

We consider a minimally coupled massless scalar field ϕ in our FRW background

$$ds_d^2 = -dt^2 + c^2 t^2 dH_{d-1}^2, \qquad dH_{d-1}^2 = d\chi^2 + \cosh^2\chi \, dH_{d-2}^2, \tag{3.95}$$

where the scale factor $a(t) = ct$ is correct at late times. If this FRW spacetime comes from a CdL decay, the scale factor has to behave like $a(t) = t + \mathcal{O}(t^3)$ for small t, so that the big bang $t = 0$ is just a coordinate singularity.

We are interested in the large t behavior of the equal-time correlator

$$G(t, \chi, \Delta\tilde{\chi}) \equiv \langle \phi(t, \chi, \Delta\tilde{\chi}) \phi(t, \chi, 0) \rangle, \tag{3.96}$$

where we have put the two points on a hypersurface of constant χ, corresponding to a given energy scale as discussed in Section 3.4.2. In particular, $\chi = 0$ corresponds to the UV and $\chi \gg 1$ corresponds to the IR of the dual field theory. We use $\Delta\tilde{\chi}$ to denote the geodesic separation of the two points in the $\mathbb{H}_{d-2}$ directions. In Appendix 3.A we organize the correlation function into an expansion in the large t and large $\Delta\tilde{\chi}$ limit. The first two leading terms turn out to be

$$G_{\text{leading}}(t, \chi, \Delta\tilde{\chi}) \sim \Delta\tilde{\chi} + 2 \log\cosh\chi, \tag{3.97}$$

$$G_{\text{subleading}}(t, \chi, \Delta\tilde{\chi}) \sim \frac{t^{(d-2)(\sqrt{1-1/c^2}-1)}}{\cosh^{d-2}\chi} e^{-(d-2)\Delta\tilde{\chi}/2} (\Delta\tilde{\chi} + 2\log\cosh\chi), \tag{3.98}$$

up to terms that are "pure gauge".[18] The same leading term was obtained in [21, 22].

We rewrite the correlation function in terms of the geodesic distance ΔX in $d-1$ dimensions, which was derived in Section 3.5.1 to be $\Delta X \approx t_{UV} e^{c\Delta\tilde{\chi}/2}$. From the coordinate transformation (3.12), t_{UV} and t are related by

$$t_{UV} = t(\cosh\chi)^c. \tag{3.99}$$

The leading contribution (3.97) to the correlation function becomes

$$G_{\text{leading}}(t,\chi,\Delta X) \sim \log\frac{\Delta X}{t_{UV}} + c\log\cosh\chi = \log\frac{\Delta X}{t}, \tag{3.100}$$

where we have used (3.99) in the last equality. We note that this leading term is present for both $c > 1$ and $c = 1$, and it is independent of the dimension d. This suggests an interpretation of it as the contribution from the zero mode of ϕ localized on the UV slice.

The subleading contribution to the correlation function in terms of ΔX is

$$G_{\text{subleading}}(t,\chi,\Delta X) \sim \frac{t^{(d-2)(\sqrt{1-1/c^2}-1)}}{\cosh^{d-2}\chi}\left(\frac{t_{UV}}{\Delta X}\right)^{(d-2)/c}\left(\log\frac{\Delta X}{t_{UV}} + c\log\cosh\chi\right) \tag{3.101}$$

$$= \frac{t^{(d-2)(\sqrt{1-1/c^2}-1+1/c)}}{(\Delta X)^{(d-2)/c}}\log\frac{\Delta X}{t}, \tag{3.102}$$

where we have used (3.99) in the second line. This term is dominated by contributions from the pseudotachyonic modes, and is present only for $c > 1$. This is the case we have focused on in this chapter, which has a warped geometry with a consistent description in terms of a low-energy $(d-1)$-dimensional dual.

In order to holographically interpret these results for $c > 1$ in detail, it is necessary to understand better the behavior of a strongly coupled field theory with time and scale dependent couplings on a $(d-1)$-dimensional FRW background. The strong

[18] This is because the massless correlator on a compact space such as the Euclidean CdL geometry is only well-defined up to arbitrary constants and linear functions of the coordinates. See a more detailed discussion in Section 3.A.1.

coupling will limit our ability to compute, but it will be interesting to see if one can determine enough about this theory to make detailed comparisons with results such as (3.101). We will leave an in-depth study of this for future work.

3.6 Future directions: Magnetic flavors and time-dependent QFT

This work raises many interesting questions, which we have only begun to explore. In this section we describe a few of them.

On the gravity side, we have seen that in the presence of sufficiently many magnetic flavor branes to uplift AdS/CFT to cosmology, one has simple time-dependent solutions, whereas the would-be static solutions are singular (as observed before in [75] via another class of time-dependent F-theory solutions). We have exhibited a warped metric on these solutions, and have obtained results consistent with the interpretation of the corresponding low energy region as a $(d-1)$-dimensional holographic dual.

It would be very interesting to understand directly from a field-theoretic point of view where the distinction between $\Delta n < 0$ and $\Delta n \geq 0$ comes from. If there is a condition on the number of magnetic flavors (holding fixed other quantities) which corresponds to $\Delta n < 0$, the above results may suggest that time-dependent effects in field theory could change this condition. Time dependent couplings affect the scaling dimensions of the corresponding operators in the effective Lagrangian.[19] On sufficiently short timescales, of course, the system becomes insensitive to the time-dependent couplings. Perhaps this is related to the finite cutoff we are left with in our late-time non-gravitational field theories.

Even at finite times, the holographic description of our system will be very interesting to develop further. The dual theory has time-dependent running couplings and (depending on our choice of conformal frame) in general lives on its own FRW geometry. These features render it somewhat complicated to match in detail the correlation functions computed in Section 3.5 and Appendix 3.A to quantities in the

[19] One interesting new effect of time-dependent couplings in quantum field theory was discussed in [124].

holographic dual, a task we therefore leave to (near-)future work.

A crucial step in a holographic formulation of cosmology is the identification of the correct microscopic degrees of freedom. In the solutions presented in this work, such states are predominantly given by string junctions extended between the magnetic flavor branes. We computed the number of degrees of freedom $\tilde{N}_{\rm dof}$ in several ways, and found agreement between the gravity and field theory sides. This generalizes the microscopic calculation of the de Sitter entropy of [7] to a time-dependent cosmology. While some of our results are specific to the class of solutions presented in Section 3.2, our methods suggest a concrete framework for holographic cosmology, which may have wider applications. Yet another method would be to put the system at finite temperature by adding a black brane and computing its entropy – we hope to pursue this calculation further.

Finally, we expect our results here to translate into a clearer understanding of appropriate observables in cosmological spacetimes. There have been a number of interesting attempts to find a consistent framework in which to define probabilities in cosmology. In our view, this program will likely benefit from concrete study of the structure of UV complete time-dependent backgrounds, in the same way as occurred in black hole physics. There, analyzing the dynamics of brane solutions in string theory led to black hole entropy counts and ultimately to the AdS/CFT correspondence. The details of particular examples may not be of central importance in the end, but can provide much needed checks and may lead us toward the right principles.

On this note, it would be extremely interesting to determine to what extent the magnetic flavor branes which play a key role here (and in other landscape constructions which use F-theory [36]) are generic in cosmological solutions with holographic duals. In general there is a longer list of "uplifting" possibilities, including starting from a larger total dimensionality $D > 10$ (the more generic case) and/or compactifying on more general curved manifolds [33]. Magnetic flavors bring in a new source of strong coupling – in addition to the strong 't Hooft coupling required to formulate large-radius gravity – and it would be interesting to further understand their role in the theory.

3.A Correlation functions in general CdL geometry

In this appendix we develop an exact formalism for calculating correlation functions in a general CdL geometry. One of our main goals is an explicitly Lorentzian formula (3.133) for the real-time correlator in the FRW region of the CdL geometry, so that one can apply it without having to analytically continue the Euclidean modes into Lorentzian signature. This is very desirable in any calculation away from the thin-wall limit, because in general the exact eigenmodes are not analytically tractable. One can certainly make approximations or compute them numerically, but these are not useful for analytic continuation because one cannot reliably continue an approximate solution.[20] Instead, we can derive an exact Lorentzian formula (3.133), and if necessary make approximations from there. This is the approach of this appendix.

In Section 3.A.1 we deveop a Euclidean prescription (3.119) for the correlation function. This is a relatively straightforward generalization of the discussion in Appendix A of [21, 22] to arbitrary dimensions and arbitrary scale factors.[21] In Section 3.A.2 we analytically continue (3.119) to an exact, Lorentzian formula (3.133), with extra care given to the choice of integration contours. Section 3.A.3 applies the Lorentzian prescription to our FRW spacetime. Finally, in Section 3.A.4 we briefly outline how to generalize this to a massive correlation function.

3.A.1 Euclidean prescription

The Euclidean CdL instanton in d dimensions is characterized by the isometries of a $(d-1)$-dimensional sphere. It is the Euclidean version of a closed FRW universe. Let

[20] A toy example is the $\tanh x$ function, which is well approximated by 1 for large, real x, but we certainly cannot continue this approximate result to the imaginary axis. A class of exact CdL solutions showing this explicitly will appear in [11].

[21] Correlation functions in general dimensions were also calculated in [125] in the thin-wall limit. In this appendix we work more generally, partly because our FRW spacetime with $c > 1$ is not in the thin-wall limit.

us work in the conformal coordinates:

$$ds_d^2 = a(X)^2(dX^2 + d\Omega_{d-1}^2), \qquad d\Omega_{d-1}^2 = d\theta^2 + \sin^2\theta\, d\Omega_{d-2}^2, \tag{3.103}$$

where X varies from $-\infty$ to $+\infty$. The smoothness of the instanton requires that the scale factor vanish as $\xi + \mathcal{O}(\xi^3)$ at the two tips, where ξ is the proper coordinate in the X direction. In the conformal coordinates this means $a(X)$ approaches (up to constant factors) e^X as $X \to -\infty$, and approaches e^{-X} as $X \to +\infty$.

We calculate the two-point function of a minimally coupled massless scalar field ϕ. It is convenient to consider the rescaled field

$$\hat{\phi} = a(X)^{k_0}\phi, \qquad \text{where} \quad k_0 \equiv \frac{d-2}{2}, \tag{3.104}$$

which has a canonical kinetic term. Note that k_0 is the momentum gap for the normalizable eigenmodes of the Laplacian on the unit $(d-1)$-dimensional hyperboloid. We let G and $\hat{G}$ denote the correlator of ϕ and $\hat{\phi}$ respectively. The rotational symmetry of the $d-1$ sphere may be used to bring one of the two points to $\theta = 0$, so that the correlator $\hat{G}(X, X', \theta)$ depends on no other angular coordinates and satisfies the Laplace equation with a delta function source:

$$\left[-\partial_X^2 - \nabla_{S^{d-1}}^2 + U(X)\right] \hat{G}(X, X', \theta) = \frac{\delta(X - X')\delta(\theta)}{S_{d-2}\sin^{d-2}\theta}, \tag{3.105}$$

where $S_n = 2\pi^{(n+1)/2}/\Gamma((n+1)/2)$ is the volume of the unit n-sphere, and the potential $U(X)$ is defined as

$$U(X) = \frac{b''(X)}{b(X)} = k_0^2 - \frac{k_0\Phi'^2 + d\, a(X)^2 V(\Phi)}{2(d-1)}, \qquad \text{where} \quad b(X) \equiv a(X)^{k_0}. \tag{3.106}$$

Here Φ is the scalar field sourcing the metric and has a canonical kinetic term. Its potential[22] $V(\Phi)$ between the two tunneling points $\Phi(X = \pm\infty)$ is nonnegative for decays from de Sitter to de Sitter or to FRW with a zero cosmological constant (if

[22]It is important not to confuse the "Schrödinger potential" $U(X)$ with the potential $V(\Phi)$ which sources the geometry. It is also important to distinguish the two scalar fields ϕ and Φ.

one assumes the null energy condition), so $U(X)$ is bounded from above by k_0^2 and asymptotes to this bound as $X \to \pm\infty$.

The correlator $\hat{G}(X, X', \theta)$ can be obtained as an expansion in the eigenmodes of the "Schrödinger operator" $[-\partial_X^2 + U(X)]$. The result is

$$\hat{G}(X, X', \theta) = \int_{-\infty}^{+\infty} \frac{dk}{2\pi} u_k(X) u_k^*(X') G_k(\theta) + \sum_{\kappa} u_{i\kappa}(X) u_{i\kappa}^*(X') G_{i\kappa}(\theta), \qquad (3.107)$$

where the first term is an integral over the orthonormal continuum modes satisfying the "Schrödinger equation"

$$\left[-\partial_X^2 + U(X)\right] u_k(X) = (k^2 + k_0^2) u_k(X), \qquad (3.108)$$

with the boundary conditions

$$u_k(X) \to e^{ikX} + R(k) e^{-ikX} \quad (X \to -\infty), \quad u_k(X) \to T(k) e^{ikX} \quad (X \to +\infty), \qquad (3.109)$$

$$u_{-k}(X) \to T_r(k) e^{-ikX} \quad (X \to -\infty), \quad u_{-k}(X) \to e^{-ikX} + R_r(k) e^{ikX} \quad (X \to +\infty), \qquad (3.110)$$

where $k > 0$ is understood. One can show that these coefficients are related by

$$T(k) = T_r(k), \qquad \frac{R(k)}{R_r^*(k)} = -\frac{T(k)}{T_r^*(k)}, \qquad |R(k)|^2 + |T(k)|^2 = 1. \qquad (3.111)$$

The second term in (3.107) is a discrete sum over the normalized bound states. They satisfy the Schrödinger equation (3.108) with $k = i\kappa$. There is always at least one bound state for a compact Euclidean CdL: the zero mode $u_{ik_0}(X) \propto a(X)^{k_0}$. For $d \leq 4$ one can show that this is the only bound state using a technique of supersymmetric quantum mechanics [21, 22]. For $d > 4$ there may be additional bound states.

The $G_k(\theta)$ that appears in (3.107) is the Green's function on S^{d-1} with an appropriate mass:

$$\left[-\nabla^2_{S^{d-1}} + (k^2 + k_0^2)\right] G_k(\theta) = \frac{\delta(\theta)}{S_{d-2}\sin^{d-2}\theta}. \tag{3.112}$$

The solution may be written in terms of the hypergeometric function:

$$G_k(\theta) = \frac{(2\sqrt{\pi})^{1-d}}{\Gamma\left(\frac{d-1}{2}\right)}\Gamma(k_0+ik)\Gamma(k_0-ik)\ {}_2F_1\left(k_0+ik, k_0-ik, \frac{d-1}{2}, \cos^2\frac{\theta}{2}\right), \tag{3.113}$$

which is a meromorphic function in k. It has simple poles located at

$$k = \pm i(k_0 + n), \qquad n = 0, 1, 2, \cdots \tag{3.114}$$

due to the Gamma functions in (3.113). In even dimensions the hypergeometric function simplifies to an elementary function. For example, in $d = 4$ (3.113) as a function of complex θ becomes

$$G_k(\theta) = \frac{\sinh\left[k(\pi-\theta)\right]}{4\pi\sinh(k\pi)\sin\theta}, \qquad \text{for} \quad 0 < \mathrm{Re}(\theta) < 2\pi. \tag{3.115}$$

The Green's function $G_{i\kappa}(\theta)$ for the bound states is also given by (3.113). The only subtlety appears when we consider the zero energy bound state $a(X)^{k_0}$ with $k = ik_0$, for which $G_k(\theta)$ hits a pole and diverges. This reflects the fact that the massless correlator on a compact space is ill-defined because we cannot put a single source there without violating Gauss's law.[23] The two-point function for the derivative of a massless field is well-defined and physical, so one may say that the massless correlator is well-defined up to arbitrary constant and/or linear terms in the coordinates. These terms are called "pure gauge". Therefore we may get a finite massless Green's function by subtracting an infinite constant from $G_{ik_0}(\theta)$. For example in $d = 4$ one

[23]The left hand side of (3.112) integrates to zero, but the right hand side does not. This may be solved by subtracting an inhomogeneous term proportional to the inverse of the volume of the compact space.

prescription is

$$G_{ik_0}(\theta) = \lim_{k\to ik_0}\left[G_k(\theta) - \frac{1}{2\pi^2(k^2+1)}\right] + \frac{1}{8\pi^2} = \frac{\cot\theta}{4\pi}\left(1-\frac{\theta}{\pi}\right). \tag{3.116}$$

Before we analytically continue to the Lorentzian signature, let us rewrite the expansion (3.107) in a simpler form. Instead of using $u_k(X)$ we might want to write the correlator in terms of eigenmodes that have simpler asymptotic behavior as $X \to -\infty$, as this is where we cross to the FRW region. Let us call this new set of eigenmodes $v_k(X)$, defined with the boundary condition $v_k(X) \to e^{ikX}$ as $X \to -\infty$ for both positive and negative k. We may write them in terms of the old eigenmodes:

$$v_k(X) = \frac{u^*_{-k}(X)}{T^*_r(k)}, \qquad v_{-k}(X) = \frac{u_{-k}(X)}{T_r(k)}, \qquad k>0. \tag{3.117}$$

After some algebra, one finds that in terms of the new eigenmodes the continuum contribution in (3.107) becomes

$$\hat{G}_c(X,X',\theta) = \int_{-\infty}^{+\infty}\frac{dk}{2\pi}\left[v_k(X)v_{-k}(X') + R(k)v_{-k}(X)v_{-k}(X')\right]G_k(\theta), \tag{3.118}$$

where the reflection coefficient $R(k)$ is extended from $k>0$ to a meromorphic function on the complex k-plane. For $k<0$ one can show $R(k) = R^*(-k)$. One may ask what we have achieved by rewriting (3.107) as (3.118). It turns out[24] that the bound-state contribution in (3.107) can be accounted for, up to pure gauge, by simply deforming the integration contour for the second term in (3.118). Specifically, the massless correlator (3.107) simplifies to

$$\hat{G}(X,X',\theta) = \int_{-\infty}^{+\infty}\frac{dk}{2\pi}v_k(X)v_{-k}(X')G_k(\theta) + \int_C\frac{dk}{2\pi}R(k)v_{-k}(X)v_{-k}(X')G_k(\theta), \tag{3.119}$$

where C is a contour that goes from $k=-\infty$ above the double pole $k=ik_0$ to $k=+\infty$, as shown in Figure 3.1. In the limit $X,\, X'\to-\infty$, the second integrand

[24]This may be shown by expanding the Green's function in terms of eigenmodes of the Laplacian on S^{d-1} (discarding the zero mode). This expansion exactly matches the sum of contributions from the simple poles enclosed by C_a as shown in Figure 3.2a.

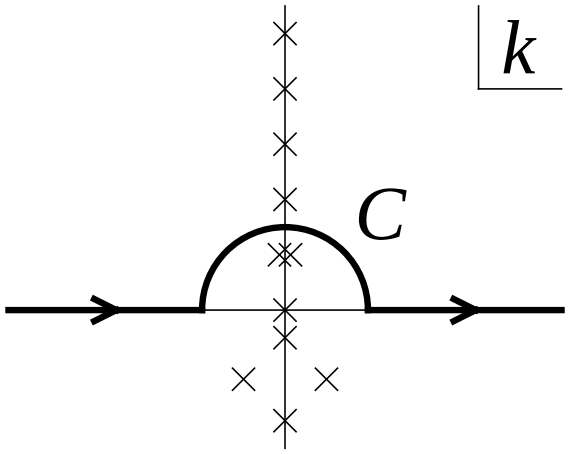

Figure 3.1: Contour C going from $k = -\infty$ above the double pole $k = ik_0$ to $k = +\infty$. Remember $k_0 \equiv (d-2)/2$. The simple poles above the double pole are located at $k = i(k_0 + n)$, $n = 1, 2, 3, \cdots$. The locations of the simple poles below the double pole are for illustration purposes only and should not be taken too seriously. They depend on the reflection coefficient $R(k)$, and also on whether we are considering the second integrand in (3.119) or in (3.133). The pair of poles away from the imaginary axis are resonance poles.

in (3.119) asymptotes to $e^{-ik(X+X')}$, so we may push the contour C up to C_a, picking up the simple poles at $k = i(k_0 + n)$, $n = 1, 2, 3, \cdots$. This is shown in Figure 3.2a.

Note that $R(k)$ has a simple pole at $k = ik_0$ (corresponding to the zero mode) and a zero at $k = -ik_0$, so the second integrand in (3.119) has a double pole at ik_0 and is regular at $-ik_0$. It is precisely the residue at the double pole that cancels with the zero energy bound state contribution up to pure gauge. For $d > 4$ there may be additional bound states, corresponding to additional simple poles between $k = 0$ and $k = ik_0$. There could also be resonance poles, all of which must lie in the lower half plane. As we will see in the next two subsections, these additional poles need to be taken into account when calculating the exact correlation function, but at the order we work, they do not contribute to our final result.

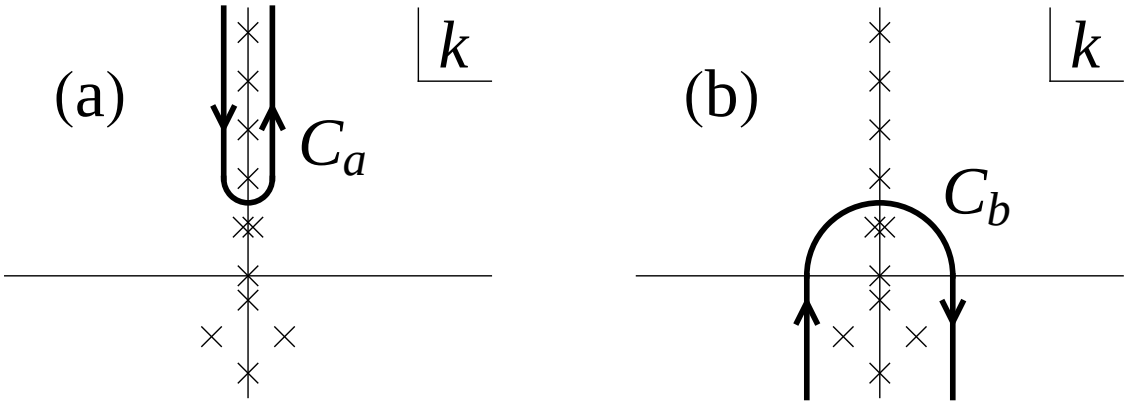

Figure 3.2: (a) Contour C_a surrounding simple poles at $k = i(k_0 + n)$, $n = 1, 2, 3, \cdots$. (b) Coutour C_b surrounding a double pole at $k = ik_0$ and simple poles below ik_0. In general there could also be resonance poles away from the imaginary axis in the lower half plane, in which case the contour C_b needs to enclose them as well.

3.A.2 Lorentzian prescription

Now that we have (3.119) for the massless correlator in the Euclidean CdL geometry, we can analytically continue it to the FRW geometry

$$ds_d^2 = a(T)^2(-dT^2 + dH_{d-1}^2), \qquad dH_{d-1}^2 = dr^2 + \sinh^2 r \, d\Omega_{d-2}^2. \tag{3.120}$$

The prescription for the analytic continuation in our conformal coordinates is given by

$$X \to T + \frac{i\pi}{2}, \quad \theta \to ir, \quad a(X) \to ia(T), \quad v_k(X) \to v_k(T)e^{-k\pi/2}, \tag{3.121}$$

so that $v_k(T)$ similarly satisfies a "Schrödinger equation"

$$\left[-\partial_T^2 + U(T)\right] v_k(T) = (k^2 + k_0^2)v_k(T), \quad U(T) \equiv \frac{\ddot{b}(T)}{b(T)}, \quad b(T) \equiv a(T)^{k_0}, \tag{3.122}$$

with the simple boundary condition $v_k(T) \to e^{ikT}$ as $T \to -\infty$.

The Lorentzian correlator $\hat{G}(T,T',r)$ satisfies

$$\left[-\partial_T^2+\nabla^2_{\mathbb{H}_{d-1}}+U(T)\right]\hat{G}(T,T',r)=\frac{i\delta(T-T')\delta(r)}{S_{d-2}\sinh^{d-2}r}, \tag{3.123}$$

and is therefore given (for sufficiently negative $T+T'$) by analytically continuing the Euclidean correlator (3.119):

$$\hat{G}(T,T',r)=i^d\hat{G}(X\to T+\frac{i\pi}{2},X'\to T'+\frac{i\pi}{2},\theta\to ir)\equiv\hat{G}_1+\hat{G}_2 \tag{3.124}$$

$$=\int_{-\infty}^{+\infty}\frac{dk}{2\pi}v_k(T)v_{-k}(T')G_k(r)+\int_{C_a}\frac{dk}{2\pi}R(k)v_{-k}(T)v_{-k}(T')\tilde{G}_k(r), \tag{3.125}$$

where $G_k(r)$ and $\tilde{G}_k(r)$ are defined as

$$G_k(r)=i^dG_k(\theta\to ir),\qquad \tilde{G}_k(r)=i^de^{k\pi}G_k(\theta\to ir) \tag{3.126}$$

except for the subtlety mentioned below for $\tilde{G}_k(r)$. Let us call the two integrals in (3.125) $\hat{G}_1$ and $\hat{G}_2$ respectively. Note that our choice of the contour C_a in $\hat{G}_2$ is correct only for sufficiently negative[25] $T+T'$. On the other hand, we are most interested in the massless correlator at late times. If we naïvely increase $T+T'$ without deforming the contour C_a, at some point the integral would diverge. A standard way of solving this problem is to pull the contour down to C which goes from $k=-\infty$ above the double pole $k=ik_0$ to $k=+\infty$, as shown in Figure 3.1. Once this is done and the new integral on C agrees with the old one on C_a for sufficiently negative $T+T'$, we simply use the new integral as the definition for any values of $T+T'$. To evaluate this new integral for large $T+T'$, one can legally deform the contour from C to C_b as shown in Figure 3.2b (at least for some of the terms in the integrand), picking up the double and simple poles below the contour. This last step will be done on a case-by-case basis in the next subsection. Here we first obtain the correct expression for the new integral on C that is valid for any T and T'.

It turns out that we cannot naïvely deform the contour from C_a to C in $\hat{G}_2$. If we

[25] One can see from (3.130) that "sufficiently negative" here means $T+T'\ll -r$.

do that, the integral on C would diverge, as we will show shortly. This is different from the situation before the analytic continuation, where it does not matter whether we choose C or C_a, as long as $X + X'$ is sufficiently negative. The main difference is the additional $e^{k\pi}$ factor inside $\tilde{G}_k(r)$, which comes from analytically continuing $v_{-k}(X)v_{-k}(X')$ to $v_{-k}(T)v_{-k}(T')$ in $\hat{G}_2$.

A hint that something subtle is going on is that we could multiply the integrand of $\hat{G}_2$ by any number of $e^{2(k-ik_0)\pi}$ factors without changing the integral on C_a. The reason is simply that the integral on C_a is equal to the sum of residues at the simple poles $k = i(k_0+n)$, $n = 1, 2, 3, \cdots$, and $e^{2(k-ik_0)\pi}$ is simply 1 at all these poles, so none of the residues are changed. On the other hand, factors such as $e^{2(k-ik_0)\pi}$ definitely matter when the integral is performed on C. In fact, there is a unique prescription for this factor for which the integral on C is actually convergent. This is the correct prescription, which we will find in exact form below.

Let us use the connection formula for the hypergeometric function

$$\begin{aligned} {}_2F_1(a,b,c,z) = {} & \frac{\Gamma(c)\Gamma(b-a)}{\Gamma(b)\Gamma(c-a)}(-z)^{-a}{}_2F_1\left(a, 1+a-c, 1+a-b, \frac{1}{z}\right) \\ & + \frac{\Gamma(c)\Gamma(a-b)}{\Gamma(a)\Gamma(c-b)}(-z)^{-b}{}_2F_1\left(b, 1+b-c, 1+b-a, \frac{1}{z}\right) \end{aligned} \tag{3.127}$$

to decompose the $\tilde{G}_k(r)$ into two terms:

$$\begin{aligned} \tilde{G}_k(r) &= i^d e^{k\pi}\frac{(2\sqrt{\pi})^{1-d}}{\Gamma\left(\frac{d-1}{2}\right)}\Gamma(k_0+ik)\Gamma(k_0-ik)\ {}_2F_1\left(k_0+ik, k_0-ik, \frac{d-1}{2}, \cosh^2\frac{r}{2}\right) \\ &= -\frac{1}{4\pi^{d/2}(4z)^{k_0}}\left[e^{2k\pi}(4z)^{-ik}\Gamma(k_0+ik)\Gamma(-ik)\ {}_2F_1\left(k_0+ik, \frac{1}{2}+ik, 1+2ik, \frac{1}{z}\right)\right. \\ &\qquad \left. +(4z)^{ik}\Gamma(k_0-ik)\Gamma(ik)\ {}_2F_1\left(k_0-ik, \frac{1}{2}-ik, 1-2ik, \frac{1}{z}\right)\right], \end{aligned} \tag{3.128}$$

where z is defined as $\cosh^2(r/2)$. For $d = 4$ this decomposition looks very simple:

$$\tilde{G}_k(r) = \frac{e^{k\pi}\sinh\left[k(\pi - ir)\right]}{4\pi i\sinh(k\pi)\sinh r} = \frac{e^{2k\pi - ikr} - e^{ikr}}{8\pi i\sinh(k\pi)\sinh r}. \tag{3.129}$$

In general dimensions this decomposition may look complicated, but each term has a simple asymptotic behavior at large r. Specifically as $r \to \infty$, z goes to $e^r/4$, both hypergeometric functions in (3.128) goes to 1, and we have

$$\tilde{G}_k(r) \approx -\frac{1}{4\pi^{d/2} e^{k_0 r}} \left[e^{2k\pi} e^{-ikr} \Gamma(k_0 + ik)\Gamma(-ik) + e^{ikr}\Gamma(k_0 - ik)\Gamma(ik) \right]. \quad (3.130)$$

As $k \to \pm\infty$ along the real axis, the absolute value of the products of Gamma functions in (3.130) becomes

$$|\Gamma(k_0 + ik)\Gamma(-ik)| = |\Gamma(k_0 - ik)\Gamma(ik)| \approx 2\pi |k|^{\frac{d-4}{2}} e^{-|k|\pi}. \quad (3.131)$$

Clearly the first term in (3.130) diverges as $k \to +\infty$, while the second term goes to zero as $k \to \pm\infty$. As we argued earlier, we treat this divergence by multiplying the first term by a factor of $e^{-2(k-ik_0)\pi} = (-1)^d e^{-2k\pi}$, changing the exact form (3.128) of $\tilde{G}_k(r)$ into

$$\begin{aligned} \tilde{G}_k(r) = -\frac{1}{4\pi^{d/2}(4z)^{k_0}} \Bigg[& (-1)^d (4z)^{-ik} \Gamma(k_0 + ik)\Gamma(-ik)\ {}_2F_1\left(k_0 + ik, \frac{1}{2} + ik, 1 + 2ik, \frac{1}{z}\right) \\ & + (4z)^{ik}\Gamma(k_0 - ik)\Gamma(ik)\ {}_2F_1\left(k_0 - ik, \frac{1}{2} - ik, 1 - 2ik, \frac{1}{z}\right)\Bigg], \quad (3.132) \end{aligned}$$

where again $z = \cosh^2(r/2)$. This does not change the integral on C_a, but enables us to legally deform the contour from C_a to C for sufficiently negative $T + T'$. In terms of this improved $\tilde{G}_k(r)$ the Lorentzian correlator is

$$\hat{G}(T, T', r) = \hat{G}_1 + \hat{G}_2 = \int_{-\infty}^{+\infty} \frac{dk}{2\pi} v_k(T) v_{-k}(T') G_k(r) + \int_C \frac{dk}{2\pi} R(k) v_{-k}(T) v_{-k}(T') \tilde{G}_k(r), \quad (3.133)$$

which looks the same as (3.125) except for the contour C. This is our final, exact expression for the massless correlator in any open FRW spacetime resulting from a

CdL decay, valid for any T, T', and r. Here $G_k(r)$ is given by (3.126) as

$$G_k(r) = i^d \frac{(2\sqrt{\pi})^{1-d}}{\Gamma\left(\frac{d-1}{2}\right)} \Gamma(k_0 + ik)\Gamma(k_0 - ik)\ {}_2F_1\left(k_0 + ik, k_0 - ik, \frac{d-1}{2}, \cosh^2\frac{r}{2}\right). \tag{3.134}$$

Before concluding this section, let us comment on the structure of (3.133). In order to calculate the Lorentzian correlator, we only need the eigenmodes $v_k(T)$ and the reflection coefficient $R(k)$. For $v_k(T)$ we solve the "Lorentzian Schrödinger equation" (3.122) with the boundary condition $v_k(T) \to e^{ikT}$ as $T \to -\infty$. For $R(k)$ we in principle need to solve the "Euclidean Schrödinger equation" (3.108). We cannot in general hope to calculate the complete Lorentzian correlator by knowing only $a(T)$ but not $a(X)$ (or vice versa); an example is provided by the thin-wall limit discussed in [21, 22], where the Lorentzian scale factor $a(T) = e^T$ is exactly the same as that of flat space in Milne coordinates, but the massless correlator still has a nontrivial term due to the specific vacuum chosen by the CdL geometry. From the perspective of (3.133), the choice of vacuum is encoded in the reflection coefficient $R(k)$ which must in general be calculated from the Euclidean scale factor $a(X)$. Usually $R(k)$ is not analytically tractable away from the thin-wall limit, but fortunately all we need to know in order to calculate the leading behavior of $\hat{G}_2$ is the fact that $R(k)$ always has a simple pole at $k = ik_0$, and all other poles lie below it.

3.A.3 Our FRW spacetime

Let us now apply (3.133) to our FRW model

$$ds_d^2 = -dt^2 + a(t)^2 dH_{d-1}^2, \tag{3.135}$$

where the scale factor $a(t)$ asymptotes to ct at late times. Near the big bang singularity $t = 0$ the scale factor $a(t) = t + \mathcal{O}(t^3)$ as required by the smoothness of the CdL instanton. Going to the conformal coordinates $T = \int dt/a(t)$, the scale factor $a(T)$ approaches (up to constant factors) e^T as $T \to -\infty$, and approaches e^{cT} as $T \to +\infty$. Therefore the "Schrödinger potential" $U(T)$ asymptotes to k_0^2 as $T \to -\infty$ and $c^2k_0^2$ as $T \to +\infty$. This means that the eigenmodes $v_k(T)$ have the following asymptotic

behavior

$$v_k(T) \to e^{ikT} \qquad (T \to -\infty), \tag{3.136}$$

$$v_k(T) \to \alpha_k e^{iT\sqrt{k^2-(c^2-1)k_0^2}} + \beta_k e^{-iT\sqrt{k^2-(c^2-1)k_0^2}} \qquad (T \to +\infty), \tag{3.137}$$

where α_k and β_k are analogous to reflection and transmission coefficients. For $k > k_0\sqrt{c^2-1}$ the eigenmodes are oscillatory at large T; for smaller k they are exponentially decaying or growing. These are pseudotachyonic modes.

The exact eigenmodes $v_k(T)$ are difficult to solve analytically except for perhaps unrealistically simple $U(T)$ such as a step potential. Fortunately, we are most interested in the equal-time massless correlator at large T and large r, for which both $v_k(T)$ and $\tilde{G}_k(r)$ simplify. Specifically in the large T limit $v_{-k}(T)v_{-k}(T)$ in $\hat{G}_2$ becomes

$$v_{-k}(T)^2 \approx \alpha_{-k}^2 e^{-2iT\sqrt{k^2-(c^2-1)k_0^2}} + \beta_{-k}^2 e^{2iT\sqrt{k^2-(c^2-1)k_0^2}} + 2\alpha_{-k}\beta_{-k} \equiv v_- + v_+ + v_0, \tag{3.138}$$

where we have changed the sign of the exponent in $v_{-k}(T)$ because we choose the square root to have a branch cut between $k = \pm k_0\sqrt{c^2-1}$. In the large r limit (3.132) simplifies to

$$\tilde{G}_k(r) \approx -\frac{1}{4\pi^{d/2}e^{k_0 r}}\left[(-1)^d e^{-ikr}\Gamma(k_0+ik)\Gamma(-ik) + e^{ikr}\Gamma(k_0-ik)\Gamma(ik)\right] \equiv \tilde{G}_- + \tilde{G}_+. \tag{3.139}$$

Therefore the integrand of $\hat{G}_2$ in (3.133) can be decomposed into six terms:

$$\hat{G}_2(T,T,r) \approx \int_C \frac{dk}{2\pi} R(k)(v_- + v_+ + v_0)(\tilde{G}_- + \tilde{G}_+), \tag{3.140}$$

where for large $|k|$ we have $v_\pm \sim e^{\pm i2kT}$ and $\tilde{G}_\pm \sim e^{\pm ikr}/\sinh(k\pi)$ up to powers of k.

In the large T, large fixed r limit that we are interested in (i.e. $T \gg r \gg 1$) we may deform the contour from C to C_a for the three terms $v_+(\tilde{G}_- + \tilde{G}_+) + v_0\tilde{G}_+$, and deform the contour to C_b for the other three: $v_-(\tilde{G}_- + \tilde{G}_+) + v_0\tilde{G}_-$. If we are interested in the large r, large fixed T limit (i.e. $r \gg T \gg 1$) instead, we simply switch the contours for $v_+\tilde{G}_-$ and $v_-\tilde{G}_+$. In both cases (or more generally, in any

large T, r limit), the leading behavior of $\hat{G}_2$ can be shown to come from the residue of the $v_-\tilde{G}_-$ term at the double pole $k = ik_0$. This can be evaluated up to numerical factors:

$$\hat{G}_2(T,T,r) \sim e^{2ck_0T}(2T+r), \qquad G_2(T,T,r) = \frac{\hat{G}_2(T,T,r)}{a(T)^{k_0}a(T)^{k_0}} \sim 2T + r, \tag{3.141}$$

where G_2 is the corresponding piece of the original correlator for ϕ. The first term $2T$ is a pure gauge because it is linear in the coordinates. The second term r is not, because it is actually the geodesic distance on $\mathbb{H}_{d-1}$ between the two points of the correlation function.

To study the holographic dual of our FRW model, we rewrite the metric in hyperbolic slicing

$$ds_d^2 = -dt^2 + a(t)^2(d\chi^2 + \cosh^2\chi\, dH_{d-2}^2), \qquad dH_{d-2}^2 = d\tilde{\chi}^2 + \sinh^2\tilde{\chi}\, d\Omega_{d-3}^2. \tag{3.142}$$

Let us put both points of the correlator on a hypersurface of constant χ, with a separation of $\Delta\tilde{\chi}$ in the $\tilde{\chi}$ direction. Their geodesic distance on $\mathbb{H}_{d-1}$ is therefore

$$r = \operatorname{arccosh}(\cosh\Delta\tilde{\chi}\cosh^2\chi - \sinh^2\chi) \approx \Delta\tilde{\chi} + 2\log\cosh\chi, \tag{3.143}$$

where the approximation holds for large $\Delta\tilde{\chi}$ and any χ. For large χ the second term on the right hand side of (3.143) simply becomes 2χ, but let us not commit ourselves to that limit. In terms of χ and $\Delta\tilde{\chi}$ the leading behavior of G_2 from (3.141) becomes

$$G_2(t,\chi,\Delta\tilde{\chi}) \sim \Delta\tilde{\chi} + 2\log\cosh\chi. \tag{3.144}$$

This term is present for both $c > 1$ and $c = 1$, and it is independent of the dimension d. This suggests an interpretation as the contribution from the zero mode of ϕ localized on the UV slice.

The leading behavior of the other term in the correlator, namely $\hat{G}_1$, is dominated by the contributions of the pseudotachyonic modes. The most pseudotachyonic mode

is the one with $k = 0$, given by

$$v_0(T) \sim e^{k_0 T\sqrt{c^2-1}}. \tag{3.145}$$

In the large r limit $G_0(r)$ as defined in (3.134) goes like $re^{-k_0 r}$, so the first term in the correlator (3.133) becomes

$$\hat{G}_1(T,T,r) \sim re^{2k_0 T\sqrt{c^2-1}-k_0 r}, \quad G_1(T,T,r) \sim re^{2k_0 T(\sqrt{c^2-1}-c)-k_0 r}, \tag{3.146}$$

which we rewrite in terms of t, χ, and $\Delta\tilde{\chi}$ as

$$G_1(t,\chi,\Delta\tilde{\chi}) \sim \frac{t^{(d-2)(\sqrt{1-1/c^2}-1)}}{\cosh^{d-2}\chi} e^{-(d-2)\Delta\tilde{\chi}/2}(\Delta\tilde{\chi} + 2\log\cosh\chi). \tag{3.147}$$

This term is present only for $c > 1$, in which case there is a warped geometry with a consistent description in terms of a low-energy $(d-1)$-dimensional dual.

3.A.4 Massive correlation functions

We have hitherto focused on massless correlation functions, but it is rather straightforward to generalize it to massive correlation functions, as we outline below. This provides an alternative way of calculating the massive Green's functions for the KK modes, closed strings, and 7-7 strings in Section 3.5.1.

Let us consider a scalar field ϕ with mass $m(t)$ which we allow to be time-dependent. We can use the same techniques developed in Sections 3.A.1 and 3.A.2 to calculate its correlation function. The only difference is that we need to add a corresponding mass term $a(X)^2 m(X)^2$ to the "Schrödinger potential" $U(X)$, and similarly add $-a(T)^2 m(T)^2$ to $U(T)$. This makes the potential $U(X)$ shallower, and the bound states either have larger eigenvalues (for small masses) or simply disappear (for large masses). This means that the reflection coefficient $R(k)$ no longer has a pole at $k = ik_0$. The pole is moved down to between $k = ik_0$ and $k = 0$ if there is still a bound state. Therefore, the formulae for both the Euclidean correlator (3.119) and the Lorentzian correlator (3.133) are fully correct, as long as we define the contour C

to go from $k = -\infty$ to $k = +\infty$, in a way that goes just below $k = ik_0$ but always above any possible poles corresponding to bound states.

The pseudotachyonic modes disappear for sufficiently large masses due to the additional term $-a(T)^2 m(T)^2$ in the "Schrödinger potential" $U(T)$. One can show that in this case the leading term in the correlation function agrees with the estimates in Section 3.5.1.

Chapter 4

Unitarity bounds and RG flows in time dependent quantum field theory

4.1 Motivations

Unitarity is essential to any closed quantum mechanical system such as Lorentzian-signature quantum field theory. In conformal field theory, operator dimensions are bounded in a way that derives from unitarity. For example for scalar operators $\mathcal{O}$ in a d-dimensional theory, the condition

$$\Delta_{\mathcal{O}} \geq (d-2)/2 \tag{4.1}$$

follows from the positivity of the norm of states created by $\mathcal{O}$ and its descendants. If one couples additional fields χ to the CFT via couplings of the form $\int d^d x g \chi \mathcal{O}$, the same condition (4.1) arises from the optical theorem for forward scattering of χ (see [126] for a clear recent discussion and [127, 128] for general results on constraints from conformal invariance).

One reason unitarity bounds are interesting is that they can help determine aspects of the infrared physics of nontrivial quantum field theories. For example, in

supersymmetric QCD below the Seiberg window of conformal field theories, one can use this unitarity bound along with other symmetries to show that the theory cannot flow to a CFT [129, 130]. In other examples, such as [131, 132], unitarity bounds help to establish that a certain field decouples from the rest of the theory in the infrared.

In this chapter, we are concerned with the question of what happens to the infrared physics and unitarity bounds in field theories which have a time dependent coupling $g(t)$.[1] More specifically, we will study the infrared limit of field theories with spacetime dependent couplings that approximately preserve scale invariance but not Poincaré invariance over a wide range of spacetime scales. Consider a coupling of the form

$$\int d^d x \mathcal{L}_g = \int dt d^{d-1}\vec{x}\, g(t,\vec{x})\mathcal{O}, \tag{4.2}$$

with $g(t) \sim t^\alpha$ or $g(t,\vec{x}) \sim (t^2 - \vec{x}^2)^{\alpha/2}$, at sufficiently late times, or sufficiently well within the forward light cone, respectively. As we rescale the coordinates $x^\mu \to \lambda x^\mu$, the coupling transforms by the rescaling

$$g(x) \to \lambda^\alpha g(x). \tag{4.3}$$

If we perturb a CFT by $\int d^d x \mathcal{L}_g$ (4.2), the nontrivial scaling of g (4.3) affects the question of whether $\mathcal{L}_g$ dominates at late times and large distance scales. If $\mathcal{L}_g$ does dominate in the infrared and become marginal under our scaling by λ, then the nontrivial scaling of g also affects the scaling of the operator $\mathcal{O}$. This suggests that unitarity conditions and scaling dimensions of the infrared theory may be modified by the presence of $g(x)$. Another way to organize this question, which we will consider below as well, is to realize the spacetime dependent coupling dynamically, as the profile of an additional field $g(x)$ in the theory.

To answer our question, we will analyze the infrared behavior of correlation functions in simple, tractable theories with such a coupling $g(x)$. Clearly, the effects of the spacetime dependence of the coupling become unimportant on short enough scales, schematically $\Delta x \ll g/\partial g$. For this reason, we focus on an infrared, late-time regime

[1] Works on spacetime dependent couplings and RG flows in QFT include [133, 134, 135, 136, 137].

which we define carefully below. At shorter distance scales, we cross over to static physics. We will consider examples below in which this static theory is well defined up to energy scales much larger than the scale $\partial g/g$, including a class of fully UV complete examples.

The general motivations to study time dependent quantum field theories are very simple. Time dependent backgrounds are generic, and have important applications in fields as diverse as cosmology[2] and condensed matter physics.[3] On a more theoretical front, it remains a major challenge to derive a framework for cosmology including the effects of horizons, singularities, and transitions among metastable configurations; various interesting approaches are being pursued.[4] Recently, by uplifting AdS/CFT solutions to cosmological ones (de Sitter and other FRW solutions), we made some progress on this question, and encountered the above issue. Our uplifting procedure [16, 7, 9] introduces a number n of (p, q) 7-branes, which introduce magnetic flavors into the dual theory. For n greater than a certain integer n_* (depending on the dimensionality and other details of the example), one finds no static AdS/CFT solution. However, for $n > n_*$ one does find a controlled time dependent solution, which furthermore admits a warped metric indicating a low energy field theory dual.[5] We analyzed the basic properties of this putative dual in several different ways, achieving consistent results. As we will show below by using the most supersymmetric class of examples, the problem with would-be static theories in the range $n > n_*$ can be traced to unitarity. Our gravity solutions suggest that the time dependent background relaxes this condition. Moreover, in our FRW solutions, the dual effective field theory is cut off at an energy scale proportional to $\partial g/g \sim 1/t$.

This led us to the above (more general) question, which we will address in much simpler examples than those of [9]. In particular, we will focus on a theory with a

[2](ultimately providing a simple theory of the origin of structure in the universe)

[3]For example, quenching and thermalization is an interesting probe of field theories at finite density [138, 139, 140, 141]. Nonequilibrium processes are also useful for stimulating interesting low temperature phases [142, 143, 124].

[4]Some recent approaches can be found in [144, 20, 72, 82, 73, 18, 19, 7, 9, 145, 21, 22, 78, 146, 83, 147]. Other recent work on this general subject includes, for instance, [148, 149, 150, 151, 152, 153, 154, 155, 156, 157, 93].

[5]A different class of solutions was analyzed in [75].

spacetime dependent semi-holographic [28, 94, 27, 18, 158, 159, 160] coupling $g(x)$ between a large-N conformal field theory and a scalar field, including the simplest case corresponding to double trace renormalization group flows [161, 162, 163, 164, 165, 79, 166, 167, 168, 169]. This system and its infrared unitarity for constant coupling was analyzed recently in [170] in the case where the large-N CFT has a large-radius holographic dual. Here, we determine the effects of the spacetime dependence of $g(x)$ on the relevance of the coupling and the analysis of unitarity in the infrared theory. In particular, we will find – as anticipated in the FRW example just mentioned – that spacetime dependent couplings can produce new interacting theories with approximate scale invariance in the infrared for a wider range of flavors than in the corresponding static theory. Our results about the infrared physics will apply for parametrically long times at large N.[6]

This chapter is organized as follows. In §4.2, we present our main example, a semi-holographic model in which we can compute the needed amplitudes explicitly. In §4.3, we analyze spacetime dependent couplings involving fermions, finding similar results. Then in §4.4, we consider supersymmetric gauge theories with time dependent couplings; this provides a concrete UV completion of a class of models like those of §4.2, and makes contact with our motivations from FRW holography. Finally, we conclude in §4.5 with additional comments and potential generalizations of our results. Several useful results are explained in more detail in the Appendix.

4.2 Spacetime dependent double trace flows and semiholographic models

Let us now analyze in detail our main example. We will study the RG evolution of a large-N CFT in d dimensions perturbed by a spacetime dependent coupling to a

[6] This is reminiscent of other large-N field theories for which scaling symmetry holds over a wide range of scales but not arbitrarily far into the infrared.

scalar field ϕ:[7]

$$S = S_{CFT} - \frac{1}{2}\int d^d x\,(\eta^{\mu\nu}\partial_\mu\phi\partial_\nu\phi + m^2\phi^2) + \int d^d x\, g(x)\mathcal{O}\phi\,, \tag{4.4}$$

where $\mathcal{O}$ is an operator in the CFT. A related question that will be addressed is what happens when a CFT is deformed by a space-time dependent double-trace operator,

$$S = S_{CFT} + \int d^d x\,\lambda(x)\mathcal{O}^2\,. \tag{4.5}$$

These two systems are closely related: when the coupling g in (4.4) is relevant, integrating out a massive ϕ produces a double-trace deformation with $\lambda = g^2/(2m^2)$.

For many purposes, it is useful to think of $g(x)$ as a dynamical field rolling in a potential. Then questions about unitarity and backreaction from interactions and particle production can be understood more directly in the theory where g is a dynamical field. This will be explored in detail in Appendix §4.A, while in the rest of this section $g(x)$ will be treated as an external coupling.

While in general it is a hard problem to determine the RG evolution of a QFT with spacetime dependent couplings, we will use the fact that in the large-N limit the infrared dynamics can be calculated explicitly. We will first recall what happens in the static case, and then incorporate the effects of spacetime dependence. Various results and calculations are relegated to Appendices §4.B and §4.C.

4.2.1 RG flow in the static limit

Let us begin with the static case. The Lagrangian including the coupling between the CFT and ϕ is

$$L = L_{CFT} - \frac{1}{2}(\eta^{\mu\nu}\partial_\mu\phi\partial_\nu\phi + m^2\phi^2) + g\,\mathcal{O}_\pm\phi \tag{4.6}$$

[7]Throughout, we will use mostly plus conventions for the metric signature. Our QFT conventions are those of Weinberg [171].

with $\mathcal{O}_\pm$ a CFT operator of dimension

$$\Delta_\pm = \frac{d}{2} \pm \nu \ , \ \ \nu > 0 \, , \tag{4.7}$$

at the unperturbed $g = 0$ fixed point, where $[g] = 1 \mp \nu$. The two-point function is normalized as

$$\langle \mathcal{O}_\pm(x) \mathcal{O}_\pm(y) \rangle = \frac{1}{[(x-y)^2]^{\Delta_\pm}} \, . \tag{4.8}$$

We analyze, in turn, three possibilities: coupling $\mathcal{O}_-$ or $\mathcal{O}_+$ to ϕ when $0 < \nu < 1$, or coupling $\mathcal{O}_+$ to ϕ for $\nu > 1$.

First, consider the effect of coupling $\mathcal{O}_-$ to ϕ. Unitarity of $\mathcal{O}_-$ requires $\nu < 1$, and the coupling g is relevant. At low energies the kinetic term for ϕ is negligible; integrating out ϕ sets

$$\phi = \frac{g}{m^2} \mathcal{O}_- \, . \tag{4.9}$$

This produces a double-trace term $\frac{g^2}{2m^2} \mathcal{O}_-^2 \subset L$, which is a relevant deformation of dimension 2ν. It is known that this triggers a flow from $\mathcal{O}_-$ to $\mathcal{O}_+$, which we now review.

In order to calculate the dimension $\Delta(\mathcal{O}_-)$ in the infrared, it is convenient to first compute the two-point function for ϕ and then use (4.9) to obtain the correlator for $\mathcal{O}_-$. At large N, loops containing ϕ are negligible, and the ϕ two-point function is given by a geometric series which sums to

$$\langle \phi(p) \phi(-p) \rangle = \frac{-i}{p^2 + m^2 - g^2 c_{-\nu} (p^2)^{-\nu}} \, . \tag{4.10}$$

This calculation is derived using path integrals in Appendix §4.B. In particular, it uses the Fourier transform of the unperturbed correlator (4.8) for $\mathcal{O}$,

$$\langle \mathcal{O}_\pm(p) \mathcal{O}_\pm(-p) \rangle = -i \, c_{\pm\nu} \, (p^2 - i\epsilon)^{\pm\nu} \ , \ c_\nu \equiv 2^{-2\nu} \pi^{d/2} \frac{\Gamma(-\nu)}{\Gamma(\frac{d}{2} + \nu)} \, . \tag{4.11}$$

(Here $p^2 = -(p^0)^2 + (p^i)^2$, and in what follows the $i\epsilon$ prescription will be implicit in

our formulas.) The last term in the denominator of (4.10) dominates at low energies,

$$\langle\phi(p)\phi(-p)\rangle \approx i\frac{(p^2)^\nu}{g^2 c_{-\nu}}\,, \tag{4.12}$$

corresponding to an operator of dimension Δ_+. Thus, $\Delta_{IR}(\mathcal{O}_-) = \Delta_+$, and we recover the double-trace flow from $\mathcal{O}_-$ to $\mathcal{O}_+$.

Next, let us instead couple $\mathcal{O}_+$ to ϕ, still in the range $0 < \nu < 1$. The $g\mathcal{O}_+\phi$ interaction is relevant, and the two-point function for ϕ becomes

$$\langle\phi(p)\phi(-p)\rangle = \frac{-i}{p^2 + m^2 - g^2 c_\nu (p^2)^\nu}\,. \tag{4.13}$$

The difference with the previous case is that now the g^2 contribution is less important than the mass term, so at low energies the correlator can be expanded in inverse powers of the mass,

$$\langle\phi(p)\phi(-p)\rangle \approx \frac{-i}{m^2}\left(1 + \frac{g^2}{m^2}c_\nu (p^2)^\nu + \dots\right)\,, \tag{4.14}$$

corresponding to an operator of dimension Δ_+.[8] This implies that the dimension of $\mathcal{O}_+$ does not change in flowing to the IR. This may be understood by noting that the double trace deformation $\frac{g^2}{2m^2}\mathcal{O}_+^2 \subset L$ obtained by integrating out ϕ is actually an irrelevant perturbation of the $g = 0$ conformal fixed point.

Finally, we come to the range $\nu > 1$ and consider an interaction $g\mathcal{O}_+\phi$ ($\mathcal{O}_-$ does not exist in this case since it would violate the unitarity bound). This was the static theory studied in [170]. The propagator for ϕ is still given by (4.13) but, crucially, now g is irrelevant. As a result, in the IR we simply have the original CFT plus a decoupled scalar field. Conversely, in the UV g becomes strong at a scale of order

$$\Lambda_g \approx \frac{1}{g^{\frac{1}{\nu-1}}}\,. \tag{4.15}$$

Choosing for simplicity a mass parameter $m \ll \Lambda_g$, for $\nu > 1$ the propagator (4.13)

[8] The first term in (4.14) gives a contact term that has to be subtracted when relating ϕ and $\mathcal{O}$ inside the path integral via $\phi = \frac{g}{m^2}\mathcal{O}$.

has a new pole at $p^2 \approx 1/(c_\nu g^2)^{1/(\nu-1)}$, which moreover has a residue with the opposite sign as the usual one at $p^2 \approx -m^2$. We thus learn that the theory has a tachyonic ghost and violates unitarity around the scale Λ_g. If we anyway continue past Λ_g towards the UV, we may interpret the ϕ two-point function as giving an 'inverse' RG flow to $\mathcal{O}_-$. Of course, the theory by itself is inconsistent and needs a UV modification above the scale Λ_g.

At this point it is useful to discuss a physical way of deriving unitarity bounds in the static theory proposed by [126], which we will then apply to the time dependent theory. The idea is to couple a probe scalar χ to the operator of interest $\mathcal{O}$ via $\chi\mathcal{O} \subset L$; then requiring that the $\chi \to \chi$ amplitude satisfy the optical theorem reproduces the unitarity bound for $\mathcal{O}$. In more detail, in terms of (4.11),

$$\mathrm{Im}\,\mathcal{A}(\chi \to \chi) \propto \mathrm{Im}\, i\langle \mathcal{O}(p)\mathcal{O}(-p)\rangle \propto -c_\nu \sin(\pi\nu)\,. \tag{4.16}$$

Then $\mathrm{Im}\,\mathcal{A} \geq 0$ for $\nu > -1$, which is the unitarity bound $\Delta_+ \geq \frac{d-2}{2}$ for $\mathcal{O}_+$.

To summarize, the interaction $g\phi\mathcal{O}$ can either give a flow from $\mathcal{O}_-$ to $\mathcal{O}_+$ in the IR, a double trace deformation $\mathcal{O}_+^2$ that is irrelevant at the $g = 0$ fixed point with the scalar ϕ becoming strongly coupled in the IR, or a theory where ϕ decouples in the IR but its interaction with $\mathcal{O}_+$ is nonrenormalizable and violates unitarity around its strong coupling scale Λ_g (above which we would formally get $\mathcal{O}_-$). In what follows we will study how all this is modified when g becomes spacetime dependent.

4.2.2 Spacetime dependent case

Having reviewed the static limit, we now consider a spacetime dependent interaction

$$g(x)\phi\mathcal{O}_+ \subset L \tag{4.17}$$

and study the long distance dynamics. Since we are interested in the possibility of a new scale invariant regime at long distance, we will assume a power-law dependence approaching

$$g(x) \to g_0(t^2 - \vec{x}^2)^{\alpha/2} \quad \text{or} \quad g(x) \to g_0|t|^\alpha\,,\ \alpha > 0\,, \tag{4.18}$$

well within the forward light cone, or at late times, respectively. With this in mind, in what follows we denote (4.18) simply by $g(x) = g_0|x|^\alpha$. We will show in §4.A that this dependence arises when a dynamical field g rolls in a potential $V \propto -g^{2\left(1-\frac{1}{\alpha}\right)}$.[9]

Before getting into any detailed calculation, let us start simply by noting the scaling of the double trace interaction induced by our mixing term (4.17), taking the rest of the Lagrangian to depend on ϕ simply as $m^2\phi^2$. Integrating out ϕ leads as in the static case to a double trace deformation

$$\int d^d x \, \frac{g(x)^2}{m^2} \mathcal{O}_+^2. \tag{4.19}$$

With the spacetime dependent $g(x)$ in (4.18), the effective coupling is g_0^2/m^2. This has dimension

$$\left[\frac{g_0^2}{m^2}\right] = 2(\alpha - \nu)\,. \tag{4.20}$$

This indicates that the condition for relevance of (4.17) is shifted by α relative to the static case, to $\alpha > \nu$. As a result, we expect that even for cases with $\nu > 0$ in which the double trace deformation would be irrelevant in the static case (including cases with $\nu > 1$ in which the irrelevant deformation leads to a pathological theory in the UV), as long as $\alpha > \nu$ the term (4.17) will be relevant. Our calculations of correlation functions below will bear this out.[10]

We are particularly interested in how (4.18) modifies the dynamics in the range $\nu > 1$, for which in the static theory unitarity violation arises in the UV and ϕ becomes a free field in the IR. It is important to point out that for $\nu > 1$ the theory will still need a UV completion or cutoff, because at momenta much larger than the rate of change $\partial g/g$, the static limit is recovered. On the other hand, we will show that for momenta $\Delta p \ll (\partial g/g)$ the spacetime dependent interaction changes the theory in important ways, depending on the relation between α and ν. Similar effects will be found when $0 < \nu < 1$, though in this range the theory is UV complete since the static theory is consistent at high energies.

[9] For even α, it is possible choose a state defined by analytically continuing to the Euclidean theory with $g(x) = g_0|x|^\alpha$ and imposing regularity at $x^\mu = 0$.

[10] We will also generalize to include the possibility that ϕ itself also starts with a kinetic term $-\int d^d x (\partial\phi)^2$ in the UV.

The calculation of the two-point function of ϕ is similar to the static one (4.10), and can be done directly in position space for a general $g(x)$. Denoting the propagators of the unperturbed $g = 0$ theory by

$$\begin{aligned} K^{-1}_{\mathcal{O}_+}(x,y) &\equiv i\langle \mathcal{O}_+(x)\mathcal{O}_+(y)\rangle_{g=0} = c_\nu \int \frac{d^dp}{(2\pi)^d} e^{ip(x-y)}(p^2-i\epsilon)^\nu = \frac{i}{[(x-y)^2]^{\Delta_+}} \\ K^{-1}_{\phi}(x,y) &\equiv i\langle \phi(x)\phi(y)\rangle_{g=0} = \int \frac{d^dp}{(2\pi)^d} \frac{e^{ip(x-y)}}{p^2+m^2-i\epsilon}\,, \end{aligned} \tag{4.21}$$

the two-point function for ϕ including quantum effects from $\mathcal{O}_+$ insertions but ignoring ϕ loops becomes

$$\langle \phi(x)\phi(x')\rangle = -iK^{-1}_\phi(x,x') - i\int d^dz_1 d^dz_2 K^{-1}_\phi(x,z_1) g(z_1) K^{-1}_{\mathcal{O}_+}(z_1,z_2) g(z_2) K^{-1}_\phi(z_2,x') + \dots \tag{4.22}$$

This is again a geometric series, which in matrix notation sums to[11]

$$\langle \phi(x)\phi(x')\rangle = -i\left(K_\phi - gK^{-1}_{\mathcal{O}_+} g\right)^{-1}(x,x')\,. \tag{4.23}$$

Recall that the static derivation requires large N at fixed g, so that internal loops containing ϕ are suppressed by powers of $1/N$. In the present spacetime dependent situation, we need to be more careful about this since our specified $g(x)$ grows at large x. Ignoring ϕ loops as we just did is valid as long as $g(x) \ll N^\gamma$, with $\gamma \sim 1$ depending on the details of the CFT OPEs. Thus, at large N and for a power-law interaction, the correlator (4.23) starts receiving corrections at parametrically large distances $|x| \sim N^{\gamma/\alpha}$. In what follows we restrict to scales where such effects are negligible.

We thus find that at large N, quantum effects from the spacetime dependent interaction can be calculated explicitly in our semiholographic model, and they lead

[11] Here the inverse $K^{-1}(x,y)$ means $\int_z K(x,z)K^{-1}(z,y) = \delta^d(x-y)$, and g can be thought of as a diagonal matrix $g(x,y) = g(x)\delta^d(x-y)$. Appendix §4.B presents a similar derivation in gaussian theories directly from the path integral.

to the effective action for ϕ

$$S_{\text{eff}}[\phi] = -\frac{1}{2}\int d^dx\, d^dx'\, \phi(x)\left((-\partial_x^2+m^2)\delta^d(x-x') - \frac{ig(x)g(x')}{[(x-x')^2]^{\Delta_+}}\right)\phi(x')\,, \quad (4.24)$$

which is equivalent to (4.23). Note that the factor of i appearing in the last term of the effective action does not necessarily violate unitarity, since this is a nonlocal term. Our analysis so far has been for a general $g(x)$. Next we will specialize to (4.18) and we will analyze how the decoupling of ϕ in the static limit is modified by the spacetime dependence in the action (4.24).

4.2.3 Long distance propagator

Let us now focus on momenta $\Delta p \ll (\partial g/g) \sim 1/|x|$ and determine the propagator when the last term in (4.24) dominates. This will be valid in a certain range of ν and α that we find below by requiring the effects from $K_\phi(x,x')$ to be negligible.

Ignoring the first two terms in (4.24) and keeping only the contributions proportional to $g(x)g(x')$, the effective action becomes

$$S_{\text{eff}}[\phi] = \frac{1}{2}\int d^dx\, d^dx'\, \frac{i\tilde\phi(x)\tilde\phi(x')}{[(x-x')^2]^{\Delta_+}}\,, \quad (4.25)$$

with $\tilde\phi(x) \equiv g(x)\phi(x)$. From this it is clear that the $\tilde\phi$ propagator is – up to a sign which we will determine next – that of $\mathcal{O}_-$. In particular, Fourier transforming $\tilde\phi(x)$ we obtain

$$S_{\text{eff}}[\phi] = \frac{1}{2}\int \frac{d^dp}{(2\pi)^d}\,\tilde\phi(p)\tilde\phi(-p)\,c_\nu(p^2-i\epsilon)^\nu, \quad (4.26)$$

where again the coefficient

$$c_\nu = 2^{-2\nu}\pi^{d/2}\frac{\Gamma(-\nu)}{\Gamma(\frac{d}{2}+\nu)}\,. \quad (4.27)$$

From (4.26), the two-point function for $\tilde\phi(p)$ is

$$\langle\tilde\phi(p)\tilde\phi(-q)\rangle = i\delta^d(p-q)\,\frac{(p^2-i\epsilon)^{-\nu}}{c_\nu}\,. \quad (4.28)$$

We can then Fourier transform back to position space and get

$$\langle\tilde{\phi}(x)\tilde{\phi}(x')\rangle = \frac{i}{c_\nu}\int\frac{d^dp}{(2\pi)^d}\,e^{ip\cdot(x-x')}(p^2-i\epsilon)^{-\nu} = \frac{-1}{c_\nu c_{-\nu}[(x-x')^2]^{\Delta_-}}\,. \tag{4.29}$$

Recalling the relation between $\tilde{\phi}(x)$ and $\phi(x)$, we arrive at our final expression for the two-point function

$$\langle\phi(x)\phi(x')\rangle = \frac{-1}{c_\nu c_{-\nu}g(x)g(x')[(x-x')^2]^{\Delta_-}}\,, \tag{4.30}$$

up to corrections from the first two terms in (4.24).

We now recall that the massive case is equivalent to a spacetime dependent double trace deformation (4.19) of the original CFT. From the relation between ϕ and $\mathcal{O}_+$ and the result (4.30), we conclude that the double trace perturbation induces a flow for $\mathcal{O}_+$ between the UV two-point function (4.8) and a long distance/late times correlator

$$\langle\mathcal{O}_+(x)\mathcal{O}_+(x')\rangle = \frac{-m^4}{c_\nu c_{-\nu}g(x)^2g(x')^2[(x-x')^2]^{\Delta_-}}\,. \tag{4.31}$$

This is one of our main results, exhibiting the effects of the spacetime dependent coupling on the IR dynamics. While translation invariance has been broken explicitly, the power-law dependence of this correlator signals the appearance of a new scale invariant regime. This two-point function implies that, under a dilatation $(x,x')\to\lambda(x,x')$, the operator transforms as $\mathcal{O}_+\to\lambda^{-\left(\frac{d}{2}-\nu+2\alpha\right)}\mathcal{O}_+$. We should also stress that this regime is approximate, being modified by small nonadiabatic effects as well as by $1/N$ corrections.

Relevance condition

Before exploring the physics contained in this result, let us analyze its regime of applicability. In other words, we need to find out when the last term in (4.24) is relevant and dominates in the IR. We first analyze this with a simple scaling argument which reproduces (4.20) in the case that the ϕ mass dominates, and then show the same result by expanding the two-point function.

Under the dilatation $(x, x') \to \lambda(x, x')$, the term $\partial_x^2 \delta^d(x - x')$ transforms with weight $d + 2$, $m^2 \delta^d(x - x')$ transforms with weight d, and $g(x)g(x')/[(x - x')^2]^{\Delta_+}$ transforms with weight $2(\Delta_+ - \alpha)$ in either the Lorentz invariant case $g(x) = g_0|x|^\alpha$ or the purely time-dependent case $g(x) = g_0|t|^\alpha$. Therefore the $g(x)g(x')$ term is more relevant than the other terms if we satisfy

$$\alpha > \begin{cases} \nu\,, & m \neq 0 \\ \nu - 1\,, & m = 0 \end{cases} \tag{4.32}$$

We may reproduce these conditions by expanding the full two-point function (4.23) around $K_\phi = 0$:

$$\langle \phi(x)\phi(x') \rangle = i \left[(gK_{\mathcal{O}_+}^{-1} g)^{-1} + (gK_{\mathcal{O}_+}^{-1} g)^{-1} K_\phi (gK_{\mathcal{O}_+}^{-1} g)^{-1} + \cdots \right](x, x')\,. \tag{4.33}$$

The leading term here is given by (4.30). The subleading term from K_ϕ can be neglected if

$$\left| (gK_{\mathcal{O}_+}^{-1} g)^{-1} K_\phi (gK_{\mathcal{O}_+}^{-1} g)^{-1}(x, x') \right| \ll \left| (gK_{\mathcal{O}_+}^{-1} g)^{-1}(x, x') \right|\,. \tag{4.34}$$

We ask when this is true and the two-point function is well approximated by (4.30) at long distance/late times (for large $|x|$, $|x'|$, and $|x - x'|$). We show in Appendix §4.C.1 that the condition is the same as (4.32). These results are in agreement with the effective dimension (4.20) calculated in the UV.

We may also ask under what conditions the free fixed point $g = 0$ is stable. In other words we expand the full two-point function (4.23) (and the one for $\mathcal{O}$) around $g = 0$, and ask when the subleading terms are much smaller than the leading one. We show in Appendix §4.C.2 that this condition is precisely the opposite of (4.32). This is what we expect: if (4.32) is satisfied, our theory is dominated in the IR by the last term in the effective action (4.24), otherwise it is dominated by the first two terms in (4.24), giving a free, decoupled scalar field.

When the coupling is a function of t only, $g = g_0|t|^\alpha$, it is more convenient to study the relevance of the different terms in the action by first Fourier transforming

the spatial coordinates. This gives, in Euclidean space,

$$S_{\text{eff}} = -\frac{1}{2}\int_{t,t',\vec{p}} \phi_{\vec{p}}(t)\left((\partial_t^2 + m^2 + \vec{p}^2)\delta(t-t') - C_\nu g(t)g(t')|\vec{p}|^{2\nu+1}\frac{K_{\nu+\frac{1}{2}}(|\vec{p}||t-t'|)}{(|\vec{p}||t-t'|)^{\nu+\frac{1}{2}}}\right)\phi_{-\vec{p}}(t') \tag{4.35}$$

where C_ν is a positive constant from the Fourier transform of $1/[(t-t')^2+\vec{x}^2]^{\Delta_+}$ with respect to $\vec{x}$. The two-point function in this mixed representation reads

$$\langle\phi_{\vec{p}}(t)\phi_{-\vec{p}}(t')\rangle = \left(K_{\phi,\vec{p}} - gK^{-1}_{\mathcal{O}_+,\vec{p}}g\right)^{-1}(t,t') \tag{4.36}$$

where $K_{\phi,\vec{p}}$ and $gK^{-1}_{\mathcal{O}_+,\vec{p}}g$ refer to the first and second term in (4.35). The condition that the $gK^{-1}_{\mathcal{O}_+,\vec{p}}g$ term dominates (which is still given by (4.34) but now in the mixed $(t,\vec{p})$ basis) gives again $\alpha > \nu$ in the massive case and $\alpha > \nu - 1$ in the limit $m = 0$, in agreement with (4.32).

4.2.4 Infrared physics and unitarity: two wrongs make a right

We would now like to generalize and analyze standard unitarity conditions in our theories. In ordinary quantum field theory, a theory that is well defined at a scale Λ will retain unitarity in the infrared. With a good UV complete theory, in other words, it is not that unitarity bounds can fail; but they are useful in helping constrain the low energy behavior of the theory. We expect that the same holds for systems like ours which are static at high energies but are subject to nontrivial time dependent effects at lower energies.

Above the scale $\partial g/g$, the coupling in our theory becomes effectively static. We may UV complete the theory in various ways; in §4.4 we will describe a supersymmetric completion and in Appendix §4.A we will describe a partial UV completion in which the time dependent coupling is the homogeneous mode of a dynamical field. Without implementing such a procedure, however, starting at any given time we may tune the value of the coupling to obtain a separation of scales between the scale Λ_g

in which the static coupling becomes strong and the scale $\partial g/g$. This hierarchy eventually breaks down at late times when $\alpha > \nu - 1$, but can be tuned to apply over a parametrically long region in time.[12]

Let us now turn to a direct analysis of unitarity conditions in our theories. We have found that time dependence can significantly affect the infrared behavior of correlation functions. It is particularly interesting to consider $\nu > 1$. In this case, for constant coupling g (i.e. $\alpha = 0$), the semiholographic mixing term in the Lagrangian is irrelevant; the operator we are considering has dimension Δ_+ in the infrared, rather than flowing to an operator of dimension Δ_- (which would violate the unitarity bound). However, in the time dependent version of the $\nu > 1$ theory, with $g(t) = g_0|t|^\alpha$, if we choose α appropriately we have seen that the semiholographic deformation can dominate in the infrared. Moreover, at long distances this theory has a two-point function for $\tilde{\phi}$ (4.29) which scales like that of an operator of dimension $\Delta_- < (d-2)/2$. In addition, from (4.29) we see that the two-point function in position space is negative for some ranges of ν, including $1 < \nu < 2$. In a conformal field theory, either of these features would imply a failure of unitarity. The negative two-point function would correspond to a negative norm state created by $\tilde{\phi}$. If the two-point function of $\tilde{\phi}$ were positive, the subunitary operator dimension Δ_- would imply that the descendant $\partial^2\tilde{\phi}$ creates a state of negative norm.[13]

In our case, on scales where the time dependent coupling affects the physics we lose the constraints of conformal symmetry, and we cannot compute the norm of states as in the static conformal field theory. However, we can use the method discussed recently for conformal field theories in [126] to obtain a unitarity condition both in the static and time dependent theories. In that way of organizing the problem, we use the momentum space propagator (4.28) to compute the imaginary part of the

[12] In some cases, it may happen that the theory is sensible even when the nominal scale Λ_g goes below the scale $\partial g/g$, but we have not fully analyzed such cases. A toy model in which we set up the corresponding question appears in Appendix §4.D. A related question is whether one can implement a cutoff at the scale $\partial g/g$; this arises at the level of a radial cutoff in the holographic models of FRW cosmology in [9].

[13] For a primary operator $\mathcal{O}$ in a CFT, the norm of the state created by the descendant $\partial^2\mathcal{O}$ can be related to an expression containing the two-point functions $\langle\mathcal{O}\partial^2\mathcal{O}\rangle$ and $\langle\partial^\mu\mathcal{O}\partial^2\mathcal{O}\rangle$ as well as $\langle\partial^2\mathcal{O}\partial^2\mathcal{O}\rangle$, which are easily computed by taking derivatives of the propagator $1/|x-y|^{2\Delta_-}$. The final result has a sign equal to $\mathrm{sgn}(\Delta_- - (d-2)/2)$.

forward scattering amplitude for Fourier modes, which must be positive for unitarity. This quantity, as shown in [126], has a sign equal to $\mathrm{sgn}[C(\Delta - (d-2)/2)]$ for an operator of dimension Δ with two-point function $C/|x-y|^{2\Delta}$.

We can now come to the key point: the imaginary part of the scattering amplitude calculated using (4.28) has a sign equal to that of $-\sin(\pi\nu)/c_\nu$. See also the discussion around (4.16). This is positive for all ν (recall $\nu > 0$), implying a positive imaginary part for the forward scattering amplitude. This is consistent with the general expectation that all theories in the class we are discussing – including both spacetime dependent ($\alpha \neq 0$) and static ($\alpha = 0$) cases – are unitary in the infrared.

It is important for this argument that the sign of the position space propagator only determines the sign of the norm of a state in the static case. Of course on short scales where the time dependent couplings do not affect the physics, the theory reverts to a static one. But on those scales, the correlation function is not of the form (4.28) (4.29), and the unitarity conditions are the familiar ones. With a sensible completion of the theory above the scale $\partial g/g$, such as those mentioned at the beginning of this section, the static unitarity conditions are satisfied in this regime.

4.3 Spacetime dependent RG flow for fermionic operators

Our analysis so far has focused on scalar operators. Now we will couple a fermion ψ to a fermionic operator $\mathcal{O}_f$ in a large-N CFT via a spacetime dependent interaction[14]

$$L = L_{CFT} - i\bar{\psi}\bar{\sigma}^\mu\partial_\mu\psi - \frac{1}{2}m\psi\psi + g(x)\psi\mathcal{O}_f + c.c. \tag{4.37}$$

[14]We employ the two-component notation of [172, 173], which is well adapted for calculations in $d = 4$. All the fermions are Weyl and transform as $(1/2, 0)$; also, $\bar{\psi}_{\dot{\alpha}} \equiv (\psi_\alpha)^\dagger$. In this section we will restrict our discussion to $d = 4$; however, the results below can be adapted to other dimensions by changing the representations of γ matrices.

and study the RG evolution. In the massive case (4.37) leads to a spacetime dependent double trace perturbation of the original CFT,

$$\int d^d x \, \frac{g(x)^2}{m} \mathcal{O}_f^2 \,, \tag{4.38}$$

and we will determine its effects at long distances. The main conclusions are similar to the ones described in §4.2: at large N the system has an effectively gaussian description which, for large enough α, flows to an approximately scale invariant regime controlled by the time dependent coupling. As before, this will also be consistent with scaling arguments around the UV fixed point. More explicit calculations for the fermionic gaussian model are relegated to Appendix §4.B.

One motivation for looking at fermionic theories comes from supersymmetry. For instance, the UV completion that we discuss in §4.4 is based on supersymmetric QCD and features an interaction between the fermionic part of the meson superfield and a fermionic operator made of magnetic quarks. We should nevertheless stress that our analysis below does not assume supersymmetry, and in fact we will find that the basic fermionic double trace flow is not related directly by supersymmetry to the previous bosonic double trace result. Another application of the fermionic version (which would be an interesting future direction), is to semiholographic Fermi surfaces with time dependent interactions. The static version of this model was proposed by [160] in $2+1$ dimensions. Static double-trace fermionic deformations have been studied recently in [174, 175]; from the bulk perspective, the double-trace operator generated by (4.38) corresponds to a Majorana-type deformation in the classification of [174].

4.3.1 Results for the static theory

As in the bosonic case, we will see that the new IR regime dominated by the time dependent coupling has a simple description in terms of a static correlator for $\tilde{\psi}(x) \equiv g(x)\psi(x)$, so it is useful to first analyze the static version of the theory.

We find it convenient to denote the fermionic CFT operators that couple to ψ by

$\mathcal{O}_{f\pm}$, with dimensions at the $g = 0$ fixed point parametrized by

$$\Delta_{f\pm} = \frac{d}{2} \pm \left(\nu - \frac{1}{2}\right) . \tag{4.39}$$

Both operators are unitary for $0 < \nu < 1$, corresponding to the standard and alternate quantizations of fermionic fields in AdS/CFT. Quantum corrections will again be given by a geometric series containing the $\mathcal{O}_f$ propagator,

$$\langle \mathcal{O}_f(x)\overline{\mathcal{O}}_f(y)\rangle = -i\sigma^\mu \frac{\partial}{\partial x^\mu} \frac{1}{[(x-y)^2]^{\Delta_f - \frac{1}{2}}} = (2\Delta_f - 1)\frac{i\sigma\cdot(x-y)}{[(x-y)^2]^{\Delta_f+\frac{1}{2}}} . \tag{4.40}$$

The dependence on the coordinates and σ matrices is fixed by Lorentz and conformal invariance, and the normalization has been chosen to be consistent with our normalization (4.21) in cases when there is supersymmetry.[15] We will also need the correlator in momentum space,

$$\langle \mathcal{O}_{f+}(p)\overline{\mathcal{O}}_{f+}(q)\rangle = i\sigma\cdot p\, c_{\nu-1}(p^2 - i\epsilon)^{\nu-1}\,\delta^d(p-q) . \tag{4.41}$$

The result for $\mathcal{O}_{f-}$ follows by replacing $\nu - 1 \to -\nu$.

Resumming the geometric series with quantum corrections from $\mathcal{O}_{f\pm}$ gives a self-energy for ψ proportional to the propagator (4.41). After inverting the Pauli matrices, the two-point function becomes

$$\langle \psi(p)\bar{\psi}(p)\rangle = -i\sigma\cdot p\,\frac{1 - c_\gamma |g|^2 (p^2)^\gamma}{p^2\left(1 - c_\gamma|g|^2(p^2)^\gamma\right)^2 + m^2 - i\epsilon} \tag{4.42}$$

where we have defined $\gamma \equiv \pm\left(\nu - \frac{1}{2}\right) - \frac{1}{2}$ for $\mathcal{O}_{f\pm}$ respectively.

Let us now briefly discuss the different consequences of this result. We restrict to $\nu > 1/2$ so that $\Delta_{f-} < \Delta_{f+}$; choosing $\nu < 1/2$ just interchanges the roles of $\mathcal{O}_{f+}$

[15] Eq. (4.40) is then a consequence of the identity

$$\langle \mathcal{O}_f(x)_\alpha \delta_\xi \mathcal{O}_b^*(y)\rangle + \langle \delta_\xi \mathcal{O}_f(x)_\alpha \mathcal{O}_b^*(y)\rangle = 0$$

where the supersymmetry variations are given by $\delta_\xi \mathcal{O}_b = \xi \mathcal{O}_f$, $\delta_\xi \mathcal{O}_f = i\sigma^\mu \bar{\xi}\,\partial_\mu \mathcal{O}_b$. See e.g. [176] for properties of correlation functions in superconformal field theories.

and $\mathcal{O}_{f-}$. First, when ψ interacts with $\mathcal{O}_{f-}$ via $g\psi\mathcal{O}_{f-} \subset L$, the dimension of the interaction is $[g] = \nu$ and the double trace deformation $\mathcal{O}_{f-}^2$ has dimension $2\nu - 1$, so both are relevant. We need to restrict to $\nu < 1$ for unitarity. The long distance correlator becomes

$$\langle \psi(p)\bar{\psi}(p)\rangle \approx i\sigma \cdot p \, \frac{(p^2 - i\epsilon)^{\nu-1}}{c_{-\nu}|g|^2} \tag{4.43}$$

corresponding to an operator of dimension Δ_{f+}.[16] In the massive case this then describes a fermionic double trace flow from $\mathcal{O}_{f-}$ to $\mathcal{O}_{f+}$. This is the analog of the bosonic double trace flow between $\mathcal{O}_-$ and $\mathcal{O}_+$, although the fermionic version differs in the shifts by 1/2. This difference has nontrivial consequences for supersymmetric theories. It means that there cannot be a supersymmetric double trace flow between superfields $\mathcal{O}_-$ in the UV and $\mathcal{O}_+$ in the IR. For instance, if we start with a supersymmetric $(\mathcal{O}_{b-}, \mathcal{O}_{f-})$ of dimensions $(\frac{d}{2} - \nu, \frac{d}{2} - \nu + \frac{1}{2})$, the bosonic flow ends on a scalar operator of dimension $\frac{d}{2} + \nu$ that would have a fermionic partner of dimension $\frac{d}{2} + \nu + \frac{1}{2}$, while the fermionic double trace flow would give a fermionic operator of different dimension $(\frac{d}{2} + \nu - \frac{1}{2})$.

The other possibility is to couple ψ to $\mathcal{O}_{f+}$. For $1/2 < \nu < 1$, the IR limit of (4.42) is, up to contact terms,

$$\langle \psi(p)\bar{\psi}(p)\rangle \approx i\sigma \cdot p \, \frac{c_{\nu-1}|g|^2(p^2 - i\epsilon)^{\nu-1}}{m^2}\,, \tag{4.44}$$

from which we deduce that the dimension is Δ_{f+}. This behavior is consistent with the fact that the interaction $g\psi\mathcal{O}_{f+}$ is relevant, but the induced double trace deformation is actually an irrelevant perturbation of the $g = 0$ fixed point, so the dimension of $\mathcal{O}_{f+}$ is not modified in the IR. Finally, for $\nu > 1$ both $\psi\mathcal{O}_f$ and $\mathcal{O}_f^2$ are irrelevant; in the IR ψ decouples and $\mathcal{O}_+$ does not flow, as can be seen in (4.42).

[16] The correlator of a fermionic operator $\mathcal{O}_f$ of dimension Δ_f scales like $\langle \mathcal{O}_f(p)\overline{\mathcal{O}}_f(p)\rangle \sim i\sigma \cdot p\,(p^2)^{\Delta_f - \frac{d}{2} - \frac{1}{2}}$.

4.3.2 Infrared dynamics of the spacetime dependent theory

Let us now turn on a spacetime dependent interaction $g(x)\psi\mathcal{O}_{f+}$ that approaches a power law $g(x) = g_0|x|^\alpha$ at long distances. A scaling argument near the $g = 0$ fixed point gives $[g_0] = \alpha - (\nu - 1)$, implying that time dependence makes this interaction relevant for $\alpha > \nu - 1$. Similarly, the condition that the double trace $\frac{g^2}{m}\mathcal{O}_{f+}^2 \subset L$ be relevant is $\alpha > \nu - 1/2$.

The long distance correlators are computed as before using large-N factorization and are described by the gaussian model of Appendix §4.B. For large enough α as above, the self-energy for $\tilde{\psi}(x) = g(x)\psi(x)$ receives the dominant contribution from inverse of the $\mathcal{O}$ correlator (4.41), giving

$$\langle\tilde{\psi}(p)\bar{\tilde{\psi}}(p)\rangle = i\sigma\cdot p\,\frac{1}{c_{\nu-1}(p^2 - i\epsilon)^\nu}\,. \tag{4.45}$$

This is simply the previous static result (i.e. the limit of large g in (4.42)) but now valid for $\nu > 1$ as long as $\alpha > \nu - 1/2$. We note that this corresponds to a field of subunitary dimension Δ_{f-} but, as will be seen shortly, the propagator does not violate unitarity. Transforming back to position space and rewriting $\tilde{\psi}$ in terms of ψ obtains

$$\langle\psi(x)\bar{\psi}(y)\rangle = -\frac{(2\Delta_{f-} - 1)}{c_{-\nu}c_{\nu-1}}\,\frac{i\sigma\cdot(x-y)}{g(x)[(x-y)^2]^{\frac{d}{2}-\nu+1}g(y)^*}\,. \tag{4.46}$$

This is our final form for the Green's function of ψ in the regime where the effects from time dependence are dominant.

Eq. (4.46) also allows us to determine the IR limit of the flow induced by a spacetime dependent double trace deformation (4.38) of the original CFT. The result is that at long distances the $\mathcal{O}_{f+}$ two-point function becomes

$$\langle\mathcal{O}_{f+}(x)\overline{\mathcal{O}}_{f+}(y)\rangle = -\frac{(2\Delta_{f-} - 1)}{c_{-\nu}c_{\nu-1}}\,\frac{i\sigma\cdot(x-y)m^2}{g(x)^2[(x-y)^2]^{\frac{d}{2}-\nu+1}g(y)^{*2}}\,. \tag{4.47}$$

As in the scalar case, we see that the power-law time dependent coupling leads to an (approximately) scale invariant regime with scaling dimensions modified by α.

We should now discuss the unitarity constraints on this fermionic two-point function. For this, we couple $\tilde{\psi}$ to an external fermion χ by $\tilde{\psi}\chi + c.c. \subset L$ and demand that the $\chi \to \chi$ scattering amplitude obey the optical theorem [126]. It is useful to recall how this works in known static examples. Coupling $\chi\mathcal{O}_{f+} + c.c. \subset L$, where the CFT fermionic operator $\mathcal{O}_{f+}$ has two-point function

$$\langle \mathcal{O}_{f+}(p)\overline{\mathcal{O}}_{f+}(q)\rangle = i\sigma\cdot p\, c_{\nu-1}(p^2 - i\epsilon)^{\nu-1}\,\delta^d(p-q)\,, \tag{4.48}$$

the scattering amplitude is

$$\mathcal{A}(\chi\to\chi) \propto c_{\nu-1}(p^2 - i\epsilon)^{\nu-1}\,. \tag{4.49}$$

The $i\epsilon$ prescription implies that in the forward lightcone $\mathrm{Im}\,\mathcal{A} \propto -c_{\nu-1}\sin(\pi(\nu-1))$, which is nonnegative for $\nu \geq 0$. This reproduces the unitarity bound $\Delta_{f+} \geq (d-1)/2$.

Now we come to our time dependent theory, where the appearance of an operator of subunitary dimension Δ_{f-} in (4.45) would naively suggest a violation of unitarity. However, this is avoided because the propagator also comes with a coefficient $c_{\nu-1}$. Coupling our probe fermion to $\tilde{\psi}$ and requiring $\mathrm{Im}\,\mathcal{A} \geq 0$ obtains $\sin(\pi\nu)/c_{\nu-1} \geq 0$. This is satisfied for all $\nu \geq 0$. The conclusion is that as long as the UV dimension Δ_{f+} is above the unitarity bound, unitarity is preserved along the time dependent RG flow.

4.4 Unitarity bounds in supersymmetric gauge theories and FRW holography

So far we have worked with a simple class of large-N-solvable field theories exhibiting the effect of spacetime dependent couplings on infrared physics and unitarity. We focused on the infrared, noting that in some cases, unitarity problems arise in the UV. In those cases, the theory needs to be cut off or cross over to different physics at a sufficiently low scale to retain unitarity. This was implemented at the static level recently in [170], and arose in our more complicated FRW examples [9].

In this section, we will combine the methods we developed in the previous section with those of supersymmetric gauge theory. Of course, spacetime dependent couplings $g(x)$ break translation invariance and supersymmetry at a scale of order $\partial g/g$. Nonetheless, this will prove useful for two reasons:
(i) Via the relation between dimensions and R-symmetries, it provides a beautiful method to relate unitarity bounds to the infrared dynamics of static theories (see e.g. [129, 130]). We will be interested in comparing this to the infrared physics one obtains instead in the presence of spacetime dependent couplings.
(ii) Well above the scale $\partial g/g$, the results of the static theory pertain and as we will see can naturally provide a UV completion.

We begin by presenting a time-dependent version of an interesting class of models [131] with $\mathcal{N} = 1$ supersymmetry; these have the structure of the above semiholographic models in the IR, and provide a concrete UV completion of that mechanism. Then, we will return to our original motivation from [9] and consider $\mathcal{N} = 2$ supersymmetric gauge theories with time-independent couplings, such as those obtained on D3-branes probing parallel (p, q) 7-branes. In this class of theories, one can vary the hypermultiplet masses to obtain regimes where mutually nonlocal matter fields (electric and magnetic) become simultaneously light [177, 178, 179]. Our first question is why from a field theory point of view this class of theories never involves more than a certain number (here $n_* = 12$) dyonic flavors descending from (p, q) strings stretching between the D3-branes and the (p, q) 7-branes. We will trace this to a unitarity bound, which is evidently relaxed in the presence of appropriate time dependence as determined from the gravity side of the corresponding holographic models [9].

4.4.1 $\mathcal{N} = 1$ Supersymmetric QCD plus singlets: unitarity bounds and UV completion

In this section, we begin with the construction in [131].[17] In this class of models, in the deep UV one has an asymptotically free theory plus a singlet. At sufficiently low energies (well below a dynamical scale Λ), [131] gives strong evidence that the

[17] We thank K. Intriligator for suggesting this class of examples to us.

theory consists of a nontrivial CFT with an irrelevant coupling to a (different) singlet Φ, which hits the unitarity bound and decouples in the deep IR. Consequently, if we consider a large-N version of the theory then in this infrared regime the system boils down to a semi-holographic model of the kind we studied above.

Consider a four-dimensional $\mathcal{N} = 1$ gauge theory with gauge group $SU(N_c)$, fundamental + antifundamental flavors $(Q, \tilde{Q})$, and a set of singlets S that couple to some of the flavors. The flavors are divided into two sets: N'_f flavors $(Q'_a, \tilde{Q}'_a)$ are coupled to S by a superpotential

$$W = hS^{ab}Q'^{\alpha}_{a}\tilde{Q}'_{b\,\alpha} \tag{4.50}$$

(where α are the contracted gauge theory indices), while the remaining N_f flavors $(Q_i, \tilde{Q}_i)$ have no superpotential interactions. For $h = 0$ this is just SQCD with $N_f + N'_f$ flavors, which flows to a superconformal field theory in the window $\frac{3}{2}N_c < N_f + N'_f < 3N_c$. In this range, the superpotential (4.50) is relevant, and drives the theory away from the $h = 0$ fixed point. In [131], evidence was provided that the theory flows to another nontrivial SCFT.

Symmetries and anomaly cancellation are not enough to determine the dimensions of holomorphic operators at the putative new fixed point, but these dimensions can be found using a-maximization [180, 131]. The result is that at the new fixed point where (4.50) becomes marginal, the conformal dimensions are given by

$$\Delta(Q\tilde{Q}) = 2y\ ,\ \Delta(Q'\tilde{Q}') = \frac{3(n+1-x)-2y}{n}\ ,\ \Delta(S) = \frac{3(x-1)+2y}{n} \tag{4.51}$$

where

$$x \equiv \frac{N_c}{N_f}\ ,\ n \equiv \frac{N'_f}{N_f} \tag{4.52}$$

and the quantity y (which is the prediction from a-maximization) is

$$y = \frac{-3[2n(n+2)+(n(n-4)-1)x+x^2]+n\sqrt{9x^2(x-2n)^2-8n(n^2-1)x+4n^2}}{2x-2n(nx+4)}\,. \tag{4.53}$$

The gauge-invariant degrees of freedom are given by the mesons and baryons

$$\Phi = (Q\tilde{Q}) \ , \ P = (Q\tilde{Q}') \ , \ P' = (Q'\tilde{Q}) \ , \ B_r = (Q^r Q'^{N_c - r}) \, , \tag{4.54}$$

whose dimensions are determined from those in (4.51).

The nature of the infrared theory changes when

$$x > x_c(n) \equiv \frac{1}{3} + \frac{5}{3}n - \frac{1}{3}\sqrt{1 - 14n + 13n^2} \, . \tag{4.55}$$

If (4.50) were still nonzero and marginal, the meson $\Phi = (Q\tilde{Q})$ would violate the unitarity bound:

$$\Delta(\Phi) = 2\Delta(Q) < 1 \, . \tag{4.56}$$

Instead of breaking unitarity, what happens at this point is that the meson decouples, and for $x > x_c(n)$ we are left with a consistent CFT plus a free field Φ.[18]

Since for $x \lesssim x_c(n)$ Φ is weakly coupled, we can write down an effective action

$$L = L_{SCFT} + \int d^4\theta \, \Phi^\dagger \Phi + \int d^2\theta \, \lambda \, \Phi \mathcal{O} + c.c. \tag{4.57}$$

with $\mathcal{O}$ being an operator in the CFT (which we identify below) of dimension

$$\Delta(\mathcal{O}) = 3 - 2y \, . \tag{4.58}$$

For $x = x_c(n)$, Φ flows to a free field, implying that the $\Phi\mathcal{O}$ interaction is irrelevant so that Φ decouples. We see that this theory in the IR is like our semiholographic model. The main difference is that the gauge theory is unitary all the way to the UV; around the dynamical scale Λ the composite nature of Φ emerges. (Also, in the static theory the dimension of Φ is calculated using supersymmetry, and no large-N limit is required.)

In fact, Seiberg duality [129, 130] provides an explicit description for (4.57). Recall that the dual of $SU(N_c)$ SQCD with N_F flavors $(Q, \tilde{Q})$ has a gauge group $SU(N_F -$

[18] $n \geq 2$ is required here, to avoid baryons hitting the unitarity bound. Eventually, for large enough x the theory exits the conformal window and moves into the free magnetic phase.

N_c), N_F magnetic quarks $(q, \tilde{q})$ and N_F^2 singlets M with a superpotential

$$W_{mag} = qM\tilde{q}\,. \tag{4.59}$$

The singlets just correspond to the mesons $M = (Q\tilde{Q})$.

The duality generalizes very simply to the theory with extra singlets as well. Start in the UV with $N_F = N_f + N_f'$ flavors and dualize. At lower energy scales, below the dynamical scale the superpotential (4.50) becomes a mass term $S^{ab}(Q'\tilde{Q}')_{ab} \subset W$ that lifts the singlets S and the mesons $(Q'\tilde{Q}')$. Hence, at low energies the dual is a theory with gauge group $SU(N_f + N_f' - N_c)$, N_f magnetic quarks $(q, \tilde{q})$ (dual to $(Q, \tilde{Q})$), N_f' quarks $(q', \tilde{q}')$ (dual to $(Q, \tilde{Q})$), and singlets Φ, P, P' (identified in (4.54)) with superpotential

$$W_{mag} = q\Phi\tilde{q} + qP\tilde{q}' + q'P'\tilde{q}\,. \tag{4.60}$$

In the magnetic theory, the meson Φ appears as an elementary field that couples to the rest of the fields via $\Phi q\tilde{q} \subset W$. So the operator $\mathcal{O}$ above is identified with the product of magnetic quarks $q\tilde{q}$. In this dual theory, when $x \geq x_c(n)$ the coupling $\Phi q\tilde{q}$ is irrelevant and the elementary Φ becomes a free field, in agreement with the analysis in the electric theory.

The dynamics of this system can be studied at large N. Indeed, the CFT exists at large N_c and N_f' with N_f fixed, in which case loops containing Φ will be suppressed by powers of N_f/N_c and N_f/N_f'. Therefore in components we obtain a fermion ψ and a complex scalar ϕ interacting with a large-N CFT sector. The fermion couples linearly to the CFT operator $q\psi_{\tilde{q}} + \tilde{q}\psi_q$ (where ψ_q is the fermion component of the chiral superfield q and so on). In this large-N limit, the theory is in the same class of theories as our semiholographic models, and can be analyzed using similar techniques.

In particular, we wish to understand what effect a spacetime dependent coupling $\lambda(x)$ would have on the infrared physics. Let us discuss this using the magnetic dual, which is more appropriate for this purpose. We start with

$$W_{mag} \supset \lambda(x) q\Phi\tilde{q}\,, \tag{4.61}$$

where we continue to use supersymmmetric language to package the following component Lagrangian. Denoting the scalar and fermion components of Φ by ϕ and ψ respectively, the resulting classical component Lagrangian is

$$\begin{aligned} L =& L_{SCFT} - \partial_\mu \phi^* \partial^\mu \phi - i\bar{\psi}\ \not{\partial}\psi - \lambda(x)^2|\phi|^2(|q|^2+|\tilde{q}|^2) - \lambda(x)^2|q\tilde{q}|^2 - (\lambda(x)\phi\psi_q\psi_{\tilde{q}} \\ & -\lambda(x)\psi(q\psi_{\tilde{q}} + \tilde{q}\psi_q) + c.c.) \end{aligned} \tag{4.62}$$

In the deep IR, supersymmetry no longer controls our calculations, but using large N we can control the semiholographic mixing between ψ and $q\psi_{\tilde{q}} + \tilde{q}\psi_q$ in the same way as we did in §4.3, obtaining correlators which include a would-be subunitary operator combined with factors of $1/\lambda$ which restore unitarity. At shorter scales than $\lambda/\partial\lambda$, we return to the static theory, for which the double trace deformation generated by integrating out ψ is irrelevant. This theory is unitary, altogether providing a UV completion of our basic semi-holographic mechanism. In §4.3 we analyzed the fermionic case explicitly. It would also be interesting to study the full (4.62) at large N, including the effects of the quartic couplings which are absent in the theory analyzed in §§4.2 and 4.3.

Further remarks

Here we have considered a spacetime dependent coupling directly in the magnetic theory, which by itself provides a consistent UV completion for our semiholographic model. The electric theory gives a different UV theory (the two are equivalent only in the deep IR), and it is interesting to ask how to incorporate time dependence in this setup. One possibility would be to consider time dependent gauge couplings. Another option is to add new singlets N and Φ to the electric theory, with superpotential

$$W_{el} \supset Q N \tilde{Q} + \lambda(x) N \Phi \,. \tag{4.63}$$

This is the dual of (4.61) when λ is small. Note that for constant λ the second term gives masses to N and Φ; integrating out N then yields the usual relation between Φ and the electric meson, $(Q\tilde{Q}) = -\lambda\Phi$. In the time dependent case we should instead

keep these fields in the effective theory; for $x \geq x_c(n)$ we expect that $\lambda(x)$ will modify the dynamics of $(Q\tilde{Q})$, which would otherwise decouple in the static limit.

Finally, let us briefly mention another type of modification of the theory which could adjust the infrared physics in a similar way: add an extra chiral superfield X, assumed to couple in the superpotential as

$$W \sim \lambda \frac{q\Phi\tilde{q}}{X^k} \tag{4.64}$$

to good approximation at sufficiently large and homogenous X, with k some positive number (and λ constant). For instance, instanton-generated superpotentials can contain inverse powers of X. If there is a limit where we can treat X as a fixed background, then requiring that (4.64) is marginal at the fixed point obtains

$$\Delta(\Phi) = 3 - \Delta(\mathcal{O}) + k\Delta(X) \tag{4.65}$$

with $\mathcal{O} = q\tilde{q}$ as before. So the dimension of Φ would be increased by its interaction with X, leading to unitarity consistent with nonvanishing λ, unlike the original static theory in which $\lambda \to 0$ in the infrared. We have not constructed an example of this yet; it would be interesting to find a UV completion of this mechanism.

4.4.2 Seiberg-Witten theory and flavor bounds

Our next class of theories is an $\mathcal{N} = 2$ gauge theory in four dimensions, studied by Seiberg and Witten [181] as well as many other subsequent works[19]. Using these, we will make contact with our motivating examples [9]. We will show that the matter content derived from the brane construction in [9] in the case of parallel 7-branes would not be unitary with static couplings. This fits well with the fact that the dual description of the FRW spacetime solutions in [9] has time dependent couplings. However, this theory is more complicated than those analyzed above; in particular we have not isolated a simple limit in which to calculate correlation functions on the field theory side.

[19] See e.g. [182] for a review and references.

A useful way to geometrize the Coulomb branch of $\mathcal{N} = 2$ theories is as position collective coordinates of D3-branes probing sets of (p, q) 7-branes. In that language, we are interested in nontrivial fixed points which arise when a stack of N_c color branes hits a set of mutually nonlocal 7-branes. As the 3-branes approach the 7-branes, we obtain light mutually nonlocal flavors [90, 91, 177, 178, 179]. We would like to use field theory techniques to understand how many such flavors can arise in this way.

Let us focus on the case of an SU(2) gauge group, with a one complex dimensional Coulomb branch labelled by u. This captures the dynamics of the center of mass of the stack of D3-branes in the class of models just described. We work near a fixed point which we take to sit at $u = 0$. Holomorphic quantities in the theory such as the gauge coupling function, the metric on the Coulomb branch, and BPS particle masses are related to the Seiberg-Witten (SW) curve

$$y^2 = x^3 - f(u)x - g(u) \tag{4.66}$$

where x and y are complex variables, u is the local Coulomb branch coordinate and the singularity is located at $u = 0$. f and g are polynomials in u; varying their coefficients corresponds to turning on relevant deformations of the fixed point. The SW curve defines a differential λ_{SW} by

$$\frac{d\lambda_{SW}}{du} = \frac{dx}{y}\,. \tag{4.67}$$

BPS masses are given by combinations of the periods of λ_{SW} on the torus (4.66); these periods are denoted by (a, a_D) and are functions of u. Moreover, the scalar kinetic term is obtained by differentiating the Kähler potential

$$K = \mathrm{Im}(A_D \bar{A})\,. \tag{4.68}$$

The Seiberg-Witten curve also determines the dimension of the Coulomb branch coordinate u [179]; let us review how this comes about. Since the BPS masses are linear combinations of a and a_D, these periods have dimension one. This is also consistent with the Kähler potential above having dimension 2. Since $a \sim (u/y)dx$,

we find the relation between the conformal dimensions

$$\Delta(x) - \Delta(y) + \Delta(u) = 1\,. \tag{4.69}$$

Close enough to the singularity $u = 0$ that describes the CFT, f and g have a power-law dependence, which we parametrize by

$$f(u) \sim u^r\ ,\ g(u) \sim u^s\,. \tag{4.70}$$

For $2s < 3r$ ($2s > 3r$) the singularity is dominated by g (resp. f), so these cases need to be treated separately.

First, when $2s < 3r$, the SW curve for $u \to 0$ is $y^2 \approx x^3 - u^s$; since at the fixed point it should scale homogeneously under dilatations, the scaling dimensions obey

$$2\Delta(y) = 3\Delta(x) = s\Delta(u)\,. \tag{4.71}$$

Combining this with (4.69) we obtain

$$\Delta(u) = \frac{6}{6-s}\,. \tag{4.72}$$

We see that for $s > 6$ the Coulomb branch field u would violate unitarity. On the other hand, for $2s > 3r$ the singularity is dominated by f, and a similar analysis leads to the dimension

$$\Delta(u) = \frac{4}{4-r}\,. \tag{4.73}$$

This violates unitarity for $r > 4$. The set of all integers (r, s) allowed by unitarity reproduce the ADE classification of singularities [183].

Now we want to express $\Delta(u)$ in terms of the number N_f of flavors – i.e. the number of 7-branes in the $D3$–(p, q)7-brane realization of SW. N_f is given by the order of the vanishing of the discriminant

$$\Delta = 4f^3 + 27g^2 \tag{4.74}$$

at the singularity. This relates N_f to (s, r) above: for $2s < 3r$ we have $N_f = 2s$, while $N_f = 3r$ if $2s > 3r$. In terms of N_f, both (4.72) and (4.73) reduce to

$$\Delta(u) = \frac{12}{12 - N_f} \,. \tag{4.75}$$

We conclude that there is no unitary $\mathcal{N} = 2$ supersymmetric conformal field theory in this class of models for $N_f > 12$.

At this point it is useful to make contact with AdS/CFT and review how this result is obtained in the gravity side. The F-theory description of N_f 7-branes in Sen's limit of constant axio-dilaton gives a 10d metric

$$ds^2 = \eta_{\mu\nu} dx^\mu dx^\nu + \frac{dz d\bar{z}}{(z\bar{z})^{N_f/12}} \,. \tag{4.76}$$

Introducing a D3 probe parallel to the 7-branes, the worldvolume field u that describes motion along the z direction has a kinetic term

$$S = -\int d^4x \, \eta^{\mu\nu} \frac{\partial_\mu u \partial_\nu \bar{u}}{(u\bar{u})^{N_f/12}} \,. \tag{4.77}$$

From here we can read off the scaling dimension $\Delta(u) = 12/(12 - N_f)$, in agreement with the field theory result. (The relation between u and z that we used here is fixed by supersymmetry.) Nontrivial CFTs (some of which have no known field theory description) are obtained by placing N_c D3-branes near one of these ADE singularities from 7-branes [184, 44].

The gravity side provides a useful description to explore mechanisms for avoiding the unitarity violation that we just found. In particular, controlled late-time time-dependent F-theory solutions with $N_f > 12$ were found in [75] and the implications for the holographic duality were studied in [9]. There, we have a controlled gravity description with warping and hence a low energy field theory regime; but in that case the dual is strongly interacting and we have not done an independent field theoretic calculation of the effects of the time dependence. From the gravity side we can see the dual theory is defined up to a time-dependent cutoff $\Lambda \sim 1/t$; it would be interesting to understand in more detail how this holographic cutoff is realized in the dual theory.

Gravity decouples in the dual theory at late times, so this question is purely field-theoretic. Next, we will exhibit a static theory with $n > n_*$ *massive* flavors, another way to restore unitarity.

4.4.3 Static theory with $n > n_*$ massive flavors

In general, a field theory which is well defined in the UV (e.g. QED on the lattice above its Landau pole) will do something sensible at all scales. What we have shown is that it cannot retain $\mathcal{N} = 2$ SUSY and $n > n_*$ massless magnetic flavors. In the discussion so far, we have focused on the effects of time dependence on unitarity conditions. However, in this subsection we briefly mention another consistent flow in the static case in which $n > n_*$ magnetic flavors are present, but massive.

The work [16] constructed noncompact Calabi-Yau fourfolds describing intersecting (p, q) 7-branes, generalizing those in [184, 44]. These, combined with color $D3$-branes placed at the intersection, can produce AdS/CFT dual pairs with small internal dimensions. In [16] a physical criterion for singularity-freedom was articulated, matching but generalizing standard results. This limits how many 7-branes can intersect, leading to bounds of the sort described above (the details of which depend on the codimension of intersection). If we take a case with $n > n_*$, i.e. with a singular intersection, and deform it so that the 7-branes do not intersect at the same point, this can remove the singularity. It was argued in [184, 44] that generically for such F-theory configurations adding D3 color branes produces a good AdS/CFT duality. The deformation away from the singularity means that the flavors obtained from (p,q) strings are not simultaneously light; they are generically massive.

Although it would take us too far afield to describe in detail here, we have used gauge linear sigma model techniques to construct an example of a noncompact Calabi-Yau fourfold describing a configuration of 7-branes with $n > n_*$, deformed away from the would-be singular intersection. In the resulting dual theory, the excessive magnetic flavors are massive, corresponding to a smoothed out tip controlled by a deformation parameter in the superpotential of the sigma model. The model has nontrivial RG flow corresponding to bending of the branes as one evolves in the

radial direction toward the resolved singularity.

4.5 Future directions

Happy families are all alike; every unhappy family is unhappy in its own way. – Leo Tolstoy.

In this chapter, we have shown how infrared physics and unitarity conditions are consistently modified in time dependent quantum field theory, as compared to static versions of the same theory. We focused on double trace deformations and related semiholograpic theories in order to explicitly analyze these effects in tractable examples with nontrivial operator scaling. The lesson is more general, and suggests several interesting directions to pursue.

We have seen how spacetime dependent couplings affect RG trajectories, in some cases reversing the direction of flow at long distances as compared to the static version of the theory. Similarly, in cases which are classically marginal at the static level, spacetime dependent couplings will generically introduce nontrivial flow at the same order. This opens up the possibility of new fixed points, for example in spacetime dependent QED in four dimensions with sufficiently many flavors to screen the interaction at one loop.

Our results suggest a similar explanation for how the flavor content of the time dependent holographic quantum field theory in [9] (dual to an FRW geometry with a warped metric) is distinct from the flavor content allowed in the corresponding static theories. It would be interesting to pursue other examples to see how unitarity bounds are affected by spacetime dependent couplings. Examples to which we may apply these ideas include minimal models which are nonunitary at the static level, additional examples of SUSY and/or holographic gauge theories going below their static unitarity bound, and no-ghost theorems in various holographic backgrounds modified by time dependence.

4.A Dynamical couplings and unitarity

In this section, we promote the time dependent coupling to a dynamical field, and study unitarity constraints and scales in this 'parent' theory. This will provide a useful partial UV completion of the main semiholographic example in the text, one which requires a cutoff that is static and well above the energy scale of the time variation of the effective coupling coming from the rolling scalar field. A UV completion up to arbitrarily high scales is provided by the UV-supersymmetric examples in the main text.

The full action is

$$L = L_{CFT} - \frac{1}{2}\left((\partial\phi)^2 + m^2\phi^2\right) + \lambda_0\, g\phi\mathcal{O}_+ - \frac{1}{2}(\partial g)^2 - V(g) \tag{4.78}$$

where we have promoted the coupling $g(x)$ to a field. Ignoring the cubic interaction $g\phi\mathcal{O}$, we will construct a potential $V(g)$ such that at late times $g(x) \approx g_0 t^\alpha$. Then we will determine the conditions under which $g(x)$ may be considered as a background field and we can neglect effects of the cubic interaction on the dynamics of this field.

The starting Lagrangian (4.78) has only static couplings, and it will be found that $V(g)$ does not involve higher dimension operators over the range of field of interest to us. However, at the UV fixed point the cubic coupling is irrelevant, $[\lambda_0] = 2-\Delta_+ < 0$, for $d \geq 2$ and $\nu > 1$. Thus, this theory needs a UV cutoff

$$\Lambda_0 = \frac{1}{\lambda_0^{1/(\Delta_+-2)}}\,. \tag{4.79}$$

Using conservation of energy,

$$\frac{1}{2}\left(\frac{dg}{dt}\right)^2 + V(g) = V_0 \tag{4.80}$$

and inverting $t = (g/g_0)^{1/\alpha}$ gives a (late time) potential

$$V(g) = V_0 - \frac{1}{2} g_0^{\frac{2}{\alpha}} \alpha^2 g(x)^{2(1-\frac{1}{\alpha})}\,. \tag{4.81}$$

The potential is negative for large enough g, but the power $0 < 2(1 - \frac{1}{\alpha}) < 2$ for $\alpha > 0$. So g takes an infinite time to reach infinity and the system does not require a self-adjoint extension.

For our purposes, we are concerned about unitarity bounds but not model-building "taste bounds"; i.e. we are content to tune the potential as required to maintain the shape (4.81). Similarly, we may avoid strong effects of particle (or unparticle) production by coupling $\mathcal{O}$ to a sufficient number of additional operators in the CFT which do not couple directly to g. Thus, as the time dependent motion of g produces excited states of $\mathcal{O}$, it quickly shares that energy with other modes which do not directly backreact on g. This procedure may buy us a parametrically long time under which nonadiabatic effects on the underlying state of the system may be ignored, though at some point these effects become important.

The energy scale for the perturbations of the rolling scalar is given by the square root of

$$V''(g) = -(\alpha - 1)(\alpha - 2)\frac{g_0^{2/\alpha}}{g(x)^{2/\alpha}} = -(\alpha - 1)(\alpha - 2)\frac{1}{t^2}\,, \tag{4.82}$$

which is of the same order as $\partial g/g$. The range $1 < \alpha < 2$ is interesting in that $V''(g) > 0$, giving the fluctuation δg a positive mass of order $1/t$. Above the scale $\partial g/g$ we must include the dynamics of the field $g(x)$. This gives a UV completion up to the scale Λ_0 (4.79) at which we could introduce a (static) cutoff to render the theory completely well defined. As a result, the theory must be unitary on all scales; this is checked in the infrared in the main text.

4.B Gaussian theories with spacetime dependent masses

In this appendix we consider a model of time dependence given by a quadratic action with two fields coupled together via spacetime dependent masses, and perform the path integral explicitly. The kinetic terms are taken to be arbitrary kernels $K(x, y)$. This theory also captures the leading result for the effective action of a field coupled to a large-N CFT that was analyzed in §4.2 and §4.3.

4.B.1 Bosonic model

Consider a Gaussian bosonic theory of the form

$$S = -\frac{1}{2}\int d^d x d^d y \left(\phi(x) K_\phi(x,y)\phi(y) + \mathcal{O}(x) K_{\mathcal{O}}(x,y)\mathcal{O}(y)\right) + \int d^d x\, g(x)\mathcal{O}(x)\phi(x)\,. \tag{4.83}$$

In the setup of §4.2, $\mathcal{O}$ would be an operator in a nontrivial CFT, ϕ is the weakly coupled scalar, and $g(x)$ is the spacetime dependent coupling. Also, in this case the kernels K_ϕ and $K_{\mathcal{O}}$ would be translationally invariant, but in our present discussion these kernels will be arbitrary. (Of course, they should be positive definite, so that the path integral is well defined.)

Our goal is to compute the two-point functions for (4.83). For this, it is convenient to adopt a matrix notation where

$$S = -\frac{1}{2}\phi_a K_{ab}\phi_b \tag{4.84}$$

and

$$K_{ab} = \begin{pmatrix} K_\phi(x,y) & -g(x)\delta(x-y) \\ -g(x)\delta(x-y) & K_{\mathcal{O}}(x,y) \end{pmatrix} \tag{4.85}$$

Here a, b are multi-indices that distinguish both $(\phi, \mathcal{O})$ and the position coordinates; summation over repeated indices also contains an integral over positions. With our mostly plus sign conventions, we have

$$Z[J] = \int \mathcal{D}\phi\, \exp\left[-\frac{i}{2}\phi_a K_{ab}\phi_b + J_a\phi_a\right] = \exp\left[-\frac{i}{2}J_a (K^{-1})_{ab} J_b\right] \tag{4.86}$$

and the two-point function is given by

$$\langle \phi_a \phi_b \rangle = \frac{\delta^2 Z}{\delta J_a \delta J_b} = -i(K^{-1})_{ab}\,. \tag{4.87}$$

The inverse of (4.85) can be calculated using the formula for the inverse of a block

matrix

$$\begin{pmatrix} A & B \\ C & D \end{pmatrix}^{-1} = \begin{pmatrix} (A-BD^{-1}C)^{-1} & -A^{-1}B(D-CA^{-1}B)^{-1} \\ -D^{-1}C(A-BD^{-1}C)^{-1} & (D-CA^{-1}B)^{-1} \end{pmatrix}, \quad (4.88)$$

which gives

$$\begin{aligned} (K^{-1})_{ab} &= \begin{pmatrix} (K_\phi - gK_{\mathcal{O}}^{-1}g)^{-1} & K_\phi^{-1}g(K_{\mathcal{O}} - gK_\phi^{-1}g)^{-1} \\ K_{\mathcal{O}}^{-1}g(K_\phi - gK_{\mathcal{O}}^{-1}g)^{-1} & (K_{\mathcal{O}} - gK_\phi^{-1}g)^{-1} \end{pmatrix} & (4.89) \\ &= \begin{pmatrix} (K_\phi - gK_{\mathcal{O}}^{-1}g)^{-1} & K_\phi^{-1}g(K_{\mathcal{O}} - gK_\phi^{-1}g)^{-1} \\ (K_{\mathcal{O}} - gK_\phi^{-1}g)^{-1}K_\phi^{-1}g & (K_{\mathcal{O}} - gK_\phi^{-1}g)^{-1} \end{pmatrix} & (4.90) \end{aligned}$$

The two-point functions are then

$$\begin{aligned} \langle\phi(x)\phi(y)\rangle &= -i(K_\phi - gK_{\mathcal{O}}^{-1}g)^{-1}(x,y) \\ \langle\phi(x)\mathcal{O}(y)\rangle &= -i\left[K_\phi^{-1}g(K_{\mathcal{O}} - gK_\phi^{-1}g)^{-1}\right](x,y) \\ \langle\mathcal{O}(x)\mathcal{O}(y)\rangle &= -i(K_{\mathcal{O}} - gK_\phi^{-1}g)^{-1}(x,y)\,. \end{aligned} \quad (4.91)$$

These formulas reproduce the large-N result (4.23) for $\langle\phi(x)\phi(y)\rangle$ obtained by summing the geometric series with $\mathcal{O}$ propagators. However, it is important to note that for a kernel such as

$$K_{\mathcal{O}}^{-1}(x,y) = \frac{i}{[(x-y)^2]^\Delta} \quad (4.92)$$

we need to add the rest of the CFT (that is responsible for the nontrivial dimension Δ) in order to have a consistent theory. So, while the gaussian model captures correctly the two-point functions for ϕ and $\mathcal{O}$, one should keep in mind that it is not complete by itself without the remaining CFT. This is what we mean by 'effectively gaussian' in the main text.

4.B.2 Fermionic model

Let us now analyze a fermionic Gaussian theory with spacetime dependent coupling g:

$$S = \bar{\psi} K_\psi \psi - \frac{1}{2} m(\psi\psi + \bar{\psi}\bar{\psi}) + \overline{\mathcal{O}}_f K_f \mathcal{O} + g\psi\mathcal{O}_f + \eta\psi + \eta_f \mathcal{O}_f + c.c. \tag{4.93}$$

where the sources η and η_f are introduced to calculate the propagators, and are set to zero at the end. For instance, $K_\psi = -i\bar{\sigma}^\mu \partial_\mu \, \delta^d(x-y)$ for a free fermion; we follow the two-component notation of [172, 173]. As before, $\mathcal{O}_f$ plays the role of the CFT fermionic operator, so we have not included a mass term for this field.

It is useful to introduce a 'Majorana' fermion $\Psi_a \equiv (\psi, \bar{\psi}, \mathcal{O}_f, \overline{\mathcal{O}}_f)$, and similarly for the sources $N_a \equiv (\bar{\eta}, \eta, \bar{\eta}_f, \eta_f)$, such that the action can be written compactly as

$$S = \frac{1}{2} \, \bar{\Psi}_a K_{ab} \Psi_b + \bar{\Psi}_a N_a \,, \tag{4.94}$$

with

$$K_{ab} = \begin{pmatrix} K_\psi & -m & 0 & g^* \\ -m & \bar{K}_\psi & g & 0 \\ 0 & g^* & K_f & 0 \\ g & 0 & 0 & \bar{K}_f \end{pmatrix} . \tag{4.95}$$

Here $\bar{K}_\psi$ is defined by $\psi \bar{K}_\psi \bar{\psi} = \bar{\psi} K_\psi \psi$, and similarly for $\bar{K}_f$. In particular, $\bar{K}_\psi = -i\sigma^\mu \partial_\mu \, \delta^d(x-y)$ for a free fermion.

The equation of motion gives $K_{ab}\Psi_b = -N_a$, so the partition function becomes

$$Z[N_a] = \int \mathcal{D}\Psi \, e^{iS} = \exp\left[-\frac{i}{2} \bar{N}_a (K^{-1})_{ab} N_b \right] . \tag{4.96}$$

From here, the two-point functions are

$$\langle \Psi_a \bar{\Psi}_b \rangle = -\frac{\delta^2 Z}{\delta N_b \delta \bar{N}_a} = i(K^{-1})_{ab} \,. \tag{4.97}$$

The inverse $(K^{-1})_{ab}$ is calculated using (4.88). In the notation of this equation we

have, for instance,

$$A - BD^{-1}C = \begin{pmatrix} K_\psi - g^* \bar{K}_f^{-1} g & -m \\ -m & \bar{K}_\psi - g K_f^{-1} g^* \end{pmatrix} . \tag{4.98}$$

This shows that quantum effects from $\mathcal{O}_f$ shift the effective action of ψ by $K_\psi \to K_\psi - g^* \bar{K}_f^{-1} g$. The inverse of (4.98) gives

$$\begin{aligned} \langle \psi(x) \bar{\psi}(y) \rangle &= i \left[(\bar{K}_\psi - g K_f^{-1} g^*) \cdot \left((K_\psi - g^* \bar{K}_f^{-1} g)(\bar{K}_\psi - g K_f^{-1} g^*) - m^2 \right)^{-1} \right] (x, y) \\ \langle \psi(x) \psi(y) \rangle &= im \left((K_\psi - g^* \bar{K}_f^{-1} g)(\bar{K}_\psi - g K_f^{-1} g^*) - m^2 \right)^{-1} (x, y) , \end{aligned} \tag{4.99}$$

in agreement with the large-N results in §4.3.

4.C Expansion of the two-point functions

4.C.1 Expansion around the nontrivial scale-invariant regime

The two-point function (4.30) suggests that there is an approximately scale-invariant regime in our semi-holographic model. In the following we show that our theory indeed flows to this regime in the IR for a range of α.

For this we start with the full two-point function (4.23) and evaluate the corrections to (4.30) from K_ϕ. These are obtained by expanding (4.23) around $K_\phi = 0$:

$$\langle \phi(x) \phi(x') \rangle = i \left[(g K_{\mathcal{O}_+}^{-1} g)^{-1} + (g K_{\mathcal{O}_+}^{-1} g)^{-1} K_\phi (g K_{\mathcal{O}_+}^{-1} g)^{-1} + \cdots \right] (x, x') . \tag{4.100}$$

The leading term here is given by (4.30). The subleading term from K_ϕ can be neglected if

$$\left| (g K_{\mathcal{O}_+}^{-1} g)^{-1} K_\phi (g K_{\mathcal{O}_+}^{-1} g)^{-1} (x, x') \right| \ll \left| (g K_{\mathcal{O}_+}^{-1} g)^{-1} (x, x') \right| , \tag{4.101}$$

or more directly

$$\left|[(x-x')^2]^{\Delta_-}\int d^dz\,\frac{1}{g(z)[(x-z)^2]^{\Delta_-}}\,(-\partial_z^2+m^2)\frac{1}{g(z)[(z-x')^2]^{\Delta_-}}\right|\ll 1\,. \quad (4.102)$$

Let us estimate this integral in euclidean space for the power law coupling $g(x) = g_0|x|^\alpha$. Convergence at the origin (in the Euclidean version of this calculation) requires $\alpha < (d-2)/2$ when ϕ has a kinetic term, or $\alpha < d/2$ if it only has a mass term, but as mentioned above we need not extend the power law form of $g(x)$ all the way to the origin. Convergence at $z \to x, x'$ requires $\nu > 0, 1$ respectively, however, these divergences are present in the static case as well and can be cancelled by local counterterms. Convergence at large $|z|$ requires $\alpha > 2\nu - d/2$ in the massive case $m \neq 0$, or $\alpha > 2\nu - d/2 - 1$ in the massless case $m = 0$.

We would like to show (4.102) for large $|x|$, $|x'|$, and $|x - x'|$. There are (at least) two ways of taking this limit: either $|x| \sim |x'| \sim |x - x'|$, or one of them is much larger – say $|x| \gg |x'|$. In either case, a leading contribution to the integral comes from the region $|z| \sim |x'|$ and the left hand side of (4.102) is of order

$$\sim \left(-\frac{1}{|x'|^2} + m^2\right)\frac{1}{|x'|^{2(\alpha-\nu)}}\,. \quad (4.103)$$

One may verify that higher order corrections in (4.100) all come with additional powers of (4.103). Therefore all corrections from K_ϕ are negligible for large $|x|$, $|x'|$ if we have

$$\alpha > \nu \quad (4.104)$$

in the massive case $m \neq 0$, or

$$\alpha > \nu - 1 \quad (4.105)$$

in the massless case $m = 0$. These conditions are strictly stronger than the corresponding convergence conditions at large $|z|$, as long as $\Delta_- = d/2 - \nu > 0$. We conclude that our theory flows to an IR fixed point characterized by the two-point function (4.30) when (4.104) or (4.105) is satisfied.

The analog calculation in Minkowski signature would have additional divergences

on the light cone if $\Delta_- > 1$. These divergences are present already in the static limit, and are absent given an appropriate $i\epsilon$ prescription which is easy to implement in momentum space. In our case as well, this is simplest to address by Fourier transforming the factors $1/[(x-z)^2]^{\Delta_-}$ and $1/[(x'-z)^2]^{\Delta_-}$, then integrating over z. This turns the left hand side of (4.102) into an expression proportional to (considering for simplicity the term proportional to m^2)

$$m^2 c_\nu^2 \left| [(x-x')^2]^{\Delta_-} \int d^d p_1 \int d^d p_2 \left(\tilde{\frac{1}{g^2}}\right)(p_1+p_2) \frac{e^{i(p_1 x + p_2 x')}}{(p_1^2 - i\epsilon)^\nu (p_2^2 - i\epsilon)^\nu} \right| \tag{4.106}$$

with $\left(\tilde{\frac{1}{g^2}}\right)(p_1+p_2)$ the Fourier Transform of $1/g^2(z)$, a smooth function of z. For even α, this can also be done by analytically continuing the (regular) Euclidean result.

It is also worth noting that the scale covariance manifest in our IR two-point functions does not hold for all times, as we have explained above. In particular, our theory has (un)particle production due to the spacetime-dependent coupling, and $1/N$ corrections also become important at sufficiently late times.

4.C.2 Expansion around the free fixed point

We may also ask if there are other IR fixed points to which our theory could flow. Specifically, we may ask if the free $g = 0$ fixed point characterized by (4.21) is IR stable.

Let us first work in the massless case $m = 0$, so the fixed point contains a free massless scalar field decoupled from a CFT. To investigate its stability in the IR, we expand the full two-point function (4.23) around $g = 0$:

$$\langle \phi(x)\phi(x') \rangle = -i \left(K_\phi^{-1} + K_\phi^{-1} g K_{\mathcal{O}_+}^{-1} g K_\phi^{-1} + \cdots \right)(x, x') \,. \tag{4.107}$$

The leading term here is $1/|x-x'|^{d-2}$, the two-point function of a free massless scalar field. The subleading term can be neglected if

$$\left| |x-x'|^{d-2} \int d^d z \int d^d z' \frac{g(z) g(z')}{|x-z|^{d-2} |z-z'|^{2\Delta_+} |x'-z'|^{d-2}} \right| \ll 1 \,. \tag{4.108}$$

Again one could consider different ways of taking $|x|$, $|x'|$, and $|x-x'|$ to large values. Convergence of the integral at large $|z|$, $|z'|$ leads to a weaker condition than our final result. The left hand side of (4.108) is estimated to be of order $|x'|^{2(\alpha-\nu+1)}$. Therefore we conclude that the free fixed point is IR stable when $\alpha < \nu-1$. When this condition is violated, our previous result shows that the theory flows to the nontrivial fixed point characterized by (4.30).

Note that we would have arrived at the same conclusion (4.105) had we demanded that the $g(x)g(x')$ term in the effective action be a relevant deformation of the free fixed point. Indeed, under the scaling transformation

$$x \to \lambda x \ , \ x' \to \lambda x' \ , \ \phi \to \lambda^{-\frac{d-2}{2}} \phi \tag{4.109}$$

the last term in (4.24) is relevant precisely when $\alpha > \nu - 1$. So our previous explicit calculation shows that we are in a situation where scaling arguments from static QFT still apply in the presence of spacetime dependent couplings. The power law $g(x) = g_0|x|^\alpha$ has turned an interaction that would have been irrelevant in the static case into a relevant one (for $\alpha > \nu - 1$). The scale at which this coupling crosses over from irrelevant to relevant is $\Delta p \sim 1/|x|$. In other words, this is a "dangerously irrelevant" operator, with the "danger" coming from spacetime dependence.

One could also consider the massive case $m \neq 0$, where the scalar field is gapped out from the free fixed point in the IR. In this case we look at the two-point function of $\mathcal{O}_+$.[20] In the large-N limit it similarly sums to

$$\langle \mathcal{O}_+(x)\mathcal{O}_+(x')\rangle = -i\left(K_{\mathcal{O}_+} - gK_\phi^{-1}g\right)^{-1}(x,x')\,. \tag{4.110}$$

The free fixed point is stable in the IR if we can ignore the subleading corrections in the expansion

$$\langle \mathcal{O}_+(x)\mathcal{O}_+(x')\rangle = -i\left(K_{\mathcal{O}_+}^{-1} - K_{\mathcal{O}_+}^{-1}gK_\phi^{-1}gK_{\mathcal{O}_+}^{-1} + \cdots\right)(x,x')\,, \tag{4.111}$$

[20] One should in principle analyze $\langle \mathcal{O}_+\mathcal{O}_+\rangle$ also at the nontrivial scale-invariant regime, but there we have an approximate operator equation $\mathcal{O}_+(x) = m^2\phi/g(x)$ in the IR, so the analysis is similar. In the massless case we have a different operator equation $\mathcal{O}_+(x) = -\partial^2\phi(x)/g(x)$, so $\mathcal{O}_+$ is the descendant of ϕ up to a factor of $g(x)$.

where the propagator $K_\phi^{-1}(x,y)$ is approximately a delta function $\delta^d(x-y)/m^2$ in the IR. Therefore we arrive at the following condition

$$\left| |x-x'|^{2\Delta_+} \int d^d z \int d^d z' \frac{\delta^d(z-z')g(z)g(z')}{m^2|x-z|^{2\Delta_+}|x'-z'|^{2\Delta_+}} \right| \ll 1\,, \tag{4.112}$$

which can be verified to be equivalent to $\alpha < \nu$ for large $|x|$, $|x|'$, and $|x-x'|$. Again, we conclude that our theory flows to the free fixed point in the IR if $\alpha < \nu$, otherwise it flows to the nontrivial scale-invariant regime characterized by (4.30).

4.D Higher-derivative toy model

In this chapter we have focused on models that are static in the UV and exhibit time dependence at energies below the scale $\partial g/g$. It is also possible that the scale $\partial g/g$ lies above the scale Λ_g (a scale at which in the static theory ghosts can appear). With time dependent couplings, the role of Λ_g is different from what it is in the static theory; the would-be ghost solutions must be reanalyzed. Here we set up that question in a simple toy model.

Consider a scalar field

$$S = \int d^d x \left\{ (\partial\phi)^2 + g(t)(\partial^2\phi)^2 + \dots \right\} \tag{4.113}$$

There are additional solutions to the wave equation since the action is fourth order rather than second order. These solutions represent a breakdown of the theory in the standard quantization[21], however, as long as the theory is cut off in the UV before the scale at which the new solutions enter it will be well-defined and unitary. With time dependence, there will be additional terms involving $\dot{g}, \ddot{g}$ in the equation of motion which may remove the new solutions over some range of scales. We can analyze this explicitly in a class of models with $g(t) = g_0 t^\alpha$.

[21]It is however possible to quantize the time-independent theory under an alternate quantization such that the spectrum is ghost-free, since the Hamiltonian is PT-symmetric. For a discussion of these issues, see e.g. [185, 186].

The equations of motion following from the action are

$$-\nabla^2\phi + \nabla^2((g(t)\nabla^2\phi) = 0. \tag{4.114}$$

It is clear from this that there is always a solution $\nabla^2\phi = 0$. For constant $g(t)$, there is additionally a solution with $\nabla^2\phi \sim \phi/g^2$. However, for $\frac{\dot{\phi}\dot{g}}{\phi g}$ or $\frac{\ddot{g}}{g} \gg 1/g$ this solution is absent, the ansatz fails. The toy example makes the origin of the $O(\frac{1}{t})$ cutoff (which we found also in the semiholographic example) particularly transparent: for $\ddot{g} \gg 1$, the overall scale g_0 of the coupling cancels from the equation of motion, and the solutions depend on the scales of the derivatives $\frac{\partial g}{g}$, $\left(\frac{\partial^2 g}{g}\right)^{1/2}$.

Working for simplicity in flat space, for the time-independent case $\alpha = 0$, the solutions are of the form $\phi(t, \vec{x}) \propto e^{i\omega t + i\vec{k}\vec{x}}$, where

$$\omega = \pm|\vec{k}|, \pm\sqrt{\frac{1}{g} - \vec{k}^2}. \tag{4.115}$$

The first pair of solutions corresponds to the 'normal' solutions with $\partial^2\phi = 0$.

For general $\alpha \neq 1$, in the regime $\ddot{g} \sim \frac{g_0}{t^2} \gg 1$ we can drop the first term in 4.114. The solutions are separable in space and time and can be found explicitly. For a spatial ansatz $e^{i\vec{k}\vec{x}}$, there are a pair of normal solutions with time-dependent factor $e^{\pm ikt}$ and an additional pair whose positive frequency solution is

$$\propto e^{ikt}\left(\frac{-2ikt^\alpha}{1-\alpha}\right) + e^{-ikt}e^{\frac{-i\pi\alpha}{2}}(2k)^\alpha\Gamma[1-\alpha, -2ikt] \tag{4.116}$$

where we have made use of the incomplete gamma function. The additional (positive frequency) solution in the case $\alpha = 1$ is

$$\propto e^{ikt}\log(t) + e^{-ikt}Ei(2ikt) \tag{4.117}$$

The power-law dependence means that these solutions enter at an energy scale of $O(\frac{1}{t})$, which is above the static cutoff defined by the instantaneous value of the coupling for a range of parameters. Thus the analysis of unitarity conditions will be significantly different in the time dependent version of this theory as compared to the

static case.

Chapter 5

Simple exercises to flatten your potential

5.1 Motivation: realizing your potential

Inflation [187, 188, 189, 190] is a powerful framework for addressing the cosmological flatness and horizon puzzles, and for generating the primordial seeds of structure. One recent advance is the development of a model-independent "bottom-up" effective field theory framework [191, 192, 193], which organizes CMB observables in terms of the lowest dimension operators participating in the effective theory. Still, model building plays an important role, both in field theory[1] and from the "top down" in string theory. In particular, inflation is sensitive to Planck-suppressed higher dimension operators in the low energy Lagrangian (an infinite sequence of them in the case of large-field inflation with detectable tensor modes). It is therefore of interest to model inflation within a UV-complete candidate for quantum gravity, of which string theory is our best-studied example (see [195] for a recent review).

The extra degrees of freedom of string theory – arising at various mass scales up to the four-dimensional Planck scale – affect the effective action along candidate inflaton directions in field space. This has led to important constraints and complications, such as order one corrections to slow roll parameters from compactification effects

[1] See [194] for a recent example.

[196] and bounds on the inflationary energy relative to the scale of moduli stabilizing potential energy barriers [197][198].

Additional fields can play other roles, sometimes in fact contributing useful effects to model building. The string theory motivated possibility of many additional light fields assisting inflation has been addressed in works such as [199, 200], and the tendency of particle production to slow down the inflaton was analyzed in [201, 202].[2] In some circumstances, integrating out heavy fields changes the character of the inflationary mechanism, producing higher dimension operators suppressed by the inflaton. An early example of this is [153, 155] where off-diagonal Yang-Mills matrix fields renormalize the effective action for the diagonal fields. In [209] similar effects were constructed via integration out of heavy fields coupled through the kinetic term. Integrating out heavy fields can also introduce a field-dependent enhancement of the kinetic term in the inflaton equation of motion [210] or produce features in the power spectrum for small enough radius of curvature in field space (see e.g. [211] for a recent discussion). Effects of heavy fields on precision observables such as the spectral tilt and the tensor to scalar ratio were considered in [212].

In this note, we show how interactions with heavy scalar fields – such as moduli and KK modes – can help flatten the inflaton potential. This mechanism was used in the small-field models of [213, 214, 215] but can occur very generally. The reason is very simple: the heavy fields coupled to the inflaton relax to their most energetically favorable configuration. Consider, as motivation, a simple field theoretic toy model with two fields ϕ_L, ϕ_H with the following potential

$$V(\phi_L, \phi_H) = g^2\phi_L^2\phi_H^2 + m^2(\phi_H - \phi_0)^2 \ . \tag{5.1}$$

The light field ϕ_L will play the role of the inflaton in this toy model. Assuming its kinetic energy is a subdominant effect (as we will shortly confirm), the heavy field will track its instantaneous minimum, which is itself a function of ϕ_L, and so the

[2] For similar approaches using a gas of particles to slow the inflaton field on a steep potential see e.g. [203, 204, 205, 206, 207, 208].

potential takes the form

$$V(\phi_L, \phi_{H,min}(\phi_L)) = \frac{g^2\phi_L^2}{g^2\phi_L^2 + m^2} m^2\phi_0^2 \ . \tag{5.2}$$

For $\phi_L \gg m/g$, the inflationary potential is nearly flat. The Friedmann equation becomes $3H^2M_P^2 \approx m^2\phi_0^2$, and

$$H^2 \sim m^2 \frac{\phi_0^2}{M_P^2} \ . \tag{5.3}$$

We take ϕ_0 to satisfy $0 < \phi_0 \ll M_P$ so that $m \gg H$, enforcing that ϕ_H be heavy enough not to produce scalar perturbations during inflation.[3] As mentioned above, here we ignored the time derivative terms in the ϕ_H equation of motion. The ratio between $3H\dot{\phi}_H$ and a typical term $\sim g^2\phi_H\phi_L^2$ in $\partial_{\phi_H}V$ is tiny in our solution, of order $(m/g\phi_L)^4(\phi_0/\phi_L)^2$.

This mechanism can operate purely within field theory. However string theory naturally provides a wealth of heavy scalar fields coming from moduli stabilization and from Kaluza-Klein modes which may play the role of ϕ_H, as well as potentially lighter fields such as axions and certain brane positions that may play the role of the light inflaton ϕ_L. In a general compactification we expect couplings between axions, fluxes and geometry. As long as the moduli are not destabilized in the process[4] the adjustments of the heavy fields will generically go in the direction of flattening the potential. (For restricted couplings, this can fail; for example if we shifted ϕ_0 by a term proportional to ϕ_L in the above example, it becomes quadratic at large field values, and can even steepen to quartic for a finite range of ϕ_L depending on parameter choices.)

One interesting consequence of this concerns $m^2\phi^2$ chaotic inflation, a classic model [190]. The couplings in the effective action including the light and heavy fields are analytic, and the scalar potential is generically quadratic around an extremum of the potential. In string theory, a key example of such a quadratic term descends

[3] Such fluctuations from additional light fields are constrained by existing limits on isocurvature fluctuations and non-Gaussianities in the CMB. [216, 217, 218, 219, 220]

[4] Although this is a more energetically favorable outcome, it requires the fields to go over moduli-stabilizing barriers.

from couplings of the form $|B \wedge F|^2$ in the low energy effective action, where B is a two-form potential field which produces an axion upon integration over a two-cycle in the compactification. However, although the potential is quadratic near the origin, the response of the heavy fields generically flattens the potential further out. The models of [221] in which the potential ends up linear in ϕ_L for $\phi_L > M_P$ is a particular example of this. The present work aims to provide a more systematic understanding of this theoretical trend. (See [222, 223, 224] for an interesting discussion of $m^2\phi^2$ inflation from flux monodromy developed within an effective field theory framework.)

Observationally, a quadratic potential is still viable, currently sitting at the edge of the 1σ exclusion contours, with smaller powers (corresponding to flatter potentials) lying further inside the allowed region [216, 217, 218, 219, 220]. Upcoming measurements [225] are expected to significantly improve the constraints on the tensor to scalar ratio and the tilt of the power spectrum. Because of the effects of heavy fields, including the flattening effect we consider here, it would not be surprising if the $m^2\phi^2$ model gets excluded. Special choices of compactification minimizing backreaction may realize chaotic inflation with a quadratic potential, but flatter potentials such as power-law inflation $V(\phi) \propto \phi^p$ with $p < 2$ appear to arise more generically at sufficiently large values of ϕ. We illustrate the predictions of a flattening monomial power-law potential against the present status of the WMAP 7-year results for the CMB in Fig. 5.1.

This chapter is organized as follows. In the remainder of this section and the next, we introduce the general setup, further specify conditions under which the energetic argument leading to flattening of the potential applies, and describe important situations where it fails. In section 3 we give several distinct realizations of the effect in the context of axion inflation in string theory, with different fields playing the role of ϕ_H. In section 4 we make some concluding remarks.

5.1.1 Additional kinetic effects

In the toy model presented above, we solved for ϕ_H in terms of ϕ_L to good approximation by solving $\partial_{\phi_H} V(\phi_L, \phi_H) \equiv 0$; the kinetic term $\dot{\phi}_H^2$ was subdominant. In more

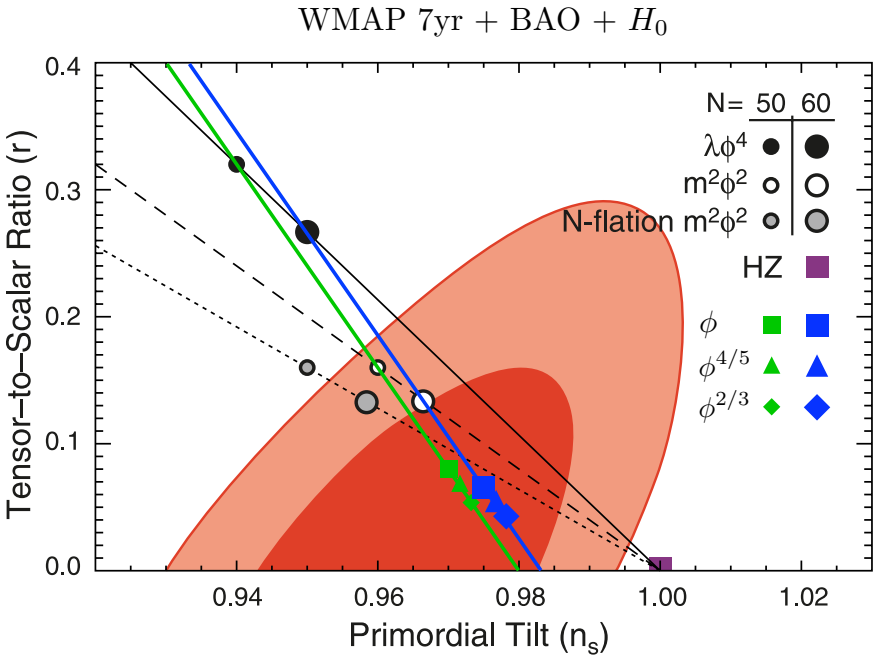

Figure 5.1: Combined data constraints on the tensor to scalar ratio r and the tilt n_s [216, 217, 218, 219, 220] together with the predictions for power-law potentials $\propto \phi^p$, $p > 0$ for 50 e-foldings (green line) and 60 e-foldings (blue line) of inflation. Flattening the potential corresponds to moving down and to the right along these lines. The colored points denote powers that have arisen in various large-field monodromy inflation models in string theory: IIB linear axion monodromy from 5-branes (squares; ϕ), IIA moving 4-brane monodromy (diamonds; $\phi^{2/3}$), and a candidate example of IIB flux axion monodromy (this work; triangles; $\phi^{4/5}$).

general examples we will need to establish whether the same approximation holds. Consider an action (for homogeneous fields) of the form

$$\int d^4x\sqrt{-g}\left\{\dot{\phi}_H^2 + G_{LL}(\phi_H)\dot{\phi}_L^2 - V(\phi_L,\phi_H)\right\} \ . \tag{5.4}$$

In integrating out ϕ_H, there are two effects that may arise from the kinetic terms. The first, discussed in [210], is that the $\dot{\phi}_H^2$ kinetic term affects the solution for ϕ_H as ϕ_L rolls. This is significant if $|d\phi_H/d\phi_L|$ is large compared to $\sqrt{G_{LL}}$. In our examples, as in the above toy model, we will check that this quantity is small.

The second, discussed in [209], arises from the coupling of ϕ_H in the light field's kinetic term $G_{LL}(\phi_H)\dot{\phi}_L^2$. If $\dot{\phi}_L^2$ is large enough during inflation, this term can significantly affect the solution for ϕ_H, leading to a nontrivial k-inflationary [226] effective Lagrangian $\mathcal{L}[(\partial\phi_L)^2,\phi_L]$. In this class of models, inflation may occur on a steep potential, with self-interactions of the field ϕ_L slowing it down (resulting in a large non-Gaussian signature in the power spectrum). The energetics of the backreaction for these more general solutions is not as simple as it is in the limit of slow roll inflation, where the heavy fields adjust in such a way as to flatten the potential when possible. Within slow roll inflation we have $\dot{\phi}_L^2 \ll V$, and this will allow us to self-consistently bound the effect in our examples below. It would be interesting to find UV-complete examples of the effects in [209, 210] in future work.

Steepening from kinetic curvature

We should emphasize that flattening of the potential is not an automatic consequence of couplings to massive fields. For example, even when the kinetic effects of the previous subsection are small it can fail, as can be seen from the following variant of our previous toy model:

$$\mathcal{L} = \frac{1}{2}\frac{\phi_H}{M_P}\dot{\phi}_L^2 + \frac{1}{2}\dot{\phi}_H^2 - g^2\phi_L^2\phi_H^2 - m^2(\phi_H-\phi_0)^2 - \mu^2\phi_L^2 \ . \tag{5.5}$$

As before, for large ϕ_L, $|d\phi_H/d\phi_L|$ is small compared to $\sqrt{G_{LL}}$ and $\dot{\phi}_H^2$ can safely be neglected, and the kinetic term $\frac{\phi_H}{M_P}\dot{\phi}_L^2$ is subdominant to the potential, so that the

effects of [209] are suppressed. The canonical field $\tilde{\phi}$ at large ϕ_L is now $\approx \frac{m}{g}\sqrt{\frac{\phi_0}{M_P}}\log(\phi_L/M_P)$, and the potential has the form

$$V_{eff}(\tilde{\phi}) \approx m^2\phi_0^2 + \mu^2 M_P^2 e^{\frac{2g\tilde{\phi}}{m}\sqrt{\frac{M_P}{\phi_0}}} \ . \tag{5.6}$$

Thus, if $G_{LL}(\phi_{H,min}(\phi_L))$ scales like a negative power of ϕ_L, then the dressed kinetic term is responsible for *steepening* the potential. This inverse power can arise for example in the case where ϕ_H descends from the overall (inverse) volume of a string compactification, leading to an increased volume at large inflaton field values (flattening the manifold, and steepening the potential). This can be neglected in examples with sufficiently strong volume-stabilizing potential barriers. In a complete example, μ would likely not be a fixed parameter, and all backreaction effects would need to be incorporated consistently.

5.2 Warmup: review of axion monodromy inflation

Our string-theoretic examples grew out of a project aimed at developing the flux version of axion monodromy inflation. Let us begin by briefly reviewing the general discussion of this mechanism in [221]. A flux version of monodromy inflation has been obtained at the level of effective field theory also in [223, 222, 224], and the phenomenology of monodromy inflation was further developed in [227, 228].

String theory naturally provides axions

$$b = \int_{\Sigma^p} B_p \ \ , \ \ c = \int_{\Sigma^p} C_p \tag{5.7}$$

coming from p-form Neveu-Schwarz–Neveu-Schwarz and Ramond-Ramond fields B_p, C_p wrapped on p-cycles in the compact directions. Assuming a single scale $L\sqrt{\alpha'}$ for the compactification geometry, the canonically normalized field is related to the

angular scalar field (5.7) by

$$\frac{\phi_b}{M_p} \sim \frac{b}{L^p} \quad , \quad \frac{\phi_c}{M_p} \sim \frac{g_s c}{L^p} \ . \tag{5.8}$$

The theory contains couplings between the axions and various fluxes and spacefilling branes that are generically present in compactifications. These couplings introduce *monodromy* in the axion direction: the system builds up potential energy as b or c traverses its basic period.

In the specific, UV-complete examples discussed in [221] the axion potential is lifted by the DBI action

$$\mathcal{S}_{DBI} = -\frac{1}{g_s \alpha'^3} \int \sqrt{det(G_{MN} + B_{MN}) \partial_\alpha X^M \partial_\beta X^N} \quad \Rightarrow \quad V(\phi_b) \propto \sqrt{1 + \left(\frac{\phi_b}{M_P}\right)^2} \tag{5.9}$$

for a spacefilling D5-brane wrapped on the 2-cycle (or its S-dual in the case of RR axions). Using the AdS/CFT correspondence, this result can be described equivalently in terms of a dual geometry plus fluxes. In that description, the monodromy arises from flux couplings of the form

$$\mathcal{L} \sim |B_2 \wedge F_3|^2 + \dots \tag{5.10}$$

or its S-dual $|C_2 \wedge H_3|^2$. Although the coupling (5.10) is quadratic, backreaction of the axion and fluxes on the geometry leads to a linear potential, as we will discuss in more detail below. This provides an explicit example of the general trend discussed in the introduction: that back reaction of the potential energy descending from (5.10) should flatten the potential, since this is energetically favorable.

Globally, however, the most energetically favorable configuration in metastable string compactifications is the runaway to large radius and/or weak coupling, or decays to negative cosmological constant. Therefore, before discussing examples of potential-flattening effects, let us first briefly review the combined conditions for maintaining moduli stabilization and the COBE normalization of the power spectrum.

As is emphasized in [221], the canonically normalized axion potential is, in the

absence of strong warping (supposing for illustration that B_2 is the inflationary axion)

$$\frac{1}{\alpha'^4}\int d^6x\sqrt{-g}|B_2\wedge F_q|^2 \sim \frac{1}{\alpha'^4}\frac{\phi_b^2}{M_P^2}\int d^6x\sqrt{-g}|F_q|^2 \ . \tag{5.11}$$

If the q-form flux lifting the axion potential makes a sufficiently subleading contribution to the moduli stabilization, one can obtain a super-Planckian field range without destabilizing the moduli.

In order to provide a successful phenomenological model of chaotic inflation, we must have a sufficient range to give $N_e = 60$ e-foldings of inflation, and the power spectrum of scalar perturbations must match the COBE normalization,

$$\Delta^2_{scalar} = \frac{H^4}{(2\pi)^2\dot{\phi}^2} \cong 10^{-9} \ . \tag{5.12}$$

For a power-law potential $V(\phi) \propto \mu^{4-n}\phi^n$, the required field range is $\Delta\phi/M_p \sim \sqrt{nN_e}$, which is $O(15)$ for the quadratic case. The COBE normalization becomes

$$\left(\frac{\mu}{M_P}\right)^{2-\frac{n}{2}}\left(\frac{\Delta\phi}{M_P}\right)^{\frac{n}{2}+1} \sim 10^{-5} \tag{5.13}$$

which becomes $\mu/M_P \sim 10^{-6}$ for a quadratic potential and $O(10^{-3})$ for a linear potential.

Let us first review the basic scales in the problem which show that it is possible for axion monodromy inflation to self-consistently satisfy the required number of e-foldings and COBE normalization. Here is an estimate of the effects of these observational constraints in the extreme case of $m^2\phi^2$ inflation, in the absence of warping (flatter potentials and warped models being easier to embed below the moduli stabilizing barrier, this is the most conservative estimate we can make). Supposing that the inflaton comes from a C_p axion lifted by the term $|C_p\wedge H_3|^2$, the flux potential is

$$\mathcal{U} = \frac{1}{\alpha'^4}\int d^6x\sqrt{-g}|C_p\wedge H_3|^2 \sim \frac{M_P^2}{\alpha'}\left(\frac{g_s c}{L^p}\right)^2\left(\frac{K}{L^3}\right)^2 \sim M_P^4\left(\frac{g_s^2K^2}{L^{12}}\right)\frac{\phi_c^2}{M_P^2} \tag{5.14}$$

where we have labeled the number of H_3 flux quanta by K. The condition for realizing

60 e-foldings of inflation without destabilizing the moduli and for matching the power spectrum to the COBE normalization then becomes (returning to the general case of q-form flux lifting the inflaton $\sim |C_p \wedge F_q|^2$)

$$15K_{inf} \ll K_{moduli} \;\; ; \;\; \frac{\mu}{M_p} \cong \frac{g_s K_{inf}}{L^{q+3}}(2\pi)^{7/2} \cong 10^{-6} \; . \tag{5.15}$$

These conditions can be satisfied for reasonable parameter values, e.g. $g_s \sim 0.02$, $K_{inf} \sim 1$, $q = 3$, $L \sim 10$. Moreover, as already mentioned, warping can naturally suppress the potential energy if the inflationary sector is localized in a region of large gravitational redshift, as in the specific examples in [221]. Therefore there is no immediate obstruction to fitting the flux-based version of axion monodromy inflation into stabilized string compactifications, avoiding catastrophic decay of the vacuum.

More generally, there may be single-sector models where the inflaton potential itself helps stabilize the moduli during inflation, competing with or even dominating over some of the terms in the moduli potential. The gravity dual of the models [221] is a familiar local example of this, where down the brane throat the axion $c = \int_{\Sigma_2} C_2$ helps stabilize the cycle Σ_2 it threads. Below we will explore potential generalizations of this which are further from a simple brane construction.

5.2.1 Flattening vs. moduli potential barriers

Before proceeding to our main flattening exercises, it is worth describing a simple example which illustrates both the flattening effect and how the requirement of moduli stabilization can cut it off. De Sitter vacua can plausibly be achieved in string theory via perturbative techniques, where localized sources of energy such as curvature, D-branes and NS5-branes, fluxes, orientifolds and others contribute to an effective potential for the four dimensional scalar fields, which is minimized to solve the equations of motion. Such constructions were introduced in [33] and discussed in [51, 52, 53, 54, 55, 56, 57, 58, 59, 60, 61]; worked examples include [48, 229, 50, 7]. It is useful to organize these mechanisms in terms of an 'abc' structure for the potential,

$$V(g) = ag^2 - bg^3 + cg^4 \tag{5.16}$$

where g is a representative modulus such as the the string coupling (with the coefficients a, b, and c depending on the other moduli). Such a potential generally arises with curvature, Neveu-Schwarz–Neveu-Schwarz fluxes, and/or supercritical dimensionality in the a term, orientifold planes in the b term, and Ramond-Ramond fluxes in the c term. This potential has a positive metastable minimum when the quantity $4ac/b^2$ is minimized as a function of the other moduli, within the window

$$1 < \frac{4ac}{b^2} < \frac{9}{8} \ . \tag{5.17}$$

Adding flux energy from an axion term will produce an effective potential of the form

$$V(g,x) = ag^2 - bg^3 + (1+x^2)cg^4 \tag{5.18}$$

where x is proportional to the axion field. Explicit examples may be found among the axions in [229, 50, 7], though we have not developed complete models.

Setting $4ac/b^2 = 1$, the potential is stabilized at a Minkowski minimum for $x = 0$, and as x is turned on, the de Sitter minimum persists as long as

$$x^2 < \frac{1}{8} \ . \tag{5.19}$$

Including backreaction, $V(g_{min}(x), x)$ is no longer quadratic, as plotted in Figure 5.2. As expected, the potential is quadratic for small values of x where backreaction can be ignored, and then flattens as x is increases. However, the flattening only starts to become significant when x is of order one, but from (5.19) it is clear that x begins to destabilize the minimum at this point.

5.3 Workout: axions pushing on heavy fields

Finally let us turn to the effects of interest in this chapter, the backreaction of the energy (5.11)(5.14) on heavy fields and its effect on the inflationary potential energy.

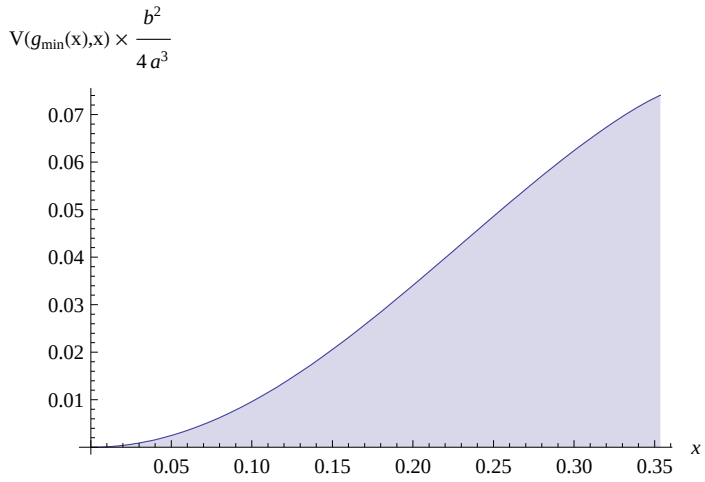

Figure 5.2: Effects of an inflationary flux on the three-term structure stabilized in a Minkowski minimum for $x = 0$.

5.3.1 Bowflux: Sloshing of flux on fixed cycles

The axion potential may be modified by rearrangement of fluxes on fixed cycles so as to minimize their energy. To illustrate this effect, we consider a model of the kind discussed by [27, 49] stabilized by three-form fluxes H_3, F_3. We add a small extra three-form flux ΔH_3 to an unwrapped cycle, and turn on an axion C_2 threading a cycle Σ_2 as the inflaton. Our candidate inflaton will be $c \sim \int_{\Sigma_2} C_2$. We minimize the other fields at a given value of c, given consistency with moduli stabilization which requires that the inflationary energy stay below the moduli-stabilizing barriers. In general the potential will descend from terms in the 10D action of the form

$$\frac{1}{g_s^2}|H_3 + \Delta H_3|^2 + |C_2 \wedge (H_3 + \Delta H_3)|^2 + |F_3|^2 \ . \tag{5.20}$$

The number of flux quanta threading a given cycle is topological and does not change, but the fluxes may slosh around on their cycles so as to minimize the total energy. If the flux ΔH_3 shifts so that its support is partially separated from that of C_2, for instance, the Chern-Simons term would be weakened, but the contribution to the potential from the $|\Delta H_3|^2$ term would increase. The competition between them

determines the optimal field configuration. In general the geometry and the axion wavefunction can adjust as well. Before considering the potential energy, C_2 minimizes its energy by forming a flat connection $c\omega_2$ (where ω_2 is a nontrivial closed form which integrates to one over Σ_2). In the presence of potential energy, it might prove energetically favorable for Kaluza-Klein modes of C_2 to turn on to reduce the second term in (5.20), at the cost of introducing a contribution to the $|F_3|^2$ term. However, to illustrate our effect, let us focus on the sloshing of ΔH_3 at fixed C_2, since the adjustment of any other modes (such as the geometry and C_2 itself) can only enhance the flattening effect.

Keeping fixed the integral of ΔH_3 over the three-cycles it threads, ΔH_3 can scrunch up in three directions w along the three-cycle to reduce its overlap with C_2. Let us denote by $\tilde{L}\sqrt{\alpha'}$ the size of the region over which the scrunched-up field ΔH_3 has support, modeling its profile locally by

$$\sqrt{\alpha'}\Delta H_3 \sim \frac{\Delta N}{\tilde{L}^3} e^{-w^2/\tilde{L}^2\alpha'} \tag{5.21}$$

where ΔN is the number of ΔH_3 flux quanta. We would like to minimize the potential energy with respect to $\tilde{L}$ and determine the effect of this on the axion potential. If the profile of C_2 were flat in the internal dimensions, shrinking $\tilde{L}$ would not be advantageous. Of course harmonic forms in nontrivial compactification manifolds are not constant. Taylor expanding (and assuming rough isotropy locally), let us model C_2 in the region of support of ΔH_3 as

$$C_2(w) \sim \frac{c}{L^2}\left(1 + \gamma \frac{w^2}{L^2\alpha'} + \dots\right) \tag{5.22}$$

where γ is a constant derived from the Taylor expansion of C_2's profile.[5] Here we are assuming ΔH_3 is centered on a local minimum of C_2, which is its preferred configuration if available (otherwise one would obtain a linear term in the expansion (5.22), with similar results).

After integrating over the internal volume, the relevant terms in the potential are

[5]Note that $C_2 \wedge H_3$ will in general include angular factors depending on the geometry. We will not write these factors here.

proportional to

$$\frac{1}{g_s^2}\left[\Delta N^2\left(\frac{L}{\tilde{L}}\right)^3+\gamma N\Delta N\left(\frac{\tilde{L}}{L}\right)^2\frac{\phi_c^2}{M_P^2}\right] \tag{5.23}$$

where N refers to the number of H_3 flux quanta and $L\sqrt{\alpha'}$ is a typical length scale in the compactification. Here the first term comes from $|\Delta H_3|^2$. The second term comes from $(C_2\wedge H_3)\cdot(C_2\wedge\Delta H_3)$, and gets its leading contribution from the w^2 term in (5.22) convolved with (5.21).[6] The potential will then minimize these two terms and be proportional to $\phi_c^{6/5}$, which is flatter than quadratic.

This illustrates the flattening mechanism, but only provides a lower bound on the effect. Adjustments of other fields including C_2 and the compactification geometry would further flatten the potential.

Bounding additional kinetic effects

As discussed above in §5.1.1, we must check whether it is a good approximation to determine the heavy field ϕ_H (in this case corresponding to KK modes of B_2) in terms of ϕ_L by solving $\partial_{\phi_H}V\equiv 0$, neglecting the contributions from the kinetic terms. The kinetic effects of [210] are small if $|\partial\phi_H/\partial\phi_L|\ll 1$, i.e. if the KK modes of B_2 that we consider make a negligible correction to C_2's kinetic term. It is straightforward to see that this may be obtained in the present example, as follows. The kinetic term for $\tilde{L}$ descends from the kinetic term for ΔH_3 and is

$$\mathcal{L}_{kin}\sim\frac{\Delta N^2M_P^2}{\tilde{L}^3L^3}(\partial\tilde{L})^2\ , \tag{5.24}$$

giving the canonically normalized field ϕ_H as

$$\phi_H\sim\frac{\Delta NM_P}{\tilde{L}^{1/2}L^{3/2}}+const\ . \tag{5.25}$$

[6] The other terms are either subleading or do not depend on $\tilde{L}$.

Minimizing the potential (5.23) with respect to L', we get

$$\frac{L}{\tilde{L}} \sim \left(\frac{\gamma N}{\Delta N}\right)^{1/5} \left(\frac{\phi_c}{M_P}\right)^{2/5} \quad . \tag{5.26}$$

Combining the above equations and writing ϕ_H as a function of ϕ_c, we get

$$\frac{d\phi_H}{d\phi_c} \sim \frac{\Delta N}{L^2} \left(\frac{\gamma N}{\Delta N}\right)^{1/10} \left(\frac{M_P}{\phi_c}\right)^{4/5} \quad , \tag{5.27}$$

which can be much smaller than 1 for a reasonable range of parameters.

5.3.2 Puffing on the kinetic term

In the previous subsection we have considered modification of the effective potential due to backreaction on the potential terms. The backreaction of the inflationary potential on the geometry can also affect the kinetic term, realizing the "running kinetic term" mechanism described in [230].

In a simple situation where the NS-NS or R-R field threads a cycle of size $L\sqrt{\alpha'}$ that is the same as the typical length scale in the compactification, the canonical normalization of the inflaton field is given in terms of the number of axion windings by

$$\frac{\phi_b}{M_P} \sim \frac{b}{L^2} \quad , \quad \frac{\phi_c}{M_P} \sim \frac{g_s c}{L^p} \tag{5.28}$$

respectively for a 2-form NS-NS and for a p-form R-R axion. If instead we consider cases where the p-form field is localized (e.g. in a throat) and is therefore threading a much smaller cycle of size $L'\sqrt{\alpha'}$, the canonically normalized field becomes

$$\frac{\phi_b}{M_P} \sim \frac{b}{L'^2}\frac{L'^3}{L^3} \sim \frac{bL'}{L^3} \quad , \quad \frac{\phi_c}{M_P} \sim \frac{g_s c}{L'^p}\frac{L'^3}{L^3} \sim \frac{g_s c L'^{3-p}}{L^3} \ . \tag{5.29}$$

Here we are considering the case that the support of the axion is of order the size $L'\sqrt{\alpha'}$ in all directions in the compactification (as occurs for example in the case that $L'\sqrt{\alpha'}$ describes the size of an internal cycle localized within a Freund-Rubin throat). Now if the inflationary flux backreacts on the size $L'\sqrt{\alpha'}$ of the wrapped cycle, L'

will become a function of the axion and this will alter the relation between b or c and the canonically normalized field. The terms of the form $|\text{axion} \wedge \text{flux}|^2$ push the geometry to expand. Given this, $L'(b)$ will vary as a positive power of b and reduce the power of ϕ_b in the potential. For example, in the case where the size $L'\sqrt{\alpha'}$ is mostly supported by $|B_2 \wedge F_3|^2$, we have $L'^4 \propto b$ and therefore $\phi_b \propto b^{5/4}$. In the case where the inflation arises from a Ramond-Ramond field, we will have $p \leq 3$ for magnetic fluxes in six compact dimensions, and so $L'(c)$ will either reduce the power of the potential or leave it unchanged.

Bounding additional kinetic effects

In this example, we solved for the heavy field L' in terms of the light field ϕ_b (or ϕ_c) by minimizing the potential in the L' direction. Let us now address the question of additional kinetic effects described in §5.1.1 in the context of the present model. Before describing the kinetic interactions of ϕ_b and L', let us note that the overall size $L\sqrt{\alpha'}$ of the compactification will not be pushed far in the process given a sufficient hierarchy between the inflationary energy and the moduli stabilizing barriers.

First, let us check whether $|d\phi_H/d\phi_L|$ is small. This requires knowledge of the kinetic term for ϕ_H, i.e. the relation between the canonically normalized field ϕ_H and the modulus L'. The kinetic term for L' descends from the ten-dimensional Einstein term, and in four-dimensional Einstein frame is given by

$$\int d^4x\sqrt{-g}M_P^2\left(\frac{L'}{L}\right)^6\left(\frac{\partial L'}{L'}\right)^2 \tag{5.30}$$

in the above example. From this, the canonically normalized field ϕ_H is

$$\phi_H \sim M_P\left(\frac{L'}{L}\right)^3 . \tag{5.31}$$

Now, from the above-mentioned scaling $L'^4 \propto b, \phi_b \propto b^{5/4}$, we obtain $\phi_H \propto \phi_b^{3/5}$ and

$$\left|\frac{d\phi_H}{d\phi_L}\right| \propto \phi_L^{-2/5} \tag{5.32}$$

which is $\ll 1$ for sufficiently large $\phi_b = \phi_L$.

Next, let us check that the kinetic term for $\phi_L = \phi_b$ does not constitute a significant source for ϕ_H as considered in [209]. To do this, write $L' \equiv L'_0 e^{\sigma'(t)/M_P}$ (note here σ' is not the canonically normalized field). The relevant terms in the effective action have the form

$$\int d^4x\sqrt{-g}\left(e^{2\sigma'/M_p}\dot{\phi}_b^2 - V(\sigma', \phi_b)\right) \ . \tag{5.33}$$

Each term in the potential scales like a power of $L' \propto e^{\sigma'/M_P}$. Varying this action with respect to σ', the first term is of order $\dot{\phi}_b^2/M_P$, much smaller than the second term which is of order V/M_p during inflation. Thus we can self-consistently ignore the effect of [209] here.

5.3.3 Weight lifting: pushing on moduli

The fact that the axion $\times$ flux energy pushes on the moduli can lead to a similar but distinct effect from the backreaction on the inflaton kinetic term just discussed. One concrete example of this is simply the one developed in [221], described in terms of its gravity dual. Again, the term $|C_2 \wedge H_3|^2$ is quadratic in the axion $c = \int C_2$. But the axion builds up effective D3-brane charge, and from that point of view the potential should be linear in cg_s, which is proportional to the effective number of D3-branes. This works out because the generalized 5-form RR flux $\tilde{F}_5 = C_2 \wedge H_3 + \dots$ backreacts on the moduli, giving a near horizon internal geometry with size $R\sqrt{\alpha'}$ depending on c as

$$R^4 \sim g_s\tilde{N} \sim g_s c\int_{S^3} H_3 \tag{5.34}$$

as in standard Freund-Rubin solutions. Folding this into the effective action, we see that it scales like

$$\mathcal{S} \sim \frac{1}{\alpha'^4}\int d^{10}x\sqrt{-G}|\tilde{F}_5|^2 + \dots \sim Vol(4d)\frac{\tilde{N}^2}{R^{10}} \times R^6 \sim \frac{\tilde{N}}{g_s}Vol(4d) \tag{5.35}$$

as befits a set of D3-branes (here $Vol(4d)$ is the volume of the worldvolume swept out by the brane). A straightforward calculation of the four dimensional effective

potential, derived for general warping in [65][66], allows one to reproduce from the gravity side the corresponding four-dimensional Einstein frame potential energy V descending from the brane throat:

$$V(c) \sim M_P^4 \left(\frac{g_s^2}{Vol}\right)^2 \frac{\tilde{N}}{g_s} \tag{5.36}$$

where Vol is the compactification volume in string units. In the specific construction [221], the kinetic term of the axion was dominated by the ultraviolet region of the compactification well outside the brane throat. Therefore, in that example the kinetic backreaction of §5.3.2 does not apply, but backreaction on the geometry (specifically, on the internal size $R\sqrt{\alpha'}$) flattens the potential from quadratic to linear. In this example, the kinetic effects are bounded much as in §5.3.2.

5.3.4 Circuit training: toward more generic UV complete examples

A general string compactification involves multiple backreaction effects that are simultaneously important. We have not fully controlled any such example in this chapter, but will note here an interesting candidate. Consider an S^3 localized down a warped throat. Put M units of RR F_3 flux on its dual cycle $\tilde{S}^3$. On the S^3 itself, put zero total units of flux, but introduce a topologically trivial configuration of h units of $H_3 = dB_2$ on one hemisphere (north of the equator, say) and $-h$ units on the other (south of the equator). This will dynamically relax back down to zero, and if the geometry were fixed the $|H_3|^2$ term would produce a quadratic potential for the integral $b \equiv \int_{equator} B_2 = h$ of B_2 over the equator of the S^3. Backreaction, however, will change this significantly. Consider starting the system in a configuration in which each hemisphere times the $\tilde{S}^3$ with flux is approximately solving the equations of motion as in [29, 27, 49]. This constitutes, in effect, a 3-brane throat and an anti-3-brane throat at the bottom of the original throat. One can set this up explicitly in terms of two close-by conifold singularities with flux. A similar construction with metastable fluxes on a noncompact Calabi-Yau geometry is studied in [231].

Each throat carries potential energy of order $\tilde{N} \sim Mb(t)$ including the backreaction of §5.3.3. Moreover, the kinetic energy of b is subject to backreaction as in §5.3.2. The four-dimensional canonically normalized field ϕ_b in four-dimensional Einstein frame is given by

$$\begin{aligned}\int d^4x\sqrt{-g_E}(\partial\phi_b)^2 &\sim \frac{1}{g_s^2\alpha'^4}\int d^{10}x\sqrt{-g_{st}}(\partial B_2)^2 \sim \frac{1}{\alpha'}\int d^4x\sqrt{-g_{st}}\left(\frac{R^6}{g_s^2}\right)\frac{(\partial b)^2}{R^4}\\ &\sim \int d^4x\sqrt{-g_E}M_P^2\left(\frac{g_s^2}{Vol}\right)\left(\frac{R^2}{g_s^2}\right)(\partial b)^2\\ &\sim \int d^4x\sqrt{-g_E}\left(\frac{M_P^2}{Vol}\right)R^2(\partial b)^2\\ &\sim \int d^4x\sqrt{-g_E}\frac{M_P^2(g_sM)^{1/2}}{Vol}b^{1/2}(\partial b)^2 \end{aligned} \tag{5.37}$$

and so $\frac{\phi_b}{M_P} \sim \frac{(g_sM)^{1/4}}{\sqrt{Vol}}b^{5/4}$. These two effects, taken together, suggest a potential

$$V(\phi_b) = \mu^{16/5}\phi_b^{4/5} \ . \tag{5.38}$$

However, in order to obtain a concrete prediction for the evolution of this system, we would require a better understanding of the region between the brane and antibrane throats and full control over all sources of backreaction in all directions in field space. This would be interesting to pursue further.

5.4 Cooldown

A quadratic inflaton potential may be the simplest possibility from a bottom-up approach, but interactions with heavier fields typically deform the effective action, flattening the potential in the cases discussed here for a simple energetic reason. This is a basic aspect of the UV sensitivity of inflation, complementary to others much discussed in the recent literature. If the upcoming round of CMB measurements become consistent with the predictions of $m^2\phi^2$ chaotic inflation, this would significantly constrain the inflaton's couplings to additional fields, including those much heavier than the inflationary Hubble scale. Conversely, if the mild trend in the data toward

flatter potentials sharpens, the considerations of this chapter may help explain the results.

In the case of axion monodromy inflation, we have outlined two specific mechanisms for backreaction to flatten the axion potential; in general the fluxes and the geometry will seek out the state of lowest energy consistent with the higher dimensional equations of motion. In general, determining the correct form of the potential seems a complicated task. Complete catalogs of the modes found in compactification geometries, such as [232, 233], may be of use in constructing more explicit examples. It would also be interesting to see if these considerations apply to other mechanisms for inflation, including general small field models and models with more generic kinetic terms where the energetic analysis is somewhat more complicated.[7]

[7]It would also be interesting to study backreaction further in models where a cycle size modulus plays the role of the inflaton such as [234] or [235].

Chapter 6

Analytic Coleman-De Luccia Geometries

6.1 Introduction

The Coleman-De Luccia (CDL) geometry [123] is essential to the study of eternal inflation (see [236, 237] and the references therein) and the string theory landscape [46, 49, 238]. Most discussions of this geometry take place in the "thin-wall" limit, where the geometries inside and outside of the bubble are pieces of de Sitter space, Minkowski space, or Anti de Sitter space, sewn together nonanalytically at the domain wall. This picture is sufficient for many qualitative questions, but is troublesome when applied to calculations of correlation functions in the CDL background [21, 9]. This often involves various analytic continuations from Euclidean to Lorentzian signature, and also from one part to another of the geometry, and pathologies can appear when the geometry is not analytic. Our goal in this chapter is to give some reasonably simple analytic expressions for "thick-wall" CDL bubbles which mediate various types of decays. There is a conservation of trouble here, however, in that we will not be able to give closed form expressions for the scalar potentials which give rise to these geometries. Rather we will work out a set of general constraints that the metric needs to obey in order for it to come from *some* scalar field theory with a potential, and then give examples of geometries which satisfy all the constraints. Since it is

the potential that usually comes out of "top-down" constructions this may not seem eminently useful, but we consider our approach to be more appropriate for "bottom-up" investigations of bulk physics in the CDL background. Similar analyses have been applied to other less-restricted cases such as thick domain walls [239, 240, 241] and FRW cosmologies [242], both of which are contained in our analytic CDL geometries.

6.2 General Properties of the Coleman-De Luccia Geometry

6.2.1 Euclidean Preliminaries

The Euclidean CDL geometry is a solution of the equations of motion for the scalar-gravity system with Euclidean action

$$S = -\frac{1}{16\pi G}\int d^d x\sqrt{g}R + \int d^d x\sqrt{g}\left[\frac{1}{2}g^{\mu\nu}\partial_\mu\phi\partial_\nu\phi + V(\phi)\right]. \tag{6.1}$$

The solution has $SO(d)$ symmetry, so we can write the metric as

$$ds^2 = d\xi^2 + a(\xi)^2\left(d\theta^2 + \sin^2\theta d\Omega_{d-2}^2\right). \tag{6.2}$$

The equations of motion for solutions with this symmetry are

$$\begin{aligned}\phi'' + (d-1)\frac{a'}{a}\phi' - V'(\phi) &= 0\\ \left(\frac{a'}{a}\right)^2 &= \frac{1}{a^2} + \frac{16\pi G}{(d-1)(d-2)}\left(\frac{1}{2}\phi'^2 - V(\phi)\right).\end{aligned} \tag{6.3}$$

If V has a local extremum at $\phi = \phi_{min}$ then there is a simple solution. When $V(\phi_{min}) = 0$ we have flat space:

$$a(\xi) = \xi. \tag{6.4}$$

When $V(\phi_{min}) = \rho_{min} > 0$, we have the sphere:

$$\begin{aligned} a(\xi) &= \ell_{ds} \sin(\xi/\ell_{ds}) \\ \ell_{ds}^{-2} &= \frac{16\pi G \rho_{min}}{(d-2)(d-1)}. \end{aligned} \tag{6.5}$$

When $V(\phi_{min}) = \rho_{min} < 0$, we have hyperbolic space:

$$\begin{aligned} a(\xi) &= \ell_{ads} \sinh(\xi/\ell_{ads}) \\ \ell_{ads}^{-2} &= -\frac{16\pi G \rho_{min}}{(d-2)(d-1)}. \end{aligned} \tag{6.6}$$

More interesting solutions will interpolate smoothly between different minima of the potential; these have the interpretation of causing bubble nucleation.[1] The geometries describing the decay of Minkowski space and AdS are noncompact and can be chosen to have $\xi \in [0, \infty)$, while the geometry describing the decay of dS space is compact and can be chosen to have $\xi \in [0, \xi_c]$. In all cases for the solution to be smooth at $\xi = 0$ we need

$$\begin{aligned} \phi(\xi) &= \phi_0 + \mathcal{O}(\xi^2) \\ a(\xi) &= \xi + \mathcal{O}(\xi^3). \end{aligned} \tag{6.7}$$

For the noncompact cases, as $\xi \to \infty$ we want ϕ to approach its value in the false vacuum and a to approach (6.4) or (6.6). When the false vacuum is dS then as $\xi \to \xi_c$ smoothness requires

$$\begin{aligned} \phi(\xi) &= \phi_c + \mathcal{O}((\xi_c - \xi)^2) \\ a(\xi) &= (\xi_c - \xi) + \mathcal{O}((\xi_c - \xi)^3). \end{aligned} \tag{6.8}$$

[1] The Euclidean solution does not actually quite reach the minimum; the more precise boundary conditions are stated momentarily. Also for vacua which have $V < 0$ it is possible for a maximum to be stable or metastable; we include this case below in our definition of a CDL geometry.

6.2.2 Lorentzian Continuation

To find the Lorentzian geometry describing the aftermath of bubble nucleation we analytically continue the Euclidean solution of the previous subsection. To get inside the bubble we define

$$\begin{aligned} \xi &= it \\ \theta &= i\rho \\ \hat{a}_1(t) &= -ia(it), \end{aligned} \tag{6.9}$$

which gives an open FRW cosmology

$$ds^2 = -dt^2 + \hat{a}_1(t)^2 \left(d\rho^2 + \sinh^2 \rho d\Omega_{d-2}^2 \right). \tag{6.10}$$

To get the Lorentzian geometry outside of the bubble we continue

$$\theta = \frac{\pi}{2} + i\omega, \tag{6.11}$$

which gives a "warped de Sitter" geometry

$$ds^2 = d\xi^2 + a(\xi)^2 \left[-d\omega^2 + \cosh^2 \omega d\Omega_{d-2}^2 \right]. \tag{6.12}$$

When the false vacuum is dS there is an additional region outside of the bubble which is up near the future boundary of the false vacuum, which we reach by

$$\begin{aligned} \xi &= \xi_c + it \\ \theta &= i\rho \\ \hat{a}_2(t) &= ia(\xi_c + it). \end{aligned} \tag{6.13}$$

Both $\hat{a}_1$ and $\hat{a}_2$ obey the Lorentzian FRW equations of motion

$$\ddot{\phi} + (d-1)\frac{\dot{\hat{a}}}{\hat{a}}\dot{\phi} + V'(\phi) = 0$$
$$\left(\frac{\dot{\hat{a}}}{\hat{a}}\right)^2 = \frac{1}{\hat{a}^2} + \frac{16\pi G}{(d-1)(d-2)}\left(\frac{1}{2}\dot{\phi}^2 + V(\phi)\right). \tag{6.14}$$

The metric and scalar produced by these continuations are guaranteed to be real because they obey equations of motion and boundary conditions that are real. In particular the simple Euclidean solutions with constant ϕ become various patches of Minkowski, de Sitter, or Anti de Sitter space. The late time behaviour inside of the bubble depends on the nature of the "true" minimum. If the minimum is infinitely far away in field space then there are many possibilities, but if the minimum is at some finite ϕ there are only three. These are Minkowski space[2]

$$\hat{a}_1(t) \to t, \tag{6.15}$$

de Sitter

$$\hat{a}_1(t) \sim e^{t/\ell_1}, \tag{6.16}$$

and Anti de Sitter[3]

$$\hat{a}_1(t) \sim \sin(t/\ell_1). \tag{6.17}$$

If the false vacuum has positive energy and is at finite field value then we also expect

$$\hat{a}_2(t) \sim e^{t/\ell_2}. \tag{6.18}$$

The full analytic continuation is illustrated in Figure 6.1.

[2]We use "$\to$" here instead of "$\sim$" to indicate $a(t) = t(1 + o(t^0))$, i.e. unlike the dS and AdS cases the prefactor must go to one.

[3]In this case late time does not make so much sense, since we expect the geometry to crunch in time of order ℓ_1 and there isn't really a good asymptotic limit.

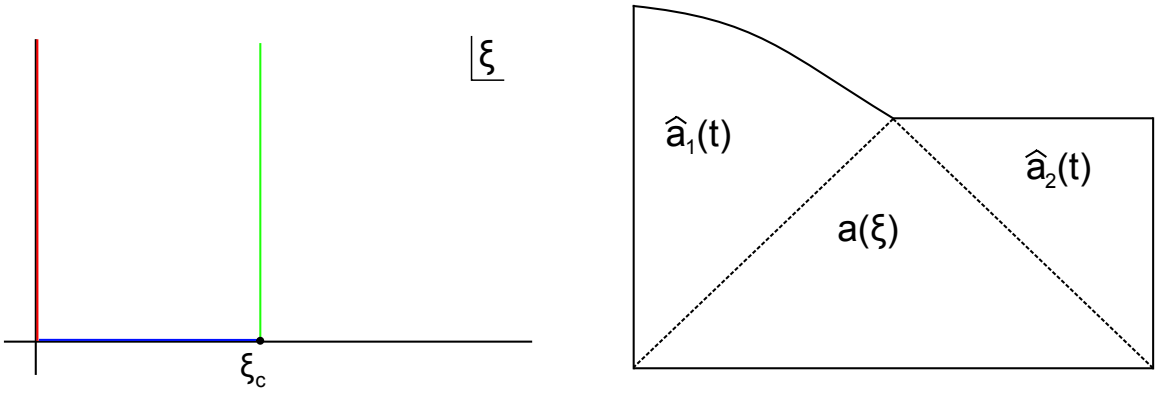

Figure 6.1: On the left we have the three regions of interest in the ξ plane for the Lorentzian continuation of a compact CDL geometry. The red line gives $\hat{a}_1(t)$, the blue line gives $a(\xi)$, and the green line gives $\hat{a}_2(t)$. On the right we show the regions of the CDL Penrose diagram that are described by these different continuations. If the geometry is noncompact then the blue line extends to infinity and the $\hat{a}_2$ region doesn't exist.

6.2.3 Constraints and a Definition

For a given potential the boundary conditions are sufficient to determine a unique solution of the equations of motion (6.3). What we will do in this section is to identify the constraints that a real and positive function $a(\xi)$ must obey in addition to the boundary conditions to ensure that a potential exists which has this $a(\xi)$ (and some $\phi(\xi)$) as a solution, and also that its analytic continuation describes a Lorentzian bubble geometry of true vacuum surrounded by false vacuum.

We begin by writing expressions for ϕ and V in terms of a:

$$\begin{aligned} \frac{8\pi G}{d-2}\phi'^2 &= \left(\frac{a'}{a}\right)^2 - \frac{1}{a^2} - \frac{a''}{a} \\ \frac{16\pi G}{(d-2)^2}V(\phi) &= \frac{1}{a^2} - \left(\frac{a'}{a}\right)^2 - \frac{1}{d-2}\frac{a''}{a}. \end{aligned} \tag{6.19}$$

The first of these make it clear that throughout the physical range of ξ we must have

$$a'^2 - aa'' - 1 \geq 0. \tag{6.20}$$

In fact if this inequality is satisfied then we can integrate the first equation in (6.19) to find $\phi(\xi)$, which we can then invert and insert into the second equation to find $V(\phi)$.[4] This inequality may appear unusual, but we show in Appendix 6.A that it is equivalent to the null energy condition in the region produced by the continuation (6.11).

Additional constraints come from the Lorentzian continuation. We want $\hat{a}_1(t)$ to be real and positive for all $t > 0$, and also to obey (6.15), (6.16), or (6.17), with the caveat that in the last case (6.17) $\hat{a}_1(t)$ need only be positive before the crunch. If the false vacuum is dS then we want $\hat{a}_2(t)$ to be real and positive for all $t > 0$ and to obey (6.18). By continuing (6.19) we see that to reconstruct the scalar field and potential we need both $\hat{a}_1$ and $\hat{a}_2$ to obey

$$\dot{\hat{a}}^2 - \hat{a}\ddot{\hat{a}} - 1 \geq 0. \tag{6.21}$$

This inequality is again equivalent to the null energy condition in these two regions. We claim that these are all of the constraints that a proposed $a(\xi)$ needs to obey to be considered a CDL geometry.

The condition that $\hat{a}_1(t)$ is real can be rewritten in a nice way by observing that in a neighborhood around $\xi = 0$ we can see from the Taylor expansion for $a(\xi)$ that it is equivalent to

$$a(-\xi) = -a(\xi). \tag{6.22}$$

By analytic continuation this equation must hold in any simply-connected region containing $\xi = 0$ in which $a(\xi)$ is analytic. Conversely, (6.22) (together with the reality and positivity of $a(\xi)$ on $(0, \xi_c)$) implies that $\hat{a}_1(t)$ is real and positive for small positive t, and by analytic continuation must be so for all $t > 0$ unless we encounter a zero or singularity. Similarly the condition that $\hat{a}_2(t)$ is real is equivalent to

$$a(\xi_c - \xi) = -a(\xi_c + \xi). \tag{6.23}$$

[4] If there are places where the inequality is saturated and ϕ comes to a rest, this inversion is slightly more subtle. This happens for example inside the bubble if the field oscillates about the true minimum before settling down, as in reheating. This subtlety does not affect our ability to find the potential since the scalar traverses all relevant parts of the potential at least once.

A final condition we would like to have is that the vacua involved are at least metastable and not unstable. If the geometry is compact then the late time behaviour (6.15-6.18) of $\hat{a}_{1,2}$ ensures that the scalar field is rolling down to a minimum in both asymptotic regions. But if the geometry is noncompact then the false vacuum is reached already in the Euclidean geometry as $\xi \to \infty$, and there is no $\hat{a}_2$. So if we do not impose an additional condition, then the constraints we have stated so far allow situations where there is an unstable Minkowski or AdS maximum that the field rolls down from, which we feel does not deserve the name of a CDL geometry since it is not a tunnelling process. If the false vacuum is Minkowski we thus need to demand that $V''(\phi(\xi)) > 0$ as $\xi \to \infty$. The simplest way to achieve this is to demand that the potential is decreasing as $\xi \to \infty$, which from (6.19) means that

$$\left(\frac{1}{a^2} - \left(\frac{a'}{a}\right)^2 - \frac{1}{d-2}\frac{a''}{a}\right)' < 0 \qquad \text{as} \quad \xi \to \infty. \tag{6.24}$$

Note that unlike our other restrictions, this one depends on the dimension d. If the false vacuum is AdS, then a maximum should be allowed if its negative mass-squared obeys the Breitenlohner-Freedman bound [243]

$$V''(\phi(\xi)) > -\frac{(d-1)^2}{4(\ell_2)^2} \qquad \text{as} \quad \xi \to \infty. \tag{6.25}$$

The potential in this inequality is written in terms of a by using (6.19). Examples of potentials with metastable maxima of this type were given in [244, 148].

We can now gather the results of this section into a definition; a function $a(\xi)$ is a "CDL Geometry" if:

(a) It is real and positive on a real interval $\xi \in (0, \xi_c)$, possibly with $\xi_c \to \infty$.

(b) Near $\xi = 0$ it obeys (6.7), and if ξ_c is finite then it obeys (6.8). If ξ_c is infinite then as $\xi \to \infty$ either $a(\xi) \sim e^{\xi/\ell_2}$ ("tunnelling from AdS") or $a(\xi) \to \xi$ ("tunnelling from Minkowski").

(c) It is analytic in a simply connected region $\mathcal{D}$ containing the real interval $[0, \xi_c]$,

the positive imaginary axis,[5] and if ξ_c is finite the ray $\mathcal{R}$ defined by $\xi = \xi_c + it$ with $t > 0$.

(d) There are no zeros of a on the positive imaginary axis or on $\mathcal{R}$ if ξ_c is finite, and throughout $\mathcal{D}$ we have $a(-\xi) = -a(\xi)$. If ξ_c is finite we also have $a(\xi_c - \xi) = -a(\xi_c + \xi)$ and the dS asymptotic (6.18).

(e) On the real interval $[0, \xi_c]$ we have the null energy condition (6.20). On the positive imaginary axis and on $\mathcal{R}$ if ξ_c is finite, we have the null energy condition (6.21).

(f) If ξ_c is infinite then for "tunnelling from Minkowski" the inequality (6.24) is satisfied, while for "tunnelling from AdS" we have (6.25).

In this definition we assumed that the false vacuum was at a finite point in field space. If we wish to restrict to cases where the true vacuum is also at a finite point in field space then we can introduce an additional requirement:

(g) For large purely imaginary ξ we have the asymptotic geometry (6.15), (6.16), or (6.17).

6.2.4 Compact Coleman-De Luccia Geometries

Before presenting our examples of CDL geometries, we will make some special observations about the compact case. We first note that the reality conditions (6.22) and (6.23) allow continuation of $a(\xi)$ to a neighborhood of the full real axis and together imply the periodicity

$$a(\xi + 2\xi_c) = a(\xi). \tag{6.26}$$

Thus for the compact case we have Fourier Analysis at our disposal. We will henceforth choose units where $\xi_c = \pi$, after which we see that we may write

$$a(\xi) = \sum_{n=1}^{\infty} c_n \sin(n\xi). \tag{6.27}$$

[5] For tunnelling to (crunching) AdS we only include the open interval between the origin and the first zero of a on the positive imaginary axis. This also applies to constraints (d) and (e).

There are no cosines because the function is odd. This form is not the most useful however because the boundary conditions (6.7) and (6.8) imply nontrivial constraints on the c_n's. We can reorganize the series using trigonometric identities to take the form

$$a(\xi) = \sin(\xi)\left[1 + f(\sin\xi) + \cos(\xi) g(\sin\xi)\right], \tag{6.28}$$

where $f(\cdot)$ and $g(\cdot)$ are even functions which go to zero as their argument goes to zero, and which are analytic in a region containing the real interval $(0, 1]$ and also the pure imaginary axis. This form is completely general; any compact CDL geometry must have it. It is convenient because it automatically incorporates the reality conditions and boundary conditions at 0 and π, so the only remaining things to check are that the scale factor is nonvanishing, the null energy condition is satisfied, and that at late times outside the bubble we have (6.18). The cosine term has a simple interpretation in that it breaks the symmetry between the two minima. In particular, the analytic continuations (6.9) and (6.13) give

$$\hat{a}_{1,2}(t) = \sinh(t)\left[1 + f(i\sinh t) \pm \cosh(t) g(i\sinh t)\right], \tag{6.29}$$

which are real because f and g are even functions. Here $\hat{a}_1$ (or $\hat{a}_2$) takes the plus (or minus) sign. Depending on the desired nature of the true vacuum we might also like to impose (6.15), (6.16), or (6.17).

6.3 Examples

In this section, we first derive some general results that illustrate the difficulty of constructing geometries that satisfy our definition. In the following subsections we then give a series of explicit examples.

In writing down functions $a(\xi)$ that obey our constraints (a)–(g), the biggest challenge is the null energy conditions (6.20) and (6.21). We first consider the case where $a(\xi)$ (or $\hat{a}(t)$) is linear with unit coefficient both at $\xi = 0$ and $\xi \to \infty$. This is

appropriate for tunnelling to or from Minkowski space. We parametrize this as

$$a(\xi) = \xi(1 + \delta(\xi)). \tag{6.30}$$

Here $\delta(\xi)$ must go to zero both at $\xi = 0$ and $\xi = \infty$, and we must have $\delta > -1$ to avoid collapse. If there is a point where $-1 < \delta < 0$, then by continuity δ must have a minimum ξ_{min} with $-1 < \delta(\xi_{min}) < 0$. The null energy condition however takes the form

$$\delta(2 + \delta) + \xi^2\delta'^2 - \delta''\xi^2(1 + \delta) \geq 0, \tag{6.31}$$

and it is easy to check that a local minimum with $-1 < \delta < 0$ necessarily violates it. Thus we must have

$$\delta \geq 0. \tag{6.32}$$

We can use this observation to constrain the behaviour of a near $\xi = 0$. We can expand $\delta(\xi) = A\xi^n + \mathcal{O}(\xi^{n+2})$, with n some even integer greater than 1. Inserting this into (6.31) we find that if $n > 2$ then we must have $A < 0$, which is not allowed because then near $\xi = 0$ we would have $\delta < 0$. So $\delta(\xi)$ must start out like $A\xi^2$ with $A > 0$. We can also rule out the possibility that δ is a rational function. If δ were rational then at large ξ it would scale like ξ^{-n} for some positive integer n. From (6.31), we find the restriction $n(n + 1) \leq 2$. The only possibility is $n = 1$, but if δ is rational then this is impossible since (6.22) requires δ to be an even function of ξ. In our examples below we overcome this by including radicals.

Another constraint of this type is that when the false vacuum is de Sitter, its radius must be greater than 1 in the units where $\xi_c = \pi$:

$$\ell_2 > \frac{\xi_c}{\pi}. \tag{6.33}$$

In the thin-wall limit, this is the statement that if we draw the Euclidean CDL instanton as a piece of a sphere glued to a piece of flat space, the hyperbolic plane, or a larger sphere, the radius of the sphere corresponding to the metastable dS vacuum is always larger than the "size" ξ_c of the instanton divided by π.[6] We show this is

[6]One can also think of this as a bound on the proper length ξ_c of the warped de Sitter region

generally true in Appendix 6.B. Note that when the "true" vacuum is also dS this also implies that $\ell_1 > 1$ since $\ell_1 > \ell_2$ by definition. This constraint implies that the even functions $f(\cdot)$ and $g(\cdot)$ in equation (6.28) cannot both be rational, as this would lead to scaling (6.18) with $\ell_2^{-1} = (n+1)$ and $n \in \mathbb{Z}$ (we are now setting $\xi_c = \pi$). This is clearly impossible if $\ell_2 > 1$. So again in the compact case we will include radicals to avoid this problem.

6.3.1 De Sitter Domain Walls

Our simplest example of a CDL geometry describes a one-parameter family of (thick) domain walls interpolating between two degenerate dS minima. Geometries that describe genuine decays are given later, as they are in general more complicated. The domain walls are simple because in these cases $a(\xi)$ is symmetric under $\xi \leftrightarrow \pi - \xi$ and therefore only involves $\sin\xi$ when written in the form (6.28). Our domain walls are given by

$$a(\xi) = c\sqrt{1 - \sqrt{1 - \frac{2}{c^2}\sin^2\xi}}, \tag{6.34}$$

where c is any constant greater than $\sqrt{2}$, as required by the reality of the inner square root. As ξ approaches 0 or π we may expand the inner square root and check the smoothness conditions (6.7) and (6.8). We also need to check the null energy condition (6.20), which reads

$$a'^2 - aa'' - 1 = \frac{(c^2-2)(c - \sqrt{c^2 - 2\sin^2\xi})}{(c^2 - 2\sin^2\xi)^{3/2}}\sin^2\xi \geq 0, \tag{6.35}$$

which is manifestly satisfied for any $c \geq \sqrt{2}$.

Next, we analytically continue (6.34) to Lorentzian signature by applying (6.9). The resulting scale factor is

$$\hat{a}_1(t) = c\sqrt{\sqrt{1 + \frac{2}{c^2}\sinh^2 t} - 1}, \tag{6.36}$$

(6.12).

whose late time behavior is

$$\hat{a}_1(t) \to \sqrt{\frac{c}{\sqrt{2}}} e^{t/2} \quad \text{as} \quad t \to \infty. \tag{6.37}$$

Matching this to (6.16), we find an asymptotically dS space with radius $\ell_1 = 2$. This agrees with the bound $\ell_2 > 1$ mentioned earlier and proven in Appendix 6.B (here $\ell_1 = \ell_2$). We still need to check the null energy condition (6.21), which is simply the analytic continuation of (6.35):

$$\dot{\hat{a}}_1^2 - \hat{a}_1 \ddot{\hat{a}}_1 - 1 = \frac{(c^2-2)(\sqrt{c^2 + 2\sinh^2 t} - c)}{(c^2 + 2\sinh^2 t)^{3/2}} \sinh^2 t \geq 0. \tag{6.38}$$

By symmetry the second analytic continuation (6.13) gives exactly the same $\hat{a}_2(t) = \hat{a}_1(t)$.

We have verified that (6.34) satisfies all conditions (a)–(g) to be a CDL geometry. We may then use (6.19) to solve for $\phi(\xi)$ and $V(\phi)$. Their analytic forms are not very illuminating, as $\phi(\xi)$ involves a hypergeometric function and $V(\phi)$ is written in terms of the inverse of $\phi(\xi)$. However, in many applications of CDL (such as calculating the correlation functions) it is $a(\xi)$ that we would like to be simple, not $V(\phi)$.

6.3.2 Decays from dS to dS

In Sec. 6.3.1 we discussed domain walls interpolating between two degenerate dS minima. When this degeneracy is broken, we arrive at the phenomenologically interesting case [245] of decays from one dS space to another with a smaller cosmological constant. We give analytic examples of such geometries in this subsection.

In order to interpolate between two dS minima with different cosmological constants, it is necessary to break the symmetry of $a(\xi)$ under $\xi \leftrightarrow \pi - \xi$. In the form (6.28) this means that $a(\xi)$ has to depend on $\cos\xi$ in addition to $\sin\xi$. Under the analytic continuations (6.9) and (6.13), $\cos\xi$ becomes $\cosh t$ and $-\cosh t$ respectively as we see in (6.29). This minus sign is crucial in making the late time behaviors of $\hat{a}_1(t)$ and $\hat{a}_2(t)$ different, which is necessary for them to describe asymptotically dS

spaces with different cosmological constants.

One of the simplest examples that we found is

$$a(\xi) = \left(\frac{1 + 10^{1/4}}{1 + \left[10 - \sin^2 \xi \left(\sqrt{2 - \sin^2 \xi} + \cos \xi \right) \right]^{1/4}} \right)^{1/2} \sin \xi. \tag{6.39}$$

One can show that this is of the form (6.28) by first writing out its Taylor expansion in terms of $\sin \xi$ and $\cos \xi$, and then eliminating all quadratic or higher order terms in $\cos \xi$ by applying $\cos^2 \xi = 1 - \sin^2 \xi$. One can check the null energy conditions (6.20) and (6.21). Upon analytic continuation we have

$$\hat{a}_{1,2}(t) = \left(\frac{1 + 10^{1/4}}{1 + \left[10 + \sinh^2 t \left(\sqrt{2 + \sinh^2 t} \pm \cosh t \right) \right]^{1/4}} \right)^{1/2} \sinh t, \tag{6.40}$$

where $\hat{a}_1(t)$ takes the plus sign and asymptotes to

$$\hat{a}_1(t) \to \frac{\sqrt{1 + 10^{1/4}}}{2^{3/4}} e^{5t/8} \quad \text{as} \quad t \to \infty, \tag{6.41}$$

and $\hat{a}_2(t)$ takes the minus sign and asymptotes to

$$\hat{a}_2(t) \to \frac{\sqrt{1 + 10^{1/4}}}{2^{3/4}} e^{7t/8} \quad \text{as} \quad t \to \infty. \tag{6.42}$$

The radii of the two dS vacua are $\ell_1 = 8/5$ and $\ell_2 = 8/7$, which again obey the bound of Appendix 6.B. We show this geometry in $d = 4$ in Figure 6.2, together with the scalar potential that gives rise to it.

A family of geometries of this type can be found by varying the parameters in (6.39) (subject to the smoothness and null energy conditions). We will not give the exact parameter space here, but we note that it is quite large. For instance, one can verify that all constraints are still satisfied if we change both constants "10" in (6.39) to any number larger than 4.2, or if we change the power 1/4 to any number between 0 and 1/4.

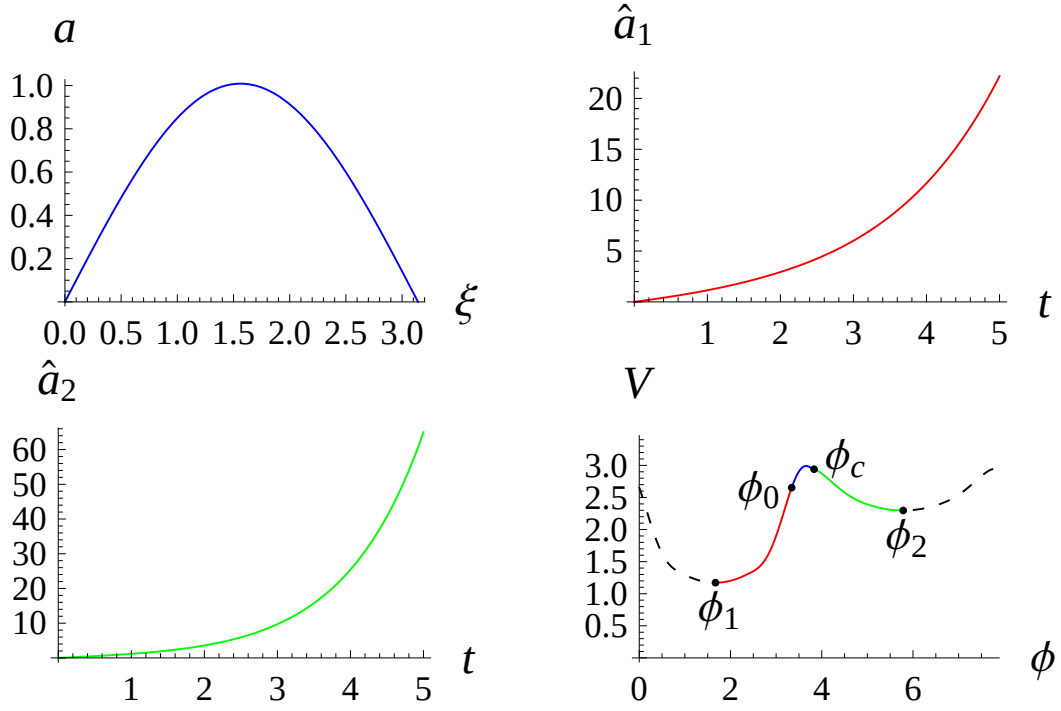

Figure 6.2: A CDL geometry describing the decay from dS to dS. We have the Euclidean geometry $a(\xi)$ on the top left, the first FRW geometry $\hat{a}_1(t)$ that asymptotes to the true dS vacuum on the top right, the second FRW geometry $\hat{a}_2(t)$ describing the parent dS on the bottom left, and the scalar potential $V(\phi)$ on the bottom right. The blue, red, and green segments are traversed by the scalar field in the three regions of the CDL geometry as depicted in Figure 6.1. The black dashed lines are "conjectures" from what we expect qualitatively – the potential there cannot be solved numerically from the CDL geometry because the field never goes there. If one could solve the potential analytically between the two minima, it can then be continued to the dashed region.

6.3.3 Decays from dS to Minkowski Space

In this subsection we consider decays from dS to asymptotically Minkowski space. These are potentially interesting for conceptual reasons, as explained in [246, 78, 247]. A "simple" geometry of this type is

$$a(\xi) = \frac{\frac{3}{2}\sin\xi}{1+\left[8-\sin^2\xi\left(\sqrt{2-\sin^2\xi}+\cos\xi\right)\right]^{1/3}} + \arcsin\left(\frac{\sin\xi}{2}\right). \tag{6.43}$$

One can check that it satisfies the smoothness conditions (6.7), (6.8) and the null energy conditions (6.20), (6.21). Upon analytic continuation we have

$$\hat{a}_{1,2}(t) = \frac{\frac{3}{2}\sinh t}{1+\left[8+\sinh^2 t\left(\sqrt{2+\sinh^2 t}\pm\cosh t\right)\right]^{1/3}} + \operatorname{arcsinh}\left(\frac{\sinh t}{2}\right), \tag{6.44}$$

where $\hat{a}_1(t)$ takes the plus sign and the exponentially growing terms cancel, leading to

$$\hat{a}_1(t) \to t \quad \text{as} \quad t\to\infty, \tag{6.45}$$

and $\hat{a}_2(t)$ takes the minus sign and asymptotes to

$$\hat{a}_2(t) \to \frac{3}{2^{4/3}}e^{2t/3} \quad \text{as} \quad t\to\infty. \tag{6.46}$$

The radius of the parent dS space is therefore $\ell_2 = 3/2$, again satisfying the bound of Appendix 6.B. We show this geometry and its potential in $d = 4$ in Figure 6.3.

As before, a family of geometries of this type can be found by varying the parameters in (6.43). Additionally, we could get CDL geometries that describe decays from dS to FRW which has a zero cosmological constant but does not have the asymptotic behavior (6.15). As discussed above (6.15) this means that the scalar field is rolling off to infinity in the FRW. A particular class of interesting FRW solutions of this type was studied in [9] and conjectured to have holographic duals. They are characterized

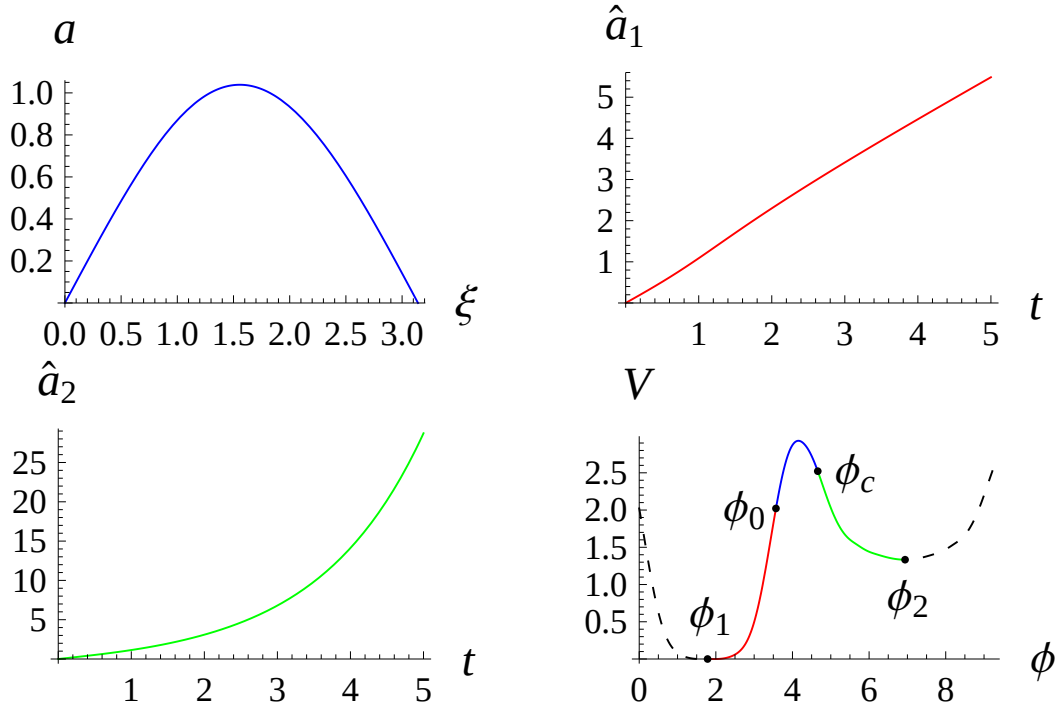

Figure 6.3: The geometry and potential describing a decay from dS to asymptotically Minkowski space. See the caption of Figure 6.2 for detailed explanations.

by the following late time behavior:

$$\hat{a}_1(t) \to ct \quad \text{as} \quad t \to \infty. \tag{6.47}$$

We give analytic CDL geometries of this type by multiplying the "arcsin" term in (6.43) by a constant $c > 1$, and multiplying the first term by $(2 - c)$ to preserve the smoothness conditions.[7] Over a range of c the null energy conditions are satisfied, and we get an asymptotically linear scale factor $\hat{a}_1(t) \to ct$ with $c > 1$.

6.3.4 Noncompact Examples

Noncompact examples have simpler functional forms, but have the added complication of the conditions (6.24) or (6.25). These decays are arguably the least interesting, since exactly Minkowski spaces are expected to be supersymmetric and stable, and metastable AdS is inherently ill-defined [248, 249, 250]. A candidate example for a decay of Minkowski space to a crunch is

$$a(\xi) = \xi \left(1 + \frac{\xi^2}{(1+\xi^2)^{3/2}}\right). \tag{6.48}$$

The radical is still necessary because of the argument given below equation (6.32). This obeys the null energy conditions (6.20) and (6.21), and crunches inside the bubble at finite time. For $d = 4$ however it corresponds to rolling down from a maximum, and we find we need to set $d = 3$ to satisfy (6.24). This can be checked analytically by expanding (6.24) to order $1/\xi^6$ at large ξ.[8] An improved example that works in $d = 4$ is

$$a(\xi) = \xi \left(1 + \frac{\xi^2}{\sqrt{1+\xi^6}}\right). \tag{6.49}$$

[7] The lower limit $c > 1$ is required by the null energy condition (6.21). The apparent upper limit $c < 2$ is superficial and can be relaxed by changing the "2" inside the arcsin in (6.43).

[8] Note that for the compact examples in the previous subsections the dimension was irrelevant. It is only for noncompact geometries that we have the inequalities (6.24) or (6.25) which depend on dimension.

We can show that the potential leading to this geometry has a metastable minimum by expanding (6.24) to order $1/\xi^{10}$. This potential is shown in Figure 6.4.

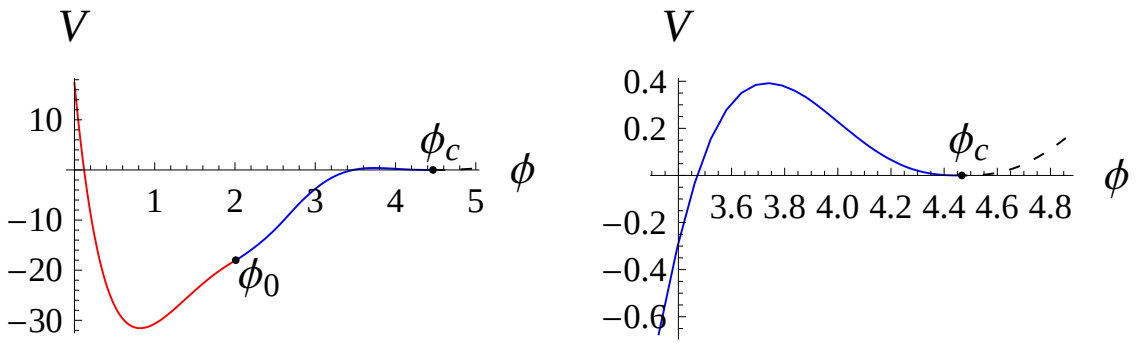

Figure 6.4: The potential $V(\phi)$ leading to a CDL geometry (6.49) describing the decay from Minkowski space to a crunching AdS. On the right we zoom in on the same potential at ϕ_c (the asymptotic field value) and see that it is a local minimum with a very shallow barrier.

A candidate family of decays of AdS to a crunch is

$$a(\xi) = (1+c)\sinh\xi - 2c\sinh\frac{\xi}{2}. \tag{6.50}$$

This example is simple enough that we can check the null energy conditions (6.20) and (6.21) analytically, finding that any $c > 0$ is allowed. It is also not hard to check that the BF bound (6.25) is satisfied for $d \geq 3$. This geometry and its potential are shown in Figure 6.5 for $c = 1$, $d = 4$.

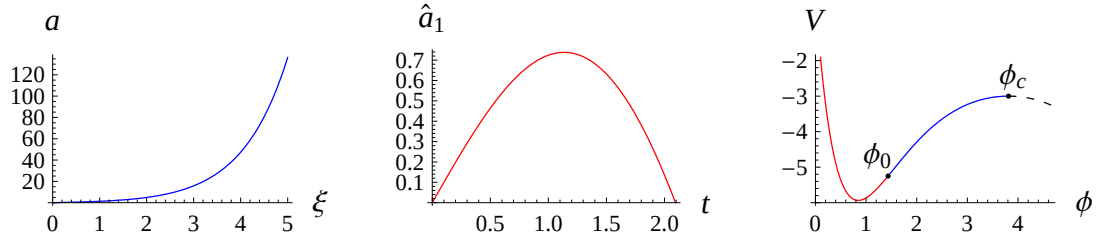

Figure 6.5: The geometry and potential for a decay from AdS to a crunch

6.A Null Energy Condition

In this appendix we show the equivalence of the inequalities (6.20) and (6.21) to the null energy condition

$$T_{\mu\nu}k^\mu k^\nu \geq 0, \tag{6.51}$$

for any null k^μ. We first apply this to the "warped de Sitter" geometry (6.12), which we rewrite as

$$ds^2 = d\xi^2 + a(\xi)^2\gamma_{ij}dx^i dx^j. \tag{6.52}$$

The Ricci tensor is

$$\begin{aligned} R_{\xi\xi} &= -(d-1)\frac{a''}{a} \\ R_{ij} &= -\left[aa'' + (d-2)(a'^2-1)\right]\gamma_{ij} \\ R_{\xi i} &= R_{i\xi} = 0, \end{aligned} \tag{6.53}$$

so the Einstein tensor is

$$\begin{aligned} G_{\xi\xi} &= \frac{(d-1)(d-2)}{2}\left[\left(\frac{a'}{a}\right)^2 - \frac{1}{a^2}\right] \\ G_{ij} &= \left[(d-2)\frac{a''}{a} + \frac{(d-2)(d-3)}{2}\left(\left(\frac{a'}{a}\right)^2 - \frac{1}{a^2}\right)\right]a^2\gamma_{ij} \\ G_{\xi i} &= G_{i\xi} = 0. \end{aligned} \tag{6.54}$$

To check the null energy condition, consider the radial null vector $k = \partial_\xi + \frac{1}{a}\partial_\omega$.[9] Contracting this with $G_{\mu\nu}$ we find (6.51) is satisfied if

$$\left(\frac{a'}{a}\right)^2 - \frac{1}{a^2} - \frac{a''}{a} \geq 0, \tag{6.55}$$

[9] Any nonradial vector can be boosted into a radial one unless it lies entirely within the dS slice, but in that case the Null Energy Condition is trivially saturated since the dS Einstein tensor is proportional to the metric.

which agrees with (6.20). We can easily continue this Einstein tensor to find the Einstein tensor for the open FRW metric (6.10), and a similar computation confirms (6.21).

6.B A Bound on Parent dS Radius

In this appendix we show that for any compact CDL geometry describing the decay of dS space, the parent dS radius (which is ℓ_2 according to (6.18)) must be greater than ξ_c/π. In the convenient units proposed in Sec. 6.2.4 where $\xi_c = \pi$, this means $\ell_2 > 1$. We will not need to know what kind of space the parent dS decays into, whether it is dS, AdS, Minkowski space, or even something else.

We prove this by using the null energy conditions (6.20) and (6.21). First, we note that it is impossible for $a(\xi)$ or $\hat{a}(t)$ to have a local minimum within their physical domains. Clearly if for example $a(\xi)$ had a local minimum, we would have $a'(\xi) = 0$ and $a''(\xi) \geq 0$ there, manifestly violating the null energy condition (6.20). Therefore it is impossible to have a contracting phase followed by an expanding phase. Combining this with the boundary conditions (6.7) and (6.8), we find that $a(\xi)$ must monotonically increase to a maximum at some ξ_m and after that monotonically decrease to 0. For $\hat{a}_2(t)$ there has to an expanding phase (6.18) at late times, so $\hat{a}_2(t)$ must be a monotonically increasing function for all $t \geq 0$.

Let us define an "energy function" $E \equiv (a'^2 - 1)/a^2$ and take its derivative

$$\frac{dE}{d\xi} = \frac{d}{d\xi}\left(\frac{a'^2 - 1}{a^2}\right) = -\frac{2a'(a'^2 - aa'' - 1)}{a^3}. \tag{6.56}$$

Using the null energy condition (6.20), we find that E never increases in an expanding phase and never decreases in a contracting phase. For a more physical argument, we note that E is equal to the total energy up to a constant coefficient, as we can see from the second equation in (6.3).[10] The total energy is drained by friction during an expanding phase and replenished by anti-friction during a contracting phase. Exactly

[10]The Euclidean equations of motion (6.3) are completely the same as the Lorentzian equations (6.14) with the inverted potential $-V(\phi)$, so we may use our usual intuition about real-time evolution.

the same statements hold for $\hat{E}_2 \equiv (\dot{\hat{a}}_2^2 - 1)/\hat{a}_2^2$.

It is therefore clear that $E(\xi)$ reaches an absolute minimum exactly as $a(\xi)$ reaches its maximum at ξ_m:

$$E(\xi) \geq E(\xi_m) = -\frac{1}{a(\xi_m)^2} \qquad \text{for} \qquad \forall \xi \in [0, \xi_c]. \tag{6.57}$$

Let us abbreviate $a(\xi_m)$ as a_m. For the expanding phase $0 \leq \xi \leq \xi_m$ we rewrite the above inequality as

$$\frac{a'}{\sqrt{1 - a^2/a_m^2}} \geq 1 \tag{6.58}$$

and integrate both sides from $\xi = 0$ to $\xi = \xi_m$, which gives

$$\frac{\pi}{2} a_m \geq \xi_m. \tag{6.59}$$

For the contracting phase $\xi_m \leq \xi \leq \xi_c$ there is a minus sign on the left hand side of (6.58). After integrating from ξ_m to ξ_c we find

$$\frac{\pi}{2} a_m \geq \xi_c - \xi_m. \tag{6.60}$$

Combining this with (6.59) we arrive at

$$\pi a_m \geq \xi_c. \tag{6.61}$$

Finally, we argue that a_m is bounded from above by ℓ_2. From the analytic continuation (6.13) we find

$$E|_{\xi=\xi_c} = \left.\frac{a'^2 - 1}{a^2}\right|_{\xi=\xi_c} = -\left.\frac{\dot{\hat{a}}_2^2 - 1}{\hat{a}_2^2}\right|_{t=0} = -\hat{E}_2|_{t=0}. \tag{6.62}$$

Physically, the field is at rest when $\xi = \xi_c$ or $t = 0$, so the total "Euclidean energy" $-V(\phi_c)$ is just minus the "Lorentzian energy". From this we have a chain of

(in)equalities

$$-\frac{1}{a_m^2} = E|_{\xi=\xi_m} \leq E|_{\xi=\xi_c} = -\hat{E}_2|_{t=0} \leq -\hat{E}_2|_{t\to\infty} = -\frac{1}{\ell_2^2}, \tag{6.63}$$

where we have the first inequality because E never decreases in a contracting phase, and the second inequality because $\hat{E}_2$ never increases in an expanding phase. The last equality comes from the asymptotically dS condition (6.18). Therefore we have

$$a_m \leq \ell_2. \tag{6.64}$$

Combining this with (6.61), we have shown the bound on the parent dS radius

$$\ell_2 > \frac{\xi_c}{\pi}. \tag{6.65}$$

This inequality cannot be saturated without saturating all the above inequalities. In particular, saturating (6.57) and (6.64) leads to $a(\xi) = \ell_2 \sin(\xi/\ell_2)$ which describes a pure dS geometry rather than a CDL decay.

Bibliography

[1] T. Banks, W. Fischler, S. Shenker, and L. Susskind, *M theory as a matrix model: A Conjecture*, *Phys.Rev.* **D55** (1997) 5112–5128, [hep-th/9610043].

[2] J. M. Maldacena, *The Large N limit of superconformal field theories and supergravity*, *Adv.Theor.Math.Phys.* **2** (1998) 231–252, [hep-th/9711200].

[3] E. Witten, *Anti-de Sitter space and holography*, *Adv.Theor.Math.Phys.* **2** (1998) 253–291, [hep-th/9802150].

[4] S. Gubser, I. R. Klebanov, and A. M. Polyakov, *Gauge theory correlators from noncritical string theory*, *Phys.Lett.* **B428** (1998) 105–114, [hep-th/9802109].

[5] G. 't Hooft, *Dimensional reduction in quantum gravity*, gr-qc/9310026.

[6] L. Susskind, *The World as a hologram*, *J.Math.Phys.* **36** (1995) 6377–6396, [hep-th/9409089].

[7] X. Dong, B. Horn, E. Silverstein, and G. Torroba, *Micromanaging de Sitter holography*, *Class.Quant.Grav.* **27** (2010) 245020, [arXiv:1005.5403].

[8] X. Dong, B. Horn, E. Silverstein, and G. Torroba, *Unitarity bounds and RG flows in time dependent quantum field theory*, arXiv:1203.1680.

[9] X. Dong, B. Horn, S. Matsuura, E. Silverstein, and G. Torroba, *FRW solutions and holography from uplifted AdS/CFT*, arXiv:1108.5732.

[10] X. Dong, B. Horn, E. Silverstein, and A. Westphal, *Simple exercises to flatten your potential*, *Phys.Rev.* **D84** (2011) 026011, [arXiv:1011.4521].

[11] X. Dong and D. Harlow, *Analytic Coleman-De Luccia Geometries*, *JCAP* **1111** (2011) 044, [arXiv:1109.0011].

[12] G. Gibbons and S. Hawking, *Cosmological Event Horizons, Thermodynamics, and Particle Creation*, *Phys.Rev.* **D15** (1977) 2738–2751.

[13] A. Strominger and C. Vafa, *Microscopic origin of the Bekenstein-Hawking entropy*, *Phys.Lett.* **B379** (1996) 99–104, [hep-th/9601029].

[14] C. G. Callan and J. M. Maldacena, *D-brane approach to black hole quantum mechanics*, *Nucl.Phys.* **B472** (1996) 591–610, [hep-th/9602043].

[15] J. M. Maldacena and L. Susskind, *D-branes and fat black holes*, *Nucl.Phys.* **B475** (1996) 679–690, [hep-th/9604042].

[16] J. Polchinski and E. Silverstein, *Dual Purpose Landscaping Tools: Small Extra Dimensions in AdS/CFT*, arXiv:0908.0756.

[17] A. Karch, *Autolocalization in de Sitter space*, *JHEP* **0307** (2003) 050, [hep-th/0305192].

[18] M. Alishahiha, A. Karch, E. Silverstein, and D. Tong, *The dS/dS correspondence*, *AIP Conf.Proc.* **743** (2005) 393–409, [hep-th/0407125].

[19] M. Alishahiha, A. Karch, and E. Silverstein, *Hologravity*, *JHEP* **0506** (2005) 028, [hep-th/0504056].

[20] A. Strominger, *The dS / CFT correspondence*, *JHEP* **0110** (2001) 034, [hep-th/0106113].

[21] B. Freivogel, Y. Sekino, L. Susskind, and C.-P. Yeh, *A Holographic framework for eternal inflation*, *Phys.Rev.* **D74** (2006) 086003, [hep-th/0606204].

[22] R. Bousso, B. Freivogel, Y. Sekino, S. Shenker, L. Susskind, et al., *Future foam: Nontrivial topology from bubble collisions in eternal inflation*, *Phys.Rev.* **D78** (2008) 063538, [arXiv:0807.1947].

[23] N. Arkani-Hamed, S. Dubovsky, A. Nicolis, E. Trincherini, and G. Villadoro, *A Measure of de Sitter entropy and eternal inflation*, *JHEP* **0705** (2007) 055, [arXiv:0704.1814].

[24] S. Dubovsky, L. Senatore, and G. Villadoro, *The Volume of the Universe after Inflation and de Sitter Entropy*, *JHEP* **0904** (2009) 118, [arXiv:0812.2246].

[25] T. Banks, *Cosmological breaking of supersymmetry? or Little lambda goes back to the future 2*, hep-th/0007146.

[26] U. H. Danielsson, A. Guijosa, and M. Kruczenski, *Brane anti-brane systems at finite temperature and the entropy of black branes*, *JHEP* **0109** (2001) 011, [hep-th/0106201].

[27] S. B. Giddings, S. Kachru, and J. Polchinski, *Hierarchies from fluxes in string compactifications*, *Phys.Rev.* **D66** (2002) 106006, [hep-th/0105097].

[28] L. Randall and R. Sundrum, *An Alternative to compactification*, *Phys.Rev.Lett.* **83** (1999) 4690–4693, [hep-th/9906064].

[29] I. R. Klebanov and M. J. Strassler, *Supergravity and a confining gauge theory: Duality cascades and chi SB resolution of naked singularities*, *JHEP* **0008** (2000) 052, [hep-th/0007191].

[30] S. S. Gubser, *AdS / CFT and gravity*, *Phys.Rev.* **D63** (2001) 084017, [hep-th/9912001].

[31] S. Hawking, J. M. Maldacena, and A. Strominger, *de Sitter entropy, quantum entanglement and AdS / CFT*, *JHEP* **0105** (2001) 001, [hep-th/0002145].

[32] A. R. Frey, *Warped strings: Selfdual flux and contemporary compactifications*, hep-th/0308156.

[33] E. Silverstein, *TASI / PiTP / ISS lectures on moduli and microphysics*, hep-th/0405068.

[34] M. Grana, *Flux compactifications in string theory: A Comprehensive review*, *Phys.Rept.* **423** (2006) 91–158, [hep-th/0509003].

[35] J. Polchinski, *The Cosmological Constant and the String Landscape*, hep-th/0603249.

[36] M. R. Douglas and S. Kachru, *Flux compactification*, *Rev.Mod.Phys.* **79** (2007) 733–796, [hep-th/0610102].

[37] F. Denef, M. R. Douglas, and S. Kachru, *Physics of String Flux Compactifications*, *Ann.Rev.Nucl.Part.Sci.* **57** (2007) 119–144, [hep-th/0701050].

[38] R. Bousso, *TASI Lectures on the Cosmological Constant*, *Gen.Rel.Grav.* **40** (2008) 607–637, [arXiv:0708.4231].

[39] F. Denef, *Les Houches Lectures on Constructing String Vacua*, arXiv:0803.1194.

[40] X. Dong, B. Horn, E. Silverstein, and G. Torroba, *work in progress*, .

[41] B. R. Greene, A. D. Shapere, C. Vafa, and S.-T. Yau, *Stringy Cosmic Strings and Noncompact Calabi-Yau Manifolds*, *Nucl.Phys.* **B337** (1990) 1.

[42] S. Hellerman, J. McGreevy, and B. Williams, *Geometric constructions of nongeometric string theories*, *JHEP* **0401** (2004) 024, [hep-th/0208174].

[43] D. Vegh and J. McGreevy, *Semi-Flatland*, *JHEP* **0810** (2008) 068, [arXiv:0808.1569].

[44] O. Aharony, A. Fayyazuddin, and J. M. Maldacena, *The Large N limit of N=2, N=1 field theories from three-branes in F theory*, *JHEP* **9807** (1998) 013, [hep-th/9806159].

[45] S. Weinberg, *Anthropic Bound on the Cosmological Constant*, *Phys.Rev.Lett.* **59** (1987) 2607.

[46] R. Bousso and J. Polchinski, *Quantization of four form fluxes and dynamical neutralization of the cosmological constant*, *JHEP* **0006** (2000) 006, [hep-th/0004134].

[47] E. Silverstein, *(A)dS backgrounds from asymmetric orientifolds*, hep-th/0106209.

[48] A. Maloney, E. Silverstein, and A. Strominger, *De Sitter space in noncritical string theory*, hep-th/0205316.

[49] S. Kachru, R. Kallosh, A. D. Linde, and S. P. Trivedi, *De Sitter vacua in string theory*, *Phys.Rev.* **D68** (2003) 046005, [hep-th/0301240].

[50] E. Silverstein, *Simple de Sitter Solutions*, *Phys.Rev.* **D77** (2008) 106006, [arXiv:0712.1196].

[51] M. P. Hertzberg, S. Kachru, W. Taylor, and M. Tegmark, *Inflationary Constraints on Type IIA String Theory*, *JHEP* **0712** (2007) 095, [arXiv:0711.2512].

[52] S. S. Haque, G. Shiu, B. Underwood, and T. Van Riet, *Minimal simple de Sitter solutions*, *Phys.Rev.* **D79** (2009) 086005, [arXiv:0810.5328].

[53] C. Caviezel, P. Koerber, S. Kors, D. Lust, T. Wrase, et al., *On the Cosmology of Type IIA Compactifications on SU(3)-structure Manifolds*, *JHEP* **0904** (2009) 010, [arXiv:0812.3551].

[54] R. Flauger, S. Paban, D. Robbins, and T. Wrase, *Searching for slow-roll moduli inflation in massive type IIA supergravity with metric fluxes*, *Phys.Rev.* **D79** (2009) 086011, [arXiv:0812.3886].

[55] U. H. Danielsson, S. S. Haque, G. Shiu, and T. Van Riet, *Towards Classical de Sitter Solutions in String Theory*, *JHEP* **0909** (2009) 114, [arXiv:0907.2041].

[56] B. de Carlos, A. Guarino, and J. M. Moreno, *Flux moduli stabilisation, Supergravity algebras and no-go theorems*, *JHEP* **1001** (2010) 012, [arXiv:0907.5580].

[57] C. Caviezel, T. Wrase, and M. Zagermann, *Moduli Stabilization and Cosmology of Type IIB on SU(2)-Structure Orientifolds*, *JHEP* **1004** (2010) 011, [arXiv:0912.3287].

[58] G. Dibitetto, R. Linares, and D. Roest, *Flux Compactifications, Gauge Algebras and De Sitter*, *Phys.Lett.* **B688** (2010) 96–100, [arXiv:1001.3982].

[59] T. Wrase and M. Zagermann, *On Classical de Sitter Vacua in String Theory*, *Fortsch.Phys.* **58** (2010) 906–910, [arXiv:1003.0029].

[60] U. H. Danielsson, P. Koerber, and T. Van Riet, *Universal de Sitter solutions at tree-level*, *JHEP* **1005** (2010) 090, [arXiv:1003.3590].

[61] D. Andriot, E. Goi, R. Minasian, and M. Petrini, *Supersymmetry breaking branes on solvmanifolds and de Sitter vacua in string theory*, *JHEP* **1105** (2011) 028, [arXiv:1003.3774].

[62] G. Shiu, G. Torroba, B. Underwood, and M. R. Douglas, *Dynamics of Warped Flux Compactifications*, *JHEP* **0806** (2008) 024, [arXiv:0803.3068].

[63] M. R. Douglas and G. Torroba, *Kinetic terms in warped compactifications*, *JHEP* **0905** (2009) 013, [arXiv:0805.3700].

[64] A. R. Frey, G. Torroba, B. Underwood, and M. R. Douglas, *The Universal Kahler Modulus in Warped Compactifications*, *JHEP* **0901** (2009) 036, [arXiv:0810.5768].

[65] S. B. Giddings and A. Maharana, *Dynamics of warped compactifications and the shape of the warped landscape*, *Phys.Rev.* **D73** (2006) 126003, [hep-th/0507158].

[66] M. R. Douglas, *Effective potential and warp factor dynamics*, *JHEP* **1003** (2010) 071, [arXiv:0911.3378].

[67] M. R. Douglas and R. Kallosh, *Compactification on negatively curved manifolds*, *JHEP* **1006** (2010) 004, [arXiv:1001.4008].

[68] E. Witten, *Phases of N=2 theories in two-dimensions*, *Nucl.Phys.* **B403** (1993) 159–222, [hep-th/9301042].

[69] T. Ishii, G. Ishiki, S. Shimasaki, and A. Tsuchiya, *T-duality, fiber bundles and matrices*, *JHEP* **0705** (2007) 014, [hep-th/0703021].

[70] E. Cremmer, B. Julia, H. Lu, and C. Pope, *Dualization of dualities. 2. Twisted selfduality of doubled fields, and superdualities*, *Nucl.Phys.* **B535** (1998) 242–292, [hep-th/9806106].

[71] S. Kachru, D. Simic, and S. P. Trivedi, *Stable Non-Supersymmetric Throats in String Theory*, *JHEP* **1005** (2010) 067, [arXiv:0905.2970].

[72] E. Witten, *Quantum gravity in de Sitter space*, hep-th/0106109.

[73] J. M. Maldacena, *Non-Gaussian features of primordial fluctuations in single field inflationary models*, *JHEP* **0305** (2003) 013, [astro-ph/0210603].

[74] D. Anninos, G. S. Ng, and A. Strominger, *Future Boundary Conditions in De Sitter Space*, *JHEP* **1202** (2012) 032, [arXiv:1106.1175].

[75] M. Kleban and M. Redi, *Expanding F-Theory*, *JHEP* **0709** (2007) 038, [arXiv:0705.2020].

[76] D. Harlow and D. Stanford, *Operator Dictionaries and Wave Functions in AdS/CFT and dS/CFT*, arXiv:1104.2621.

[77] A. W. Peet and J. Polchinski, *UV / IR relations in AdS dynamics*, *Phys.Rev.* **D59** (1999) 065011, [hep-th/9809022].

[78] D. Harlow and L. Susskind, *Crunches, Hats, and a Conjecture*, arXiv:1012.5302.

[79] I. Heemskerk and J. Polchinski, *Holographic and Wilsonian Renormalization Groups*, *JHEP* **1106** (2011) 031, [arXiv:1010.1264].

[80] O. DeWolfe, T. Hauer, A. Iqbal, and B. Zwiebach, *Uncovering the symmetries on [p,q] seven-branes: Beyond the Kodaira classification*, *Adv.Theor.Math.Phys.* **3** (1999) 1785–1833, [hep-th/9812028].

[81] O. DeWolfe, T. Hauer, A. Iqbal, and B. Zwiebach, *Uncovering infinite symmetries on [p, q] 7-branes: Kac-Moody algebras and beyond*, *Adv.Theor.Math.Phys.* **3** (1999) 1835–1891, [hep-th/9812209].

[82] D. Anninos, T. Hartman, and A. Strominger, *Higher Spin Realization of the dS/CFT Correspondence*, arXiv:1108.5735.

[83] P. McFadden and K. Skenderis, *Holography for Cosmology*, *Phys.Rev.* **D81** (2010) 021301, [arXiv:0907.5542].

[84] P. McFadden and K. Skenderis, *Observational signatures of holographic models of inflation*, arXiv:1010.0244.

[85] A. Bzowski, P. McFadden, and K. Skenderis, *Holographic predictions for cosmological 3-point functions*, *JHEP* **1203** (2012) 091, [arXiv:1112.1967].

[86] O. Aharony and E. Silverstein, *Supercritical stability, transitions and (pseudo)tachyons*, *Phys.Rev.* **D75** (2007) 046003, [hep-th/0612031].

[87] C. Vafa, *Evidence for F theory*, *Nucl.Phys.* **B469** (1996) 403–418, [hep-th/9602022].

[88] D. R. Morrison and C. Vafa, *Compactifications of F theory on Calabi-Yau threefolds. 1*, *Nucl.Phys.* **B473** (1996) 74–92, [hep-th/9602114].

[89] D. R. Morrison and C. Vafa, *Compactifications of F theory on Calabi-Yau threefolds. 2.*, *Nucl.Phys.* **B476** (1996) 437–469, [hep-th/9603161].

[90] A. Sen, *F theory and orientifolds*, *Nucl.Phys.* **B475** (1996) 562–578, [hep-th/9605150].

[91] T. Banks, M. R. Douglas, and N. Seiberg, *Probing F theory with branes*, *Phys.Lett.* **B387** (1996) 278–281, [hep-th/9605199].

[92] A. Sen, *Orientifold limit of F theory vacua*, *Phys.Rev.* **D55** (1997) 7345–7349, [hep-th/9702165].

[93] G. Horowitz, A. Lawrence, and E. Silverstein, *Insightful D-branes*, *JHEP* **0907** (2009) 057, [arXiv:0904.3922].

[94] H. L. Verlinde, *Holography and compactification*, *Nucl.Phys.* **B580** (2000) 264–274, [hep-th/9906182].

[95] L. Susskind and E. Witten, *The Holographic bound in anti-de Sitter space*, hep-th/9805114.

[96] R. Bousso, *A Covariant entropy conjecture*, *JHEP* **9907** (1999) 004, [hep-th/9905177].

[97] R. Bousso, *The Holographic principle*, *Rev.Mod.Phys.* **74** (2002) 825–874, [hep-th/0203101].

[98] S. S. Gubser, *Curvature singularities: The Good, the bad, and the naked*, *Adv.Theor.Math.Phys.* **4** (2000) 679–745, [hep-th/0002160].

[99] J. M. Maldacena and C. Nunez, *Supergravity description of field theories on curved manifolds and a no go theorem*, *Int.J.Mod.Phys.* **A16** (2001) 822–855, [hep-th/0007018].

[100] http://www.urbandictionary.com/define.php?term=technicolor+yawn.

[101] D. R. Green, A. Lawrence, J. McGreevy, D. R. Morrison, and E. Silverstein, *Dimensional duality*, *Phys.Rev.* **D76** (2007) 066004, [arXiv:0705.0550].

[102] S. A. Hartnoll, J. Polchinski, E. Silverstein, and D. Tong, *Towards strange metallic holography*, *JHEP* **1004** (2010) 120, [arXiv:0912.1061].

[103] E. Silverstein, *AdS and dS entropy from string junctions: or, The Function of junction conjunctions*, hep-th/0308175.

[104] J. A. Harvey and G. W. Moore, *Algebras, BPS states, and strings*, *Nucl.Phys.* **B463** (1996) 315–368, [hep-th/9510182].

[105] T. Damour, M. Henneaux, B. Julia, and H. Nicolai, *Hyperbolic Kac-Moody algebras and chaos in Kaluza-Klein models*, *Phys.Lett.* **B509** (2001) 323–330, [hep-th/0103094].

[106] J. Brown, O. J. Ganor, and C. Helfgott, *M theory and E(10): Billiards, branes, and imaginary roots*, *JHEP* **0408** (2004) 063, [hep-th/0401053].

[107] J. McGreevy, L. Susskind, and N. Toumbas, *Invasion of the giant gravitons from Anti-de Sitter space*, *JHEP* **0006** (2000) 008, [hep-th/0003075].

[108] J. D. Brown and M. Henneaux, *Central Charges in the Canonical Realization of Asymptotic Symmetries: An Example from Three-Dimensional Gravity*, *Commun.Math.Phys.* **104** (1986) 207–226.

[109] M. Banados, *Global charges in Chern-Simons field theory and the (2+1) black hole*, *Phys.Rev.* **D52** (1996) 5816, [hep-th/9405171].

[110] V. Balasubramanian and P. Kraus, *A Stress tensor for Anti-de Sitter gravity*, *Commun.Math.Phys.* **208** (1999) 413–428, [hep-th/9902121].

[111] M. Henningson and K. Skenderis, *The Holographic Weyl anomaly*, *JHEP* **9807** (1998) 023, [hep-th/9806087].

[112] E. Witten, *Anti-de Sitter space, thermal phase transition, and confinement in gauge theories*, *Adv.Theor.Math.Phys.* **2** (1998) 505–532, [hep-th/9803131].

[113] J. D. Brown and J. York, James W., *Quasilocal energy and conserved charges derived from the gravitational action*, *Phys.Rev.* **D47** (1993) 1407–1419, [gr-qc/9209012].

[114] G. T. Horowitz and R. C. Myers, *The AdS / CFT correspondence and a new positive energy conjecture for general relativity*, *Phys.Rev.* **D59** (1998) 026005, [hep-th/9808079].

[115] R. C. Myers, *Stress tensors and Casimir energies in the AdS / CFT correspondence*, *Phys.Rev.* **D60** (1999) 046002, [hep-th/9903203].

[116] R. Emparan, C. V. Johnson, and R. C. Myers, *Surface terms as counterterms in the AdS / CFT correspondence*, *Phys.Rev.* **D60** (1999) 104001, [hep-th/9903238].

[117] N. Birrell and P. Davies, *QUANTUM FIELDS IN CURVED SPACE*, .

[118] E. Alvarez and C. Gomez, *Geometric holography, the renormalization group and the c theorem*, *Nucl.Phys.* **B541** (1999) 441–460, [hep-th/9807226].

[119] D. Freedman, S. Gubser, K. Pilch, and N. Warner, *Renormalization group flows from holography supersymmetry and a c theorem*, *Adv.Theor.Math.Phys.* **3** (1999) 363–417, [hep-th/9904017].

[120] L. Girardello, M. Petrini, M. Porrati, and A. Zaffaroni, *Novel local CFT and exact results on perturbations of N=4 superYang Mills from AdS dynamics*, *JHEP* **9812** (1998) 022, [hep-th/9810126].

[121] A. Strominger, *Inflation and the dS / CFT correspondence*, *JHEP* **0111** (2001) 049, [hep-th/0110087].

[122] V. Sahakian, *Holography, a covariant c function, and the geometry of the renormalization group*, *Phys.Rev.* **D62** (2000) 126011, [hep-th/9910099].

[123] S. R. Coleman and F. De Luccia, *Gravitational Effects on and of Vacuum Decay*, *Phys.Rev.* **D21** (1980) 3305.

[124] N. Bao, X. Dong, E. Silverstein, and G. Torroba, *Stimulated superconductivity at strong coupling*, *JHEP* **1110** (2011) 123, [arXiv:1104.4098].

[125] D. S. Park, *Graviton and Scalar Two-Point Functions in a CDL Background for General Dimensions*, *JHEP* **0906** (2009) 023, [arXiv:0812.3172].

[126] B. Grinstein, K. A. Intriligator, and I. Z. Rothstein, *Comments on Unparticles*, *Phys.Lett.* **B662** (2008) 367–374, [arXiv:0801.1140].

[127] H. Osborn and A. Petkou, *Implications of conformal invariance in field theories for general dimensions*, *Annals Phys.* **231** (1994) 311–362, [hep-th/9307010].

[128] S. Minwalla, *Restrictions imposed by superconformal invariance on quantum field theories*, *Adv.Theor.Math.Phys.* **2** (1998) 781–846, [hep-th/9712074].

[129] N. Seiberg, *Electric - magnetic duality in supersymmetric nonAbelian gauge theories*, *Nucl.Phys.* **B435** (1995) 129–146, [hep-th/9411149].

[130] K. A. Intriligator and N. Seiberg, *Lectures on supersymmetric gauge theories and electric - magnetic duality*, *Nucl.Phys.Proc.Suppl.* **45BC** (1996) 1–28, [hep-th/9509066].

[131] E. Barnes, K. A. Intriligator, B. Wecht, and J. Wright, *Evidence for the strongest version of the 4d a-theorem, via a-maximization along RG flows*, *Nucl.Phys.* **B702** (2004) 131–162, [hep-th/0408156].

[132] D. Kutasov, A. Parnachev, and D. A. Sahakyan, *Central charges and U(1)(R) symmetries in N=1 superYang-Mills*, *JHEP* **0311** (2003) 013, [hep-th/0308071].

[133] H. Osborn, *Weyl consistency conditions and a local renormalization group equation for general renormalizable field theories*, *Nucl.Phys.* **B363** (1991) 486–526.

[134] D. Freedman and H. Osborn, *Constructing a c function for SUSY gauge theories*, *Phys.Lett.* **B432** (1998) 353–360, [hep-th/9804101].

[135] Z. Komargodski and A. Schwimmer, *On Renormalization Group Flows in Four Dimensions*, *JHEP* **1112** (2011) 099, [arXiv:1107.3987].

[136] Z. Komargodski, *The Constraints of Conformal Symmetry on RG Flows*, arXiv:1112.4538.

[137] A. Adams and S. Yaida, *Disordered Holographic Systems I: Functional Renormalization*, arXiv:1102.2892.

[138] V. E. Hubeny and M. Rangamani, *A Holographic view on physics out of equilibrium*, *Adv.High Energy Phys.* **2010** (2010) 297916, [arXiv:1006.3675].

[139] S. R. Das, T. Nishioka, and T. Takayanagi, *Probe Branes, Time-dependent Couplings and Thermalization in AdS/CFT*, *JHEP* **1007** (2010) 071, [arXiv:1005.3348].

[140] P. Basu and S. R. Das, *Quantum Quench across a Holographic Critical Point*, *JHEP* **1201** (2012) 103, [arXiv:1109.3909].

[141] V. Balasubramanian, A. Bernamonti, J. de Boer, N. Copland, B. Craps, et al., *Holographic Thermalization*, *Phys.Rev.* **D84** (2011) 026010, [arXiv:1103.2683].

[142] G. M. Eliasberg, *Film Superconductivity Stimulated by a High-Frequency Field*, *JETP Lett.* **11** (1970) 114.

[143] A. Robertson and V. M. Galitski, *Nonequilibrium enhancement of Cooper pairing in cold fermion systems*, *Phys.Rev.* **A80** (2009) 063609, [arXiv:0905.0912].

[144] R. Bousso, *The Holographic principle for general backgrounds*, *Class.Quant.Grav.* **17** (2000) 997–1005, [hep-th/9911002].

[145] T. Banks and W. Fischler, *Holographic cosmology*, hep-th/0405200.

[146] D. Harlow, S. H. Shenker, D. Stanford, and L. Susskind, *Tree-like structure of eternal inflation: A solvable model*, *Phys.Rev.* **D85** (2012) 063516, [arXiv:1110.0496].

[147] T. Hertog and J. Hartle, *Holographic No-Boundary Measure*, arXiv:1111.6090.

[148] T. Hertog and G. T. Horowitz, *Holographic description of AdS cosmologies*, *JHEP* **0504** (2005) 005, [hep-th/0503071].

[149] B. Craps, T. Hertog, and N. Turok, *Quantum Resolution of Cosmological Singularities using AdS/CFT*, arXiv:0712.4180.

[150] A. Lawrence and A. Sever, *Holography and renormalization in Lorentzian signature*, *JHEP* **0610** (2006) 013, [hep-th/0606022].

[151] A. Awad, S. R. Das, S. Nampuri, K. Narayan, and S. P. Trivedi, *Gauge Theories with Time Dependent Couplings and their Cosmological Duals*, *Phys.Rev.* **D79** (2009) 046004, [arXiv:0807.1517].

[152] K. Dasgupta, G. Rajesh, D. Robbins, and S. Sethi, *Time dependent warping, fluxes, and NCYM*, *JHEP* **0303** (2003) 041, [hep-th/0302049].

[153] E. Silverstein and D. Tong, *Scalar speed limits and cosmology: Acceleration from D-cceleration*, *Phys.Rev.* **D70** (2004) 103505, [hep-th/0310221].

[154] L. Kofman, A. D. Linde, X. Liu, A. Maloney, L. McAllister, et al., *Beauty is attractive: Moduli trapping at enhanced symmetry points*, *JHEP* **0405** (2004) 030, [hep-th/0403001].

[155] M. Alishahiha, E. Silverstein, and D. Tong, *DBI in the sky*, *Phys.Rev.* **D70** (2004) 123505, [hep-th/0404084].

[156] S. F. Ross and G. Titchener, *Time-dependent spacetimes in AdS/CFT: Bubble and black hole*, *JHEP* **0502** (2005) 021, [hep-th/0411128].

[157] G. T. Horowitz and E. Silverstein, *The Inside story: Quasilocal tachyons and black holes*, *Phys.Rev.* **D73** (2006) 064016, [hep-th/0601032].

[158] D. Marolf and S. F. Ross, *Boundary Conditions and New Dualities: Vector Fields in AdS/CFT*, *JHEP* **0611** (2006) 085, [hep-th/0606113].

[159] G. Compere and D. Marolf, *Setting the boundary free in AdS/CFT*, *Class.Quant.Grav.* **25** (2008) 195014, [arXiv:0805.1902].

[160] T. Faulkner and J. Polchinski, *Semi-Holographic Fermi Liquids*, *JHEP* **1106** (2011) 012, [arXiv:1001.5049].

[161] M. Li, *A Note on relation between holographic RG equation and Polchinski's RG equation*, *Nucl.Phys.* **B579** (2000) 525–532, [hep-th/0001193].

[162] O. Aharony, M. Berkooz, and E. Silverstein, *Multiple trace operators and nonlocal string theories*, *JHEP* **0108** (2001) 006, [hep-th/0105309].

[163] A. Adams and E. Silverstein, *Closed string tachyons, AdS / CFT, and large N QCD*, *Phys.Rev.* **D64** (2001) 086001, [hep-th/0103220].

[164] E. Witten, *Multitrace operators, boundary conditions, and AdS / CFT correspondence*, hep-th/0112258.

[165] M. Berkooz, A. Sever, and A. Shomer, *'Double trace' deformations, boundary conditions and space-time singularities*, *JHEP* **0205** (2002) 034, [hep-th/0112264].

[166] E. Pomoni and L. Rastelli, *Large N Field Theory and AdS Tachyons*, *JHEP* **0904** (2009) 020, [arXiv:0805.2261].

[167] A. Dymarsky, I. Klebanov, and R. Roiban, *Perturbative search for fixed lines in large N gauge theories*, *JHEP* **0508** (2005) 011, [hep-th/0505099].

[168] E. Kiritsis and V. Niarchos, *Interacting String Multi-verses and Holographic Instabilities of Massive Gravity*, *Nucl.Phys.* **B812** (2009) 488–524, [arXiv:0808.3410].

[169] L. Vecchi, *The Conformal Window of deformed CFT's in the planar limit*, *Phys.Rev.* **D82** (2010) 045013, [arXiv:1004.2063].

[170] T. Andrade, T. Faulkner, and D. Marolf, *Banishing AdS Ghosts with a UV Cutoff*, arXiv:1112.3085.

[171] S. Weinberg, *The Quantum theory of fields. Vol. 1: Foundations*, .

[172] J. Wess and J. Bagger, *Supersymmetry and supergravity*, .

[173] H. K. Dreiner, H. E. Haber, and S. P. Martin, *Two-component spinor techniques and Feynman rules for quantum field theory and supersymmetry*, *Phys.Rept.* **494** (2010) 1–196, [arXiv:0812.1594].

[174] J. N. Laia and D. Tong, *Flowing Between Fermionic Fixed Points*, *JHEP* **1111** (2011) 131, [arXiv:1108.2216].

[175] A. Allais, *Double-trace deformations, holography and the c-conjecture*, *JHEP* **1011** (2010) 040, [arXiv:1007.2047].

[176] F. Dolan and H. Osborn, *Superconformal symmetry, correlation functions and the operator product expansion*, *Nucl.Phys.* **B629** (2002) 3–73, [hep-th/0112251].

[177] M. R. Douglas and S. H. Shenker, *Dynamics of SU(N) supersymmetric gauge theory*, *Nucl.Phys.* **B447** (1995) 271–296, [hep-th/9503163].

[178] P. C. Argyres and M. R. Douglas, *New phenomena in SU(3) supersymmetric gauge theory*, *Nucl.Phys.* **B448** (1995) 93–126, [hep-th/9505062].

[179] P. C. Argyres, M. R. Plesser, N. Seiberg, and E. Witten, *New N=2 superconformal field theories in four-dimensions*, *Nucl.Phys.* **B461** (1996) 71–84, [hep-th/9511154].

[180] K. A. Intriligator and B. Wecht, *The Exact superconformal R symmetry maximizes a*, *Nucl.Phys.* **B667** (2003) 183–200, [hep-th/0304128].

[181] N. Seiberg and E. Witten, *Electric - magnetic duality, monopole condensation, and confinement in N=2 supersymmetric Yang-Mills theory*, *Nucl.Phys.* **B426** (1994) 19–52, [hep-th/9407087].

[182] L. Alvarez-Gaume and S. Hassan, *Introduction to S duality in N=2 supersymmetric gauge theories: A Pedagogical review of the work of Seiberg and Witten*, *Fortsch.Phys.* **45** (1997) 159–236, [hep-th/9701069].

[183] J. A. Minahan and D. Nemeschansky, *An N=2 superconformal fixed point with E(6) global symmetry*, *Nucl.Phys.* **B482** (1996) 142–152, [hep-th/9608047].

[184] A. Fayyazuddin and M. Spalinski, *Large N superconformal gauge theories and supergravity orientifolds*, *Nucl.Phys.* **B535** (1998) 219–232, [hep-th/9805096].

[185] P. D. Mannheim, *Solution to the ghost problem in fourth order derivative theories*, *Found.Phys.* **37** (2007) 532–571, [hep-th/0608154].

[186] C. M. Bender and P. D. Mannheim, *No-ghost theorem for the fourth-order derivative Pais-Uhlenbeck oscillator model*, *Phys.Rev.Lett.* **100** (2008) 110402, [arXiv:0706.0207].

[187] A. H. Guth, *The Inflationary Universe: A Possible Solution to the Horizon and Flatness Problems*, *Phys.Rev.* **D23** (1981) 347–356.

[188] A. D. Linde, *A New Inflationary Universe Scenario: A Possible Solution of the Horizon, Flatness, Homogeneity, Isotropy and Primordial Monopole Problems*, *Phys.Lett.* **B108** (1982) 389–393.

[189] A. Albrecht and P. J. Steinhardt, *Cosmology for Grand Unified Theories with Radiatively Induced Symmetry Breaking*, *Phys.Rev.Lett.* **48** (1982) 1220–1223.

[190] A. D. Linde, *Chaotic Inflation*, *Phys.Lett.* **B129** (1983) 177–181.

[191] C. Cheung, P. Creminelli, A. L. Fitzpatrick, J. Kaplan, and L. Senatore, *The Effective Field Theory of Inflation*, *JHEP* **0803** (2008) 014, [arXiv:0709.0293].

[192] L. Senatore and M. Zaldarriaga, *The Effective Field Theory of Multifield Inflation*, *JHEP* **1204** (2012) 024, [arXiv:1009.2093].

[193] X. Chen, M.-x. Huang, S. Kachru, and G. Shiu, *Observational signatures and non-Gaussianities of general single field inflation*, *JCAP* **0701** (2007) 002, [hep-th/0605045].

[194] D. Baumann and D. Green, *Inflating with Baryons*, *JHEP* **1104** (2011) 071, [arXiv:1009.3032].

[195] D. Baumann and L. McAllister, *Advances in Inflation in String Theory*, *Ann.Rev.Nucl.Part.Sci.* **59** (2009) 67–94, [arXiv:0901.0265].

[196] S. Kachru, R. Kallosh, A. D. Linde, J. M. Maldacena, L. P. McAllister, et al., *Towards inflation in string theory*, *JCAP* **0310** (2003) 013, [hep-th/0308055].

[197] R. Kallosh and A. D. Linde, *Landscape, the scale of SUSY breaking, and inflation*, *JHEP* **0412** (2004) 004, [hep-th/0411011].

[198] E. Silverstein and A. Westphal, *Monodromy in the CMB: Gravity Waves and String Inflation*, *Phys.Rev.* **D78** (2008) 106003, [arXiv:0803.3085].

[199] S. Dimopoulos, S. Kachru, J. McGreevy, and J. G. Wacker, *N-flation*, *JCAP* **0808** (2008) 003, [hep-th/0507205].

[200] R. Easther and L. McAllister, *Random matrices and the spectrum of N-flation*, *JCAP* **0605** (2006) 018, [hep-th/0512102].

[201] D. Green, B. Horn, L. Senatore, and E. Silverstein, *Trapped Inflation*, *Phys.Rev.* **D80** (2009) 063533, [arXiv:0902.1006].

[202] L. Kofman and A. D. Linde, *unpublished*, .

[203] A. Berera, I. G. Moss, and R. O. Ramos, *Warm Inflation and its Microphysical Basis*, *Rept.Prog.Phys.* **72** (2009) 026901, [arXiv:0808.1855].

[204] A. Berera and T. W. Kephart, *The Ubiquitous Inflaton in String-Inspired Models*, *Phys.Rev.Lett.* **83** (1999) 1084–1087, [hep-ph/9904410].

[205] M. Bastero-Gil, A. Berera, J. B. Dent, and T. W. Kephart, *Towards Realizing Warm Inflation in String Theory*, arXiv:0904.2195.

[206] I. Dymnikova and M. Khlopov, *Self-consistent initial conditions in inflationary cosmology*, *Grav.Cosmol.Suppl.* **4** (1998) 50–55.

[207] I. Dymnikova and M. Khlopov, *Decay of cosmological constant as Bose condensate evaporation*, *Mod.Phys.Lett.* **A15** (2000) 2305–2314, [astro-ph/0102094].

[208] I. Dymnikova and M. Khlopov, *Decay of cosmological constant in selfconsistent inflation*, *Eur.Phys.J.* **C20** (2001) 139–146.

[209] A. J. Tolley and M. Wyman, *The Gelaton Scenario: Equilateral non-Gaussianity from multi-field dynamics*, *Phys.Rev.* **D81** (2010) 043502, [arXiv:0910.1853].

[210] S. Rubin, *Effect of massive fields on inflation*, *JETP Lett.* **74** (2001) 247–250, [hep-ph/0110132].

[211] A. Achucarro, J.-O. Gong, S. Hardeman, G. A. Palma, and S. P. Patil, *Features of heavy physics in the CMB power spectrum*, *JCAP* **1101** (2011) 030, [arXiv:1010.3693].

[212] N. Bartolo and A. Riotto, *Possibly Large Corrections to the Inflationary Observables*, *Mod.Phys.Lett.* **A23** (2008) 857–862, [arXiv:0711.4003].

[213] E. D. Stewart, *Mutated hybrid inflation*, *Phys.Lett.* **B345** (1995) 414–415, [astro-ph/9407040].

[214] G. Lazarides and C. Panagiotakopoulos, *Smooth hybrid inflation*, *Phys.Rev.* **D52** (1995) 559–563, [hep-ph/9506325].

[215] D. H. Lyth and E. D. Stewart, *More varieties of hybrid inflation*, *Phys.Rev.* **D54** (1996) 7186–7190, [hep-ph/9606412].

[216] **WMAP Collaboration** Collaboration, D. Spergel et al., *First year Wilkinson Microwave Anisotropy Probe (WMAP) observations: Determination of cosmological parameters*, *Astrophys.J.Suppl.* **148** (2003) 175–194, [astro-ph/0302209].

[217] **WMAP Collaboration** Collaboration, H. Peiris et al., *First year Wilkinson Microwave Anisotropy Probe (WMAP) observations: Implications for inflation*, *Astrophys.J.Suppl.* **148** (2003) 213, [astro-ph/0302225].

[218] **WMAP Collaboration** Collaboration, D. Spergel et al., *Wilkinson Microwave Anisotropy Probe (WMAP) three year results: implications for cosmology*, *Astrophys.J.Suppl.* **170** (2007) 377, [astro-ph/0603449].

[219] **WMAP Collaboration** Collaboration, E. Komatsu et al., *Five-Year Wilkinson Microwave Anisotropy Probe (WMAP) Observations: Cosmological Interpretation*, *Astrophys.J.Suppl.* **180** (2009) 330–376, [arXiv:0803.0547].

[220] **WMAP Collaboration** Collaboration, E. Komatsu et al., *Seven-Year Wilkinson Microwave Anisotropy Probe (WMAP) Observations: Cosmological Interpretation*, *Astrophys.J.Suppl.* **192** (2011) 18, [arXiv:1001.4538].

[221] L. McAllister, E. Silverstein, and A. Westphal, *Gravity Waves and Linear Inflation from Axion Monodromy*, *Phys.Rev.* **D82** (2010) 046003, [arXiv:0808.0706].

[222] N. Kaloper and L. Sorbo, *Where in the String Landscape is Quintessence*, *Phys.Rev.* **D79** (2009) 043528, [arXiv:0810.5346].

[223] N. Kaloper and L. Sorbo, *A Natural Framework for Chaotic Inflation*, *Phys.Rev.Lett.* **102** (2009) 121301, [arXiv:0811.1989].

[224] N. Kaloper, A. Lawrence, and L. Sorbo, *An Ignoble Approach to Large Field Inflation*, *JCAP* **1103** (2011) 023, [arXiv:1101.0026].

[225] **Planck Collaboration** Collaboration, F. Bouchet, *The Planck satellite: Status & perspectives*, *Mod.Phys.Lett.* **A22** (2007) 1857–1863.

[226] C. Armendariz-Picon, T. Damour, and V. F. Mukhanov, *k - inflation*, *Phys.Lett.* **B458** (1999) 209–218, [hep-th/9904075].

[227] R. Flauger, L. McAllister, E. Pajer, A. Westphal, and G. Xu, *Oscillations in the CMB from Axion Monodromy Inflation*, *JCAP* **1006** (2010) 009, [arXiv:0907.2916].

[228] N. Barnaby and M. Peloso, *Large Nongaussianity in Axion Inflation*, *Phys.Rev.Lett.* **106** (2011) 181301, [arXiv:1011.1500].

[229] A. Saltman and E. Silverstein, *A New handle on de Sitter compactifications*, *JHEP* **0601** (2006) 139, [hep-th/0411271].

[230] K. Nakayama and F. Takahashi, *Running Kinetic Inflation*, *JCAP* **1011** (2010) 009, [arXiv:1008.2956].

[231] M. Aganagic, C. Beem, J. Seo, and C. Vafa, *Geometrically Induced Metastability and Holography*, *Nucl.Phys.* **B789** (2008) 382–412, [hep-th/0610249].

[232] D. Baumann, A. Dymarsky, S. Kachru, I. R. Klebanov, and L. McAllister, *Compactification Effects in D-brane Inflation*, *Phys.Rev.Lett.* **104** (2010) 251602, [arXiv:0912.4268].

[233] D. Baumann, A. Dymarsky, S. Kachru, I. R. Klebanov, and L. McAllister, *D3-brane Potentials from Fluxes in AdS/CFT*, *JHEP* **1006** (2010) 072, [arXiv:1001.5028].

[234] J. R. Bond, L. Kofman, S. Prokushkin, and P. M. Vaudrevange, *Roulette inflation with Kahler moduli and their axions*, *Phys.Rev.* **D75** (2007) 123511, [hep-th/0612197].

[235] M. Cicoli, C. Burgess, and F. Quevedo, *Fibre Inflation: Observable Gravity Waves from IIB String Compactifications*, *JCAP* **0903** (2009) 013, [arXiv:0808.0691].

[236] J. Garriga and A. Vilenkin, *Recycling universe*, *Phys.Rev.* **D57** (1998) 2230–2244, [astro-ph/9707292].

[237] A. H. Guth, *Eternal inflation and its implications*, *J.Phys.A* **A40** (2007) 6811–6826, [hep-th/0702178].

[238] L. Susskind, *The Anthropic landscape of string theory*, hep-th/0302219.

[239] O. DeWolfe, D. Freedman, S. Gubser, and A. Karch, *Modeling the fifth-dimension with scalars and gravity*, *Phys.Rev.* **D62** (2000) 046008, [hep-th/9909134].

[240] M. Gremm, *Four-dimensional gravity on a thick domain wall*, *Phys.Lett.* **B478** (2000) 434–438, [hep-th/9912060].

[241] C. Csaki, J. Erlich, T. J. Hollowood, and Y. Shirman, *Universal aspects of gravity localized on thick branes*, *Nucl.Phys.* **B581** (2000) 309–338, [hep-th/0001033].

[242] G. Ellis and M. Madsen, *Exact scalar field cosmologies*, *Class.Quant.Grav.* **8** (1991) 667–676.

[243] P. Breitenlohner and D. Z. Freedman, *Stability in Gauged Extended Supergravity*, *Annals Phys.* **144** (1982) 249.

[244] T. Hertog and G. T. Horowitz, *Towards a big crunch dual*, *JHEP* **0407** (2004) 073, [hep-th/0406134].

[245] B. Freivogel, M. Kleban, M. Rodriguez Martinez, and L. Susskind, *Observational consequences of a landscape*, *JHEP* **0603** (2006) 039, [hep-th/0505232].

[246] L. Susskind, *The Census taker's hat*, arXiv:0710.1129.

[247] R. Bousso and L. Susskind, *The Multiverse Interpretation of Quantum Mechanics*, *Phys.Rev.* **D85** (2012) 045007, [arXiv:1105.3796].

[248] G. T. Horowitz, J. Orgera, and J. Polchinski, *Nonperturbative Instability of AdS(5) x S**5/Z(k)*, *Phys.Rev.* **D77** (2008) 024004, [arXiv:0709.4262].

[249] D. Harlow, *Metastability in Anti de Sitter Space*, arXiv:1003.5909.

[250] J. L. Barbon and E. Rabinovici, *Holography of AdS vacuum bubbles*, *JHEP* **1004** (2010) 123, [arXiv:1003.4966].